MOLECULAR DISSECTION OF TELOMERE DYSFUNCTION AND ANALYSIS OF G-OVERHANGS IN *Arabidopsis thaliana*

A Dissertation

by

MICHELLE L. HEACOCK

Submitted to the Office of Graduate Studies of
Texas A&M University
in partial fulfillment of the requirements for the degree of

DOCTOR OF PHILOSOPHY

December 2007

Major Subject: Biochemistry

MOLECULAR DISSECTION OF TELOMERE DYSFUNCTION AND ANALYSIS OF G-OVERHANGS IN *Arabidopsis thaliana*

A Dissertation

by

MICHELLE L. HEACOCK

Submitted to the Office of Graduate Studies of
Texas A&M University
in partial fulfillment of the requirements for the degree of

DOCTOR OF PHILOSOPHY

Approved by:

Chair of Committee,	Dorothy E. Shippen
Committee Members,	Linda A. Guarino
	Alan E. Pepper
	Donald W. Pettigrew
Head of Department,	Gregory D. Reinhart

December 2007

Major Subject: Biochemistry

ABSTRACT

Molecular Dissection of Telomere Dysfunction and Analysis of G-overhangs in *Arabidopsis thaliana*.

(December 2007)

Michelle L. Heacock, B.S., Delta State University

Chair of Advisory Committee: Dr. Dorothy E. Shippen

Telomeres comprise the physical ends of chromosomes. In the absence of telomerase, the enzyme responsible for replenishing telomeric DNA, telomeres progressively shorten due to the end replication problem. Eventually telomeres reach a length where they are recruited into end-to-end chromosome fusions. Through the use of novel PCR strategies, I followed the fate of telomeres in plants lacking telomerase as they progressed into dysfunction. I uncovered two distinct structural/functional length transitions. The first transition (~1 kb) marks the onset of telomere dysfunction, where telomeres are transiently uncapped and a subset of them engage in end-to-end fusions. The second transition (~300 bp) defines complete telomere dysfunction as telomeres below this length lack G-overhangs and the vast majority of the chromosome ends fuse. Thus, these two telomere lengths define architectural transitions that link structure and function.

In addition, I uncovered a hierarchy of end-joining pathways that join dysfunctional telomeres in which the non-homologous end-joining (NHEJ) protein, KU predominates. In the absence of KU, telomeres are joined by a microhomology-mediated end-joining pathway (MMEJ) that is dependent on Mre11. I also show that

DNA ligase IV (LIG4) is the predominant enzyme that ligates dysfunctional telomeres as fusions are reduced in its absence. These studies highlight the importance of repairing DSBs and demonstrate that *Arabidopsis* possesses highly redundant means for processing dysfunctional telomeres.

The G-overhang is an essential feature of the telomere that is required for proper telomere function. I employed methods to examine G-overhang status in various mutants known to contribute to telomere maintenance in *Arabidopsis*. My analysis revealed that the putative G-overhang binding proteins POT1a, POT1b and POT1c, make modest, but distinct contributions to the G-overhangs. Additionally, I uncovered a major role for the putative telomere capping protein, CIT1 in maintenance of the G-overhang. G-overhang signals obtained from *cit1* mutants were grossly increased indicating that CIT1 is involved in either protecting the C-rich strand of the telomere from nuclease attack, or in controlling telomerase extension of the G-strand. Together, these data have provided new insight into factors that contribute to telomere integrity and have further developed *Arabidopsis* as a model for telomere biology.

DEDICATION

To my husband who has and continues to be an endless source of encouragement, grounding and support; there is no doubt that I could not have done this without him.

To the many teachers that have believed in and inspired me to keep pushing forward.

To my family and friends, I thank you for providing me with a strong foundation and reminding me to laugh at myself.

ACKNOWLEDGEMENTS

Most importantly, I am in deep gratitude to Dr. Dorothy Shippen. Her never-ending support and ability to convince me to keep reaching high has positively impacted me in more ways than I anticipated. She has patiently shown me how to acquire the tools necessary to conduct good science. Next, Dr. Donald Pettigrew, who taught the first official class in my graduate career, I could not have asked for someone better to ease the transition from undergraduate to graduate work. He spent many a time at the whiteboard answering my questions. I am grateful to Dr. Elizabeth Spangler, who took me under her wing during my first couple of years. Special thanks to Dr. Karel Riha; his enthusiasm for science is inspiring and contagious.

I thank my committee, Dr. Donald Pettigrew, Dr. Linda Guarino and Dr. Alan Pepper, for their thoughtful advice and guidance throughout my graduate career.

I would like to thank Dr. Henry Outlaw for giving me that “gentle” push to enroll at the university. It is difficult to say whether I would have ended up here if it had not been for him.

I would like to acknowledge the graduate student body and faculty of the Biochemistry/Biophysics department. I hope that the collegial atmosphere continues for years to come. I thank Juanita, Pat and Tillie for taking care of all of those pesky administrative details and making my life so much easier. Tillie has been a wonderful source of comfort and support and deserves special gratitude for continuously going the

extra mile in order to avoid and ease any potential burdens that she thought might be coming my way. Thank you for making my life easier on so many occasions.

I was fortunate enough to be able to exchange ideas with and be given suggestions on a regular basis by the members of the Kapler and McKnight labs. I will miss our weekly meetings. Dr. Geoffrey Kapler requires special mention. His ability to be sincerely interested in one's work and offer constructive criticism has made me think more critically about my experiments and data.

Of course, without saying, the members of the Shippen lab have made graduate school an enjoyable experience. They have offered me scientific advice, and most of all made me laugh. It has been an honor to be part of such a cohesive lab. I am especially grateful to Dr. Matthew Watson, Dr. Eugene Sharkirov, Kalpana and Yulia, who all have been instrumental in sharing in my accomplishments and suffering with me in my setbacks throughout this endeavor.

TABLE OF CONTENTS

CHAPTER Page

LIST OF FIGURES

Page

Page

LIST OF TABLES

Page

CHAPTER I

INTRODUCTION

The genome constantly faces double-strand breaks (DSBs) from exposure to such things as ionizing radiation (IR), reactive oxygen species (ROS) from oxidative metabolism, and replication fork stalling. DSBs can also be generated through a controlled, intentional process designed to create diversity during antibody production and meiosis. If left unrepaired, DSBs are highly detrimental to cell function.

The physical ends of natural chromosome ends are comprised of telomeres that resemble DSBs. Importantly, however, telomeres are protected from inappropriate recruitment into repair reactions (Figure 1). This protection is accomplished through formation of a higher-order structure devised to evade DNA damage surveillance mechanisms. When this structure is compromised, telomeres are recognized as sites of DNA damage and are processed accordingly (1,2). Often dysfunctional telomeres are recruited into end-to-end chromosome fusions which lead to genome instability.

In addition to canonical telomere binding proteins (TBPs), DNA damage proteins also reside at telomeres and make important contributions to the protective structure and to telomere maintenance (3). It is not known how DNA damage proteins

---

This dissertation follows the style of *Nucleic Acids Research*.

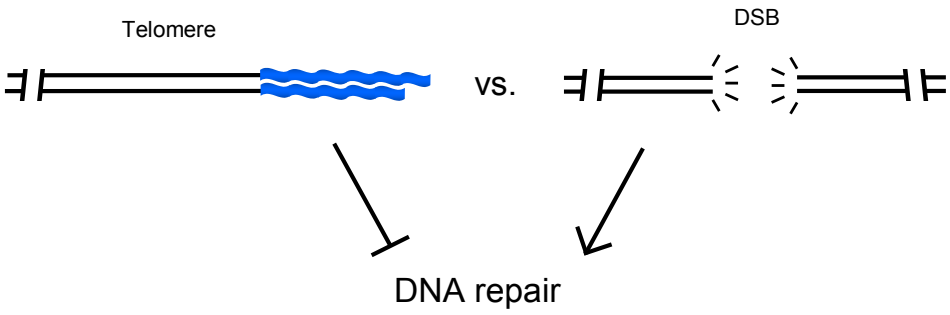

Figure 1. The fate of a double-strand break versus a telomere.

A double-strand break (radiating lines) is recruited into an end-joining reaction while a telomere (blue wavy lines) is stable and refractory to DNA repair. Adapted from (3).

can function in this paradoxical manner. Understanding the dynamic interplay between telomeres, TBPs and proteins of the DNA damage response (DDR) is a major focus of the telomere field.

Discovery of special chromosome ends

The notion that chromosome ends are distinct from internal chromosomal sequences was first suggested over seventy-five years ago by Barbara McClintock and Hermann Muller. Working independently on two different organisms, McClintock on maize (4) and Muller on Drosophila (5), both made the insightful observation that while fragmented chromosomes fused to other broken chromosomes, the natural ends of chromosomes were protected from this fate. In addition, McClintock noticed that when internal chromosome breaks fused they created dicentric chromosomes (with two centromeres) and were subsequently pulled apart during anaphase in the mitotic cycle. The new break would fuse again and the process would repeat itself. She called this process the breakage-fusion-bridge (BFB) cycle (6) (Figure 2). BFB cycles would later be shown to be one of the major contributors leading to genome instability.

Interestingly, BFB cycles were not observed in maize embyros, suggesting that something in these cells, later speculated to be telomerase, inhibited end-joining (6,7). Another key observation suggesting that chromosome ends must have unique features was made in the 1970's. Alexy Olovnikov and James Watson predicted that lagging strand synthesis of linear chromosome ends would result in continual erosion of the terminus when the most distal RNA primer was removed (8,9). This is because this region of the chromosome could not be replicated. Olovnikov correctly theorized that

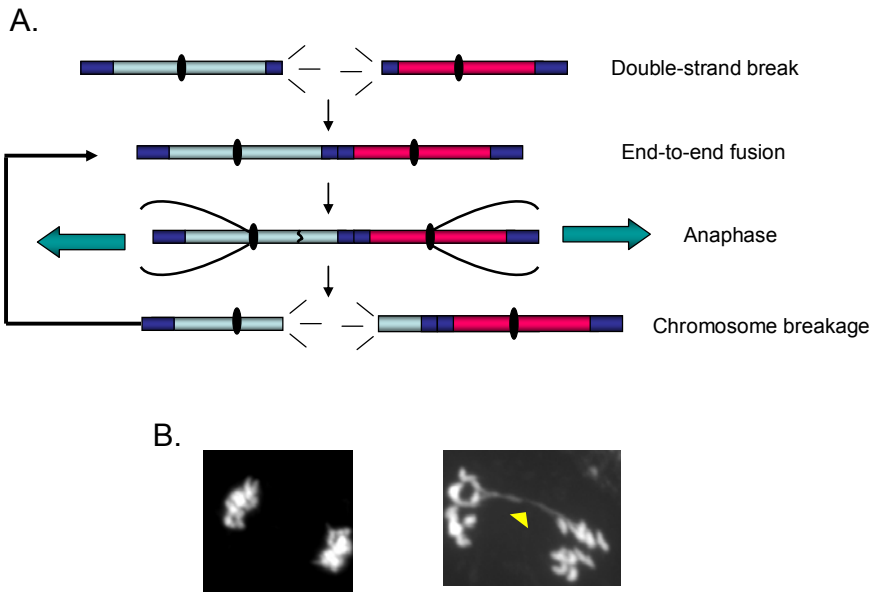

Figure 2. Breakage-fusion-bridge cycle.

(A) The repair of a double-strand break results in fusion between two chromosomes leading to a dicentric chromosome. During anaphase the fused dicentric chromosome is pulled apart resulting in a new DSB. This cycle is known as the breakage-fusion-bridge cycle. Radiating lines represent a DSB; ovals, centromere. (B) Examples of anaphases. Left panel is a wild type anaphase and right panel is an exmaple of an anaphase bridge (yellow arrowhead).

some mechanism must be in place to prevent the erosion of chromosome ends and that if not, this could ultimately lead to cellular aging. Further evidence that the chromosome terminus was special came when a unique specialized repetitive sequence at the ends of linear chromosomes was uncovered by Elizabeth Blackburn (10). These sequences were denoted telomeres, a term first coined by Hermann Muller years before (5). Telomeric DNA was subsequently demonstrated to be a functional unit that protects linear ends. Blackburn and Jack Szostak added *Tetrahymena* telomeric DNA to the end of a linear chromosome construct and introduced it into yeast (11). The *de novo* addition of yeast telomeric sequences to the *Tetrahymena* telomere tract acted to stabilize the linear chromosome. This pivotal experiment was the first to directly demonstrate that telomeres can protect linear chromosomes, and furthermore to show that there is an activity in cells that maintains telomere sequences.

What is a telomere?

Linear chromosomes must overcome a unique hurdle. Continuous erosion of chromosome ends, due to the end-replication problem, must be prevented in order to preserve internal, gene-encoding DNA sequences. In addition, as discussed above, chromosome ends must be distinguished from DSBs. Telomeres can now be defined as discrete, tandem arrays of simple DNA repeats that comprise the ends of linear chromosomes, circumvent the end-replication problem and provide chromosome end protection. In most organisms, telomeric DNA consists of a combination of thymines (Ts) and guanines (Gs). For example, the telomere repeat found at the ends of human chromosomes is $(T_2AG_3)_n$ (12), and is altered by only one thymine at *Arabidopsis* telomeres $(T_3AG_3)_n$ (13).

The length of telomeric repeat tracts differs, but it is maintained within a strict size range that is specific for a given species. For instance, telomere lengths are maintained between 275 and 300 bp in yeasts, while in human telomeres range from 10 and 15 kb (reviewed in (14), (15). Telomeric DNA consists of a double-and-single strand portions. Although bulk telomeric DNA is double-stranded, the TG-rich strand runs in the 5' to 3' direction and terminates in a single-strand extension commonly referred to as the G-overhang.

While a majority of organisms harbor telomeric DNA repeats at their chromosomal termini that are maintained by the action of telomerase reverse transcriptase (see below), examples of alternate strategies to conceal ends exist. The chromosome ends of Poxviruses and *Borrelia* are covalently-joined forming a hairpin structure (16). Here, the hairpin acts to mask chromosome ends. Another strategy is seen in *Drosophila*, where retrotransposons are periodically added to chromosome ends and form a unique chromatin structure that distinguishes the ends from DSBs (17).

Mammalian and yeast cells have devised a homologous recombination (HR) mechanism, alternative lengthening of telomeres (ALT), to maintain chromosome ends in the absence of telomerase (18,19). In budding yeast, ALT is dependent on proteins of the HR pathway and the mechanisms fall into two categories, Type I and Type II recombination (19-21). Type I recombination is dependent on Rad51 and amplifies repetitive subtelomeric regions that are present on a majority of chromosome ends. Type II recombination utilizes telomeric tracts from other chromosomes for a template for recombination and requires Rad50. The presence of alternative strategies to hide and cap chromosome ends highlights the requirement to protect linear chromosome ends.

G-overhangs

Like bulk telomeric DNA, the length of G-overhangs differs in size among organisms, but appears to correlate with the length of bulk telomere tracts. Longer G-overhangs are observed in organisms harboring longer telomere tracts (reviewed in (14)). For example, G-overhangs in *Tetrahymena* are only 14-21 nucleotides (nt), while G-overhangs of ~ 255 nt are present in vertebrates.

G-overhangs naturally occur as a consequence of lagging strand synthesis, when the most 3' RNA primer is removed (Figure 3). The G-overhang provides a substrate for telomerase elongation (discussed below). Since leading strand replication machinery produces a blunt end DNA product and yet G-overhangs are present on both chromosome ends (which are replicated by either the leading or lagging strand machineries), there must be another mechanism for their generation (14,22-27). The presence of asymmetric G-overhangs in mammalian cells (28) indicates that G-overhangs on leading and lagging strands are generated by different mechanisms. One likely mechanism is that G-overhangs are formed through a combination of telomerase and nuclease action (Figure 3). In line with this idea, studies show that absence of Mre11, a nuclease involved in DNA repair (discussed below), results in a decreased G-overhang signal (28,29), and telomere dysfunction (i.e. end-to-end fusions) due to improper telomere function (discussed further below) (30).

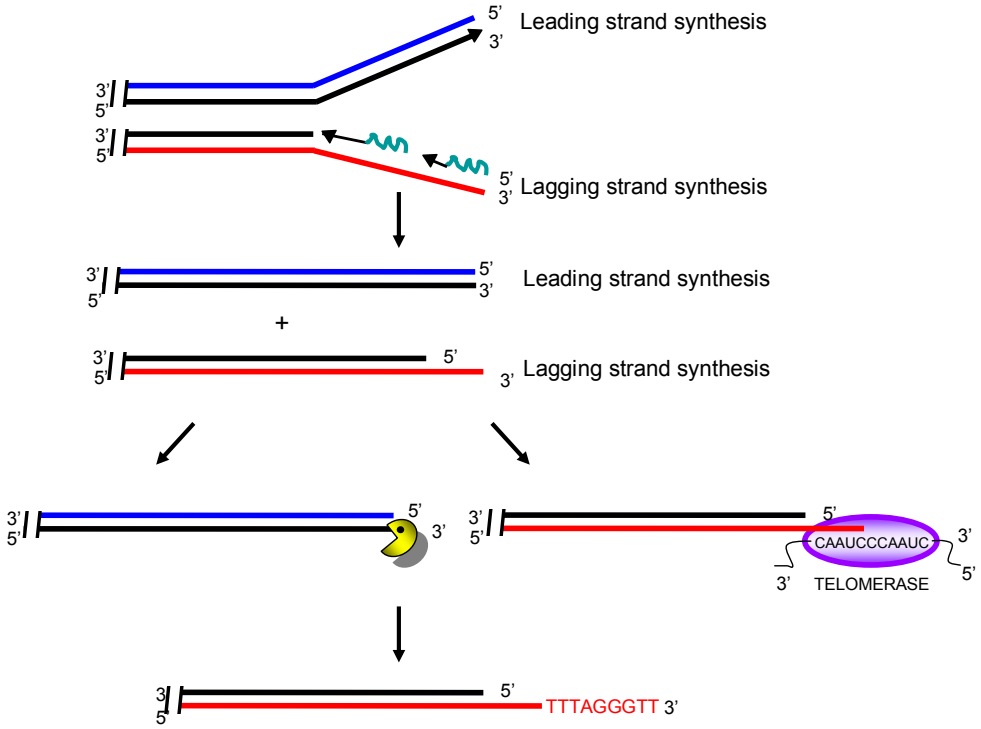

Figure 3. End replication problem and formation of the G-overhang.

The products of semi-conservative replication are denoted in black. RNA primers are shown as green wavy lines. G-overhangs are formed on the 3' end of the lagging strand when the last RNA primer is removed. Nuclease digestion of the C-strand is thought to occur on telomeres replicated by leading strand synthesis to create a G-overhang. Telomerase extends the 3' overhang through reverse transcription. The RNA subunit binds the 3' overhang. Telomerase, purple oval. Newly added telomere repeats are shown in red.

Telomeres form a higher-order structure

The special architecture of telomeres helps prevent the natural chromosome end from being inappropriately recognized as a DSB. Protection at telomeres is thought to be accomplished through the formation of a higher-order nucleoprotein capping complex known as the t-loop. The t-loop was originally observed *in vitro* using electron microscopy (EM) (31). To preserve t-loops for study, genomic DNA must be purified from isolated, cross-linked nuclei. EM studies show that the t-loop occurs when telomeres form a lariat-like structure with single-stranded DNA tucked between duplex DNA at the base (Figure 4). t-loops in human cells have been reported to range in size from 1 to 25 kb (31). As discussed below, TRF2, a core component of the telomere complex in humans, is important for formation of t-loops (32). Wang et al. show that removal of t-loop-sized telomeric tracts, cleaved in response to a mutation of TRF2, is dependent on XRCC3, a protein implicated in resolution of holliday junctions (33). These observations support the conclusion that a t-loop structure resembles a recombination intermediate (Figure 4).

While t-loops have not been observed *in vivo*, the presence of t-loops has been demonstrated *in vitro* in several organisms including mammals, plants, trypanosomes, and ciliated protozoa (34). Interestingly, t-loops have not been observed in budding yeast. The failure to observe these structures could be explained by the fact that t-loop formation involves invasion (and likely base-pairing) of the G-overhang into duplex DNA. Unlike other organisms, budding yeast telomere repeats are highly irregular, and

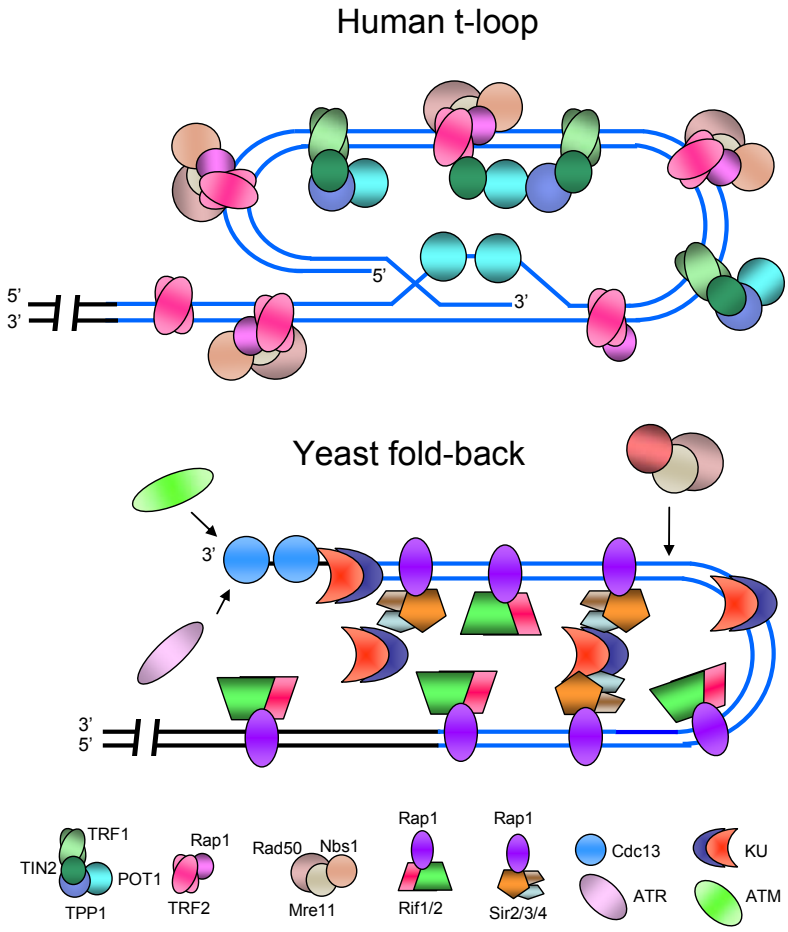

Figure 4. Proposed telomere higher-order structures.

(A) t-loop. The t-loop structure is formed by invasion of the G-overhang into the duplex telomeric DNA. POT1 localizes to both double-and-single strand portions of the t-loop. For simplicity, only proteins comprising the shelterin complex are shown bound to the telomere. (B) Yeast fold-back structure. The fold-back structure is mediated by Rap1p, Rif1/2p, Sir proteins and Ku. ATM and ATR are recruited to yeast telomeres through interactions with Cdc13p. Telomeric DNA is shown in blue. Protein legend is shown along bottom of figure. Adapted from (3).

therefore base-pairing between the G-overhang and the C-rich telomeric strand (C-strand) would be limited (35). In addition, technical limitations may prevent the observation of t-loops in yeast. Yeast telomeres are ~ 300 bp, making it difficult to separate telomeric DNA from digested bulk genomic DNA. Instead of t-loops, yeast telomeres are proposed to fold-back on themselves, the structure secured by chromatin and protein interactions (36) (Figure 4). Altogether, these observations indicate that a functional telomere is one that can form a protective cap.

Telomerase

Due to the end-replication problem, telomeres shorten with each cell division (Figure 3). After a finite number of cell divisions, telomeres reach a critical length where a protective cap can not be formed any longer and ends are recognized as a DSB (1). In most organisms, telomerase solves the end-replication problem. Telomerase is a ribonucleoprotein reverse transcriptase capable of telomere elongation using the G-overhang as a substrate ((37), reviewed in (38)). The core components of telomerase consist of an intrinsic telomerase RNA component (TERC) and the catalytic telomerase reverse transcriptase subunit (TERT).

One feature of TERC is a species-specific template region that corresponds to ~1.5 telomere repeats complementary to the G-rich telomere strand. In humans the sequence of this template is 5' CUAACCCUAAC 3' (39). Aside from the template region, TERC is not conserved at the nucleotide level among different organisms. Instead, TERCs share a highly conserved secondary structure that includes a pseudoknot, template, template boundary regions, and an H/ACA box, which is

important for telomerase RNP biogenesis (40). TERCs vary widely in size, ranging from 148 nt in ciliates to 1300 nt in yeast (reviewed in (40)).

The TERT subunit of telomerase is a reverse transcriptase (RT) that contains all seven canonical RT motifs (1, 2, A, B', C, D, E) that are conserved in other RTs. In addition to these conserved RT motifs, TERT possesses four telomerase-specific motifs. One of these motifs, the N-terminal T motif, is required for telomerase activity (41-44). TERT is a unique RT as it stably associates with the intrinsic TERC component. Another feature that distinguishes TERT from other RTs is the capability to processively add short repeats (45).

Telomerase activity can be reconstituted *in vitro* with just TERC and TERT (38). The first step in telomere addition is binding of TERC to its telomeric DNA substrate, the G-overhang (Figure 5). Correct alignment of TERC to the telomere is mediated by boundaries intrinsic to TERC (46). The processive synthesis of G-rich telomeric DNA by telomerase is accomplished by successively repeating the following steps: alignment, nucleotide addition, and translocation. After TERC has been correctly aligned, nucleotides are reversed transcribed using C-rich sequence in the RNA as a template. DNA synthesis beyond the template is prevented by secondary structures present in TERC that act as template boundary regions (47). Once the template boundary is reached, the enzyme translocates so that it is once again aligned with the G-overhang. Like conventional DNA polymerases, telomerase elongates the G-strand in a 5'- 3' manner using the 3' OH for extension (Figure 5).

The biogenesis of telomerase occurs in the nucleolus (48). Movement to the nucleus is enhanced when the enzyme is bound by a signaling protein (14-3-3) (49). Dyskerin binds the H/ACA box in TERC in the nucleolus and is involved in the

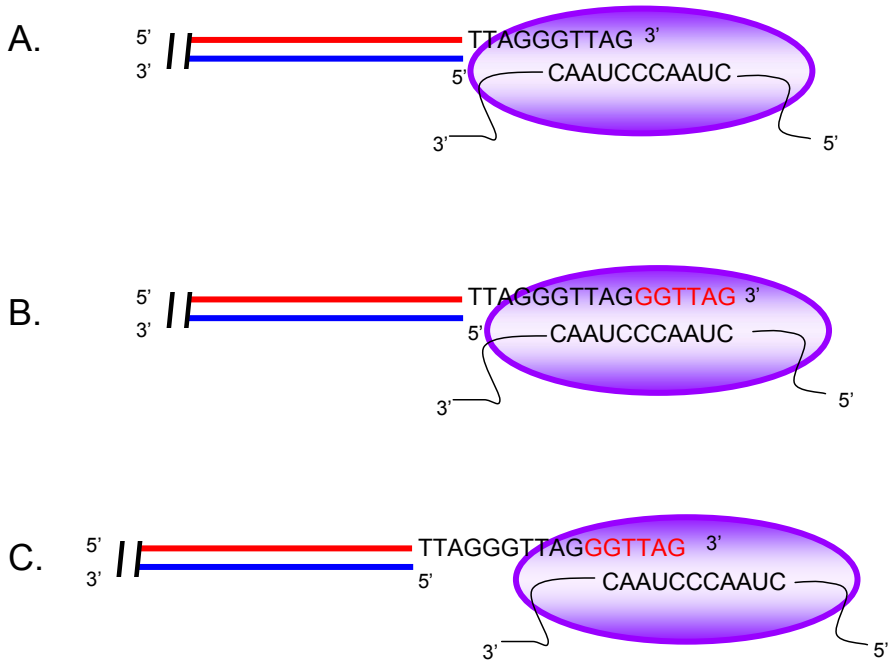

Figure 5. Model for telomere repeat addition by human telomerase.

(A) Alignment. Telomerase is oriented by Watson-Crick base pairing between the RNA template and the 3' terminus of the DNA so that the correct register of telomeric DNA repeats can be added. (B) Extension. Six nucleotides are added (shown in red). (C) Translocation. Once the 5' boundary in the RNA is reached, telomerase translocates so that another round of synthesis can occur. TERT (purple oval) and TERC (wavy line) are shown.

maturation and assembly of small nucleolar RNPs (50). Dyskerin has been implicated in telomere biology in humans as mutations lead to dyskeratosis congenita, a pathology that results in bone marrow failure due to progressive telomere shortening (reviewed in Mason et al. 2005). A role for dyskerin in telomere function has also been observed in *Arabidopsis* (K. Kannan and D. Shippen, in preparation). Interestingly, a recent report shows that the telomerase core complex consists of dimer of dyskerin, TERC and TERT (50). Therefore, dyskerin is thought to be necessary for stabilization of the telomerase RNP *in vivo*.

Telomerase is active in proliferating cells that are dividing, including those in the germline and cancer cells. The enzyme is inactive in normal somatic cells (51,52). Telomerase expression in *Arabidopsis* is similar to that in mammals where meristematic (plant germline) tissue expresses telomerase while vegetative tissues possess little or no telomerase activity (53). TERT is postulated to be the limiting factor for telomerase activity in mammals (54). In contrast to TERT, TERC is ubiquitously expressed (39,55). There are several mechanisms regulating TERT expression and telomerase activity. hTERT is proposed to be positively and negatively regulated by phosphorylation and ubiquitination, respectively (reviewed in (38)). Telomerase expression is repressed by several proteins involved in tumorigenesis, including cMyc (reviewed in (56)). Interestingly, the ciliate *Euplotes* is unique in that it contains three splice variants of TERT that are developmentally regulated (57). Therefore, in Euplotes, another form of telomerase regulation may be accomplished by developmental switches.

Telomerase can also be regulated by localization. Telomerase is sequestered in the nucleolus for most of the cell cycle and moves into the nucleus during late S/G2, a time when telomeres are replicated (58). In addition, telomerase is sequestered to the

nucleolus in response to DNA damage (58). This relocalization is likely to prevent telomerase from inappropriately adding telomere repeats de novo to DSBs, a form of chromosome healing observed in budding yeast (59). Another mode of telomerase regulation is achieved through accessibility to the telomere which can be governed by TBPs (discussed further below).

Telomere length homeostasis

The multiple processes that exist to both positively and negatively regulate telomere length result in telomere length homeostasis (Figure 6). One important way to ensure telomeres are maintained within a specific size range is to control the action of telomerase activity. As discussed above, telomerase is in limiting amounts in most cells. Furthermore, telomerase does not extend all telomeres during each cell cycle and preferentially acts on the shortest telomeres (60). It is hypothesized that telomerase access is governed by accessibility to telomere chromatin, specifically whether the telomere is in a closed or open state. Shorter telomeres are thought to be in a more open conformation (61). In support of this model, telomerase access is regulated in cis by TBPs (reviewed in (56)). A recent report shows that telomeres below wild type length are replicated earlier and these shorter telomeres have less TBPs bound (62). These data suggest that a more open chromatin state promotes telomere replication.

In actively dividing cells, such as those in the germline, the end-replication problem is circumvented by the action of telomerase. As most somatic cells do not express telomerase, telomeres progressively shorten reaching a critical length that elicits cell senescence (63), a process that prevents cells with dysfunctional telomeres

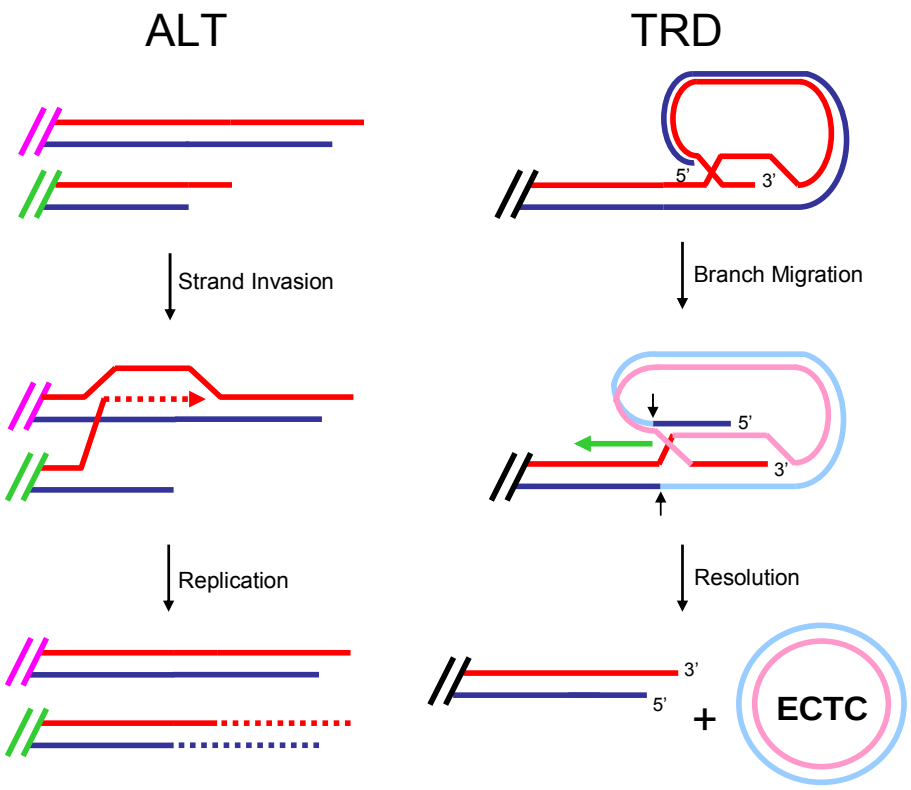

Figure 6. Strategies to maintain telomere homeostasis.

(A) Alternative lengthening of telomeres (ALT). Telomeres are elongated in the absence of telomerase using a form of HR where another chromosome end is used as a substrate for recombination. (B) Telomere rapid deletion (TRD). Telomere tracts are cleaved off in one single step. t-loops undergo branch migration (green arrow) toward the centromere, the structure is resolved (black arrows), resulting in a shortened telomere and an extra chromosomal telomere circle (ECTC). Adapted from dissertation of James M. Watson.

from dividing (see below). Therefore, cell senescence is though to be in place to limit cell division as an anticancer mechanism. A recent study demonstrated that pre-tumor cells that harbor short telomeres induce senescence (64,65). For this reason telomere length is thought to act as a molecular clock for cell division, where each cell is given an appropriate number of telomere repeats to last a lifetime.

In mammalian cells, the amount of telomere shortening observed in telomerase-deficient cells is greater then predicted from the end-replication problem (reviewed in (66)). This finding suggests that telomeres are subjected to additional activities that decrease their length. It is postulated that mammalian telomeres are routinely subjected to nuclease attack (reviewed in (66)). Another mechanism that shortens telomeres is telomere rapid deletion (TRD) (67) (see Figure 6). TRD is recombination-based mechanism observed in both budding yeast and plants that shortens elongated telomeres by bringing them back to wild type length in a single step (68,69). TRD is thought to result in deletion of t-loop sized telomere tracts, when the t-loop is subjected to holliday junction resolvase (see Figure 6).

Telomerase homeostasis also can be achieved in the absence of telomerase. While 95% of cancer cells use telomerase to maintain telomeres, there are examples of certain cancers that almost exclusively use ALT. For example, a majority of osteosarcomas employ ALT to maintain telomeres (70). In mammalian cells, ALT uses telomere tracts of a homologous chromosome as a recombination substrate to elongate telomeres.

Telomeres as nucleoprotein complexes

A functional telomere is a nucleoprotein complex consisting of telomeric DNA and the proteins that specifically bind to double- and-single-strands of telomeric DNA. Double-strand telomere binding proteins (TBPs) contact DNA through a conserved myb-like DNA binding domain (reviewed in (56). Single-strand TBPs use an oligonucleotide/oligosaccharide (OB) fold to directly bind G-overhangs (reviewed in (34)). Single-strand TBPs can also localize to double-strand telomeric DNA by protein-protein interactions with double-strand TBPs (71). In addition to proteins that directly bind telomeric DNA, many proteins contact telomeres via protein-protein interactions, forming a higher order nucleoprotein structure at the chromosome end. As discussed below, TBPs are critical for telomere length regulation, chromosome end protection and other functions ascribed to telomeres.

Double-strand TBPs

In budding yeast, double-strand telomeric DNA is bound by repressor activator protein 1 (Rap1). Rap1 is associated with two additional factors, rap1-interactor factors 1 and 2 (Rif1 and Rif2) (Figure 4). This telomere protein complex functions in negative regulation of telomere length in cis; an increase in the number of Rap1 proteins results in shorter telomeres (72-75). Thus, Rap1 is thought to function as part of a counting mechanism that determines which telomeres require elongation by telomerase (74).

Human telomeres are bound by a core complex of six proteins known as shelterin (76). Shelterin consists of: telomere repeat binding factor 1 (TRF1), telomere repeat binding factor 2 (TRF2), TIN2 (TRF1-interacting nuclear factor 2), Rap1, TPP1 and protection of telomeres 1 (POT1) (Figure 4) (76). Only three shelterin components

make direct contact with telomeric DNA: TRF1, TRF2 and POT1. TRF1 and TRF2 form homodimers to bind double-strand telomere DNA, while single-stranded telomere DNA is bound by POT1. POT1 also associates with the double-strand region of the telomeres via TTP1. TPP1 is a bridging protein that binds TIN2; TIN2 makes contacts with TRF1 and TRF2 (76).

TRF2 acts as a platform for additional proteins to localize to the telomere, and is essential for telomere capping. TRF2 null mutations are lethal (77), but dominant negative mutants of TRF2 can be used to assess the role of TRF2 at telomeres (77). TRF2 dominant-negative mutants that displace TRF2 from the telomere harbor abundant end-to-end fusions containing large tracts of telomeric DNA (2). These uncapped telomeres are recognized as sites of DNA damage as evidenced by the localization of DDR proteins involved in signaling the presence of a DSB. These proteins include γH2AX, 53BP1 and MDC1 (78). A capping function for TRF2 is further supported by studies that show that TRF2 mediates the formation of t-loops (32). TRF2 is thought to bind the double/single-strand junction at the base of the t-loop (32,79). A recent study has shown that a mutant form of TRF2 leads to an increase in TRD (33), highlighting the importance of TRF2 at the t-loop. In addition, it has been reported that TRF2 rapidly localizes to DSBs (80), however, this finding has recently been disputed (81).

TRF1 is a negative regulator of telomere length (82) and this regulation is thought to be achieved through POT1 interaction as the presence of TRF1 increases the accumulation of POT1 on double-strand portions of the telomere (83). POT1 is thought to translocate to the G-overhang where it can negatively regulate telomerase (84). This observation suggests that, similar to Rap1 in yeast, TRF1 acts as a counting

mechanism for telomere length and this message is relayed to the telomere terminus through the localization of POT1 (83).

Multiple putative double-strand TBPs have been reported in plants suggesting functional redundancy (reviewed in (85)). In *Arabidopsis*, these proteins fall into two families, characterized by whether they possess a myb-like domain and an additional myb-extension domain (86). While TRF1 and TRF2 can only form homodimers (reviewed in (76)), the putative *Arabidopsis* TBP family containing the myb and myb-extension domains can form both homodimers and heterodimers as well as bind double-strand telomeric DNA *in vitro* (86). Only two TBPs have been reported to affect telomere length in plants *in vivo* (87,88). A deficiency of *Arabidopsis* telomere binding protein 1 (TBP1) results in telomere lengthening, indicating that AtTBP1 acts as a negative regulator of telomere length (87). Likewise, in tobacco, the double-strand TBP, NgTR1 is a negative regulator of telomere length (88).

The finding that t-loops are present in pea plants (89) implies that this structure will be conserved across all multicellular eukaryotes. Thus, the identification of specific TBPs that function in telomere length regulation and capping in the *Arabidopsis* model will be critical for further developing telomere biology in this system.

Single-strand TBPs

Cdc13 is the best characterized of the single-strand TBPs. It binds G-overhangs in budding yeast and is involved in multiple aspects of telomere maintenance (reviewed in (56)). Three additional proteins, Stn1, Ten1 and Est1 localize to the G-overhang through interactions with Cdc13 (reviewed in (90)). A dynamic interplay exists between these three proteins and is critical for their telomere functions.

Cdc13 acts as a both a positive and negative regulator of telomerase (91). Positive regulation is achieved through direct recruitment of a telomerase component, ever shorter telomeres 1 (Est1) to the telomere (92). Cdc13 also interacts with Polα to coordinate lagging strand synthesis (91). Negative regulation of telomerase by Cdc13 is accomplished through binding of Stn1 to the same site of Cdc13 as Est1 (91). Once telomerase (Est1) is recruited to the telomere via Cdc13, the subsequent coordination of C-strand synthesis that is accomplished by the binding of Stn1 to Cdc13 results in negative regulation of telomerase (91).

POT1 is the single-strand telomere binding protein in fission yeast and higher eukaryotes that is the presumed ortholog of Cdc13 (93). Like Cdc13, hPOT1 is involved in regulation of telomerase access to the telomere (94). *In vitro* data indicate that POT1 binds the extreme 3' terminus of the G-overhang, providing both negative regulation of telomerase, and protecting the ends from nuclease activities (84,95,96). *In vitro* and *in vivo* data also implicate POT1 in positive regulation of telomere length (94,96-98). Another major function of POT1 is in maintenance of the G-overhang and inhibiting a DNA damage response from occurring at telomeres (see below).

Arabidopsis is unusual in that it harbors three POT1 proteins, POT1a, POT1b and POT1c, which appear to have distinct functions. AtPOT1a is a component of the telomerase ribonucleoprotein complex (99), similar to the Est1 component of telomerase in budding yeast. POT1a is required for telomerase activity *in vivo*. While the loss of POT1b does not have an obvious affect on telomeres, *pot1b* dominant-negative mutants exhibit shortened telomeres and severe genome instability (100), implicating POT1b in chromosome end protection. Preliminary data suggest that

POT1c may promote telomerase activity (Y. Surovtseva et al. unpublished data). Altogether, these data suggest that POT1 proteins are rapidly evolving in plants.

Another putative single-strand TBP has been identified in *Arabidopsis* is single-strand telomere binding protein 1 (STEP1). STEP1 localizes to the nucleus and inhibits telomerase activity *in vitro* (101). However, its *in vivo* function has not been described.

Contribution of TBPs to maintenance of G-overhangs

The importance of G-overhangs is demonstrated by several observations. First, in budding yeast, the single-strand TBP, Cdc13 functions in protection of G-overhangs. Deficiency of this protein leads to severe telomere de-regulation where G-overhangs are massively elongated leading to cell cycle arrest (102). Deficiencies in the interacting partners of Cdc13 (Ten1 and Stn1) also result in increased G-overhang signals (102-104). Therefore, G-overhang protection is shared by at least three proteins in budding yeast.

Second, G-overhangs are essential for formation of the protective t-loop structure in all organisms tested (reviewed in (34)). Several studies indicate that exposure of the G-overhang (i.e. unfolding of the t-loop) may act as a red flag that signals telomere dysfunction. When oligonucleotides corresponding to G-overhangs are introduced into cell culture the result is cellular senescence (105). Two reports from the de Lange lab highlight the importance of masking the G-overhang to chromosome end-protection and cell proliferation (2,106). One study showed that exposure of G-overhangs as a consequence of telomere uncapping leads to G-overhang degradation and immediate recruitment of telomeres into an end-joining reaction (2). The second study showed that when the nuclease responsible for removal of G-overhangs cells is

deficient and G-overhangs are intact, telomeres are not subjected to fusions (106). To complement these results, another group found that excess human POT1 protected against the reduction of G-overhang signal experienced as a result of telomere uncapping (107).

Approaches that can precisely determine the terminal sequences of both strands of the telomere tract have demonstrated that telomeres end in a precise sequence (23,108,109). Intriguingly, a study using human cells has shown that this fidelity is lost when cells are deficient in hPOT1, suggesting that POT1 directly binds G-overhangs and restricts the amount of nuclease digestion at telomeres (110). Thus, POT1 directly acts to protect the G-overhang. Together, these data indicate exposure of the G-overhang leads to fusions where removal of the G-overhang is a prerequisite for end-joining.

Finally, it should be noted that a role for POT1 proteins in G-overhang maintenance is not consistent across evolution. For example, G-overhang signals are increased in response to loss of POT1 in chicken cells, but are reduced in human cells (110-112). In mouse cells POT1 deficiency results in observable changes in the G-overhang signal intensity, however the role of POT1 in G-overhang maintenance is unknown due to two conflicting reports (113,114).

In addition to single-strand TBPs, there are a few examples where loss of double-strand TBPs affects G-overhangs. Disruption of the double-strand TBP Taz1 in *S. pombe* leads to severely elongated G-overhangs that become entangled and trigger end-to-end fusions harboring large telomere tracts (115). In addition, the loss of KU, another protein that localizes to double-strand telomeric DNA, results in elongated G-overhangs in plants and budding yeast (116,117). Finally, loss of Rad51, a protein

involved in homologous recombination, results in increased G-overhang signals in chicken cells (118).

In summary, the G-overhang is maintained by a multitude of proteins that govern various aspects of telomere structure and function. These functions include physically protecting the G-overhang, preventing nuclease degradation of the C-strand and coordinating lagging strand synthesis. It is likely that additional factors that contribute to maintenance of the G-overhang will be uncovered in the future. *In Chapter IV, I examine the status of the G-overhang in Arabidopsis plants with mutations in different telomere-related genes.*

The DNA damage response

In this section, I introduce the fundamental properties of the DNA damage response (DDR) and the proteins involved in sensing and repairing DNA damage. The basic roles of DDR proteins will be introduced to illustrate the relationship between these proteins and telomeres.

DNA damage sensing, signaling and repair are achieved via interaction of multiple proteins and pathways. In response to a DSB a cascade of responses occur that leads to recruitment of factors that amplify and transduce the DNA damage signal in order to repair the break and arrest the cell cycle. The MRN-X complex is thought to be the first protein to bind a DSB. In this capacity, MRN-X acts as a mediator of the DDR, recruiting ATM to the DSB. ATM or DNA-PKcs can phosphorylate H2AX (γH2AX) forming foci that mark the DSB (reviewed in (119). Accumulation of γH2AX is necessary for recruitment and maintenance of mediators of the DDR including 53BP1, BRCA1, MDC1 and MRN complex (reviewed in (119)).

DDR proteins

Two of the central regulators of the DDR are ATM and ATR. ATM and ATR are members of the PI3-related protein kinase (PIKK) family that function in DNA damage signaling by relaying and amplifying the DDR. ATM is predominantly involved in sensing DSBs, while ATR responds to single-strand breaks (SSBs), mainly from stalled replication forks. Upon encountering a SSB/DSB, ATM/ATR activates, through phosphorylation, proteins involved in the DDR including Mre11 and Nbs1 (78,120). Mre11 is thought to localize to a DSB prior to ATM, while Nbs1 acts downstream of ATM to assist with cell cycle control (121). Recent studies indicate ATM and Nbs1 relax the chromatin structure, leading to recruitment of downstream components of DSB repair including XRCC4 (122). ATR can substitute for ATM in ATM-deficient cells indicating overlap between the two pathways (reviewed in (119)).

DSBs are repaired by HR or NHEJ (reviewed in (119)). HR is confined to S and G2 phases of the cell cycle and relies on long stretches of homology, easily found in a homologous chromosome or sister chromatid. In contrast, NHEJ does not require homology and is a more error-prone process. NHEJ predominates during the G1 phase of the cell cycle. HR is primarily utilized by lower eukaryotes, while NHEJ is preferred in higher eukaryotes, and hence will be discussed in more detail below.

The core proteins of NHEJ are DNA Protein Kinase (DNA-PK) and XRCC4/DNA ligase 4 (LIG4). DNA-PK is comprised of KU (a heterodimer consisting of KU70 and KU80), and the catalytic subunit of DNA Protein Kinase, (DNA-PKcs). Figure 7 outlines

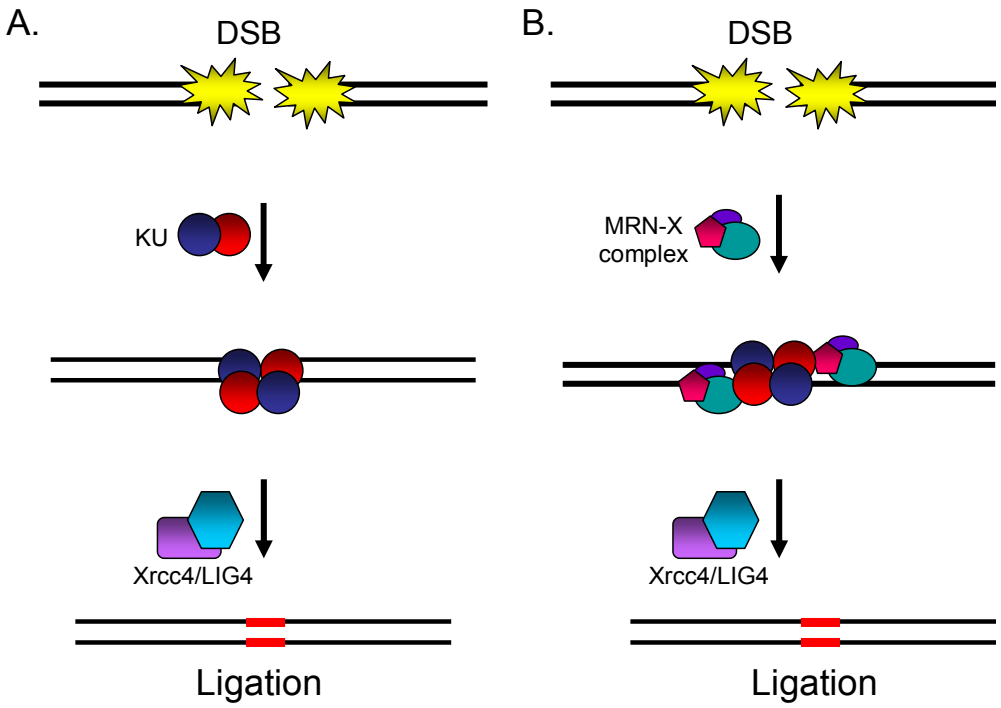

Figure 7. Non-homologous end-joining (NHEJ) double-strand break repair.

(A) Core components of NHEJ in higher eukaryotes. DSBs are bound by the Ku heterodimer which protects the ends and juxtaposes them for repair. The DSB are covalently joined by the action of DNA Ligase IV, where it is stimulated by XRCC4. (B) NHEJ end-joining in budding yeast. Budding yeast NHEJ is postulated to involve the MRX complex, which appears to aid in processing ends prior to end-joining. Ku is thought to be located closest to the DSB (reviewed in 144).

the major steps in NHEJ. In NHEJ, DSBs are initially bound by the KU heterodimer, which protects DSBs from nuclease digestion and facilitates alignment of the DSBs in juxtaposition. Once KU is bound, DNA-PKcs is recruited to the DSB. The exact contribution of DNA-PKcs to NHEJ is unclear, but current data suggest that its phosphorylation and scaffolding capabilities are important (123,124). XRCC4/LIG4 is recruited to the DSB and covalently joins the two broken ends through the ligase action of LIG4. The presence of XRRC4 stimulates the activity of LIG4 (125).

KU was first isolated from a patient with polymyositis scleroderma overlap syndrome (126) and has been well characterized with respect to its role in antibody diversity via VDJ recombination (127). *In vitro* assays show that KU can bind non-specifically to multiple types of DNA ends including blunt ends containing a 3' or 5' overhang, and hairpin structures (128,129). Multiple KU heterodimers can bind a single DSB (129). The KU crystal structure reveals that KU possesses a three domain topology (130). The C-terminal domain of KU is the site of the interaction between KU70 and KU80. This domain cradles the DNA, through non-specific contacts. The α/β barrel domain contributes minimally to heterodimerization and does not bind DNA, but is speculated to serve as a platform for binding of other proteins (130). In addition to its role in DNA repair, KU also functions in DNA replication, transcriptional regulation, inhibition of apoptosis and cellular adhesion (reviewed in (3)). These roles will not be discussed further here.

The presence of DNA-PKcs is restricted to vertebrates and likely reflects an essential function for DNA-PKcs in VDJ recombination, a vertebrate-specific process (124). Like ATM and ATR, DNA-PKcs is a Ser/Thr kinase and a member of the PIKK family. DNA-PKcs can undergo autophosphorylation and can phosphorylate other

proteins of the NHEJ pathway including KU and XRCC4 (124). Once DNA-PKcs binds a DSB, KU translocates inward so that DNA-PKcs protects the broken ends until they are ligated (reviewed in (131)). DNA-PKcs acts as a molecular scaffold facilitating recruitment of proteins including LIG4 to the DSB (reviewed in (124)). Autophosphorylation of DNA-PKcs leads to a conformational change that frees ends for the LIG4 complex to bind the DSB (132). DSBs can be joined in the absence of DNA-PKcs, suggesting that other proteins can substitute for DNA-PKcs in DSB repair (133).

The XRCC4/LIG4 complex is the most downstream component of the NHEJ pathway and acts to covalently join the two broken ends. In addition to stabilizing LIG4, XRCC4 acts to stimulate ligase activity (125). LIG4 is an ATP-dependent DNA ligase containing a conserved lysine residue that is absolutely essential for ligation (134). LIG4 was previously thought to simultaneously catalyze the covalent joining of both DSBs. However, recent studies have shown that LIG4 ligates each DNA end separately (135). This finding is interesting since recent evidence demonstrates single-strand DNA ligases can join DSBs in the absence of LIG4 (136-138).

The canonical NHEJ is not the only mechanism for end-joining. Backup DSB repair pathways have been described. In humans, the absence of KU and/or LIG4 reduces the efficiency of end-joining by ~ 10 fold, but does not abolish it (139-143). Furthermore, in the absence of KU and LIG4, DSBs can be joined by components of the base excision repair (BER) pathway (136-138). Therefore, alternative proteins capable of similar functions can substitute in DSB repair. Since DNA repair proteins from independent pathways can substitute in the absence of the predominant proteins, these data strongly underscore the importance of repairing DSBs.

One set of proteins that appears to play a key role in NHEJ in lower eukaryotes, aside from KU and LIG4, is the Mre11/Rad50/Nbs1-Xrs2 (MRN-X) complex (reviewed in (144)). MRN-X is thought to act as an alignment factor for DSBs. In budding yeast the Nbs1 component is substituted by the Xrs2 protein. The MRN-X complex can also function in the HR pathway and is essential in meiosis (120). Similar to KU, the MRN-X complex binds DSBs, but it employs a different DNA-binding strategy. A functional unit of the MRN-X complex consists of one Nbs1/Xrs2, and two Mre11 and Rad50 molecules. Mre11 makes direct contact with the DSB and is flanked by Rad50. Rad50 dimerizes forming a hinge-like structure holding together the two DSBs in close proximity (145). *In vitro* data show that the nuclease activity of Mre11 digests DNA ends to expose tracts of microhomology, thereby facilitating alignment and annealing of the two broken ends (146). This microhomology-mediated end-joining (MMEJ) has also been observed *in vivo* in budding yeast deficient for Ku (147). *In Chapter II, I present the first in vivo evidence for MMEJ in higher eukaryotes.*

A transient DDR is observed at wild type telomeres

In addition to a role in DSB repair, proteins of the DDR are necessary for the formation of the higher order t-loop structure. However, it is not fully understood why telomeres are prevented from recruitment into end-to-end fusions by DDR proteins. One possibility is that TBPs keep DDR proteins at bay. This could be accomplished by blocking an active site in the DDR protein. In support of this idea, TRF2 specifically interacts with ATM in a way that blocks the kinase domain (148).

Several studies highlight the importance of the localization of DDR components to telomeres (30,149-151). Like KU, the MRN-X complex localizes to telomeric DNA in

most organisms (150,152-154). Studies in yeast show this is a transient, cell-cycle regulated localization (150). Interestingly, in human cells Mre11 and Rad50 are present at telomeres throughout the cell cycle, while Nbs1 is recruited only during S phase (154). In human cells MRN-X, like KU (155), contacts telomeric DNA through TRF2 (154). These reports show that DDR proteins are localized to telomeres in a cell cycle-dependent manner.

In budding yeast, Takata et al. has shown that recruitment of the MRN-X complex coincides with telomere replication (150). These authors also found that MRN-X localization is necessary for recruitment of TBPs, including Cdc13, a protein that subsequently recruits telomerase to the telomere (149,150). In addition, ATM and ATR were found to be reciprocally regulated in a mutually exclusive manner at the telomere (149). Specifically, ATM is localized to telomeres throughout much of the cell cycle but is replaced by ATR in S phase, a time when the telomere is undergoing structural modifications (i.e. G-overhang formation) (149).

In human cells, wild type telomeres elicit two transient DDR signals correlating with replication through telomeres and formation of a t-loop structure (30,149,151). Jan Karlseder's lab used ChIP to determine which factors localize to telomeres in a cell cycle-dependent manner (30,149,151). The first DDR factors are recruited in response to replication fork stalling (as highly repetitive telomeric tracts are thought to present a problem for replication machinery). These proteins are MRN-X and ATM/ATR. In the second response, Mre11 and ATM are brought to telomeres, and this recruitment coincides with a reduction of POT1. Since the loss of Mre11 or ATM results in end-to-end fusions, it is proposed that these proteins promote the formation of a higher order structure (30,149,151). Importantly, these studies demonstrate that the DDR is

localized to telomeres and is not propagated to the level of cell-cycle checkpoint activation (30). This observation may explain why telomeres are not subjected to end-to-end fusions.

Because these experiments were performed in divergent organisms, the transient DDR appears to be conserved and thus may be necessary for significant architectural transitions at telomeres (30,149-151). Consistent with this prediction, the Karlseder lab demonstrated that telomeric DNA is exposed (i.e. t-loop unfolded) during late G2, a time after telomeres are replicated (30). These observations underscore the relationship between telomere structure and function and proteins of the DDR.

The role of DDR proteins in telomere maintenance

Proteins of the DDR function in various aspects of telomere maintenance. DDR proteins are involved in telomere length regulation and maintenance of the G-overhang. In some instances, these proteins make direct contact with telomerase (reviewed in (3)).

ATM/ATR

The master regulators of the DDR also contribute to telomere biology where ATM and ATR localize to the telomere and function in telomere length maintenance. Mutations in ATM in human and yeast cells result in telomere shortening (3,156,157). ATM may function in telomere length maintenance by way of recruitment of telomerase (158). Interestingly, in *Arabidopsis*, recent studies of *atm tert* mutants indicate that ATM may be involved in monitoring telomere length on homologous ends in *Arabidopsis* (Vespa et al. submitted). ATR also plays a role in telomere maintenance in *Arabidopsis* as *atr tert*

mutants results in an increased rate of telomere shortening relative to *tert* mutants alone (159).

KU

One of the major DDR proteins that contribute to telomere length maintenance is KU (reviewed in (3)). KU negatively regulates telomere length in lower eukaryotes, but positively regulates telomere length in plants (reviewed in (3)). Perhaps the most thorough characterization of KU has come through the dissection of the gene in budding yeast. In yeast, KU is involved in multiple aspects of telomere biology (160). A few of these contributions include tethering of the telomere to the nuclear periphery and a role in the telomere position effect (TPE) (161). KU functions in TPE through interactions with the silent information regulator (SIR) proteins. SIR proteins mediate a chromatin configuration that acts to prevent transcription of proximal genes (162). This chromatin configuration is achieved by KU acting as a lynchpin to bring two Sir proteins, that are normally far apart, into close contact so that the telomeric fold-back structure is achieved (36).

KU also physically interacts with telomerase in budding yeast and humans (163-166). In budding yeast, KU binds TERC and functions in positive regulation of telomere length (165), while in humans KU binds TERT (164,165). Interestingly, multiple functions of KU in telomere biology and the DNA damage response can be attributed to specific domains in KU (160,167). A recent paper from Alison Bertuch's lab has provided some insight as to how KU can be involved in these multiple, apparently conflicting, functions (167). The authors mapped the locations of key residues in KU70 and KU80 that are specific to telomere versus DNA repair functions. They present a

two-face model in which the residues that face outward toward the chromosome terminus are involved in DNA repair, while residues that face inward give rise to specific telomere functions (Ribes-Zamora et al. 2007). Furthermore, although a clear role for KU in telomerase regulation has not been determined in human cells, it is likely to be reminiscent of that in budding yeast as the key residues are conserved (167).

Studies in *Arabidopsis* and yeast show a loss of KU results in increased G-overhang signals (116,117). While the status of the G-overhang throughout the cell-cycle is not known in *Arabidopsis*, KU deletion in budding yeast leads to an increase in G-overhang signals throughout the cell-cycle (116). This finding is in contrast to telomerase-dependent increase in G-overhang signals normally only observed during S-phase of wild type yeast cells (26). Intriguingly, a function for KU in G-overhang maintenance has not been observed in vertebrate cells (118,168), suggesting that KU's functions in telomere biology are not universally conserved.

DNA-PKcs

A role for DNA-PKcs in telomere length regulation in vertebrates is observed in some cases. However, this role differs from that of KU in mouse cells. While a loss of KU in a telomerase deficient mouse background does not lead to an increase in telomere shortening, double *dna-pkcs/tert* mouse cells experience accelerated telomere shortening (169). These results indicate that KU and DNA-PKcs make distinct contributions to telomere length maintenance.

MRN-X complex

Like KU, the MRN-X complex contributes to bulk telomere length regulation and G-overhang maintenance. Telomere shortening occurs in budding and fission yeast deficient for Mre11 or Rad50 (153,170-174). Similarly, in fission yeast the loss of Nbs1 leads to a modest decrease in telomere length (175).

Mre11 has been implicated in the formation of G-overhangs due to its nuclease activity. Although Mre11 possesses 3' to 5' exonuclease capabilities (146), *in vivo* evidence indicates that Mre11 resects DSBs in the 5' to 3' direction, the opposite polarity necessary to process G-overhangs (176,177). It is possible that Mre11 modulates the recruitment of additional, unknown nuclease(s) to process the G-overhang. Budding yeast cells deficient for Mre11 do not possess the increased G-overhang signals normally present in S-phase (14), indicating that KU and Mre11 may be playing opposing roles in regulating G-overhangs. A function for Mre11 in G-overhang maintenance, together with the observation that Mre11 is recruited to telomeres in a cell-cycle-dependent manner (150), suggest that Mre11 prepares the G-overhang for elongation by telomerase and then facilitates proper telomere folding after replication is complete.

Mre11 is also implicated in G-overhang maintenance in fission yeast (178). This role is revealed in the context of a deficiency of the double-strand TBP protein Taz1. Fission yeast mutant for *taz1*$^{-/-}$ possess grossly elongated G-overhangs (179). The increase in G-overhang signals is thought to be promoted by Mre11 (178).

The MRN-X complex is also implicated in telomere biology in higher eukaryotes. In *Arabidopsis*, two groups report no change in telomere length in Mre11 mutants (180,181), while another found an increase in telomere length (182). Similar to budding

yeast, a deficiency in Nbs1 in human cells results in shortened telomeres (183). The MRN-X complex also appears to function in maintenance of the G-overhang in human cells. In particular, a reduction of Mre11 leads to decreased G-overhang signals, but only in the presence of telomerase (28). This observation supports a role for Mre11 in substrate preparation for telomerase binding.

In conclusion, a deficiency of DDR proteins or TBPs can lead to alterations in the status of the G-overhang, arguing that G-overhangs are maintained by the concerted action of these two types of proteins. It is likely that DNA repair proteins "prepare" the G-overhang so that the telomere tract is able to assume the proper protective conformation. Thus, the major function of TBPs may be to facilitate this conformational change and inhibit telomere end-joining by ensuring a full-blown DDR is not elicited.

The role of DNA damage proteins in telomere dysfunction

Although a primary function of telomeres is to block a DDR, there are three cases where the DDR is not held at bay: 1) when telomeres are uncapped; 2) when telomeres are critically shortened; and 3) when DDR proteins are removed from telomeres. In all instances, telomeres are recognized as sites of DNA damage as evidenced by the localization of γH2AX and 53BP1(1,78).

Efficient telomere maintenance by telomerase is the first line of defense against telomere dysfunction. In all organisms, the absence of telomerase results in progressive telomere shortening with each cell division (reviewed in (184). Telomeres eventually reach a critical length where they are perceived as DSBs and ultimately recruited into end-to-end fusions. Studies in mammalian systems show that the

shortest telomeres in a population are most often involved in fusions (185,186). In *Arabidopsis*, as in mammalian cells, loss of telomerase results in progressive telomere shortening accompanied by an increasing incidence of anaphase bridges. Most telomerase-deficient plants reach the terminal phenotype (arrested in vegetative growth and sterile) by the eighth generation of this mutant. In this stage up to half of anaphases in dividing cells are involved in bridges (187). *In Chapter II, I define the shortest functional telomere in late generation tert and tert ku70 mutants and in Chapter III I define a transitional telomere length that marks the onset of telomere dysfunction in Arabidopsis.*

In contrast to a gradual onset of telomere dysfunction by progressive loss of telomeric DNA due to telomerase inactivation, more pronounced chromosome end deprotection can be observed in response to deficiency of TBPs (as described above) or to loss of function of telomere-bound DDR proteins.

Several NHEJ proteins are required for chromosome end protection. ATM and ATR function in protection of functional telomeres from fusion (188-191). The loss of ATM in budding yeast results in telomere fusions and a synergistic increase in fusions is observed in a telomerase background (188,191). This finding indicates that ATM modulates telomere capping. In *Arabidopsis* and mice, a deficiency in ATM in a telomerase background leads to an abrupt and early onset of the terminal phenotype (159,192), although bulk telomeres do not shorten faster. However, recent studies in *Arabidopsis* suggest that individual telomere tracts may be subjected to increased TRD in *atm tert* mutants, giving rise to critically shortened telomeres that promote genome instability (Vespa et al. submitted). A loss in ATR alone does lead to end-to-end fusions, but double *atr* and *atm* mutants exhibit a low level of telomere fusions (159).

Moreover, the combined loss of ATR and telomerase results in a greatly accelerated rate of telomere shortening (Vespa et al. 2005).

Mice deficient in KU exhibit telomere end-to-end fusions (193,194). Although a direct role of KU in telomere capping has not been observed in other model systems (reviewed in (184), KU is necessary for chromosome end protection in the context of a telomerase deficiency in fission yeast and in *Arabidopsis* (195,196). In these systems, *tert ku70* mutants exhibit end-to-end fusions and accelerated telomere shortening, indicating that the absence of telomerase and/or shortened telomeres exacerbates the *ku* phenotype.

Similar to KU, DNA-PKcs is involved in telomere capping in vertebrates; loss of DNA-PKcs results in telomere end-to-end fusions (169,197-199). Curiously, studies in mice demonstrate that *dna-pkcs tert* mutants exhibit accelerated telomere shortening, while *ku80 tert* mutants do not (198). Therefore, the role for DNA-PKcs in telomere biology is distinct from its function in NHEJ. The kinase activity of DNA-PKcs is required for telomere end-to-end fusions (200), but the exact contribution of this enzymatic activity is unknown. Some insight has been reported by Bailey et al. who reported that the loss of kinase activity results specifically in chromatid-type of fusions (201). This finding indicates that end-joining events occur after DNA replication. Autophosphorylation of DNA-PKcs facilitates the dissociation of DNA-PKcs from DNA (132). Therefore, if autophosphorylation were impaired, DNA-PKcs may become more tightly bound to the telomere and impede access of factors necessary to process telomeres for proper capping.

Mechanisms of joining dysfunctional telomeres

Since telomeres resemble a DSB, the formation of a higher-order structure at the chromosome end acts to hide telomeres from a DDR. However, when this structure is compromised, the result is telomere dysfunction and telomeres are recruited into an end-joining reaction. While some DDR proteins contribute to proper telomere capping and telomere length maintenance, they are also instrumental in facilitating end-joining reactions involving dysfunctional telomeres. Interestingly, the requirement for particular DDR proteins in telomere end-joining reactions is variable amongst different organisms. In addition, telomere end-joining reactions within a particular organism may be mediated by different proteins depending on the nature of the dysfunction. Since telomeres are comprised of inverted repeats and homology can not be used, it is reasonable to expect that dysfunctional telomeres are joined by the NHEJ pathway.

In human cells the fusion of uncapped telomeres that arise as a consequence of TRF2 mutation is dependent on LIG4 (2). In contrast, telomere dysfunction that occurs from progressive telomere shortening through a telomerase deficiency results in telomere fusions that are LIG4-independent (202). One explanation for these conflicting findings is that the mechanism of DNA repair depends on the mode of telomere dysfunction. Since uncapped telomeres and critically shortened telomeres both elicit a DDR (1,2), the choice of mechanism used to join chromosome ends is not due to a failure to elicit a DDR. It has been speculated that uncapped telomeres may result in an altered chromatin structure which is recognized by different repair machinery than eroded telomeres (202). Alternatively, uncapped telomeres that are still long may retain TBPs that function in inhibiting particular end-joining pathways.

Arabidopsis as a model organism

Arabidopsis thaliana is fast emerging as a desirable model organism to study telomere biology (reviewed in (203)). Its small genome size and readily available mutants make it an attractive genetically-tractable organism. Double and triple mutants can easily be generated by simple genetic crosses. Furthermore, due to the high tolerance of plants to genome instability, many mutations in DDR proteins and telomere-related genes that are lethal in mammals are viable in *Arabidopsis*.

Telomere tracts in *Arabidopsis* are much shorter than in mammals and range from 2- 5 kb in length, making them amenable to standard techniques for monitoring telomere dynamics. In contrast to most other model organisms, *Arabidopsis* harbors unique subtelomeric sequences on a majority (8/10) of chromosomes ends. This allows one to precisely measure the dynamics of a particular telomere tract, including monitoring when it is recruited into an end-to-end fusion.

Many DDR proteins that are present in humans are conserved in *Arabidopsis*. Thus, *Arabidopsis* has been utilized to study fundamental aspects of DNA repair in higher eukaryotes (reviewed in (204). DSB repair is largely studied using plasmid rejoining assays, and the first report of such an assay was in tobacco (205). Through the use of these assays, it was determined that *Arabidopsis* prefers NHEJ over HR, similar to other higher eukaryotes (reviewed in (206)). Since *Arabidopsis* is highly tolerant to genome instability, this makes it an ideal system to study DSB repair. This advantageous characteristic is illustrated well in late generation *tert* mutants, as plants can survive for up to ten generations in the absence of telomerase, even though up to half of their chromosomes are involved in end-to-end fusions (187).

Dissertation overview

In Chapter II, I will discuss how dysfunctional telomeres are recruited into end-to-end fusions in *Arabidopsis*. I report the isolation and characterization of end-to-end chromosome fusion junctions. I uncovered a hierarchy of three end-joining pathways in *Arabidopsis*: KU-dependent, KU-independent and KU-Mre11-independent. These data provide the first evidence for microhomology-mediated end-joining in a higher eukaryote. Finally, I showed that the shortest functional telomere length in *Arabidopsis* is 300 bp, approximately the size of a yeast telomere.

In Chapter III, I show that telomere fusions are observed in the absence of KU and LIG4. I demonstrate that end-to-end chromosome fusions occur at a lower frequency in the absence of KU and LIG4 and that these fusion events are mechanistically distinct form KU-independent NHEJ and canonical NHEJ. Furthermore, I provide evidence of a novel transition point for telomeres. I found that the onset of telomere fusions occurs once a telomere reaches ~ 1 kb. However, since only a small fraction of telomeres engage in end-to-end fusions, 1 kb appears to represent a length at which telomeres become transiently uncapped. Thus, 1 kb and 300 bp represent key structural and functional transitions for *Arabidopsis* telomeres.

Finally, in Chapter IV, I discuss the development and optimization of assays to detect G-overhangs at *Arabidopsis* telomeres. I was successful in optimizing the in-gel hybridization technique to determine bulk G-overhang signals. My data indicate that *Arabidopsis* POT proteins play modest, but distinct roles in maintenance of the G-overhang. The most profound results were obtained with *cit1* mutants where G-overhang signals that were up to ten-fold higher than wild type. These data strongly implicate *cit1* in protection of the C-strand.

Altogether my data provide new insight to *Arabidopsis* telomere structure and function and pave the way for further development of this model system.

CHAPTER II

MOLECULAR ANALYSIS OF TELOMERE FUSIONS IN *Arabidopsis* REVEALS MULTIPLE PATHWAYS FOR CHROMOSOME END-JOINING*

Summary

End-to-end fusion of critically shortened telomeres in higher eukaryotes is presumed to be mediated by non-homologous end-joining (NHEJ). Here we describe two PCR-based methods to monitor telomere length and examine the fate of dysfunctional telomeres in *Arabidopsis* lacking the catalytic subunit of telomerase (TERT) and the DNA repair proteins KU70 and Mre11. PETRA (Primer Extension Telomere Repeat Amplification) relies on the presence of an intact G-overhang, and thus measures functional telomere length. The minimum functional telomere length detected was ~300-400bp. PCR amplification and sequence analysis of chromosome fusion junctions revealed exonucleolytic digestion of dysfunctional ends prior to fusion. In *ku70 tert*

---

*Reprinted with permission from Heacock, M., Spangler, E., Riha, K., Puizina, J., and Shippen, D.E. 2004. Molecular analysis of telomere fusions in *Arabidopsis*: multiple pathways for chromosome end-joining. *EMBO J* **23**, 2304-2313.

mutants, there was a greater incidence of microhomology at the fusion junction than in *tert* mutants. In triple *ku70 tert mre11* mutants chromosome fusions were still detected, but microhomology at the junction was no longer favored. These data indicate that both KU70 and Mre11 contribute to fusion of critically shortened telomeres in higher eukaryotes. Furthermore, *Arabidopsis* processes critically shortened telomeres as double-strand breaks, using a variety of end-joining pathways.

Introduction

It is essential that cells have an effective mechanism to differentiate telomeres from DNA double-strand breaks. Proper telomere maintenance requires the functional elements of the telomere itself, as well as recognition by systems that would otherwise signal the presence of DNA damage. Telomeres have a distinctive nucleoprotein structure characterized by a G-rich repetitive DNA sequence ending in a 3' single-strand overhang, which is thought to assume a complex secondary structure (t-loop) to sequester the chromosome terminus in a sheltered position (34). Specific DNA binding proteins recognize and associate with either double-strand or single-strand telomeric repeat sequences providing further protection for the terminus.

One function of the telomere is to prevent end-to-end chromosome fusion. Fusions can be induced through perturbation of the telomeric DNA sequence or depletion of telomere-associated proteins, such that the structure of the telomere is fundamentally altered (184). Telomerase activity is necessary for telomere maintenance. In addition, the appropriate complement of telomere-associated proteins must be present to assure that the telomere assumes a fully capped configuration, and is excluded from processing by DNA damage repair systems.

End-to-end chromosome fusion is a common outcome in cells with dysfunctional telomeres, suggesting that uncapped chromosome ends are often recognized and processed as DNA double strand breaks (184). In both mammals and yeast, fusion of chromosomes with critically shortened telomeres requires components of the NHEJ pathway. Moreover, several DNA repair proteins, including KU and the MRX complex (Mre11, Rad50 and Xrs2/Nbs1), localize to telomeres in wild type cells, and are essential for recognition or maintenance of the telomere (184).

The precise role of DNA repair proteins at the telomere is unclear, and varies between different species. For example, loss of KU function via disruption of the *KU70* or *KU80* genes leads to altered telomere tract extension in *Arabidopsis,* but chromosome fusion is not observed (196,207,208). In contrast, telomere length is not dramatically altered in mammalian cells in the absence of KU, but end-to-end chromosome fusions are formed, consistent with uncapping of the telomere (168,197). Fusion of critically shortened telomeres proceeds efficiently without KU70 in *Arabidopsis* (117), but requires KU function in mammalian cells (194). Fusion of uncapped telomeres can also occur in the absence of conventional KU-dependent NHEJ in yeast (195,209). Together, these observations imply that dysfunctional telomeres can be joined by alternative NHEJ pathways. Examination of DNA double-strand break repair in yeast lacking KU demonstrated a distinct pathway of microhomology-mediated end joining (MMEJ) that requires the MRX complex (147). Although the biochemical properties of the mammalian Mre11 protein indicate that it has the potential to function in NHEJ (146,210), this hypothesis has not been tested *in vivo*, as null mutations involving the MRX complex are lethal (211).

Arabidopsis is emerging as an attractive higher eukaryotic model for telomere biology because it displays a remarkable tolerance to telomere dysfunction and genome instability. Progressive telomere shortening in telomerase mutants ultimately leads to sterility and massive genome instability. However, terminal generation plants are viable despite end-to-end fusion of up to half of the chromosomes (117,187). Thus, *Arabidopsis* provides a rich source of material to examine the outcome of chromosome fusion at the molecular level. In addition, the DNA sequences immediately adjacent to the telomeric repeats in *Arabidopsis* are not highly repetitive, and regions of unique sequence are present near most chromosome ends. Hence, the *Arabidopsis* genome is well suited to the independent analysis of telomeres from various chromosome arms, and offers the potential to examine the fate of individual telomeres in different genetic settings.

Here we report the development of two PCR-based methods that exploit the unique subtelomeric DNA sequences at *Arabidopsis* telomeres to precisely measure the length of the telomeric tract of individual chromosomes and to amplify and characterize chromosome fusion junctions arising from telomere dysfunction. We show that the minimum functional telomere length in *Arabidopsis* is 300-400bp. Sequence analysis reveals that when KU is functional chromosome fusion junctions formed between critically shortened telomeres display hallmarks of conventional NHEJ with evidence of exonucleolytic processing and frequent small insertions (139,212). However, when critically shortened telomeres associate in the absence of KU70 the architecture of the fusion joint is altered, and a more homology-driven mechanism mediates fusion. Remarkably, fusion of critically shortened telomeres still occurs in triple *ku70 tert mre11* mutants, but the junctions display a significant decrease in microhomology. These data

not only provide *in vivo* evidence that Mre11 contributes to MMEJ reactions in higher eukaryotes, but also illustrate the complexity of NHEJ pathways.

Materials and methods

Plant growth and DNA preparation

The generation of *A. thaliana tert* and *ku70 tert* lines was described previously (117,187). Plants with a T-DNA insertion in the *MRE11* gene were obtained from the Salk collection (line 054418) (213). Triple *tert ku70 mre11* lines were created via the crossing scheme outlined in the figure on page 69. *A. thaliana* plants were grown at 23°C in an environmental growth chamber with a 16/8 hr light/dark photoperiod. DNA was extracted from whole plants 4-5 weeks after germination as previously described (196). DNA concentration was determined by agarose gel electrophoresis, using lambda DNA digested with HindIII as a standard.

Subtelomeric DNA sequences and chromosome-specific PCR primers

Terminal DNA sequences for seven *Arabidopsis* chromosome arms were identified in GenBank (1R, AC074299; 1L, AC007323 and AC074298; 2R, AC006072; 3L, AC067753; 3R, AL732522; 4R, AL035708 and Z12169; 5L, AB033277; 5R, AB033278). Unique subtelomeric primers directed 5' to 3' toward the telomeric repeat were designed for each, as indicated below.

Determination of telomere length

For PETRA, primer extension was performed using from a primer bound to the telomeric G-overhang (PETRA-T 5'-

CTCTAGACTGTGAGACTTGGACTACCCTAAACCCT-3'), followed by PCR amplification using a chromosome-specific subtelomeric primer (1R 5'-CTATTGCCAGAACCTTGATATTCAT-3'; 1L 5'-AGGACCATCCCATATCATTGAGAGA-3'; 2R 5'-CAACATGGCCCATTTAAGATTGAACGGG-3'; 3R 5'-CTGTTCTTGGAGCAAGTGACTGTGA-3'; 3L 5'-CATAATTCTCACAGCAGCACCGTAGA-3'; 4R 5'-TGGGTGATTGTCATGCTACATGGTA -3'; 5R 5'-CAGGACGTGTGAAACAGAAACTACA-3'; 5L 5'-AGGTAGAGTGAACCTAACACTTGGA-3') and second primer (PETRA-A 5'-CTCTAGACTGTGAGACTTGGACTAC-3') that recognizes sequence complementary to the 5' non-telomeric sequence present on PETRA-T. Primer extension reactions (50 µl) included 1X DNA PolI buffer (Promega), 250 µM dNTPs, 0.2 µM PETRA-T primer, 500ng genomic DNA and 9 units DNA PolI (Promega). The reaction was incubated at 16°C for 1 hr, and then overnight at 25°C. The next day DNA was recovered by ethanol precipitation, and suspended in 20 µl water. Each chromosome-specific PCR reaction (50 µl) included 1X ExTaq buffer (TaKaRa), 200 µM dNTPs, 0.4 µM PETRA-A primer, 0.4 µM subtelomeric primer, 1/10 of the DNA recovered from the primer extension, and 2 units ExTaq (TaKaRa). Samples were incubated at 96°C for 5 min, followed by 20-25 cycles of: 94°C for 15 sec, 60°C for 30 sec and 72°C for 2 min, with a final incubation at 72°C for 10 min. A 15 µl aliquot of the PCR products was separated by electrophoresis through a 0.8-1% agarose gel, and transferred to a nylon membrane. Membranes were probed with a ^{32}P end-labeled telomeric oligonucleotide $(T_3AG_3)_4$. Hybridization was performed at 55°C O/N, in a buffer consisting of 0.25 M sodium phosphate Buffer, pH 7.5, 7% SDS, and 1 mg/ml BSA. Filters were washed in 2XSSC/0.1% SDS and

0.2XSSC/0.1% SDS, twice each for 10 min at 55°C. Hybridization signals were detected using a STORM PhosphorImager (Molecular Dynamics) and the data were analyzed using IMAGEQUANT software (Molecular Dynamics). Terminal restriction fragment (TRF) analysis was performed as described (187).

PCR amplification, cloning and sequence analysis of fusion junctions

Chromosome fusion junctions were amplified by PCR using subtelomeric primers in various pairwise combinations. Primer sequences were as indicated above, with the following exceptions: 1L 5'-ACAAGGATAGAAATAGAGCATCGTC-3'; 3L 5'-AGACGAGGAGACTAGGAACG-3'; 3R 5'-GTATGGATGCCGGGAAAGTTGCAGACAA-3'; 5L 5'-CGACAACGAC GACGAATGACAC-3'; 5R 5'-TCGGTTGTCGTCTTCAAG-3'. PCR reactions (20 µl) contained 1 x ExTaq reaction buffer (TaKaRa), 125 µM dNTPs, 0.5 µM each primer, 0.5 units ExTaq (TaKaRa) and 100 ng genomic DNA. Samples were incubated at 96°C for 2 min, followed by 34 cycles of: 96°C for 30 sec, 55°C for 1 min and 72°C for 1 min, with a final incubation at 72°C for 5 min. A 10 µl aliquot of the PCR products was separated by electrophoresis through a 1% agarose gel, and transferred to a nylon membrane. Membranes were hybridized with a ^{32}P end-labeled $(T_3AG_3)_4$ or a specific subtelomeric oligonucleotide located distal to the primer used for PCR (3L 5'-CATAATTCTCACAGCAGCACCGTAGA-3'; 1R 5'-ACAAACACAGTCAATCCTGC-3') as probes. Hybridization and signal detection were performed as above.

For cloning of PCR products, unincorporated primers were removed using QIAquick PCR Purification Kit (Qiagen). Products were then ligated into the pDRIVE vector (Qiagen) and transformed into SURE® competent cells (Stratagene). Fusion

clones were detected by colony hybridization, using probes as described above. DNA was prepared from clones of interest using a QIAprep Spin Miniprep Kit (Qiagen). DNA sequence reactions were performed using the BigDye Reaction Mix (Perkin Elmer-ABI), and products were evaluated using an ABI PRISM 377 DNA Sequencer.

Statistical methods

An unpaired T-test was used to compare telomere lengths between mutant plants at different generations of propagation. Nonparametric data was compared using a Wilcoxan rank sum test. Comparison between categorical variables was completed using the chi-square test. A P value ≤ 0.05 was considered significant.

Results

Unique subtelomeric sequences in *Arabidopsis*

A search of the *Arabidopsis* genomic sequence database yielded terminal DNA sequence information for the eight non-rDNA bearing *Arabidopsis* chromosome arms (214-216). To confirm the sequence in wild type plant stocks segregated from the *tert* mutant line (ecotype Columbia), subtelomeric sequences from 1R, 1L, 2R, 3L, 3R 4R, 5L and 5R (where R corresponds to South and L to North; *Arabidopsis* Genome Initiative, 2000) were amplified via PCR using a telomeric repeat primer in combination with a chromosome-specific primer. The PCR products were cloned and sequenced. Only minor deviation from the published sequence was noted, specifically involving chromosomes 2R and 4R. Although a subtelomeric primer was designed for chromosome 3R, we were unable to isolate the most distal subtelomeric sequence for that chromosome. Pairwise BLAST analysis showed limited regions of homology within

the 2kb of subtelomeric DNA immediately proximal to the start of each telomere repeat sequence, with the exception of chromosomes 1R and 4R, which share an extensive region of homology. No highly repetitive sequences were identified near the telomeric repeats (Figure 8).

A novel PCR method to monitor individual telomere size

The presence of unique subtelomeric sequences in *Arabidopsis* allowed us to examine telomere length for individual chromosome ends. We devised a PCR-based technique called PETRA that requires the G-overhang, a key structural element necessary for telomere function, and can accurately determine telomere length at multiple chromosome ends from a single plant.

The principle of PETRA is outlined in Figure 9A. An adaptor primer (PETRA-T) is hybridized to the 3' G-rich overhang at the chromosome terminus. PETRA-T consists of 12 nucleotides complementary to the telomeric G-strand at its 3' end, with a 5' end that bears a unique sequence tag. Once annealed, the PETRA-T primer is extended by DNA PolI; the formation of PETRA products is dependent upon the action of DNA PolI Figure 9C, and we previously showed that this primer extension reaction requires the presence of an intact G-overhang (217). In the next step of PETRA, telomeres of specific chromosome arms are amplified by PCR using a unique subtelomeric primer and PETRA-A, a primer whose sequence is identical to the tag on the 5' terminus of PETRA-T. PCR products are detected by Southern hybridization using a telomeric repeat probe.

We tested the PETRA assay by evaluating the 2R telomere in a fourth generation (G4) *tert* mutant. Terminal restriction fragment (TRF) analysis of genomic

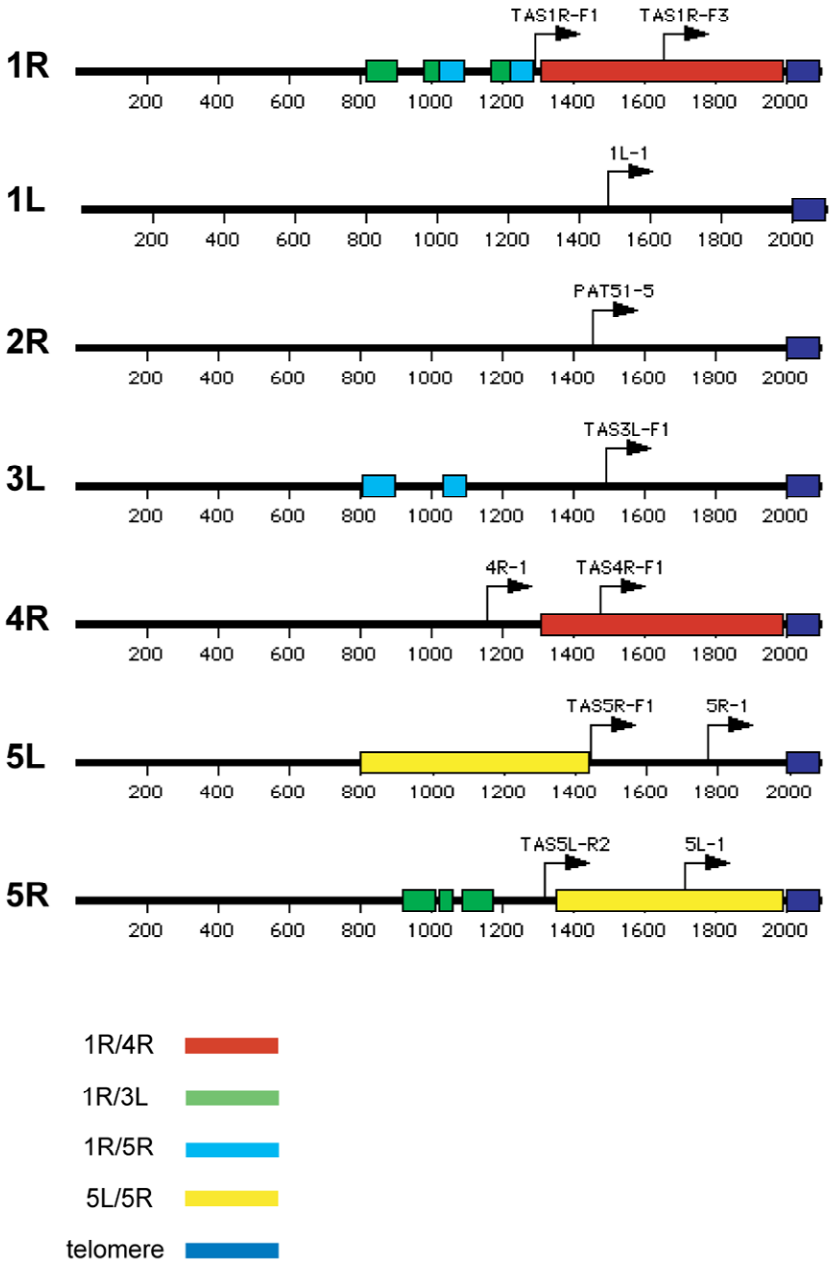

Figure 8. Unique subtelomeic regions in *Arabidopsis*.

Diagram depicting regions of subtelomere homology for 7/10 Arabidopsis chromosome arms. Arrows, location of primer using for PETRA and fusion PCR; rectangles, regions of homology shared between different chromosomes.

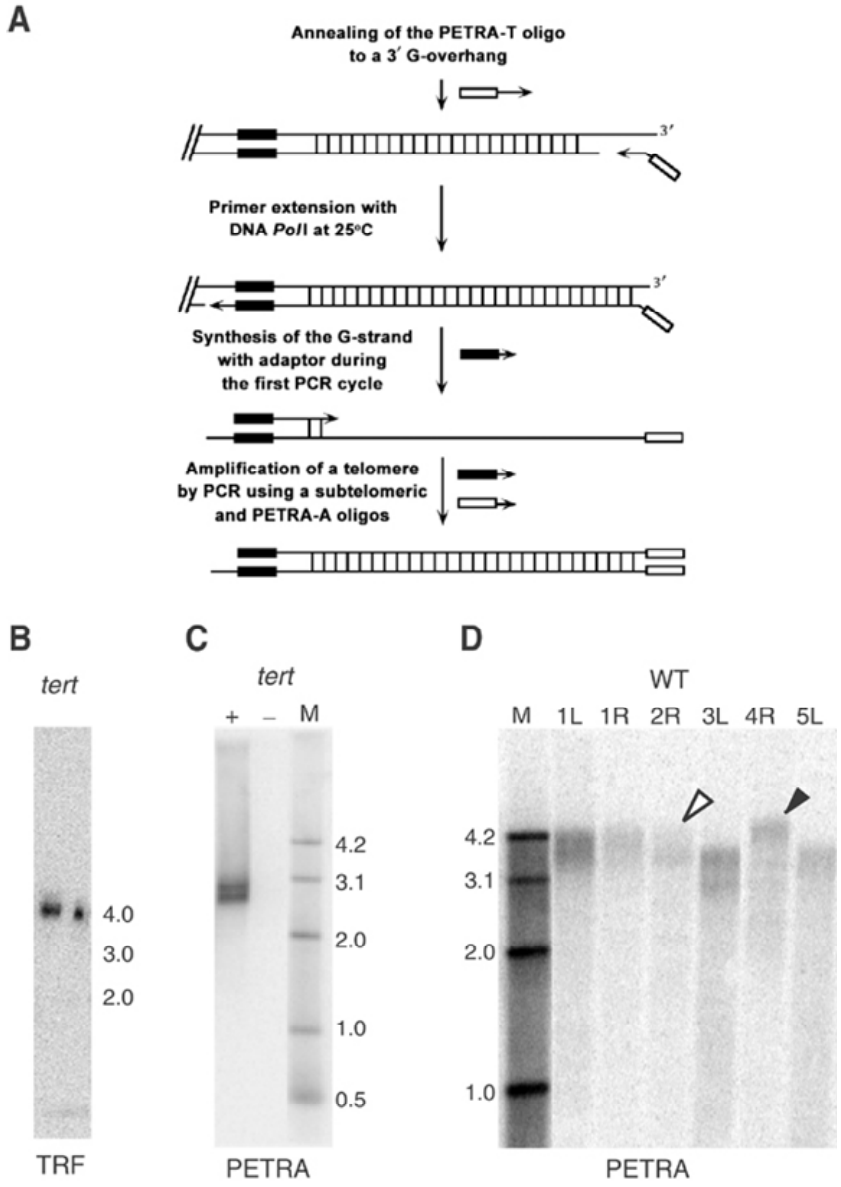

Figure 9. Measurement of telomere length by PETRA.

(A) Diagram of the PETRA method. (B) Measurement of telomere length by TRF analysis for the right arm of chromosome 2 (2R) from a G4 *tert* mutant. The probe is an oligomer that recognizes a unique subtelomeric region of 2R. The calculated telomere length is ~ 2.2 kb. (C) PETRA for 2R using the same DNA sample was carried out in the presence (+) or absence (-) of DNA *Pol*I. A doublet of bands is resolved, yielding a calculated telomere length of 2.2 and 2.4 kb. (D) PETRA for six different chromosome arms using a wild type DNA template. A single diffuse band is detected for most chromosomes; calculated telomere length ranges from 3030 to 4300 bp. Open arrowhead, shortest telomere; closed arrowhead, longest telomere.

DNA digested with HindIII detected a single 4 kb band (Figure 9B). Since the HindIII site is located 1.8 kb proximal to the telomeric repeats, the size of the telomere at 2R in this plant is approximately 2.2 kb. PETRA reactions were performed with the same DNA, using a 2R primer that binds 500bp upstream from the telomeric repeats. A doublet of bands (2.7 and 2.9 kb) was resolved (Figure 9C) indicating that the 2R telomere in this plant is comprised of two subpopulations of 2.2 and 2.4 kb in length. PETRA analysis of telomere length for other individual plants typically revealed only one or two bands for each chromosome arm, including 2R. Sequence analysis confirmed that PETRA products represent the predicted subtelomeric and telomeric sequences for the targeted chromosome (data not shown). These findings correlate well with previous TRF analysis of *tert* mutants using subtelomeric probes (187), and demonstrate that PETRA provides a sensitive and accurate measure of telomere length on individual chromosome arms.

Telomere size in telomerase deficient mutants

In mammalian cells lacking telomerase the shortest telomere is the one most often involved in fusions (185), implying the existence of a minimum functional telomere length below which the telomere is uncapped and available to participate in fusion events. To examine the relationship between telomere length, loss of telomere function and the formation of chromosome fusions in *Arabidopsis*, we determined telomere length for individual chromosome arms in different generations of *tert* mutants (Table 1).

PETRA detected a single diffuse band for most chromosome ends in wild type (Figure 9D) and a much sharper band in telomerase deficient mutants (Figure 10A and B). Telomere length varied considerably between the different chromosome ends and

Table 1. Summary of PETRA results for *tert* and *ku70 tert* mutants[a]

tert	P	1L	1R	2R	3L	4R	5L	5R	Ave	Range
G5, line 69										
1	WT	1530	1280	1600 2150	1490	1250 1530	1640	880	1480	1270
2	WT	1470	1260	2200	1420	1250	ND	890	1415	1310
3	WT	1490 1230	1330	1940	1220	1020	1600 1380	580	1310	1360
4	WT	1460	1180	2280 2090 1840	1520	1190	1770	990	1590	1290
G9, line 69										
1	II-T	920	ND	410	510	ND	810 580	500	620	510
2	II-T	600 500	360	300	440	ND	780	540	500	480
3	II-T	950	ND	520	620	ND	790	890 320	680	630
4	II-T	890	390	520	730	ND	930	ND	690	540
5	II-T	660	300	310	440	ND	700	610	500	400
6	II-T	900	ND	350	460	ND	460	710 550	570	550
7	II-T	1040	460	1150	750	ND	880	710	830	690
Pool	T	710 530	**360**	**1140**	**590**	ND	880	760 260	650	880
ku70 tert										
G4, line 52										
1	I	ND	1160 700	ND	910	1600	ND	1100	1090	900
2	I	ND	470	1100	970	1620	ND	630	960	1150
3	I	ND	**640**	1180	**980 800**	2670 2290 2020 1460	ND	1010	1450	2030
4	I	ND	1400	2570 1470	2010 1550	3200	ND	1610 820	1830	2380
5	I	ND	**1310**	2210 1410	**1660**	3070	ND	1390	1840	1760
6	I	ND	960	1100 1340	720	1900	ND	770	1130	1180
7	I	ND	810	840 1150	670	1530	ND	720	950	860
8	T	ND	**730**	1030	**740**	2280 2050	ND	1170	1330	1550
9	T	640 420	**360**	1040	**1390 970**	ND	ND	440	750	1030
Pool	T	ND	740 540 480	1080	1030 700	1690 1560	ND	650 590	910	1210

[a]Values in bold indicate chromosomes for which fusion PCR products were cloned. Phenotypes (P) for the mutants are indicated. ND=not determined.

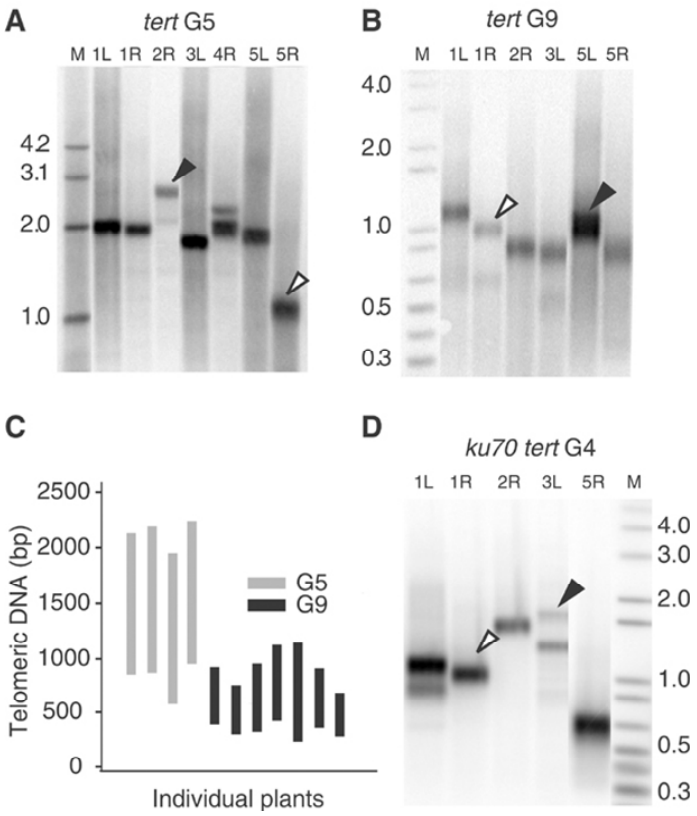

Figure 10. Telomere length analysis for *tert* and *ku70 tert* mutants.

Panels (A) and (B) show PETRA results for individual *tert* plants (line 69) at G5 and G9, respectively. Chromosome arm evaluated is indicated. Telomere length in G5 ranges from 880 to 2150 bp, while telomere length in G9 ranges from 300 to 700 bp. The shortest (open arrowhead) and longest (closed arrowhead) telomeres are indicated. (C) Bar graph illustrates the range of telomere length measured for G9 and G5 *tert* plants (line 69). Table I provides a summary of telomere length measurements. (D) PETRA results for a single *ku70 tert* plant at G4 (line 52). Telomere length ranges from 360 to 1390 bp.

no single telomere was consistently found to be the shortest or the longest in different generations (Table 1). As expected, bulk telomere length was significantly reduced in G5 *tert* mutants (Figure 10A) relative to wild type and diminished further by G9 (P=.0003) (Figure 10B). However, the size distribution of the telomere tracts (range between longest and shortest telomere) in an individual plant was dramatically compressed in G9 mutants relative to G5 (Figure 10C). On average, G5 telomeres covered a 1310bp range (n=4), while in G9 telomeres occupied a much narrower distribution of 630bp (n=7).

In *tert* plants cytogenetic evidence for chromosome fusion, manifest by the presence of anaphase bridges, correlates with the onset of developmental and growth defects that are either mild (Type I) or moderate (Type II). The phenotype worsens in successive generations, and by G9 most plants exhibit abundant anaphase bridges with severe growth defects and sterility, hence the designation terminal (T) (187). To determine the size of the shortest telomeres in *Arabidopsis* that still retain a G-overhang, PETRA analysis was performed for seven individual G9 *tert* mutants displaying either a Type II or T phenotype (Table 1). The shortest telomeres detected were 300-460bp (mean=360bp). The minimum telomere length found for a pool of terminal G9 plants was even shorter at 260bp.

Due to an accelerated rate of telomere shortening, anaphase bridges are first detected cytogenetically in *ku70 tert* mutants (line 52) in G2, with many plants reaching the terminal phenotype by G4 (218). To determine the minimal telomere length in this setting, we used PETRA to evaluate two G4 *ku70 tert* mutants that displayed a T phenotype (Figure 10D; Table 1). In these plants, the shortest telomere measured 360

and 730bp, respectively. The minimal telomere measured for a pool of terminal *ku70 tert* mutants was 480bp (n=4), a value slightly higher than for *tert* mutants.

Molecular analysis of chromosome fusion junctions in *tert* mutants

To further examine the relationship between telomere length and loss of function, we developed a PCR assay to detect chromosome fusions that exploits the existence of chromosome-specific PCR primers to amplify fusion junctions between chromosome ends (Figure 11A). The primers used for fusion PCR were positioned approximately 500bp from the telomere tract and were directed toward the chromosome terminus. Various combinations of primers were used to survey all possible combinations of chromosome ends for fusion. PCR products were detected by Southern blot, using either a telomeric repeat or a specific subtelomeric probe. PCR products were abundant in reactions carried out with a G9 *tert* DNA template (Figure 11B), and typically displayed a heterogeneous pattern of hybridization, with products of varied size that sometimes appeared as a broad smear. PCR products could be obtained for all chromosome arms surveyed, although some specific primer combinations gave negative results. PCR products were occasionally generated in wild type DNA samples (Figure 11B), but sequence analysis indicated that these rare products resulted from fortuitous amplification of interstitial sequences (data not shown).

To test whether the generation of fusion PCR products paralleled the onset of cytogenetic defects, DNA was prepared from wild type and successive generations of *tert* mutant plants (line 20; G4-G7), and PCR was performed using primers specific for chromosomes 1R and 3L. PCR products were not obtained in wild type or G4 DNA samples (Figure 11C; data not shown). In G5 faint bands were detected, and in G6 and

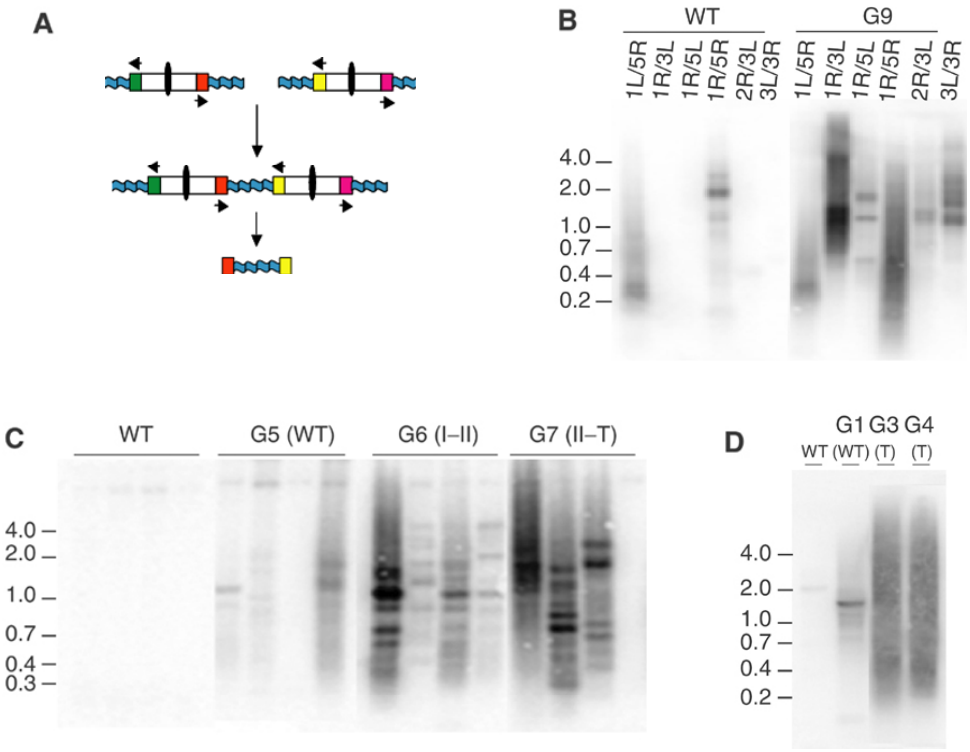

Figure 11. PCR amplification of chromosome fusion junctions.

(A) PCR strategy for amplification of fusion junctions. Arrows denote unique subtelomeric primers directed toward the chromosome terminus. PCR amplification occurs only when two subtelomeric regions are joined end-to-end (oval: centromere; wavy line: telomere). (B-D) Southern blot analysis of fusion PCR products using a telomeric repeat sequence probe. Panel B shows fusion PCR results for different subtelomeric primer combinations, using template DNA isolated from a wild type plant and a pool of terminal G9 *tert* plants. Chromosome arms analyzed are indicated. Panels C and D show fusion PCR results using the primers for chromosomes 1R and 3L, with template DNA prepared from different generations of *tert* (line 20) and *ku70 tert* (line 52) mutants. Results for a single plant are shown in each lane. Plant phenotypes are indicated in parentheses.

G7 products of greater complexity and abundance were observed (Figure 11C). A similar result was obtained with DNA from *ku70 tert* mutants (line 52) (Figure 11D). A faint band was detected in G1 plants, products of varied size were evident in G2 (data not shown), and abundant products resulting in a broad smear of hybridization were obtained using DNA from G3 and G4. These findings correlate well with the onset of cytogenetic abnormalities for both of these lines (187,218) and indicate that our PCR approach is a sensitive method for detecting chromosome fusions.

To further characterize the structure of the fusion junctions, and to correlate these structures with telomere length, we cloned fusion PCR products generated using *tert* and *ku70 tert* DNA samples that had previously been subjected to PETRA analysis. Three different primer combinations (1R-3L, 3R-3L, 2R-3L) were used to amplify chromosome fusion junctions. 39 clones from *tert* mutants (Type II or T phenotype) and 38 from *ku70 tert* mutants (Type I or T phenotype) were evaluated. Southern blot analysis showed that the majority of the clones contained telomeric DNA and sequences from both chromosome arms, consistent with fusion of heterologous chromosomes (data not shown).

DNA sequence analysis revealed that 74 of the clones had a structure consistent with end-to-end chromosome fusion, with two chromosome arms present in a head-to-head orientation (Figure 12). Three basic configurations were observed: telomere-telomere, telomere-subtelomere and subtelomere-subtelomere. Telomere-telomere fusions made up only 11% of the clones for *tert,* but at 43% represented a significantly larger proportion for *ku70 tert* (P=.002). Similar to what has been described for telomere-telomere fusions in yeast (209,219) were unable to sequence completely through the fusion junction in these clones. Telomere-subtelomere fusions were the

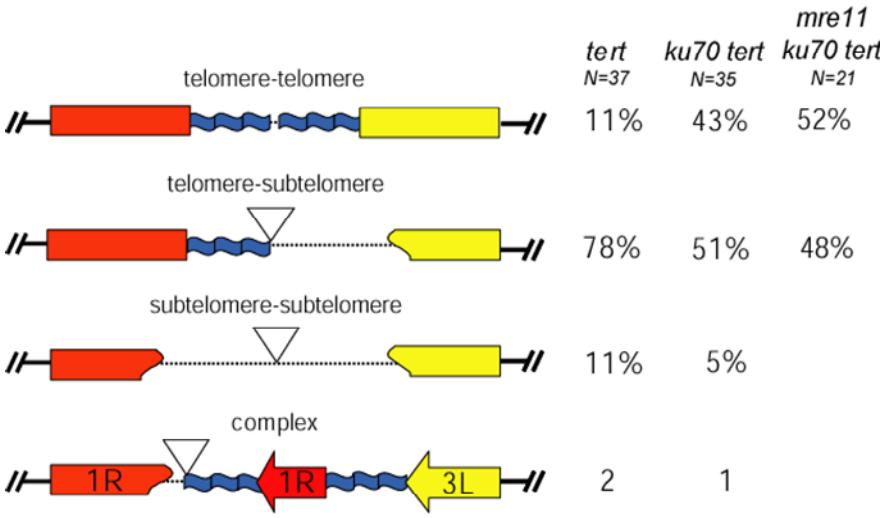

Figure 12. Structure of chromosome fusion junctions isolated from *tert*, *ku70 tert* and *ku70 tert mre11* mutants. For simplicity only heterologous chromosome fusion events are depicted. The extent of sequence deletion varied. Occasionally short regions of new sequence were inserted at the fusion junction (Tables 2, 3, and 4). Dotted lines indicate truncation of telomeric and/or subtelomeric DNA. Inverted triangles denote inserted sequences. The percentage showing a particular fusion structure for each genotype is indicated. Three examples of complex fusion junctions were isolated, but not included in the comparative analysis of fusion junction sequences.

most abundant isolates obtained from both *tert* (78%) and *ku70 te*rt (51%) mutants. In contrast, subtelomere-subtelomere fusions represented only 11% of the total for *tert* and 5% for *ku70 tert*. In three additional clones a more complex fusion junction was observed. The example shown in Figure 12 is typical of these isolates. Two copies of 1R were fused in a telomere-subtelomere configuration; the copy of 1R with an intact terminal sequence was truncated 69bp proximal to the telomere, and the 3L telomere was fused at that point.

Telomeric DNA captured in the fusion junctions must arise from an uncapped telomere. Since PETRA suggested that the shortest functional telomeres were approximately 300-400bp, it was of interest to determine how much telomeric DNA remained at the fusion junctions. The total length of the telomere tract for telomere-telomere fusions was determined by restriction mapping (Tables 2 and 3), but because we could not sequence completely across the fusion junction in these clones, the relative contribution of telomeric DNA from each chromosome end is unknown. Telomere tracts could be precisely measured in the telomere-subtelomere fusions by DNA sequence analysis. For the clones obtained from G9 *tert* mutants, telomeric DNA ranged from 122-457bp (mean=265bp) (Figure 13A; Table 2). A similar value was obtained for clones derived from G4 *ku70 tert* mutants, where telomere tracts ranged from 52-400bp (mean=241bp; Table 3). While the lengths of the telomere tracts in the fusion junctions roughly correlated with the shortest functional telomeres detected by PETRA, it is striking that these domains were often fused directly to subtelomeric DNA. Hence, dysfunctional telomeres generated by a telomerase deficiency often appear to be substrates for exonuclease attack prior to end-joining.

Table 2. Summary of sequence results for *tert* fusion PCR clones[a]

Clone number	Plant generation	Chr. arms	Source of telo repeat	Length of telo repeat[b]	Chr. deleted	Deletion Length[c]	Insertion	Homology
Telomere-telomere								
1	**G6**	**1R-3L**	**both**	**530**	**N/A**	**0**	**ND**	**ND**
2	G6	1R-3L	both	570	N/A	0	ND	ND
3	**G9**	**1R-3L**	**both**	**540**	**N/A**	**0**	**ND**	**ND**
4	**G9**	**3L-3L**	**both**	**370**	**N/A**	**0**	**ND**	**ND**
Telomere-subtelomere								
5	G6	1R-3L	1R	186	3L	349	0	4
6	G6	1R-3L	1R	122	3L	352	0	0
7	**G6**	**1R-3L**	**1R**	**198**	**3L**	**349**	**0**	**6**
8	G6	1R-3L	1R	219	3L	348	6	0
9	G8	1R-3L	1R	180	3L	115	10	0
10	G8	1R-3L	1R	122	3L	206	0	3
11	G8	1R-3L	1R	149	3L	346	0	3
12	G8	1R-3L	3L	498	1R	359	0	4
13	**G9**	**1R-3L**	**3L**	**292**	**1R**	**300**	**0**	**3**
14	**G9**	**1R-3L**	**1R**	**219**	**3L**	**64**	**6**	**0**
15	**G9**	**1R-3L**	**1R**	**197**	**3L**	**401**	**7**	**0**
16	**G9**	**1R-3L**	**1R**	**122**	**3L**	**404**	**1**	**0**
17	**G9**	**2R-3L**	**3L**	**400**	**2R**	**0***	**25**	**0**
18	**G9**	**3L-3L**	**3L**	**457**	**3L**	**143**	**0**	**4**
19	**G9**	**3R-3L**	**3L**	**271**	**3R**	**ND**	**ND**	**0**
20	**G9**	**3R-3L**	**3L**	**306**	**3R**	**ND**	**ND**	**0**
21	**G9**	**3R-3L**	**3L**	**291**	**3R**	**ND**	**145**	**0**
22	**G9**	**3R-3L**	**3L**	**334**	**3R**	**ND**	**ND**	**4**
23	**G9**	**3R-3L**	**3L**	**334**	**3R**	**ND**	**ND**	**0**
24	**G9**	**3R-3L**	**3L**	**201**	**3R**	**ND**	**ND**	**0**
25	**G9**	**3R-3L**	**3L**	**283**	**3R**	**ND**	**17**	**0**
26	**G9**	**3R-3L**	**3L**	**283**	**3R**	**ND**	**1**	**0**
27	**G9**	**3R-3L**	**3L**	**283**	**3R**	**ND**	**1**	**0**
28	**G9**	**3R-3L**	**3L**	**251**	**3R**	**ND**	**6**	**0**
29	**G9**	**3R-3L**	**3L**	**243**	**3R**	**ND**	**24**	**0**
30	**G9**	**3R-3L**	**3L**	**269**	**3R**	**ND**	**73**	**0**
31	**G9**	**3R-3L**	**3L**	**198**	**3R**	**ND**	**0**	**1**
32	**G9**	**1R-3R**	**1R**	**152**	**3R**	**ND**	**17**	**0**
33	**G9**	**1R-3R**	**1R**	**170**	**3R**	**ND**	**0**	**2**
Subtelomere-subtelomere								
34	G8	1R-3L	N/A	0	1R/3L	80/255	0	3
35	G8	1R-3L	N/A	0	1R/ 3L	459/366	0	2
36	G8	1R-3L	N/A	0	1R/3L	227/293	0	2
37	G8	1R-3L	N/A	0	1R/3L	44/54	9	0
Complex fusion								
38	G6	1R-1R-3L					0	0
39	G6	1R-1R-3L					0	0

[a]Values shown in bold indicate samples where PETRA was also performed. [b]Telomere repeat is shown in base pairs. [c]Length of deletion indicates the amount of subtelomeric DNA lost. Asterisk denotes a clone in which the entire 2R telomere tract is deleted, but the subtelomeric DNA is intact. ND, not determined; N/A, not applicable

Table 3. Summary of sequence results for *ku70 tert* fusion clones

Clone number	Plant generation	Chr. arms	Source of telo repeat	Length of telo repeat[a]	Chr. deleted	Deletion length[b]	Insertion	Homology
Telomere-telomere								
1	G3	1R-3L	both	415	N/A	0	ND	ND
2	G3	1R-3L	both	415	N/A	0	ND	ND
3	G4	1R-3L	both	365	N/A	0	ND	ND
4	G4	1R-3L	both	765	N/A	0	ND	ND
5	G4	1R-3L	both	1065	N/A	0	ND	ND
6	G4	1R-3L	both	315	N/A	0	ND	ND
7	G3	1R-3L	both	990	N/A	0	ND	ND
8	G3	1R-3L	both	1200	N/A	0	ND	ND
9	G3	3L-3L	both	1190	N/A	0	ND	ND
10	G3	1R-3L	both	715	N/A	0	ND	ND
11	G4	1R-3L	both	870	N/A	0	ND	ND
12	G4	1R-3L	both	400	N/A	0	ND	ND
13	G4	1R-3L	both	260	N/A	0	ND	ND
14	G4	1R-3L	both	700	N/A	0	ND	ND
15	G3	1R-3L	both	715	N/A	0	ND	ND
16	G3	1R-3L	both	715	N/A	0	ND	ND
Telomere-subtelomere								
17	G3	1R-3L	3L	341	1R	190	0	7
18	G4	1R-3L	1R	161	3L	91	9	0
19	G4	1R-3L	1R	222	3L	224	0	3
20	G4	1R-3L	1R	368	3L	262	0	6
21	G4	1R-3L	1R	229	3L	224	0	3
22	G4	1R-3L	1R	394	3L	262	0	6
23	G4	1R-3L	1R	164	3L	262	0	
24	G4	1R-3L	1R	184	3L	262	0	6
25	G4	1R-3L	3L	294	1R	309	0	3
26	G4	1R-3L	3L	286	1R	338	0	4
27	G4	1R-3L	1R	348	3L	3	0	2
28	G4	1R-3L	1R	106	3L	224	0	3
29	G4	1R-3L	1R	400	3L	226	0	3
30	G4	1R-3L	1R	52	3L	240	0	5
31	G4	1R-3L	3L	>469	1R	103	0	5
32	G3	1R-3L	3L	444	1R	329	0	12
33	G3	1R-3L	3L	524	1R	190	6	0
34	G4	3L-3L	3L	>100	3L	180	0	3
35	G4	3L-3L	3L	160	3L	293	0	0
Subtelomere-subtelomere								
36	G3	3R-3L	N/A	0	3L/ 3R	260/>365	0	3
37	G4	1R-3L	N/A	0	1R/3L	142/137	0	1
Complex fusion								
38	G4	1R-1R-3L					0	8

[a]Telomere repeat is shown in base pairs. [b]Length of deletion indicates the amount of subtelomeric DNA lost. Chr., Chromsome; ND, not determined; N/A, not applicable

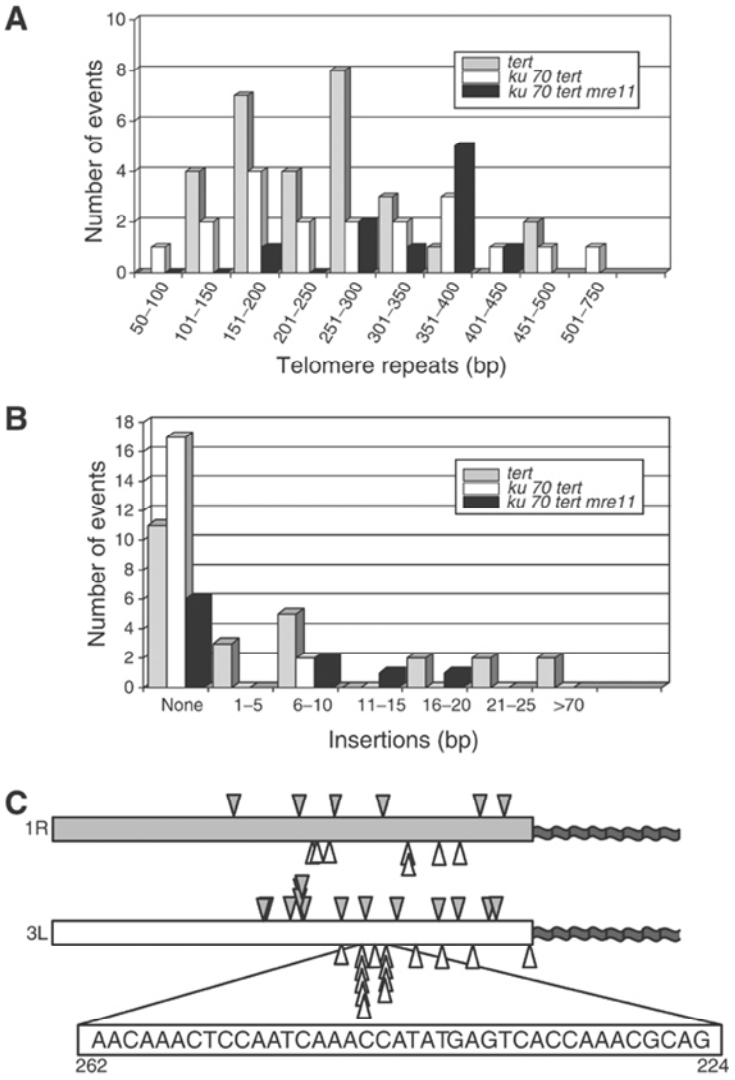

Figure 13. Chromosome fusion junction sequences from *tert*, *ku70 tert* and *ku70 tert mre11* mutants.

(A) Histogram showing the amount of telomeric DNA at the fusion junction in subtelomere-telomere clones: *tert* (gray bars), *ku70 tert* (white bars) and *ku70 tert mre11* (black bars). (B) Histogram showing the size and abundance of DNA insertion sequences at the fusion junctions. (C) Distribution of the point of fusion within the deleted subtelomere for telomere-subtelomere fusion events involving 1R and 3L in *tert* and *ku70 tert* mutants. Closed arrowheads, *tert* fusions; open arrowheads, *ku70 tert* fusions. A 39bp segment of subtelomeric sequence from 3L is expanded; this sequence was a preferred substrate for end-joining in the *ku70 tert* background.

Structural differences at the fusion junctions of *tert* and *ku70 tert* mutants

Sequence analysis revealed intriguing differences at fusion junctions formed in the presence or absence of KU. Fifty-four percent of the *tert* fusion junctions evaluated contained an insertion of a short region (1-145bp) of filler DNA (Figure 13B; Table 2). In previous studies on NHEJ, small insertions arise from both genomic and extrachromosomal DNA (Kirik et al., 2000). The origin of insertion sequences in our clones could not be determined. Significantly fewer of the *ku70 tert* clones harbored insertion sequences (10%; P=.001) and these were much shorter (6-9bp) (Figure 13B; Table 3). Overall, most insertions were less than 20bp, and all of the longer insertions were found in the *tert* fusion junctions.

Deletion of sequences at the fusion junction was common for both *tert* and *ku70 tert* mutants. For *tert* clones, the extent of erosion of subtelomeric DNA sequences varied substantially, spanning 44-459bp (Table 2). The fusion points were distributed fairly evenly throughout the region of the subtelomeric DNA, although a 6bp region of chromosome 3L exhibited a slight preference for the fusion site (Figure 13C). Erosion of subtelomeric sequences was also variable in clones derived from *ku70 tert* mutants, extending from 3bp to greater than 365bp (Figure 13C; Table 3). However, in contrast to *tert* mutants, *ku70 tert* mutants displayed a stronger bias in the choice of the fusion substrate. For 10 of the 15 fusion junctions involving the subtelomeric region of chromosome 3L, joining occurred within a 39bp region located 224-262 nucleotides from the beginning of the telomere tract (Figure 13C). This region has a similar sequence and C+A content to that of telomeric DNA, suggesting that in the absence of KU**,** homology between the ends plays a more significant role in the end-joining reaction. In support of this notion, nearly all of the *ku70 tert* telomere-subtelomere

fusions (83%) included a small region of perfect overlapping homology at the fusion junction, extending for up to 12bp (Table 3). In contrast, only 39% of the *tert* telomere-subtelomere clones displayed overlapping homology (Table 4), indicating a significant increase in microhomology (P=.006). This analysis confirms that *Arabidopsis* has the capacity to use both KU-dependent and KU-independent mechanisms for fusion of critically shortened telomeres. The data further indicate that the KU-independent mechanism has a greater reliance on DNA homology, with a concomitant decrease in the frequency of insertions at the fusion junction.

The role of Mre11 in fusion of critically shortened telomeres

In yeast, microhomology-mediated end-joining (MMEJ) is a KU-independent mechanism for repair of DNA double-strand breaks that requires Mre11 (147). Therefore, we asked whether Mre11 contributes to KU-independent fusion of critically shortened telomeres. An Mre11 homolog has been characterized in *Arabidopsis* (182). As predicted, mutations in this gene (*mre11-1* and *mre11-2*) result in increased sensitivity to DNA damage. In addition, telomeres were elongated in the mutants suggesting that Mre11 contributes to telomere length maintenance. The *mre11-1* allele resulted in severe developmental defects and sterility.

In this study we specifically focused on the DNA repair function of Mre11 in *Arabidopsis*, using fusion PCR to assess the contribution of Mre11 in joining critically shortened telomeres. For our experiments we used an *mre11* allele, *mre11-3,* which harbors a T-DNA insertion within the conserved phosphoesterase domain IV (181). *mre11-3* mutants showed vegetative growth defects and sterility, consistent with the phenotypes described for the *mre11-1* mutant (182). However, in contrast to the

Table 4. Summary of sequence results for *ku70 tert mre11* fusion clones[a]

Clone number	Chr. arms	Source of telo repeat	Length of telo repeat[a]	Chr. deleted	Deletion length[b]	Insertion	Homology
Telomere-telomere[b]							
1	1R-3L	both	410	NA	NA	ND	ND
2	1R-3L	both	491	NA	NA	ND	ND
3	1R-3L	both	906	NA	NA	ND	ND
4	1R-3L	both	978	NA	NA	ND	ND
5	1R-3L	both	806	NA	NA	ND	ND
6	1R-3L	both	533	NA	NA	ND	ND
7	1R-3L	both	573	NA	NA	ND	ND
8	1R-3L	both	734	NA	NA	ND	ND
9	1R-3L	both	642	NA	NA	ND	ND
10	1R-3L	both	851	NA	NA	ND	ND
11	1R-3L	both	522	NA	NA	ND	ND
Telomere-subtelomere							
12	1R-3L	1R	189	3L	328	6	0
13	1R-3L	3L	316	1R	432	0	3
14	1R-3L	3L	357	1R	61	0	3
15	1R-3L	3L	375	1R	495	8	0
16	1R-3L	3L	267	1R	455	0	4
17	1R-3L	3L	351	1R	295	0	1
18	1R-3L	3L	364	1R	330	0	0
19	1R-3L	3L	355	1R	151	18	0
20	1R-3L	3L	268	1R	37	11	0
21	1R-3L	3L	404	1R	153	0	2

[a]Telomere repeat is shown in base pairs. [b]Length of deletion indicates the amount of subtelomeric DNA lost. Chr., Chromsome; ND, not determined; N/A, not applicable

previous study we did not detect telomere elongation in the *mre11-3* mutant (data not shown). A detailed description of the *mre11-3* mutant, including an assessment of its impact on meiosis and genome stability, will be presented elsewhere (181).

To determine whether Mre11 plays a role in MMEJ of critically shortened telomeres in *ku70 tert* mutants, we generated *ku70 tert mre11* triple mutants by genetic crossing (Figure 14A). Because disruption of Mre11 results in complete sterility, sustained propagation of a triple *ku70 tert mre11* mutant was impossible. However, since end-to-end chromosome fusions can be detected as early as G1 of *ku70 tert* double mutants, we reasoned that it would be possible to assess the impact of Mre11 dysfunction on chromosome fusion within a single generation of plant growth. Triple mutant plants (*ku70 tert mre11*) and *ku70 tert* siblings heterozygous for the insertion in Mre11 (*ku70 tert MRE11*$^{+/-}$) were obtained by self-pollination of *KU70*$^{+/-}$ *TERT* $^{+/-}$ *MRE11*$^{+/-}$ plants. These plants were designated as G1, representing the first generation of growth without active telomerase. Self-pollination of G1 *ku70 tert MRE11*$^{+/-}$ plants yielded G2 triple mutants (*ku70 tert mre11*), representing two generations of growth without active telomerase. TRF analysis showed that bulk telomere length in *ku70 tert mre11* G2 plants was comparable to that of sibling plants that retained Mre11 function (Figure 14B; and data not shown). Thus, Mre11 dysfunction does not appear to significantly affect telomere length in a *ku70 tert* background.

Fusion PCR was performed using DNA prepared from G1 and G2 *ku70 tert mre11* plants to investigate the contribution of Mre11 to the fusion of short telomeres. As shown in Figure 6C, PCR products consistent with chromosome fusion were obtained from DNA samples prepared from G1 plants and were more abundant in G2 plants. The increased abundance of PCR products in G2 demonstrates that the

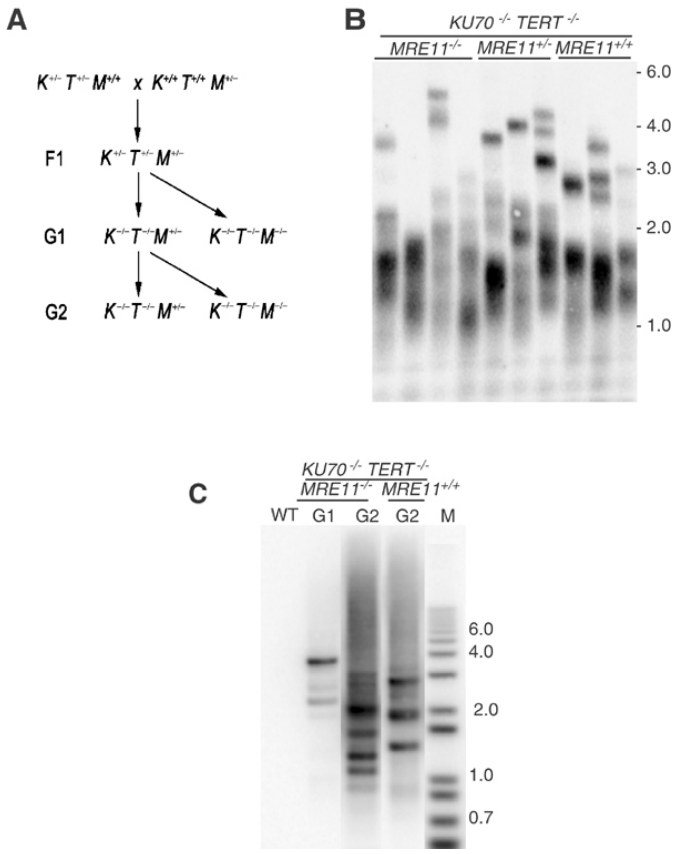

Figure 14. Telomere length and chromosome fusions in *ku70 tert mre11* mutants.

(A) Triple *ku70 tert mre11* mutants were obtained by crossing a plant doubly heterozygous for T-DNA insertions in the *TERT* and *KU70* genes with a plant heterozygous for a T-DNA insertion in *MRE11*. F1 plants heterozygous for all three mutations were self-pollinated and F2 plants homozygous for the *tert* and *ku70* mutations, and either heterozygous or homozygous for the insertion at *MRE11* were identified by PCR. This population, designated G1, represents the first generation of plants without active telomerase. Second generation (G2) *tert ku70 mre11* triple mutants were derived from self-pollination of a single G1 *tert ku70 MRE11+/-* plant. (B) TRF analysis in G2 *tert ku70 mre11* triple mutants was performed using a telomere probe to detect all chromosome arms. No consistent difference in telomere size was detected in *tert ku70 mre11* triple mutants compared to Mre11 proficient siblings. (C) Fusion PCR products are present in *ku70 tert mre11* G1, and are more abundant in G2. Fusion PCR products were generated using 1R and 3L primers.

frequency of chromosome end-to-end fusions correlates with telomere shortening and not with Mre11 inactivation. Sequence analysis of cloned PCR products supports the idea that Mre11 contributes to the formation of fusion junctions. Although the frequency of telomere-telomere and telomere-subtelomere fusions was similar in *ku70 tert* and *ku70 tert mre11* mutants (Figure12), sequence analysis revealed striking differences in the structure of telomere-subtelomere fusion junctions. Only 50% of the *ku70 tert mre11* clones displayed short regions of microhomology (1-4bp) compared to 81% in *ku70 tert* mutants (Tables 3 and 4). Moreover, small insertions were observed in 10% of the *ku70 tert* clones (6-18bp), while 40% of the *ku70 tert mre11* clones harbored insertions (Tables 3 and 4). Overall, the fusion junctions obtained from *ku70 tert mre11* mutants closely resembled junctions isolated from *tert* single mutants. These findings provide strong evidence that Mre11 contributes to the MMEJ reaction at critically shortened telomeres. Moreover, the detection of chromosome end-to-end fusions in plants deficient for both KU70 and Mre11 demonstrates that *Arabidopsis* can process dysfunctional telomeres via a variety of distinct NHEJ mechanisms, only a subset of which have been previously characterized.

Discussion

The primary function of the telomere is to define and protect the ends of chromosomes, allowing those termini to be distinguished from DNA double-strand breaks. Loss of telomere function may be precipitous as when cells are depleted of telomere binding proteins such as Taz1 or TRF2, or gradual as in telomerase-deficient mutants (184). However, in both settings formation of end-to-end fusions is a common outcome. In this study we used two different PCR strategies to follow the fate of individual chromosome

ends in *Arabidopsis* mutants experiencing telomere dysfunction through loss of telomerase. *Arabidopsis* is particularly amenable for such studies since most of its chromosome ends contain unique subtelomeric sequences. By contrast, yeast and mammalian telomeres are abutted by complex repetitive elements. Recently, a method comparable to our PETRA approach, termed STELA, was employed to measure telomere length on the short arms of the human sex chromosomes (220). However, application of STELA to other telomeres awaits the identification of additional unique subtelomeric sequences. PETRA not only allows us to simultaneously evaluate telomere length for multiple chromosome ends, but because it relies on the presence of an intact G-overhang, it is designed to detect the shortest functional telomeres in a population. PCR amplification of fusion junctions complements PETRA, since telomere fusion is a definitive indicator of loss of function.

Analysis of critically shortened telomeres

PETRA confirmed that telomere length decreased progressively through successive generations of telomerase mutants. However, we unexpectedly found that the telomere length distribution narrows sharply in later generations. It is conceivable that shorter telomeres that have lost their G-overhang exist in the population but are rapidly recruited into fusions. Removal of the G-overhang is necessary for chromosome fusion in human cells with dysfunctional TRF2 (106). Alternatively, there may be selective pressure applied to germline cells, such that only progeny harboring telomeres within the functional range are produced. A telomere surveillance mechanism has been reported for mice wherein cells bearing dysfunctional telomeres are eliminated from the germ cell precursor pool by apoptosis (221).

The shortest telomeres detected by PETRA are found in plants displaying the terminal phenotype. This value is approximately 300 bp in *tert* mutants, and is slightly longer in terminal *ku70 tert* mutants. By contrast, the shortest telomeres detected using a similar PCR technique in telomerase-deficient yeast were only ~50 bp long (222), six times smaller than the shortest telomeres in *Arabidopsis*. This difference may reflect alternative modes of telomere capping in these species. Whereas telomere protection in yeast is mediated through the binding of Cdc13 protein to the G-overhang (223), chromosome termini in plants are apparently sheltered in t-loops (89). The length of the shortest telomeres in *Arabidopsis* may correspond to the minimal size required for efficient t-loop formation *in vivo*.

Nucleolytic processing of dysfunctional telomeres

Little is known about the molecular mechanisms that process exposed chromosome termini and their role in triggering chromosomal aberrations. The initial stages of double-strand break repair typically involve nucleolytic degradation to create ends suitable substrates for downstream reactions (224). Studies in yeast reveal that deprotected telomeres are also subject to exonucleolytic resection (225). In fission yeast, inactivation of the Pot1 telomere protein leads to rapid and extensive loss of telomeric DNA followed by chromosome circularization (93). In KU70 deficient budding yeast chromosome ends are subject to degradation via exonuclease 1 (226). Furthermore, in telomerase deficient yeast, chromosome fusion is preceded by extensive telomere shortening (188,225). Although relatively little information is available concerning the processing of critically shortened telomeres in higher eukaryotes, sequence analysis of a small number of chromosome fusion junctions

formed in late generation telomerase-deficient mice revealed a complete loss of telomeric DNA (185).

Our results in *Arabidopsis* support the notion that exonucleolytic processing of critically shortened telomeres occurs prior to fusion. Among the 98 clones we sequenced, the large majority involved telomere-subtelomere fusions. The extent of nucleotide deletion in these junctions is consistent with what occurs prior to repair of endonuclease-induced double-strand breaks in plants (212). We considered the possibility that these clones represent secondary fusion events resulting from initial telomere-telomere fusion followed by one round of the BFB cycle. Since our PCR primers are targeted to sequences very close to the telomere tract, breakage of the dicentric chromosome in the next mitosis would have to have occurred in the immediate vicinity of the original fusion point, followed by a second round of fusion with another non-functional telomere. While three of our clones did display a complex structure consistent with such a secondary fusion (Figure 12), the vast majority appear to reflect a primary fusion event.

We suspect that telomere-telomere and sister chromatid fusions are under-represented in our study due to the inherent difficulty in generating PCR products across large palindromic regions. Indeed, *in situ* hybridization studies demonstrate that fusion of homologous chromosomes occurs frequently in late generation telomerase-deficient *Arabidopsis* (227), yet we identified only five examples of such junctions in our PCR survey. Nevertheless, it is striking that the incidence of telomere-telomere fusions detected was significantly higher in *ku70 tert* double mutants than in *tert* singles. Analysis of telomere length by PETRA revealed that the telomeres of chromosomes 1R and 3L, which form frequent end-to-end fusions, are slightly longer in terminal *ku70 tert*

plants than in *tert* single mutants. These findings, coupled with the observation that telomere loss is markedly accelerated in *ku70 tert* mutants (117), argue that KU70 contributes to telomere protection in *Arabidopsis.* Unlike mammals (168,197), this capping function is revealed only in the context of a telomerase deficiency (196).

The role of NHEJ in fusing critically shortened telomeres in *Arabidopsis*

Our data strongly support the contention that critically shortened telomeres are processed as double-strand breaks and are subject to NHEJ reactions. Both KU and Lig4 have been implicated in the fusion of aberrant telomeres in yeast and mammals (2,179,188,194,209). However, end-to-end chromosome fusions can also occur by other pathways, as telomere associations can form in the absence of KU in mammalian cells (197), fission yeast (195), and *Arabidopsis* (218). We investigated the mechanism of chromosome fusion in *Arabidopsis* by comparing the nucleotide sequences of fusion junctions formed in *tert* and *ku70 tert* mutants. In *tert* mutants, the fusion junctions are consistent with conventional KU-dependent NHEJ, harboring small insertions, deletions and microhomology. By contrast, chromosome fusion appears to proceed via a more homology-driven process in the absence of KU. In particular, we noted a marked increase in the incidence of overlapping microhomology, with a strong bias for joining of canonical telomere tracts to telomere-related sequences in the subtelomeric region. This finding supports the view that KU acts in NHEJ as an alignment factor that holds DNA ends in apposition to facilitate accurate repair (139). KU binding has been shown to inhibit exonucleolytic attack (178), but in its absence sequence homology between the DNA ends plays a more prominent role in proper alignment and efficient synapsis (147). The shift in the structure of the chromosome junctions formed in *tert* versus *ku70*

tert mutants demonstrates that KU contributes to the fusion of dysfunctional telomeres in *Arabidopsis*. However, in the absence of KU, an alternative and efficient NHEJ pathway operates.

The outstanding feature of this KU-independent NHEJ pathway is increased microhomology at the fusion junction. Since studies in yeast demonstrated a KU-independent MMEJ pathway that requires the MRX complex, we asked whether Mre11 contributes to the fusion of critically shortened telomeres in a higher eukaryote by creating a triple mutant deficient in Tert, KU70 and Mre11. Remarkably, *Arabidopsis* retained the capacity to mediate chromosome fusions in this setting. Sequence analysis of the fusion junctions supports a role for Mre11 in the fusion of critically shortened telomeres, as microhomology at the junction was reduced relative to that seen in double mutants lacking KU70 and TERT.

These findings demonstrate an *in vivo* role for Mre11 in NHEJ in higher eukaryotes. The discovery that inactivation of both KU-dependent NHEJ and Mre11-dependent MMEJ does not abolish end-to-end chromosome fusions in plants with critically shortened telomeres is unexpected, as nearly all end-joining activities in yeast are attributed to these two pathways (147). We conclude that plants possess at least three genetically distinct end-joining mechanisms that can efficiently substitute for each other and may directly compete in DNA repair. The robust and redundant nature of end-joining pathways is further illustrated by the capacity of *Arabidopsis ku70, ku80* and *lig4* mutants for T-DNA integration (228-230). Since higher eukaryotes rely primarily on NHEJ to repair double strand breaks, redundant end-joining activities may have evolved to ensure genome stability.

CHAPTER III

TELOMERE DYNAMICS AND FUSION OF CRITICALLY-SHORTENED TELOMERES IN PLANTS LACKING DNA LIGASE IV*

Summary

In the absence of the telomerase, telomeres undergo progressive shortening and are ultimately recruited into end-to-end chromosome fusions via the non-homologous end joining (NHEJ) double-strand break repair pathway. Previously, we showed that fusion of critically shortened telomeres in *Arabidopsis* proceeds with approximately the same efficiency in the presence or absence of KU70, a key component of NHEJ. Here we report that DNA ligase IV (LIG4) is also not essential for telomere joining. We observed only a modest decrease (three-fold) in the frequency of chromosome fusions in triple *tert ku70 lig4* mutants versus *tert ku70* or *tert*. Sequence analysis revealed that, relative to *tert ku70,* chromosome fusion junctions in *tert ku70 lig4* mutants contained less

---

*Reprinted with permission from Heacock, M.L., Idol, R.A., Friesner, J.D., Britt, A.B., and Shippen, D.E. 2007. Telomere dynamics and fusion of critically shortened telomeres in plants lacking DNA ligase IV. *Nucleic Acids Res.*

microhomology and less telomeric DNA. These findings argue that the KU-LIG4 independent end-joining pathway is less efficient and mechanistically distinct from KU-independent NHEJ. Strikingly, in all the genetic backgrounds we tested, chromosome fusions are initiated when the shortest telomere in the population reaches ~ 1 kb, implying that this size represents a critical threshold that heralds a detrimental structural transition. These data reveal the transitory nature of telomere stability, and the robust and flexible nature of DNA repair mechanisms elicited by telomere dysfunction.

Introduction

A primary function for the telomere is to confer a protective end structure that prevents natural chromosome ends from being inappropriately recognized as double-strand breaks (DSBs). This is accomplished by the specialized architecture at the chromosome terminus. In most eukaryotes telomeres are comprised of stretches of TG-rich repeated DNA sequences that terminate in a single-strand overhang (G-overhang), and are bound by double- and single-strand specific telomere proteins (76). For added protection, telomeres can assemble into a higher order t-loop configuration that apparently unfolds in S phase to allow telomerase access for telomeric DNA synthesis.

Telomere function can be disrupted by prolonged telomerase inactivation or by perturbation of telomere binding proteins. In such settings the telomere triggers a DNA damage response and is processed as a DSB (3). One outcome is the fusion of aberrant telomeres end-to-end through the non-homologous end-joining (NHEJ) repair pathway (3). Telomere fusion leads to the formation of dicentric chromosomes that in anaphase form bridges only to be broken when chromosomes are segregated. The

new DSBs induce breakage-fusion-bridge cycles, resulting in chromosome rearrangements that severely compromise genome stability.

The core components of the NHEJ machinery include LIG4/XRCC4 and the KU70/80 heterodimer (231). The KU complex acts to juxtapose two DSBs in alignment, while LIG4 and its stabilizing partner, XRCC4, ligate the two ends. In budding and fission yeast, the absence of KU and/or LIG4 leads to severe defects in end-joining; a 10-400 fold decrease in NHEJ has been reported (172,195,232,233). Likewise, mammalian cells deficient in KU and/or LIG4 display up to a 10-fold decrease in NHEJ (139-143). In both yeast and mammals, KU-independent end-joining pathways have been described, which rely on microhomology for alignment of the termini. In yeast, microhomology-mediated end-joining (MMEJ) is driven by the MRX complex (147). *In vitro* studies in human cells also demonstrate that the MRN complex utilizes microhomology to mediate end-joining (146), but it is currently unclear whether this pathway operates *in vivo*. Recent studies also implicate PARP1 and XRCC1/DNA ligase 3 (LIG3) in the repair of DSBs in mammalian cells lacking KU and LIG4 (136-138).

In addition to its role in DSB repair, KU localizes to telomeres where it functions both in telomere length maintenance and chromosome end protection (3). Notably, the loss of KU in vertebrates and fission yeast results in an increased incidence of end-to-end chromosome fusions (168,193,234-236). In this respect it is paradoxical that KU, a key component of the NHEJ machinery, actively blocks telomere fusion. How KU can provide stability to chromosome ends without engaging NHEJ is unclear, but one possibility is that telomere binding proteins occlude active sites on KU essential to DNA repair (148).

As in DSB repair, fusion of dysfunctional telomeres can be mediated by canonical NHEJ as well as alternate end-joining pathways. In budding yeast, LIG4 is required for joining dysfunctional telomeres to internal DSBs (188). Similarly, studies in both fission yeast and mammalian cells indicate that the fusion of dysfunctional telomeres is dependent on LIG4 (2,179,237). Notably, in the latter study where telomere de-protection was induced by the loss of an essential telomere binding protein, telomeres remained in an open, stabile configuration with intact G-overhangs, even though the ends were recognized as DNA damage (237). In contrast, dysfunctional telomeres that arise in fission yeast and mammalian cells as a consequence of a long-term telomerase deficiency fuse efficiently in the absence of LIG4 (195,202). Hence, the context in which the telomere is de-protected may influence its processing by DNA repair machinery.

Due to its genetic tractability and high tolerance for genome instability, *Arabidopsis* is a useful model for studying the consequences of telomere dysfunction. Wild type *Arabidopsis* telomeres range in size from 2-5 kb (238), but in mutants lacking the telomerase catalytic subunit, TERT, telomeres shorten by approximately 200-500 bp per generation, ultimately triggering the formation of abundant end-to-end chromosome fusions (53,187). In the terminal generation of the mutants, where plants were sterile and unable to propagate to the next generation, the shortest functional telomere bearing an intact G-overhang is only ~300 bp (180).

We previously showed that critically shortened telomeres fuse with approximately the same efficiency in the presence or absence of KU (117), arguing that plants employ highly flexible pathways for NHEJ. Since *Arabidopsis* telomeres are abutted by unique subtelomeric sequences on most chromosome arms, it is feasible to

investigate mechanisms of chromosome end-joining at the molecular level using PCR. Chromosome fusion junctions arising in *tert* mutants display canonical NHEJ signatures, including the insertion of filler DNA, microhomology and nucleotide deletions (180). The average amount of telomere DNA captured in chromosome fusion junctions is 270 bp, consistent with the length of the shortest functional telomere. While the overall architecture of fusion junctions is similar in *tert ku70* mutants, insertion of filler DNA is reduced and the majority of fusions possess microhomology, suggesting a microhomology-dependent back-up pathway. Consistent with this prediction, chromosome fusions that arise in triple *tert ku70 mre11* mutants display decreased microhomology and increased insertions (180), strongly implicating the MRX/N complex in a backup pathway for chromosome end-joining.

Here we examine the role of LIG4 in telomere fusion. We find that critically shortened telomeres can still fuse in plants lacking LIG4 and KU, with only a modest decrease in frequency. However, the chromosome fusion junctions display different sequence signatures than in *tert ku70* mutants, and the termini exhibit evidence for increased nucleolytic processing prior to fusion, arguing that the KU-LIG4 independent repair pathway is both mechanistically distinct, and less efficient than KU-independent NHEJ. Finally, we report a novel and critical size threshold for *Arabidopsis* telomeres that heralds the onset of chromosome end de-protection.

Material and methods

Plant growth and MMS treatment

Arabidopsis thaliana were grown and DNA was extracted as described (196) with an exception noted below. For methyl methanesulfonate sensitivity (MMS), seeds of wild-

type, *ku70* and *lig4-4* were sterilized in 50% bleach and plated on solid 0.5 BM media (239). Four-day-old seedlings were transferred to separate wells of a 24-well plate containing liquid 0.5 BM medium containing 0%, 0.006%, 0.008% or 0.01% MMS (Aldrich) and incubated in a shaker with constant light. Seedlings were scored after three weeks.

Generation of lig4 mutants and complementation of MMS sensitivity in *lig4-4* *Arabidopsis thaliana* plants with a T-DNA insertion in *AtLIG4* were obtained from the Salk collection (line 04427) (213). Heterozygous plants were identified using PCR with primers Lig4-8 (5' GTGATTTGAAACTAGTCTGTG 3'), Lig4-9 (5' CAGCAAACCGATTCAGAGATG 3') and LbA-1 (5' TGGTTCACGTAGTGGGCCATCG 3'). Plants heterozygous for T-DNA insertion in *KU70* and *TERT* (53,196) were crossed to heterozygous *lig4-4*. PCR was used to identify a triple heterozygous plant in F1, and this plant was self-pollinated to produce a segregating F2 population (Figure 15A). All single, double, and triple mutants along with wild type plants were identified by PCR from this population. The genomic *LIG4* coding sequence (Genbank Accession: AB023042) was PCR-amplified using DNA from wild-type *Arabidopsis* plants and placed under direction of the cauliflower mosaic virus promoter and the octopine synthase transcriptional terminator and cloned into a vector (240) for use in agrobacterium-mediated plant transformation (228). The MMS sensitivity of the *lig4-4* mutation was complemented with this genomic construct (data not shown). The experiment shown in the last panel of Figure 15C was performed with DNA from plants derived from a cross between *tert* and *lig4-1* mutants (228). The *lig4-1* allele produces a *LIG4* transcript, 3' of the T-DNA insertion site presumably from a cryptic promoter

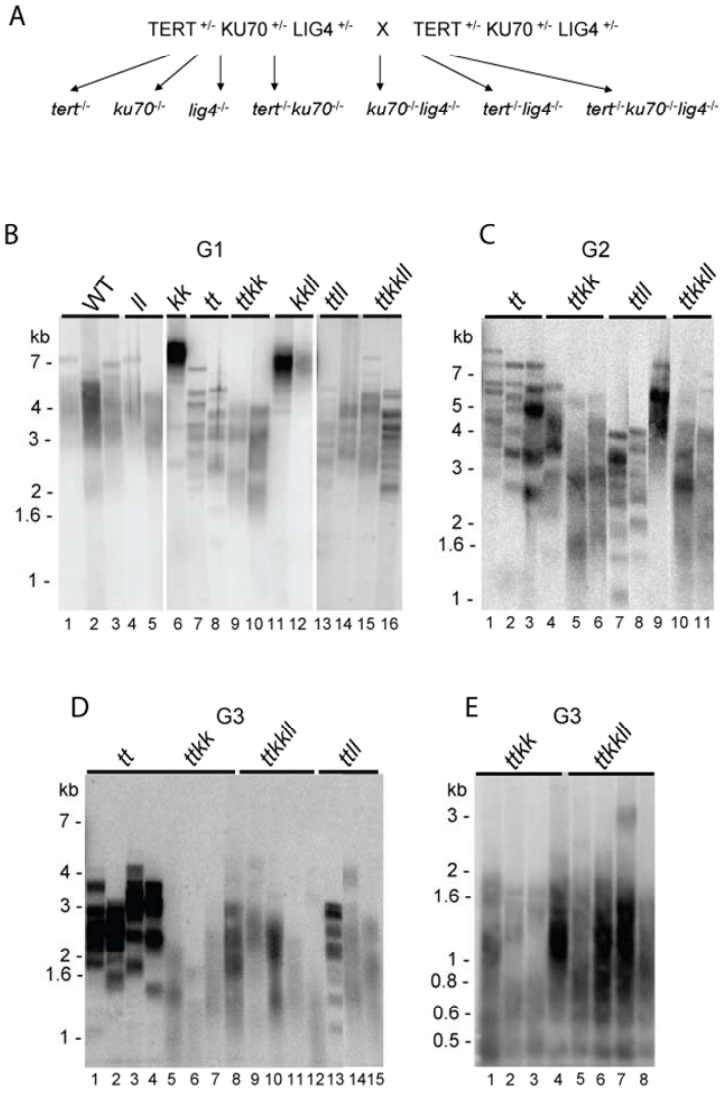

Figure 15. Characterization of telomere length in *tert ku70 lig4* mutants.

(A) Schematic representation of genetic crosses showing the segregation of various *lig4* mutants resulting from self-pollination of a triple heterozygous *TERT+/- KU70+/- LIG4+/-* parent. (B-D) TRF analysis of generation 1 (G1) (B), G2 (C), and G3 (D) mutant combinations arising from segregation of the triple heterozygote shown in (A). The right panel in Figure 16C shows TRF data for *tert* mutants carrying the *lig4-1* allele. (E) TRF analysis of G3 *tert ku70* and *tert ku70 lig4* mutants that have reached the terminal phenotype. Genotype abbreviations are as follows: wild type (WT), *lig4* (*ll*), *ku70* (*kk*), *tert* (*tt*), *ku70 lig4* (*kkll*), *tert lig4* (*ttll*) and *tert ku70 lig4* (*ttkkll*). The differences in hybridization signals reflect slight variations in the amount of DNA loaded in each lane.

within the T-DNA. However, due to the presence of stop codons within the inserted T-DNA construct, this allele likely produces a non-functional protein. In support, *lig4-1* mutants exhibit sensitivity to DNA damage, expected from the loss of a DNA repair protein.

Nucleic acid extraction, RT-PCR and telomere fusion PCR

DNA was extracted using the CTAB method (69). For RT-PCR, total RNA was extracted from flowers using the TriReagent solution (Sigma, St. Louis, MO). Reverse transcription was performed using 1μg of total RNA with SuperScript III (Invitrogen) and oligo dT at 55°C. The following primer pairs were used: Lig4-1 (5' ATGACGGAGGAGATCAAATTCAGCG 3') with Lig4-2 (5' TGACCCACTTCATCTCCTGAGC 3'), Lig4-8 with Lig4-9 (both sequences described above), and Lig4-5 (5' GGGAACCTGGAGATCGTAGTGG 3') with Lig4-6 (5' TGC CCTTGATATCCGATACATCAG 3'). Telomere fusion PCR was performed as previously described (180).

TRF, subtelomere analysis and PETRA

For TRFs and subtelomere analysis, approximately ~ 1μg of DNA was digested with 30 U of the restriction endonuclease TruI overnight at 65°C. DNA was recovered by ethanol precipitation, suspended in water and loaded into a 0.8% agarose gel run at 50V for ~ 16 hours. The gel was transferred onto a nylon membrane (Hybond), hybridized with a [γ^{32}P]ATP end-labeled $(T_3AG_3)_4$ oligonucleotide in a buffer containing 0.25 M sodium phosphate buffer (pH 7.5), 7% SDS and 1 mg/mL BSA. Hybridization signals were detected using a STORM PhosphorImager (Molecular Dynamics) and the

data were analyzed using IMAGEQUANT software (Molecular Dynamics). Specific subtelomeres were assessed in the same manner except that the DNA was digested overnight at 37°C with 30 U of PveII and SpeI in order to release intact subtelomeres (and their respective telomeres) from the bulk of genomic DNA. The probes used in the detection of the subtelomeres 1L, 2R, and 5L are described previously (238). The length of specific telomere tracts was also determined using PETRA as described previously (69) except that in most cases whole plant tissue was used.

In-gel hybridization

In-gel hybridization was performed essentially as described (111) with some modifications. Approximately 300mg of plant tissue was extracted using a GE DNA extraction kit (product code 27-5237-01) as per the manufacturer's instructions, except that the tissue was incubated at 37°C. Extracted DNA was incubated with SSB protein (Promega) to a final concentration of 2µg/mL, to protect the single-stranded G-overhang from degradation. The DNA was then subjected to digestion using 30 U of each of the restriction endonucleases, HaeIII and HinfI overnight at 37°C. The gel was hybridized with a [γ^{32}P]ATP end-labeled $(TA_3C_3)_3$ oligonucleotide. To ensure the signal obtained was from a single-stranded 3' G-overhang, DNA was either mock or treated with T4 DNA polymerase (utilizing its 5' to 3' exonuclease activity). As expected, a loss of signal was observed in the samples treated with 24 U of T4 DNA polymerase (see Figure 16B). Agarose gels were denatured and re-hybridized using the same probe. The single-strand G-overhang signals were obtained by calculating the volume of the signal in each lane and then normalizing the signal using the hybridization signal

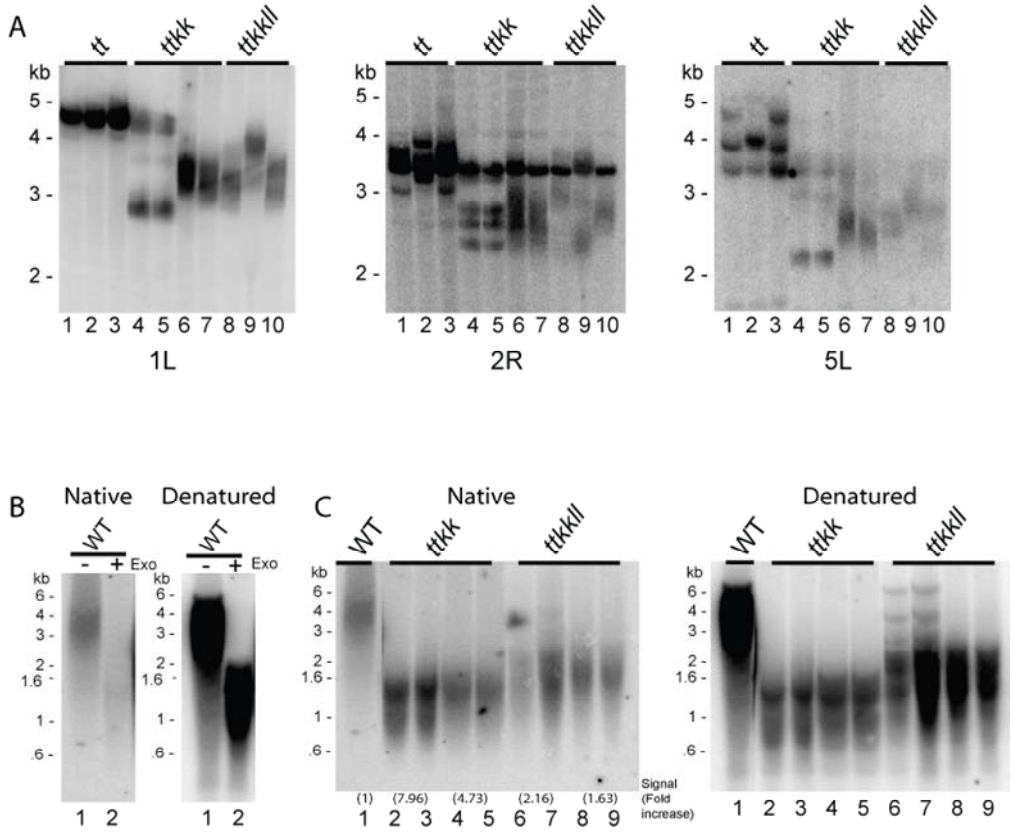

Figure 16. Subtelomere and G-overhang analysis in *tert ku70 lig4* mutants.

(A) Subtelomere TRF analysis using probes specific for 1L (left blot), 2R (middle blot) and 5L (right blot). DNA was analyzed from *tert*, line 12 (lanes 1-3), *tert ku70*, line 12 (lanes 4-7) and *tert ku70 lig4*, line 9 (lanes 8-10). (B) In-gel hybridization of DNA isolated from wild type plants under native (left panel) and denaturing conditions (right panel). Lane 2 from each gel shows DNA subjected to T4 DNA polymerase (Exo) treatment, demonstrating the signal is dependent on the G-overhang. (C) In-gel hybridization of DNA isolated from wild type and mutant plants. The wild type control is shown in lane 1. Duplicate DNA obtained from line 3 for *tert ku70* are shown in lanes 2-5 and from two separate pools from three separate plants from line1 for *tert ku70 lig4* are shown in lanes 6-9. The hybridization signal for each lane was normalized to the wild type sample and average fold increase over the wild type signal is reported. The denatured gel showing bulk telomeres is shown on the right. All gels were hybridized with a [γ^{32}P] ATP radiolabeled $(TA_3C_3)_3$ telomere repeat probe. Genotype abbreviations used are as stated in Figure 15.

obtained from the denatured gel. The single-strand G-overhang signal obtained from wild type was set to one and each sample was normalized to this value.

Cytogenetic analysis

Mitotic anaphases were obtained from pistils of unopened floral buds as described in (187) but 8-hydroxyquinoline was omitted. Squashes were analyzed with a Zeiss epifluorescence microscope. The anaphase bridges were scored as a percentage of total anaphases (Table 5).

Statistical analysis

Statistical analysis was performed using a student's t-test and a P-value less than 0.05 was considered significant.

Results

LIG4 is not required for telomere length homeostasis in *Arabidopsis*

We characterized a SALK T-DNA insertion line for *LIG4*, which we term *lig4-4*, where the insertion lies in the 6th exon (Figure 17A). To determine whether the *LIG4* gene was still functional, RT-PCR was conducted to monitor the level of *LIG4* mRNA (Figure 17B). Although we detected evidence for transcripts both upstream and downstream of the T-DNA insertion, no RT-PCR products were observed with primers flanking the T-DNA junction (Figure 17B). Since this region includes the conserved active site lysine required for catalytic activity, the data argue that LIG4 is inactive. Consistent with this conclusion, treatment of *lig4-4* mutants with 0.01% of the DSB-inducing agent MMS led to growth arrest, while wild type plants thrived under the same conditions (data not

Table 5. Summary of cytogenetic analysis

Genotype	Anaphase bridges	Total anaphases	Percent bridges[a]
Generation 3			
tert ku70 (line 3)	108	1641	6.6
tert ku70 (line 12)[b]	237	1060	22.3
tert ku70 lig4 (line1)	5	1714	0.3
tert ku70 lig4 (line 9)[b]	46	762	6
Generation 4			
tert ku70 (line 3)	340	1195	28.4
tert ku70 lig4 (line1)	139	1354	10.3

[a]For each generation, genoptype and line, the total number of anaphase bridges was divided by the total anaphases observed. [b]Indicates the generation and line where the plants were terminal.

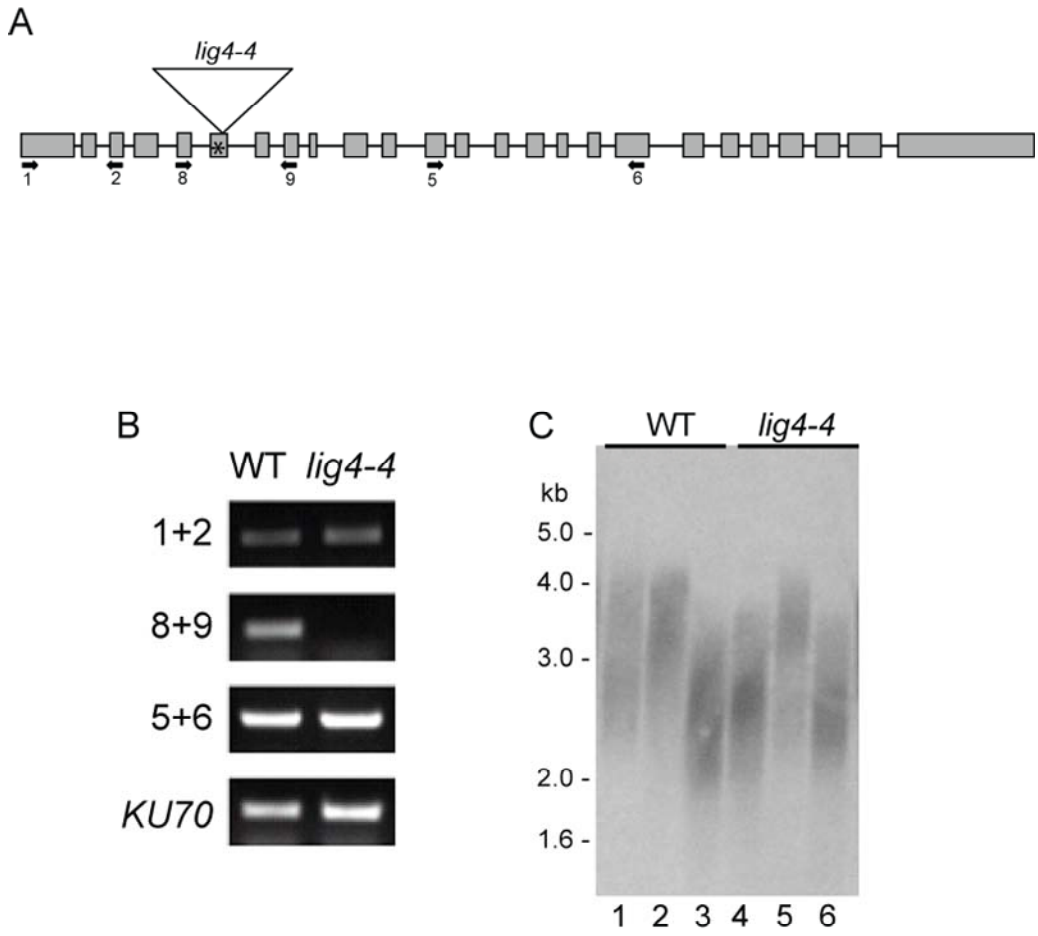

Figure 17. Characterization of the *lig4-4* mutant.

A) Schematic representation of the Arabidopsis LIG4 gene showing positions of 25 exons (rectangles); the T-DNA is inserted in the 6th exon (triangle). The active site lysine is indicated by an asterisk. Primer positions are denoted by arrows. (B) RT-PCR analysis using primer combinations shown in (A). There is no transcript detected with primers that flank the T-DNA junction using primers 8 and 9. Products downstream of the T-DNA insertion likely are derived from a cryptic promoter in the T-DNA construct. (C) Terminal Restriction Fragment (TRF) analysis of lig4-4 mutants and wild type plants segregated from LIG4-4+/- plants. Although telomeres in lig4-4 mutants (lanes 4-6) appear more variable in length than in wild type (lanes 1-3), they fall within wild type range.

shown). We verified that the DNA repair defect was linked to the *LIG4* gene by transforming a wild type genomic copy of *LIG4* into *lig4-4*. MMS hypersensitivity of the transformants was abolished (data not shown). We conclude that the *lig4-4* is a null allele of *LIG4*.

As expected from previous analysis of other *lig4 Arabidopsis* lines (228,230), *lig4-4* mutants were viable and showed no developmental defects under normal growth conditions (data not shown). To determine if LIG4 contributes to telomere maintenance in *Arabidopsis*, terminal restriction fragment (TRF) analysis was performed on DNA isolated from *lig4-4*. Although individual telomere lengths varied slightly, there was no significant difference in the telomere tracts of mutants versus their wild type siblings. All telomeres migrated in the 2-5 kb range (Figure 17C), compare lanes 1-3 to lanes 4-6). In agreement with previous studies in yeast and mammals (193,195,230,233) (193,195,233), and a previous report for *Arabidopsis* (230), we conclude that LIG4 is not required for telomere length homeostasis. Furthermore, consistent with their wild type phenotype, *lig4-4* mutants do not display evidence for genome instability (see below).

Disruption of LIG4 does not accelerate the onset of the terminal phenotype in plants with critically shortened telomeres

To investigate the role of LIG4 in promoting telomere fusions, the *lig4-4* allele was crossed into a genetic background where telomeres are rapidly shortening. Telomeric DNA is lost two to three-fold faster in plants null for both *TERT* and *KU70*, and mutants reach the terminal phenotype as early as the third generation (G3) of the mutant (117). In contrast, *tert* mutants typically survive until at least G8 (187). To accelerate our

analysis of LIG4, we generated a plant heterozygous for *TERT*, *KU70* and *LIG4* and allowed it to self-pollinate to create a triple *tert ku70 lig4* mutant (Figure 15A). From this cross we isolated all combinations of single, double and triple mutants and evaluated bulk telomere length from each genotype combination by TRF. Figure 15 shows the results of this analysis for successive generations of mutant lines arising from the triple heterozygote. As expected, telomere shortening was observed in all the plants lacking a functional *TERT* gene (Figure 15B, lanes 7-10, 13-16), and was accelerated in double *tert ku70* mutants (Figure 15B, lanes 9 and 10). Furthermore, as expected, *ku70* mutants displayed greatly extended telomeres (Figure 15B, lane 6), consistent with our previous observation that KU70 acts as a negative regulator for telomere length (196).

Although there were some variations in telomere length among sibling plants, inactivation of *LIG4* in combination with a *KU70* or *TERT* deficiency gave rise to telomere phenotypes that were similar to those associated with single mutants in G1 (Figure15B). As expected, *LIG4* deficiency did not abolish telomere extension in *ku70* mutants, nor did telomere length vary significantly in *tert lig4* versus *tert* or in *tert ku70* versus *tert ku70 lig4*. However, in G2 and G3, the rate of telomere shortening appeared to be slightly faster in several *tert lig4* mutants relative to *tert* (Figure 15C, left panel, compare lanes 1-3 with 7 and 8; middle panel, compare lanes 1-4 with 5, 6 and 8; Figure 15D compare lanes 1-4 with 13-15). Furthermore, PETRA analysis of individual telomeres in later generation *tert lig4* mutants showed telomeres that were somewhat shorter than in *tert* (data not shown). Confounding these results, however, was a three-generational analysis of *tert lig4* mutants (G1-G3) derived from a second LIG4 mutant allele (*lig4-1*; (228)). Similar to *lig4-4*, *lig4-1* appears to be a null allele displaying the sensitivity to DNA damage (228). These double mutants did not reveal evidence for

accelerated telomere shortening relative to their *tert* counterparts (Figure 15C, right panel; data not shown). Therefore, our genetic analysis indicates that LIG4 may make a modest contribution to telomere length regulation in the context of a telomerase deficiency, but further studies are needed to address this possibility.

Notably, a generational analysis failed to reveal differences in the rate of telomere shortening in triple *tert ku70 lig4* mutants versus *tert ku70* (Figure 15E). Consistent with similar rates of telomere attrition, both *tert ku70* and *tert ku70 lig4* reached the terminal phenotype as early as G3 or G4. To correlate this phenotype with telomere length, we sought to determine the minimal functional telomere length in the most severely affected, developmentally-arrested plants using Primer Extension Telomere Repeat Amplification (PETRA) (180). PETRA is a sensitive, PCR-based technique that targets specific telomere arms using a primer directed at a unique subtelomeric sequence and a primer that anneals to the 3' G-overhang. This approach allows us to accurately measure telomere length on 7/10 chromosome ends (180). We define a functional telomere as harboring an intact G-overhang, and hence the minimal functional length corresponds to the shortest PETRA products generated. The shortest telomeres that we could detect in a pool of terminal *tert ku70* mutants was 360 bp (180) and in the two fourth generation *tert ku70 lig4* mutants were 320 and 450 bp (Figure 18A and Table 6). These data support our conclusion that 300 bp represents the minimal functional length for *Arabidopsis* telomeres, below which the telomere is unable to maintain a G-overhang and block end-to-end fusion. Thus, the failure of *tert ku70*

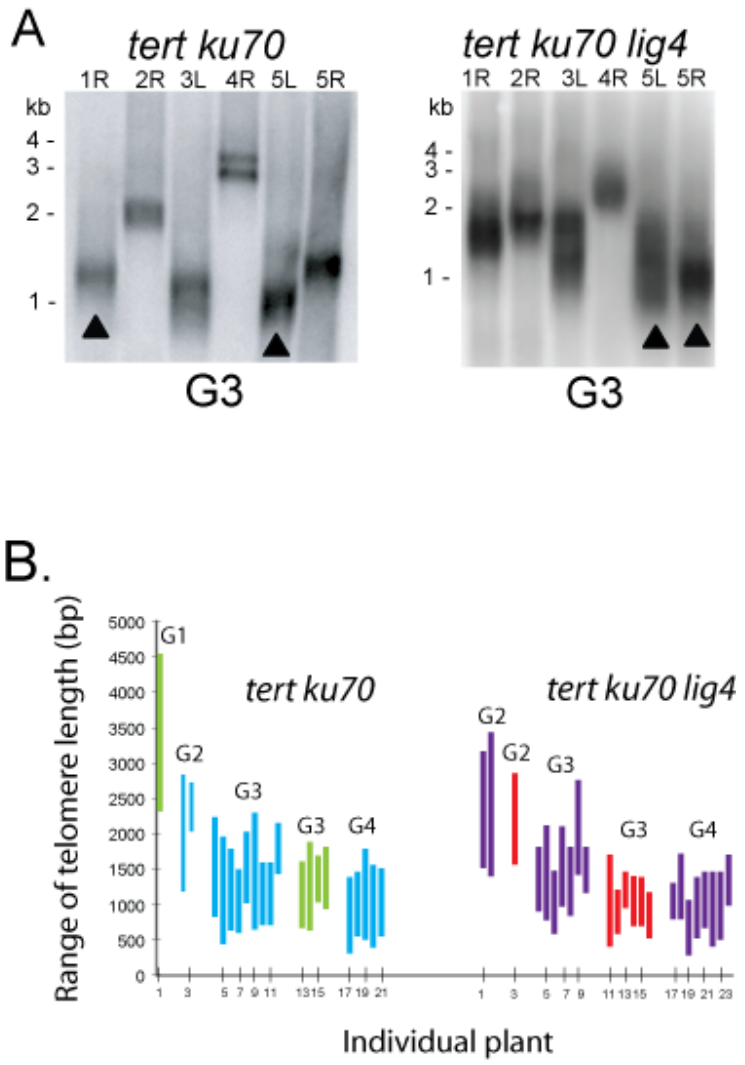

Figure 18. Analysis of telomeres in *tert ku70 lig4* mutants.

(A) Representative PETRA data for G3 *tert ku70* and *tert ku70 lig4* mutants. Closed arrows indicate the two shortest telomere tracts, determined by subtracting the length determined by PETRA from the relative position of the chromosome-specific primer on the subtelomere DNA target. (B) Summary of PETRA results for individual plants from *tert ku70* and *tert ku70 lig4* lines. Vertical lines represent that range of telomere lengths (shortest to longest) detected in each plant. Blue and green lines represent *tert ku70* line 3 and line 12; purple and red lines denote *tert ku70 lig4* lines 1 and 9. The generation for each line is denoted above each group of vertical lines.

Table 6. Summary of PETRA and fusion analysis for *tert ku70 lig4*[a]

	Chromosome Arm								TF/PCR		Bridges
Plant	1L	1R	2R	3L	4R	5L	5R	Range	1R+3L	5L+5R	(%)
G2, line 1											
1	X	X	2800 2240	1960 **1560**	3020 2510	3120 2740	2700 2070	1560	-	-	0
2	X	X	2740 2090	2200 1780 1690	3080 2590	3400 2740 2070	2810 2260 **1450**	1950	-	-	0
G2, line 9											
3	X	X	2420 1920	2750 2380 **1610**	2820	2270 1980	2130 1650	1140	-	-	0
G3, line1											
4	X	X	1780	1500 **950**	1700	X	1740	830	+	-	1.6
5	X	X	1290	1030	2080 1750	1260 **820**	1110	1260	ND	ND	ND
6	X	1450	1450	1240	910	1060	1230 970 **630**	820	-	-	0.59
7	**1010**	1430	1660	1180	2060	1420	1080	1050	-	+	0.26
8	X	X	1690	1590 **880**	1650	1720	1780 1500	900	-	ND	0
9	X	X	2720	**1460**	2230	1490	1640	1260	-	-	0
10	X	X	1780 1530	1680 1370	X	1740 **1200**	1560	580	-	-	0
G3, line9											
11	X	X	1670	1430	1670	890	**450** 890 1240	1420	-	-	10.42
12	X	750	1060	1170 740	1100	690	**630**	540	-	+	4.44
13	X	**990**	1330	1420	1380	1410	1270 1090	430	-	ND	9.33
14	X	850	1360	1140 830	X	**730**	1000 870	630	+	+	3.4
15	X	**730**	890	1350	X	1120	1170	620	+	ND	ND
16	X	**560**	890	1140	X	1030	650	580	-	-	ND
G4, line 1											
17	X	X	1180	910	1260	1130 990	1180 **840**	420	-	+	ND
18	X	X	1420	1210	1680	1210 860	**840**	840	-	-	ND
19	X	X	880	670	1020	670	540 **320**	700	-	-	15.1
20	X	X	1350	640	1120	670	**560**	790	-	+	13.3
21	X	X	1430	980	940	800	1060 **700**	730	ND	ND	6.9
22	800	X	1240 1420	1160 720	**450** 1170	1040 800	1070 710 470	970	-	+	13
23	1040	820	1360	1100	1380 860	580	1430 940 **540**	890	-	+	18
24	X	X	1490 **1020**	1080	1160	1390	1660	640	-	+	5

[a]Telomere lengths are indicated in base pairs. Values in bold denote the shortest telomere in the population. ND, not determined; NA, not applicable; X, no signal detected; +, fusion PCR product detected; -, no fusion PCR product detected.

lig4 to proliferate beyond G3 or G4 is likely due to the accumulation of non-functional telomere caps.

LIG4 is not essential for the fusion of critically shortened telomeres

We asked whether LIG4 is necessary to fuse critically shortened telomeres by comparing the efficiency of chromosome end-joining events in *tert ku70* versus *tert ku70 lig4* plants. Telomere fusion was evaluated initially using conventional cytogenetics to detect bridged chromosomes in anaphase. Two independent lines from *tert*, *tert ku70*, *tert lig4* and *tert ku70 lig4* mutants were analyzed for three consecutive generations (Table 5). As expected, no anaphase bridges were observed in G1 or G2 of any of the mutants (data not shown). However, beginning in G3 anaphase bridges were observed in both lines of *tert ku70* and *tert ku70 lig4* mutants. Thus, LIG4 is not required for chromosome fusions in cells with critically shortened telomeres.

For plants that had not reached the terminal phenotype, and which had comparable telomere lengths, the percentage of anaphase bridges was not statistically different. For example, the percentage of anaphase bridges in G3 *tert ku70* line 3 was 6.6 % and in G4 *tert ku70 lig4* line 1 was 10.3% (Table 5). However, comparison of chromosome fusion rates in terminal generation mutants revealed that the efficiency of end-joining was modestly reduced in the absence of *LIG4* (Table 5). In G3 *tert ku70 lig4* (line 9) 6% of the anaphase showed bridges, while in G3 *tert ku70* (line 12) 22.3% of the anaphases harbored bridges. This difference is statistically significant (P=0.04). A similar trend was observed with two other lines in G4; the number of anaphase bridges in *tert ku70 lig4* line 3 was reduced relative to *tert ku70* line 1 mutants (10.3%

versus 28.4%; P=0.002). Thus, the frequency of chromosome end-joining events appears to be decreased in the absence of LIG4 by a factor of ~ 3-fold.

To verify that the anaphase bridges we observed reflect telomere fusions, we analyzed these same samples using telomere fusion PCR with primers directed outward from the right arm of chromosome 1 (1R) and the left arm of chromosome 3 (3L) (180). Southern blot analysis of the PCR products using a telomeric DNA probe gave a signal for *tert ku70 lig4* reactions, although it was reduced compared with *tert ku70* (Figure 19A). Notably, results from telomere fusion PCR correlated well with the reduced frequency of anaphase bridges for the majority (75%) of *tert ku70 lig4* samples tested (Tables 5 and 6).

One explanation for the decreased amount of telomere fusion PCR products is that chromosome ends in the triple mutants were subjected to extensive nucleolytic degradation into the subtelomeric region prior to fusion, which could eliminate primer binding sites. However, when PCR was performed with primers directed at slightly more internal sites on the chromosome, product abundance was not increased. An alternative possibility is that the telomere arms we targeted were not critically shortened, and hence would not be recruited into fusions. To address this issue, we determined the length of individual telomere tracts using PETRA. PETRA showed that the 5L and 5R telomeres were the very shortest in *tert ku70 lig4* mutants (Figure 18A and Table 6). When telomere fusion PCR was repeated using 5L and 5R primers, additional weak products were evident from several triple mutants after hybridization with a telomere repeat probe (Figure 19A). Hybridization of the blots with a probe directed to the 5L or 5R subtelomere also yielded only a faint signal (data not shown).

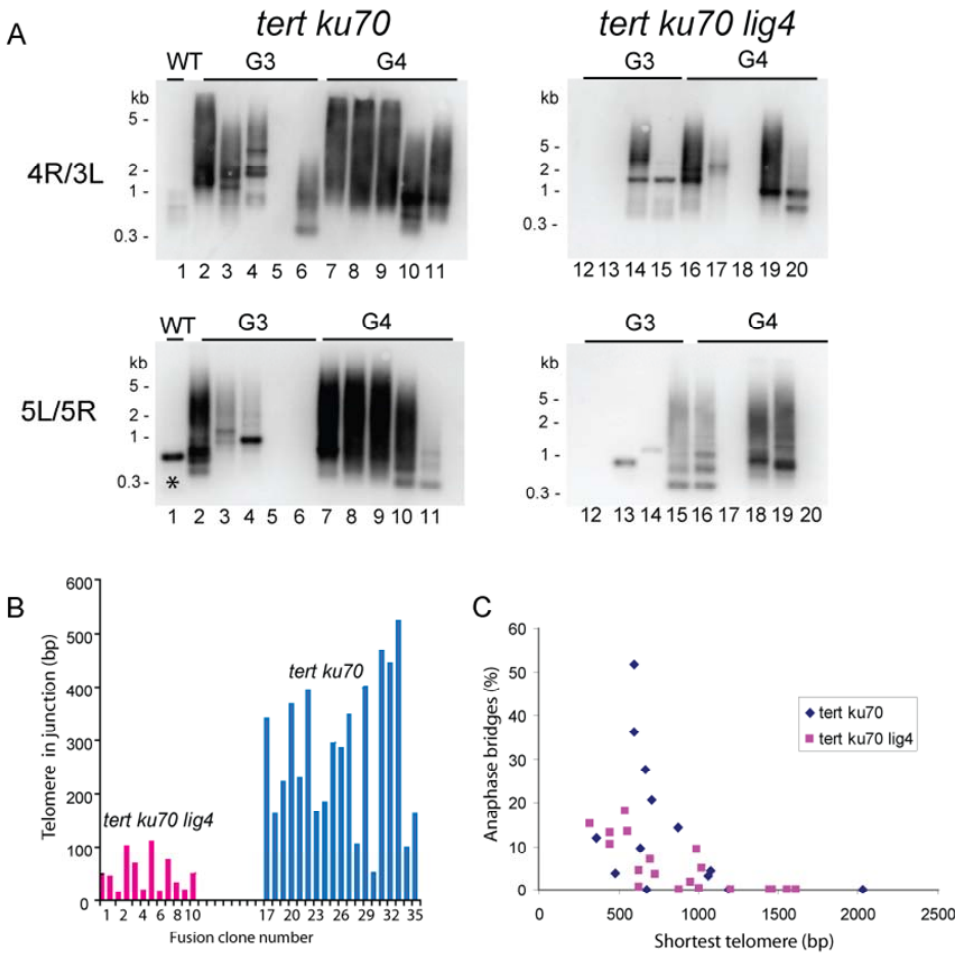

Figure 19. Telomere length and the onset of end-to-end fusions in *lig4* mutants.

(A) Results are shown from telomere fusion PCR performed on individual wild type and G3 and G4 *tert ku70* and *tert ku70 lig4* mutants. The primers used for PCR are indicated on the left. Blots were hybridized with a radiolabeled telomere repeat probe. Non-specific bands are occasionally observed (*) in this assay, but can be discerned by sequencing the cloned product. (B) Graph illustrating the amount of telomeric DNA in fusion junctions arising from *tert ku70 lig4* (pink bars) and *tert ku70* mutants (blue bars). Data were obtained from sequence analysis of telomere fusion PCR products derived from *tert ku70 lig4* mutants (this study) and from *tert ku70* mutants (180). (C) Graph illustrating the relationship between shortest telomere and the frequency of anaphase bridges in G1-G4 of *tert ku70* and *tert ku70 lig4*.

These data support the conclusion that the frequency of chromosome end-joining reactions is reduced in the absence of LIG4.

Chromosome fusion junctions formed in the absence of KU70 and LIG4 display unique sequence signatures

In accordance with their reduced abundance, telomere fusion PCR products from triple mutants were difficult to clone. Nevertheless, sequence analysis was performed on 11 independent clones. We noted several interesting distinctions in the structure of fusion junctions formed in the presence and absence of LIG4. First, although the use of microhomology (defined by at least one nucleotide overlap) was prevalent in *tert ku70 lig4* mutants, the amount of base pair overlap captured in the junctions was reduced in these mutants relative to *tert ku70* (avg=2 versus ave=4.6 perfect nucleotide overlap, respectively; P=0.02). Although the number of clones analyzed is small, these data suggest that end-joining reactions in the absence of both KU and LIG4 are mechanistically distinct from the KU-independent pathway. Second, critically shortened telomeres were more prone to nuclease attack in *tert ku70 lig4* than in *tert ku70*. We observed a substantial decrease in the number of chromosome fusions that involved the direct joining of two telomere tracts. In *tert ku70* mutants, 43% of the junctions reflected telomere-telomere joining, while this was true for only 18% of junctions analyzed from *tert ku70 lig4* mutants (Table 7; (180)). In this regard, the chromosome fusion events in the triple mutant more closely resembled *tert* mutants, where only 11% of the junctions analyzed involved direct telomere-telomere joining (180). In both *tert* and *tert ku70 lig4* mutants, the large majority of fusions (78% and 73%, respectively)

Table 7. Characterization of chromosome fusion junctions in *tert ku70 lig4* mutants

Type of fusion[a]	*tert ku70* N=31[b]	*tert ku70 lig4* N=11
Telomere-telomere	43%	18%
Telomere-subtelomere	51%	73%
Subtelomere-subtelomere	5%	9%
Complex	1%	0%
Features of fusion junctions		
Deletion of subtelomere sequence	220 bp	220 bp
Telomeric repeat retained at fusion site	270 bp	50 bp
Microhomology at fusion junction[c]	81%	66%
Insertion of filler DNA at fusion junction	10%	0%

[a]Telomere fusion PCR products were cloned and sequenced as previously described (180). Percentages indicate the relative fraction of a particular type of fusion. [b]Previous data obtained from (180). [c]Percentage of clones possessing microhomology, (perfect base pair overlap) at the fusion junction.

corresponded to telomere-subtelomere joining events, in which one chromosome end had lost all of its telomeric DNA prior to fusion.

Additional evidence that critically shortened telomeres are more susceptible to nuclease attack in *lig4* mutants was revealed when the amount of telomeric DNA captured in the fusion junctions was considered. Five-fold less telomeric DNA was associated with fusions cloned from *tert ku70 lig4* than from *ku70 tert* (average of 50 bp of telomeric DNA versus 270 bp, P=0.01) (Figure 19B and Table7).

Two additional assays were performed to investigate the extent to which chromosome ends in tert ku70 lig4 are subjected to nucleolytic attack (Figure 16). First, subtelomeric TRF analysis was employed. While the profile of bulk telomeres in terminal generation plants detected by standard TRF blots is indistinguishable in *tert ku70* and *tert ku70 lig4* mutants, a subset of chromosome ends could have suffered extensive nuclease attack. Although we did not have sufficient genomic DNA from terminal generation mutants to evaluate all the chromosome arms, analysis of the 1L, 2R and 5L telomeres indicated that at least these three termini have not been extensively degraded (Figure 16A). Second, we performed in-gel hybridization to monitor the status of the G-overhang in terminal generation *tert ku70 lig4* mutants. Telomere uncapping in LIG4-deficient mammalian cells does not result in any loss of G-overhangs (237). In contrast, in two separate experiments, we observed only a two to three-fold decrease in the G-overhang signal for *tert ku70 lig4* mutants relative to *tert ku70* (Figure 16C; data not shown). This finding is not unexpected, as PETRA, which relies on the presence of an intact G-overhang, consistently yielded products in terminal *tert ku70 lig4* mutants.

From these experiments we conclude that critically shortened telomeres in *Arabidopsis tert ku70 lig4* mutants are subjected to increased, but not catastrophic nuclease attack, which likely reflects the decreased efficiency of end-joining catalyzed by a KU-LIG4 independent repair pathway.

Identification of a novel, critical size threshold for *Arabidopsis* telomeres

To gain a deeper understanding of the molecular trigger for telomere dysfunction and chromosome fusion in plants undergoing progressive telomere erosion, we monitored the dynamics of individual telomere tracts through consecutive generations of *tert ku70* and *tert ku70 lig4* mutants**.** PETRA analysis revealed that the absence of LIG4 did not affect the stochastic nature of which telomere is the shortest. For example, in one G4 *tert ku70 lig4* mutant the shortest telomere was 5R (320 bp), while in another plant it was 4R (450 bp) (Table 6). Similarly, the range of telomere lengths (i.e. the difference between the shortest and longest telomere in a given plant) was approximately the same in *tert ku70* and *tert ku70 lig4* mutants. The average range of telomere lengths for the two G3 *tert ku70* lines was 990 bp and 930 bp in G4 (Figure 18B and Table 8). For *tert ku70 lig4* the range was 820 bp and 750 bp, respectively (Figure 18B and Table 6).

Despite the stochastic nature of telomere dynamics in all the genetic backgrounds we examined (*tert*, *tert ku70*, *tert ku70 lig4*), the onset of telomere fusions strongly correlated with the presence of at least one telomere in the population that was 1 kb or below in length (Figure 19C and Tables 6 and 8). In *tert ku70* mutants 94% of the plants (15/16) shown to contain telomere fusions by our PCR assay harbored a

Table 8. Summary of PETRA and fusion analysis for *tert ku70* [a]

	Chromosome Arm								TF/PCR		Bridges
Plant	1L	1R	2R	3L	4R	5L	5R	Range	1R+3L	5L+5R	%
G1, line 12											
1	3190	2900	4500	2850	2910	2850	**2350**	2150	ND	ND	ND
G2, line 3											
2	X	X	2310	2030 **1190**	X	2840	2050 1590	1650	-	-	0
3	X	X	2730	X	2400	2650	**2030**	700	-	-	0
G3, line 3											
4	X	1200 1450	1600 1950	1120 1570 1390	1260 500 2200	1200 1840	**870** 1370	1330	+	-	14.1
5	X	1830 1340	1930	1060 750	950	890 1340 **480**	590	1450	+	ND	3.74
6	X	**680** 1540	1740	1370 680	1180 1670	1410 770	1650	1060	+	+	0
7	X	X	X	**640**	1430	1460	1140	820	+	+	9.6
8	X	1650 1210 **970**	1900	1360	1980	1500	1150 1060	1010	+	ND	3.2
9	X	**690**	1860	2040	2260 1850	2010 1520	1920 1230	1570	+	ND	ND
10	X	X	1560	X	1550	**760**	1010	800	ND	ND	ND
11	X	760	1560 1220	X	1560	**750**	1010	810	+	ND	ND
12	X	X	1600	1600	1640 2110	1480 1660 1850	**1480**	630	+	ND	ND
G3, line 12											
13	X	780	1570	**710**	1530	750	950	860	+	ND	20.5
14	X	**670**	1120 1450	830	1840	760	870	1170	+	ND	27.4
15	X	**1080**	X	1130	X	1230	1650	570	-	-	4.3
16	X	**980**	1780	1100	1560	1140	980	800	+	-	ND
G4, line 3											
17	X	970	960 360	960 860	1160 **300**	1340 1080	1250	1040	+	+	11.9
18	X	1050 1280	1080 1330	830 1000	1420 990 **600**	1040 730 1370	910 1400	820	+	+	51.6
19	X	**550**	1440 1110	850	1740 1380	970	970	840	+	+	ND
20	X	480	770	900	1520 1290	1430 810	880 690 **440**	1080	+	ND	ND
21	X	**600**	1480	940	1320	1080	740	880	+	+	36.3

[a]Telomere lengths are indicated in base pairs. Values in bold denote the shortest telomere in the population. ND, not determined; NA, not applicable; X, no signal detected; +, fusion PCR product detected; -, no fusion PCR product detected.

telomere of less than or equal to 1 kb (Table 8). For *tert ku70 lig4* mutants this value was 90% (9/10) (Table 6). Similarly, when samples showing cytogenetic evidence for chromosome fusions from *tert ku70 lig4* mutants are included with samples showing positive telomere fusion PCR data, 87% of the plants contain at least one telomere that is less than or equal to ~ 1kb in length (Table 6). This correlation was also evident when data from both *tert ku70* and *tert ku70 lig4* are combined (Figure 19C). Thus, although bulk telomeres continue to shorten until they reach the minimal functional size of ~300 bp, our data indicate 1kb represents a critical length threshold. Telomeres that drop below this length have lost the ability to efficiently cap the chromosome terminus and begin to participate in end-joining reactions.

Discussion

Here we exploit the genetic tractability of *Arabidopsis* to examine DNA repair pathways that are elicited in mutants experiencing progressive telomere erosion. Specifically, we evaluated the role of LIG4 in promoting the formation of end-to-end chromosome fusions. By employing plants that were doubly deficient in TERT and KU70, our analysis was expedited as telomeres shortened two to three times faster in this background than in single *tert* mutants (218). Furthermore, by inactivating both *KU* and *LIG4*, we severely crippled the conventional NHEJ machinery, allowing us to investigate potential backup mechanisms for DSB repair. As with yeast and mammals, we found that LIG4 does not make a significant contribution to telomere length maintenance in *Arabidopsis* (193,195,230,233). Interestingly, we observed a slight increase in the rate of telomere shortening in *tert* mutants carrying the *lig4-4* allele, but not the *lig4-1*. However, since *tert lig4-4* mutants are viable through at least G6 as are their *tert*

siblings (M. Heacock and D. Shippen, unpublished data), LIG4 appears to play only a minor role in telomere length maintenance when telomerase is inactivated. Consistent with this conclusion, we found that bulk telomeres shorten at the same rate in *tert ku70 lig4* mutants as in *tert ku70* mutants. In both settings plants typically reach the terminal phenotype in G3 or G4.

To evaluate the role of LIG4 in joining dysfunctional telomeres, we monitored genome integrity in plants with shortening telomeres using a combination of cytogenetic analysis and telomere fusion PCR. As with *ku* mutants (117), we found that chromosome fusions can be readily detected in plants lacking both LIG4 and KU. Since NHEJ is favored in higher eukaryotes by 1000-fold over homologous recombination (241), the other well-characterized DSB repair pathway, our findings reveal a second backup mechanism for DSB repair that does not involve canonical NHEJ. Studies in yeast and mammals support this conclusion. LIG4-independent fusion of critically shortened telomeres has been reported in fission yeast (195), and very recently in mammalian cells (202). Intriguingly, evidence for a backup pathway of DNA ligation in *Arabidopsis* has also been described in *lig4* mutants during T-DNA integration, a process thought to be mediated by NHEJ (228,230). As in the current study, Friesner and Britt (228) report that T-DNA integration is reduced by three-fold in the absence of LIG4.

Although little is known about this alternative mechanism for NHEJ, our data provide some insight into how it may engage dysfunctional telomeres. Several lines of evidence indicate that the backup pathway is less robust than KU-independent NHEJ. In addition to the three-fold reduction in anaphase bridges, we found that telomere fusion PCR products were less abundant in *tert ku70 lig4* relative to *tert ku70,* even

when primers were used that specifically targeted the very shortest telomeres in the population. Furthermore, critically shortened telomeres in plants lacking both KU and LIG4 appear more vulnerable to nuclease attack than in plants deficient only in KU. Not only is the incidence of telomere-telomere fusions decreased, but also reduced is the length of the telomeric DNA tract captured in fusion junctions in *tert ku70 lig4* mutants compared to all of the other genetic backgrounds we have examined, including *tert*, *tert ku70*, *tert lig4* and *tert ku70 mre11* (Figure 18B and Table 7) (180).

We hypothesize that the increased nucleolytic digestion of dysfunctional telomeres in *tert ku70 lig4* mutants is a reflection of reduced efficiency of repair. We found no evidence for extensive degradation of individual chromosome ends. Preliminary data from four independent telomere fusion clones from G5 *tert lig4* mutants revealed an average of 125 bp of telomeric DNA in the junctions (M. Heacock and D. Shippen, unpublished data), more than twice the amount of telomeric DNA recovered from fusions in triple *tert ku70 lig4* mutants. Thus, the presence of KU in *tert lig4* mutants may limit nucleolytic digestion of dysfunctional telomeres (178). It is noteworthy that G-overhang signals in terminal *tert ku70 lig4* mutants are reduced relative to *tert ku70* double mutants. Hence, although critically shortened telomeres lose their ability to effectively block NHEJ, they largely retain their capacity to protect the chromosome terminus.

What is the mechanism for chromosome end-joining in the absence of KU and LIG4? Our sequence analysis reveals that chromosome fusion junctions in *tert ku70 lig4* mutants utilize shorter tracts of microhomology; *tert ku70* mutants employ twice the amount of perfect nucleotide overlap (180). Thus, end-joining by the LIG4-KU independent pathway appears to be mechanistically distinct from the KU-independent

pathway. The MRN complex, which has been implicated in KU-independent fusion of critically shortened telomeres in *Arabidopsis* (180), is known to mediate end-joining primarily through the use of microhomology (146,147) in an alternative pathway only partially dependent on LIG4 (147). As we see only a small difference in the level of microhomology at fusion junctions, we can not rule out the possibility that MRN joins dysfunctional telomeres in KU-LIG4 mutants. Alternatively, end-joining could be mediated through a PARP1/LIG3-dependent pathway akin to what has been described in mammals (136-138). Although there is a clear PARP1 ortholog in the *Arabidopsis* genome, LIG3 is absent. LIG1 could act in combination with *PARP1* to join DNA ends, as *in vitro* studies indicate that the mammalian LIG1 can join double-strand DNA breaks (242). It is also possible that LIG6, a DNA ligase unique to *Arabidopsis* whose function is unknown, substitutes for LIG4 (243).

Whatever the mechanism of end-joining dysfunctional telomeres, the molecular triggers for this reaction appear to be remarkably consistent in the presence or absence of key components of the NHEJ machinery. Our data indicate that *Arabidopsis* telomeres undergo at least two distinct structural changes en route to complete dysfunction. By measuring individual telomere tracts in plants undergoing progressive telomere shortening, we discovered that chromosome fusions are first initiated when the shortest telomere in the population reaches a size of ~ 1 kb. One caveat of our experiments is that the PETRA technique can currently measure telomere lengths on only 7/10 *Arabidopsis* chromosome ends. Thus, it is formally possible that telomeres shorter than 1kb are required to trigger chromosome fusions. Nevertheless, our data argue strongly that telomeres breach a length threshold at or near 1kb. At this point, telomere tracts may be unable to assume a stable t-loop configuration, perhaps due to

the reduced occupancy of some essential telomere binding proteins. An alternative, but not mutually exclusive model is that the reduced occupancy of telomere proteins on the shortened telomere releases the constraints on the telomere-associated DNA damage proteins, allowing them to instigate a DNA damage response that activates repair. Since plants survive for multiple generations after the initial onset of telomere dysfunction and their telomeres continue to shorten, this length threshold does not automatically incite significant genome instability. We speculate that shortened, "meta-stable" telomeres can assume an alternative structure that affords the terminus protection from a full-blown DNA damage response. Such a structure could be a simple fold-back conformation proposed for yeast telomeres (36,244,245). As telomere erosion continues, the incidence of chromosome fusions increases until the telomere tract reaches the minimal length of residual function (~300 bp) (180). Below this second size threshold, all of the features that distinguish the telomere from a DSB are lost.

CHAPTER IV

G-OVERHANGS

Summary

The G-rich strand of telomeric DNA terminates in a 3' single-strand extension known as the G-overhang. G-overhangs are an essential feature of the telomere and are required for formation of the protective structure known as the t-loop. To study factors that contribute to the maintenance of G-overhangs in *Arabidopsis*, we sought to develop an assay that can precisely measure the length of G-overhangs. We describe several strategies towards obtaining a higher resolution assay. We also discuss modifications to the current in-gel hybridization protocol, which is widely used to detect bulk G-overhangs in other systems, to make this assay more reliable and sensitive for studying *Arabidopsis* telomeres. Using in-gel hybridization, we uncovered proteins that make contributions to G-overhang maintenance. We demonstrate that the putative G-overhang binding proteins POT1a, POT1b, and POT1c make modest, but unique, contributions to the G-overhang. The most striking result was obtained for *cit1* mutants. CIT1 is thought to contribute to telomere capping in *Arabidopsis* (Y. Surovetseva et al. unpublished data). In-gel hybridization performed on *cit1* mutants revealed a grossly increased hybridization signal (up to 10-fold higher than wild type). This result strongly indicates that CIT1 plays a crucial role in telomere architecture.

Introduction

Telomeric DNA is comprised of discrete, tandem arrays of TG rich sequences consisting of a double-strand and single-strand component. Both telomeric tracts

terminate in a precise sequence indicative of tight regulation, possibly through the action of nucleases (23,108,109). The TG-rich telomere strand runs 5' to 3' toward the end of the chromosome and terminates in a single-strand extension referred to as the G-overhang. The G-overhang invades the duplex telomeric DNA to form a higher order structure known as the t-loop (31) (Figure 20). G-overhangs are essential for t-loop formation (31). As discussed earlier, the transient DDR that is elicited at the telomere might help facilitate the dynamics of folding and unfolding of the G-overhang.

Although mammals, plants and protozoa utilize a t-loop strategy to hide the natural ends of chromosomes, analogous capping architectures have been discovered in other organisms (34). For example, in budding yeast the telomere is thought to assume a simple fold-back structure. The major advantage of such architectures is that they effectively mask telomere ends, preventing them from being inappropriately recognized as a double-strand break. This chapter will focus on the G-overhang, how it is formed, the factors that contribute to its maintenance and methods we employed to study its status.

G-overhang generation

Removal of the most distal RNA primer after replication by lagging strand synthesis provides a natural G-overhang which is a substrate for telomerase (Figure 21). In contrast, DNA synthesized by leading strand replication produces blunt ends. G-overhangs have been detected on both ends of a chromosome (22,24,28,108,246-248) (249), indicating that an additional mechanism must be in place to generate G-overhangs on blunt ends.

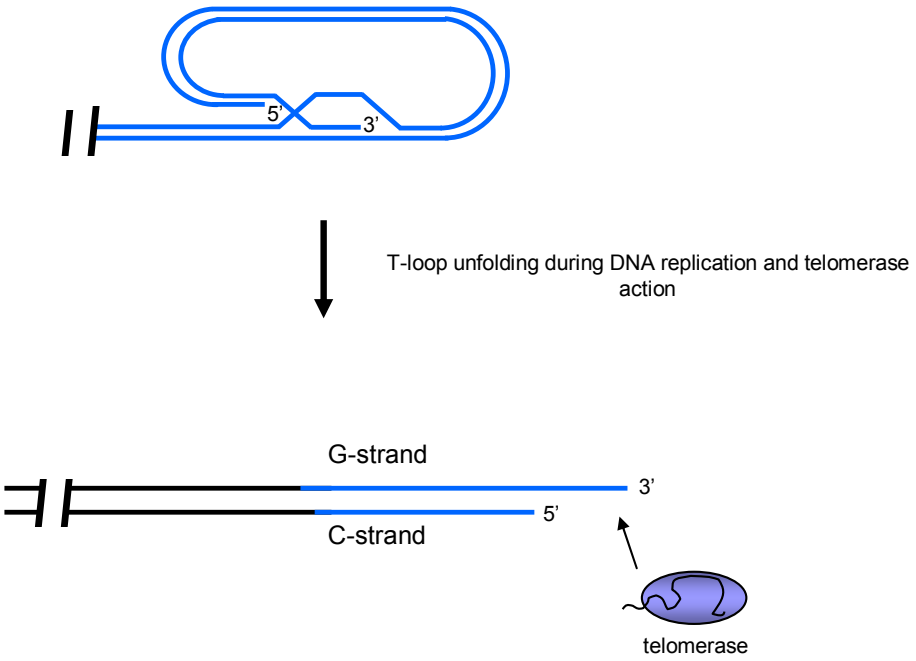

Figure 20. Proposed structure for telomeres.

The 3' G-rich telomere overhang invades and displaces double strand telomeric DNA forming a t-loop. During DNA replication and telomerase action the t-loop is presumed to unfold (bottom). Telomeric DNA in blue, telomerase, purple oval, RNA subunit, swiggly line, non-telomeric DNA is black.

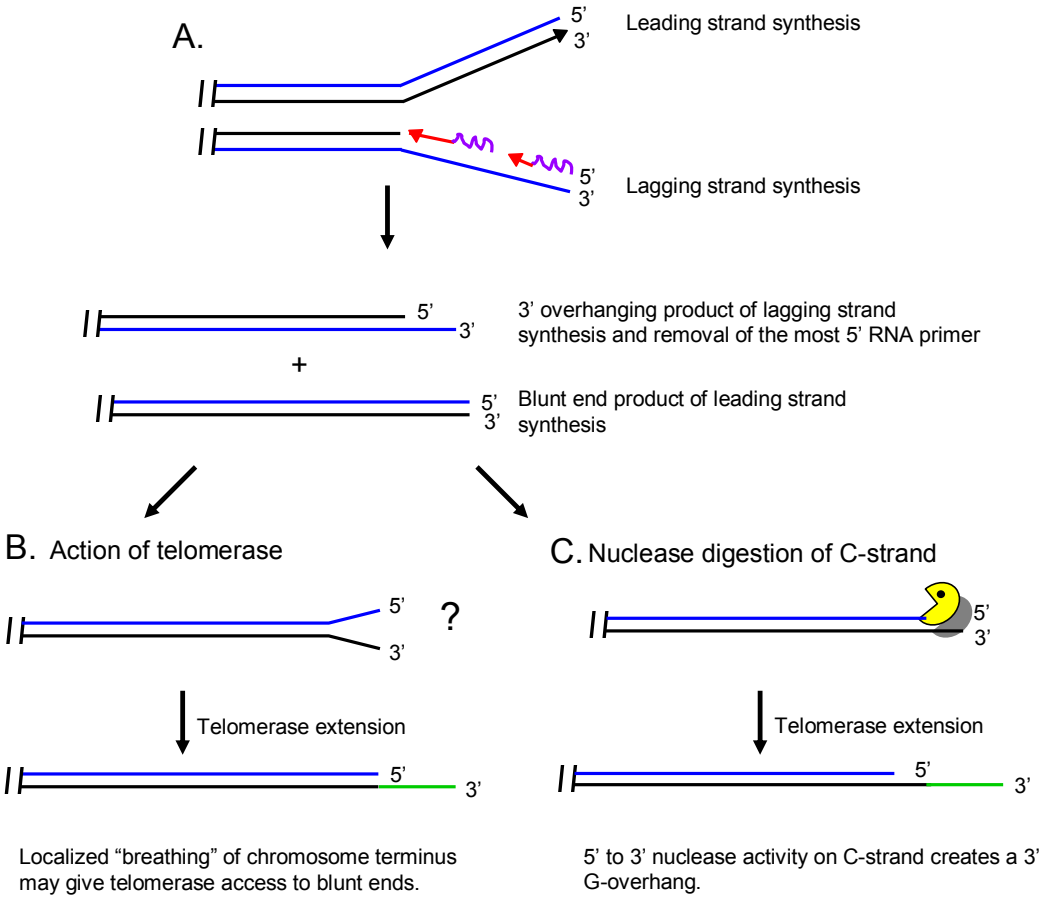

Figure 21. Strategies for G-overhang generation.

(A) The G-rich strand is generated by leading strand synthesis and the C-strand by lagging strand synthesis. Newly-replicated stands are denoted in red and black. Removal of the last RNA primer (shown in purple) results in a G-overhang on the 3' end resulting from lagging strand synthesis. (B) G-overhang on the 3'end resulting from leading strand synthesis would be observed if the DNA underwent breathing to create single-strand DNA that could used by telomerase (telomere addition shown in green). (C) A 5' to 3' nuclease digestion of the C-strand creates a 3' overhang on the G-strand.

Two possibilities for creation of G-overhang include telomerase and nuclease digestion (Figure 21). While blunt ends can not be extended *in vitro* by telomerase (250), a minimum of 4-6 nt are required (250). However, the situation *in vivo* may involve transient breathing of blunt ends providing access for telomerase to extend (Figure 21B). Since telomerase only extends single-strand G-rich DNA, blunt ends would not be a substrate for telomerase (Figure 21B). Importantly, telomerase can not be the sole mechanism of G-overhang generation as G-overhangs are detected in the absence of telomerase (22,117,251). While telomerase plays a role in G-overhang formation, another mechanism for G-overhang formation is nuclease digestion of the C-strand (Figure 21C). One nuclease that has been implicated in generation of G-overhangs on telomeres in wild type cells is the DNA repair protein Mre11. *In vitro* data show that Mre11 possesses 3' to 5' exonuclease activity, but this is the opposite polarity to generate G-overhangs (146). However, *in vivo* studies demonstrate that Mre11 promotes generation of 3' overhangs at DSBs (reviewed in (210,252)). In yeast and human cells, the absence of Mre11 leads to only a partial decrease in G-overhang signals (28,29). One possibility is that Mre11 prepares the chromosome terminus for subsequent recruitment of additional nucleases to the G-overhang. In support of this hypothesis, Mre11 is recruited to telomeres in a cell cycle-dependent manner (30,150) and a deficiency in Mre11 leads to telomere dysfunction in human cells (30,151). Interestingly, studies in budding yeast have shown that the nuclease activity of Mre11 is not required for telomere length maintenance, but is required for de novo telomere addition (253,254).

Although the identity of additional nucleases necessary for generation of G-overhangs is currently unknown at wild type telomeres, nucleases that process

dysfunctional telomeres have been characterized and will be discussed further below. In summary, the G-overhang appears to be created and maintained by a combination of telomerase action to extend pre-existing 3' overhangs and carefully controlled nuclease activity on the C-strand to create this substrate for telomerase.

G-overhang binding proteins

Both double-stranded and single-stranded portions of telomeric DNA are bound by sequence-specific proteins that function in telomere capping and length maintenance (reviewed in (34,76)). G-overhang binding proteins have been implicated in telomerase recruitment, protection of G-overhangs and the entire chromosome ends (reviewed in (255) (Table 9).

The G-overhang binding protein in fission yeast and higher eukaryotes is protection of telomeres (POT1). POT1 encodes two oligosaccharide/oligonucleotide (OB) folds that are required for sequence-specific recognition of single-strand G-rich telomeric DNA (34). In mammals, reduction of POT1 elicits a ten-fold increase in G-overhang signals in one study (114), while another study reported no change (113). These conflicting results may be due to differing amounts of residual POT1 after knockdown. Interestingly, in human cells, POT1 deficiency results in loss of the stringent manner in which the C-strand telomere strands terminate (110). This finding suggests that hPOT1 participates in the precise regulation of terminal nucleotides at telomeres. For example, hPOT1 binding may govern the amount of nuclease digestion at G-overhangs.

Table 9. Proteins that contribute to G-overhang maintenance

Organism	Gene	Mutation	G-overhang signal	Ref.
Single-celled organisms				
Tetrahymena	*POT1a*	CA	NC	Jacob et al. 2007
Tetrahymena	*POT1b*	CA	NC	Jacob et al. 2007
S. cerevisiae	*CDC13*	ts	significant increase is signal	Garvin et al. 1995, Zubko et al. 2004
	STN1	ts	increase in signal	Grandin et al. 2001
	TEN1	ts	increase in signal	Grandin et al. 1997
	KU70	KO	increased signal throughout cell cycle	Gravel et al. 1999, Bertuch and Lundblad 2004
	MRE11	KO	reduction in signal	Larrivee et al. 2004
S. pombe	*POT1*	KO	ND	Baumann and Cech 2000
K. lactis	*KU80*	KO	ND	Carter et al. 2007
Plants				
A. thaliana	*POT1a*	KO	1.5 fold increase	this study
	POT1b	KO	0.5 fold decrease	this study
	POT1c	OE	4 fold decrease in signal in telomere length both variants relative to WT	this study
	KU70	KO	3 fold increase	Riha et al. 2002; this study
	CIT1	PM	6 fold increase in signal	this study
Vertebrates				
H. sapiens	*POT1*	shRNA	2 fold decrease	Hockemeyer et al. 2005, Xin et al. 2007, Yang et al. 2005
M. musculus	*POT1a*	Genetrap	NC	Hockemeyer et al. 2006
		CA	2 fold increase	Wu et al. 2006
	POT1b	Genetrap	10 fold increase	Hockemeyer et al. 2006
		aa change	2 fold decrease	He et al. 2006
DT40 (*G. gallus*)	*POT1*	CA	2-3 fold increase	Churikov et al. 2006
	RAD51	KO	1.5 fold increase	Wei et al. 2002

CA, conditional allele; NC, no change; ND, not determined; ts, temperature sensitive; KO, knockout; OE, overexpression; PM, point mutation; aa, amino acid change.

Arabidopsis is unusual in that it contains three POT1-like proteins: POT1a, POT1b, and POT1c (99,100). The contribution of the *Arabidopsis* POT proteins in G-overhang maintenance has not been assessed until this study.

In budding yeast, the G-overhang is bound by Cdc13 (reviewed in (56)). Bound to Cdc13 are Ten1 and Stn1 proteins that are also involved in maintenance of G-overhangs. A deficiency in Ten1 and Stn1 results in elongated G-overhangs, but not to the extent observed in Cdc13 mutants (102-104,256).

G-overhangs can also be perturbed in response to loss of proteins that protect the C-strand from degradation. Table 9 presents an overview of the proteins that contribute to G-overhang maintenance in various organisms.

Intriguingly, although KU functions in telomere length maintenance in most organisms studied (reviewed in (3)) its role in C-strand protection is limited to budding yeast and plants (116,117,163). The elongated G-overhangs observed in budding yeast lacking KU80 are dependent on Exo1, a 3' to 5' nuclease (257) that has been implicated in processing dysfunctional telomeres (226,256).

In contrast to a KU deficiency, the grossly extended G-overhangs in Cdc13 mutants are only partially generated by Exo 1 (226). In this instance, another, unidentified, nuclease was found to contribute to the extended G-overhangs (256). The nuclease(s) whose action results in increased G-overhang signals in *Arabidopsis ku70* mutants has not been uncovered. Thus, nucleases that promote C-strand resection at dysfunctional telomeres are likely to be distinct from those that process normal telomeres.

The role of the G-overhang in genome integrity

The importance of protecting G-overhangs is reinforced by sequestration of these structures into t-loops (31). When proteins essential for telomere capping are perturbed and the G-overhang becomes accessible, end-to-end chromosome fusions arise in the cell (reviewed in (3)). A prerequisite for telomere-to-telomere fusions is removal of G-overhangs, implying that accessibility of G-overhangs can trigger an end-joining reaction (106). Deliberate G-overhang exposure has been implicated in senescence in human cells (105). One group showed that the G-overhang signal decreases as a consequence of continuous cell division (258), but another group showed that senescent cells do not exhibit any change in G-overhang signal relative to wild-type (259). Thus, the precise role of the G-overhang in maintaining genome stability and cell proliferation is unknown. However, these data indicate that the G-overhang is critical for proper telomere function.

Methods for monitoring G-overhang status

Several assays have been employed to monitor G-overhang status. One method used to estimate the fraction of telomeres that contain a G-overhang is primer extension nick translation (PENT) (217,246). PENT relies on extension of a primer that hybridizes to the G-overhang. Primer extension is performed under non-denaturing conditions using DNA PolI and dGTP is not provided so that extension will stop once non-telomeric sequence is reached, producing a nick. This allows the newly-synthesized telomere strands that contain G-overhangs to be separated from interstitial and telomere tracts without G-overhangs (that have not been primer-extended) by alkaline gel electrophoresis. DNA products are visualized by hybridizing with a G-strand telomeric

probe. This technique has been used to show that telomeres on both ends of the chromosome contain G-overhangs in human cells (246). In *Arabidopsis*, PENT analysis shows that only half of the telomeres contain a G-overhang that is more than 30 nucleotides long (217). This difference could suggest that half of *Arabidopsis* telomeres contain blunt ends, but this assay could not detect G-overhangs less than 30 nucleotides long. Thus, a more likely explanation is asymmetry between leading versus lagging strand G-overhangs as observed in other systems (24,260).

One of the most widely-utilized methods to assay for G-overhangs is in-gel hybridization (25,26). In-gel hybridization has been successfully employed as a standard approach to determine bulk G-overhang signals in most organisms (reviewed in (14)). In in-gel hybridization, G-overhangs are detected using a radiolabeled telomere oligonucleotide that will anneal to the single-strand G-rich telomeric DNA portion of bulk genomic DNA.

The most desirable methods for analyzing G-overhangs should provide precise measurement of G-overhang length. Higher resolution has been attained through ligation and/or primer extension of an oligonucleotide designed to bind the G-overhang. Three methods of this nature were used in this study. They are telomere oligonucleotide primer extension (TOPE), telomere oligonucleotide ligation assay (T-OLA) (261) and ligation-mediated primer extension (LMPE) (24). TOPE involves primer extension of a radiolabeled oligonucleotide that is designed to anneal G-rich telomeric DNA (Figure 22). The products of primer extension are separated from bulk genomic DNA and their size reflects that length of the G-overhang.

In T-OLA, radiolabeled oligonucleotides directed to the G-overhang are annealed along single-stranded DNA (Figure 23). Any oligonucleotides that have

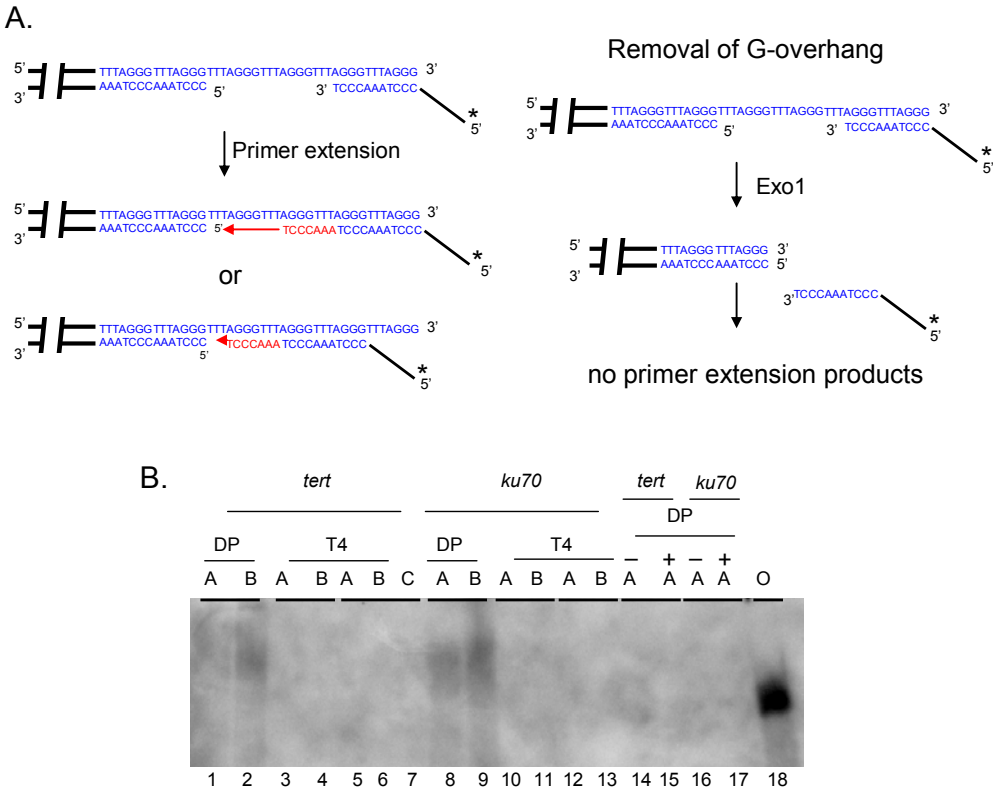

Figure 22. Detection of G-overhangs by Telomere Oligonucleotide Primer Extension (TOPE).

(A) Overview of TOPE. A radiolabeled oligonucleotide (asterisk) is pre-annealed to genomic DNA and primer extended in the presence of DNA PolI or T4 DNA polymerase. Alternate binding of the oligonucleotide is indicated. Incorporation of nucleotides is shown in red. As a control, G-overhangs are removed with Exo1 (right). (B) Results from TOPE. TOPE was performed on DNA isolated from G4 *tert* (lanes 1-7, 14,15) or *ku70* mutants (lanes 8-13, 16,17), followed by primer extension in the presence of DNA PolI (DP) (lanes 1, 2, 8, 14-17) or T4 DNA Pol (T4) (lanes 3-6, 10-13). DNA was mock treated (-) or treated with Exo1(+) to remove G-overhangs (lanes 14-17). Lane 7 is a control containing loading dye. Two DNA concentrations were utilized for reactions shown in lanes 1-6 (A=0.5ug and B=1.5 ug); C=control (no DNA); O=labeled oligonucleotide marker.

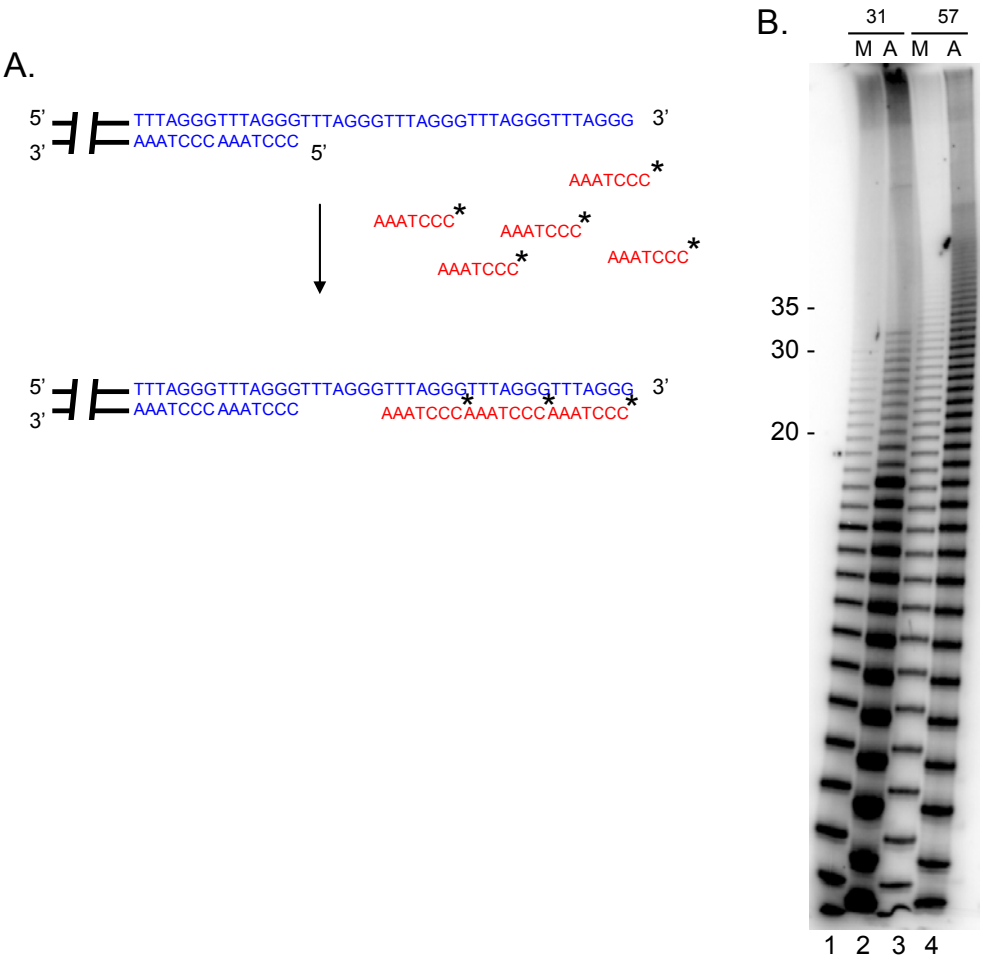

Figure 23. Overview and controls for T-OLA.

(A) Schematic of T-OLA. A 7-mer oligonucleotide containing C-strand, monomer (M), in red, or G-strand, antimonomer (A) telomere repeats is radiolabeled and annealed to genomic DNA. Annealed oligos are ligated using T4 DNA ligase and denatured products are separated in an acrylamide gel (adapted from Barbara Zellinger). (B) T-OLA products have a ladder appearance indicative of differing lengths of ligation products. Results shown are from a denatured plasmid DNA containing 31 (lanes 1,2) or 57 (lanes 3,4) telomere repeats. Number of telomere repeats is indicated on the left.

annealed are ligated and these products produce a ladder-like banding pattern where the higher molecular weight bands correspond to the length of the longest G-overhangs (262).

LMPE differs from T-OLA as primer extension occurs from oligonucleotides that have been ligated onto the end of the G-overhang. Specifically, one of the oligonucleotides contains a protrusion of additional G-telomeric repeats used to help guide the duplex to the G-overhang. This oligonucleotide is used as a site for primer extension. The size of the G-overhang corresponds to the length of these products (24).

Arabidopsis G-overhangs

A combination of in-gel hybridization and PENT has been previously employed to estimate that G-overhangs in *Arabidopsis* are ~ 30 nucleotides long (217). In-gel hybridization has shown that *ku70* mutants exhibit increased G-overhang signals compared to wild type (117). This increase in signal is attributed to a role for KU70 in C-strand protection and not G-overhang elongation as *tert ku70* mutants also show increased G-overhang signals (117). However, the in-gel hybridization protocol used in these studies was not completely reliable and was insufficient to detect a signal in wild type plants (117). As discussed above, PENT showed that ~ half of the telomeres in *Arabidopsis* contain G-overhang signals more than 30 nucleotides long (217). Thus, G-overhangs may be very short on some *Arabidopsis* telomeres, making in-gel hybridization unreliable.

In this study we employed ligation-based strategies to measure G-overhangs. We discuss our efforts to develop a higher resolution assay to detect G-overhangs with

the goal of understanding telomere structure/function as it relates to G-overhangs in *Arabidopsis* to further develop *Arabidopsis*.

Several strategies were employed. The methods we used include TOPE, T-OLA, and LMPE. In addition, I sought to further optimize the in-gel hybridization method. Below I outline our rationale and the results from these approaches. I also discuss data obtained using our modified in-gel hybridization protocol. I also study the effect of different mutations in G-overhangs in *Arabidopsis*.

Materials and methods

Plant growth and DNA preparation

Plants were grown as previously described (180). Genomic DNA was either isolated as previously described (180), or using a GE genomic DNA extraction kit (Heacock et al. submitted).

Telomere oligonucleotide primer extension (TOPE)

1 pmol of radiolabeled PETRA-T oligonucleotide (5' CTCTAGACTGTGAGACTTGGACTACCCTAAACCCT 3') was annealed to either 500ng or 1.5 µg genomic DNA at 25°C for 10 min in a tube containing 240 µM dNTPs, 1 X DNA PolI buffer or T4 DNA Pol buffer. Reactions were primer extended by adding 10 U of DNA PolI (Promega) or 10 U of T4 DNA polymerase (Promega) for 1 h at 16°C (Figure 21 top). G-overhangs were removed prior to primer extension using 20 U of ExoI (USB) at 37°C for 16 h. Primer extension products were separated from genomic DNA by boiling in SDS and separated by electrophoresis in a 10% acrylamide gel.

Ligation-mediated primer extension (LMPE)

LMPE was performed as previously described with some modifications (Wei et al. 2001). In one experiment, guide oligonucleotides were separately annealed to the unique oligonucleotide and ligated onto genomic DNA (Figure 24). 20 pmol of LMPE 1 (unique) oligonucleotide (5' CTCTAGACTGTGAGACTTGGACTA 3') was radiolabeled with 0.1mCi of γ^{32}P-[ATP] using 10 U T4 polynucleotide kinase (Fermentas) and1 X T4 PNK buffer in a 30 µL reaction. The reaction products were purified using a Qiagen column and eluted in 60 µL. Radiolabeled unique oligonucleotides were annealed separately to guide oligonucleotides. Seven different annealing reactions consisted of 7 µL of radiolabeled unique oligonucleotides added to 1.5 pmol of one of seven following guide oligonucleotides: TG1 5' TAGTCCAAGTCTCACAGTCTAGAGCCCTA 3', TG2 5' TAGTCCAAGTCTCACAGTCTAGAGCCTAA 3', TG3 5' TAGTCCAAGTCTCACAGTCTAGAGCCTAAA 3', TG4 5' TAGTCCAAGTCTCACAGTCTAGAGTAAAC 3', TG5 5' TAGTCCAAGTCTCACAGTCTAGAGAAACC 3', TG6 5' TAGTCCAAGTCTCACAGTCTAGAGAACCC 3' or TG7 5' TAGTCCAAGTCTCACAGTCTAGAGTCCCA 3'. Annealing was performed by boiling unique/guide oligonucleotide combinations for 5 min and allowing the reaction to cool to room temperature. 7 µg genomic DNA (previously digested to release the terminal restriction fragment (180), 160 U DNA ligase (NEB), and 1mM ATP were added to annealing reactions and ligated overnight at room temperature. Reactions were either ethanol precipitated or purified using Qiagen columns, resuspended or eluted, respectively, in 30 µL of H_2O and separated by electrophoresis in a 0.9% agarose gel. For another experiment, a mix of guide oligonucleotides were annealed to the unique

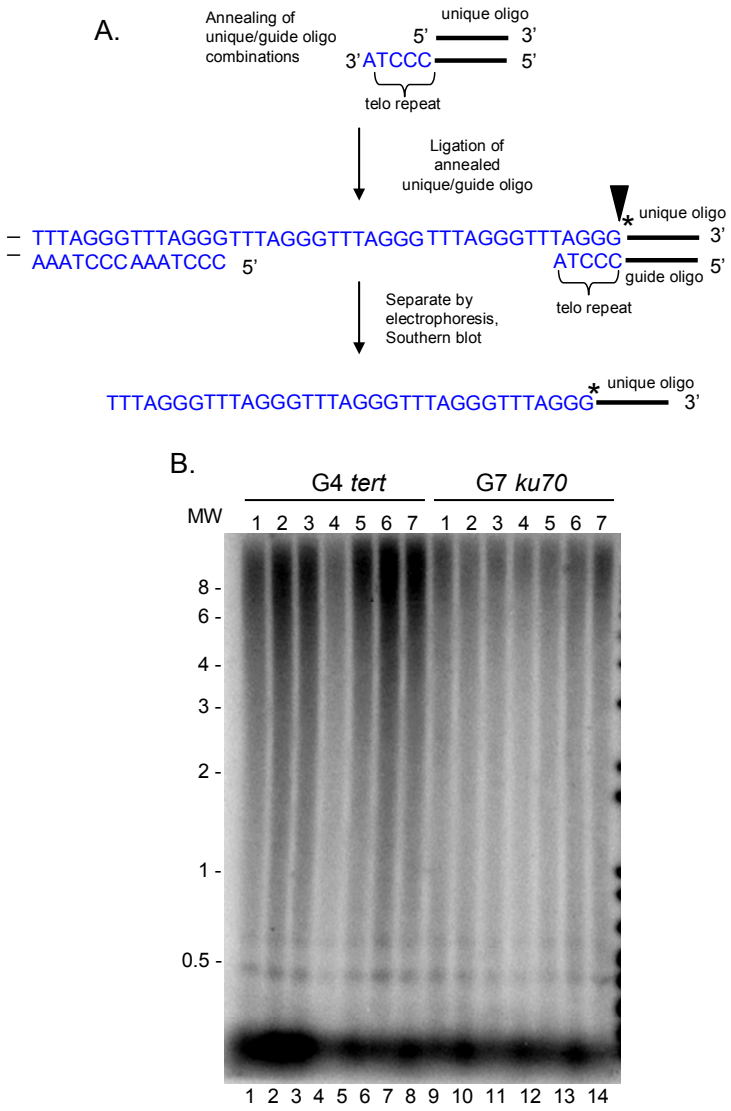

Figure 24. Overview of control ligation to test applicability of LMPE in *Arabidopsis*.

(A) Genomic DNA is digested to release telomeric fragments. Radiolabeled unique oligos are separately annealed to each of the seven guide oligonucleotides (shown in Figure G7; TG1-7). The annealed unique/guide combinations are ligated to genomic DNA, separated by electrophoresis, Southern blotted. Triangle represents the site of ligation. (B) Results of control ligation reactions performed on digested DNA from G4 *tert* mutants (lanes 1-7) and G7 *ku70* mutants (lanes 8-14). DNA was separated in a 0.9% agarose gel. Guide oligonucleotides used are indicated on the top of the gel. Molecular weight markers are shown in kilobase pairs on the left

oligonucleotide and primer extended using genomic DNA extracted using a kit (GE genomic DNA isolation kit) (Figure 25). In this experiment, 2.5 pmol of each of the seven guide oligonucleotides (sequence above) were mixed and radiolabeled as described above and the reaction was eluted in 40 µL of buffer EB (Qiagen). 3.5 µL of radiolabeled guide oligonucleotide mix was annealed to 1.7 pmol of unique oligonucleotide in 10 X ligation buffer using the same conditions as described above. Ligation reactions consisted of ~ 500 ng of genomic DNA, 1 X ligation buffer, 1 mM ATP, and 20 U DNA ligase (Fermentas) in a 50 µL total volume. Ligation reactions were performed overnight at room temperature. Reactions were purified the next day. Proteins were extracted using one-third volume of protein precipitation buffer from the GE DNA extraction kit. Precipitated DNA was resuspended in 40 µL H_2O to be utilized in primer extension reactions. Primer extension was performed in a 50 µL volume, consisting of 250 µM dNTPs, 1 X Klenow buffer and 5 U Klenow minus Exo (Fermentas). Primer extension reactions were purified as described in ligation reactions and resuspended in 20 µL H_2O. Ligation products were separated from genomic DNA by boiling in SDS and separated in a 12 % acrylamide gel. Control reactions included omitting DNA ligase (Figure 25, lane 1) and removing G-overhangs prior to ligation (Figure 25, lanes 3 and 5).

Telomere Oligonucleotide Ligation Assay (T-OLA)

Genomic DNA was extracted as previously described (Heacock et al. submitted). This protocol was provided by the Riha lab as adapted from (258). 10 pmol of the monomer (5’ CCCTAAA 3’) or anti-monomer (5’ GGGATTT 3’) was radiolabeled for 15 min at 37°C using 0.06 miC γ^{32}P-[ATP] in a 20 µL reaction containing 10 U T4 polynucleotide

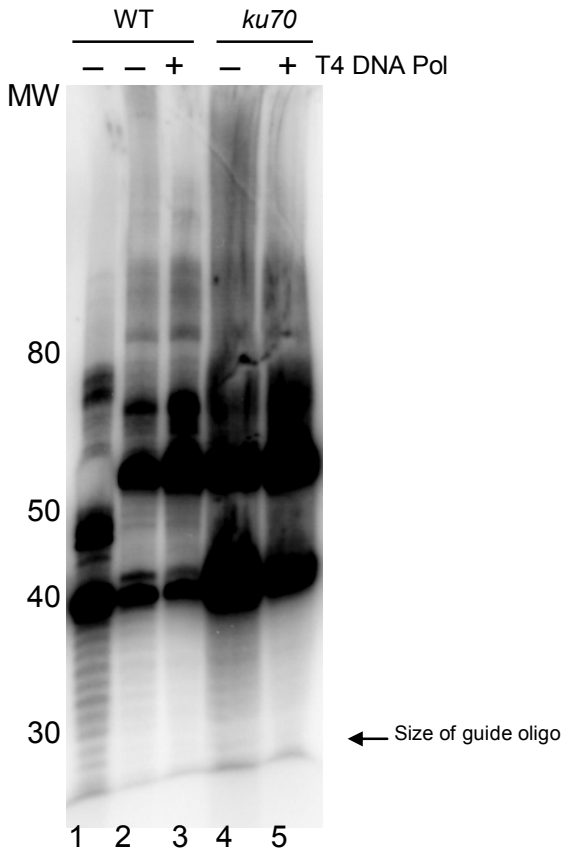

Figure 25. Application of LMPE on *Arabidiopsis* genomic DNA.

LMPE performed on DNA isolated from wild type (lanes 2 and 3) and G7 *ku70* (lanes 4 and 5) plants. A control reaction in the absence of ligase is shown in lane 1. Samples were treated with (+) or without (–) T4 DNA Pol to remove the G-overhang. Molecular weight in base pairs is indicated on the left and the migration position of the guide oligonucleotide is indicated with an arrow on the right.

kinase (Fermentas) and 10 X T4 PNK buffer. Unincorporated γ^{32}P-[ATP] could not be removed as the oligonucleotides are below the size limit and pass through a Qiagen column. ~1 pmol of radiolabeled monomers or anti-monomers were annealed to ~ 500 ng non-denatured genomic DNA at room temperature in a 19 µL reaction containing 1 X T4 DNA ligase buffer. Annealing reactions were ligated for 2 h at 25°C by the addition of 10 U T4 DNA ligase. DNA was extracted from ligation reactions by ethanol precipitation and resuspended in 10 µL of H_2O. 10 µL of formamide loading dye (80 % formamide, 10 mM EDTA, 1 mg/mL xylene cyanol, 1 mg/mL bromophenol blue and 40% sucrose) was added to each sample and ligation reactions are separated from genomic DNA by boiling for 5 min prior to loading into a denaturing 10% polyacrylamide gel. Products were visualized using a STORM phosphorimager (Molecular Dynamics). The highest molecular weight band should reflect the longest G-overhang in the sample. G-overhangs were removed in a 100 µL volume using 20 U Mung bean exonuclease in 1 X Mung bean exonuclease buffer. Digestions were performed overnight at 30°C and DNA was purified by ethanol precipitation. Removal of G-overhangs was verified by the failure to produce products in an independent reaction (PETRA) that requires an intact G-overhang.

In-gel hybridization

In-gel hybridization was performed described (refer to Chapters III and IV).

Results

Telomere oligonucleotide primer extension (TOPE)

Detection of G-overhangs using telomere oligonucleotide primer extension (TOPE) involves primer extension of an oligonucleotide that is bound to the G-overhang. This oligonucleotide is radiolabeled with ^{32}P-ATP and annealed to non-denatured genomic DNA (Figure 22A). The annealed, radiolabeled oligonucleotide is then extended using an enzyme that lacks 5' to 3' exonuclease and strand displacement activities, thereby limiting the substrate to single-stranded G-overhangs. Primer extension products are denatured and separated by electrophoresis in an acrylamide gel. The product size reflects the length of the G-overhang. Since the primer can bind anywhere along the G-overhang, multiple bands are expected where the band with the highest molecular weight reflects the longest G-overhang in the population (Figure 22A).

T4 DNA Pol and DNA Poll were used to primer extend *Arabidopsis* DNA in TOPE. Since DNA Poll possesses 5' to 3' exonuclease activity and therefore can extend into the C-strand, telomere tract products with higher molecular weight should be observed when DNA Poll was employed. As a negative control, G-overhangs were removed with Exo1, a 3' to 5' exonuclease, prior to the annealing reaction. TOPE was performed on DNA obtained from G4 *tert* and G7 *ku70* mutants. As expected, products were observed in primer extension reactions using DNA Poll. However, signals observed in *ku70* mutants were are only slightly stronger compared to *tert* mutants (Figure 22B, compare lanes 1-7 and 8-13) and we did not observe expected size differences in molecular weight, where *ku70* mutants should have an elongated G-overhang (117). In addition, a second problem with TOPE was that no primer extension products resulted when T4 DNA polymerase was used for primer extension (Figure 22B, lanes 3-6, 10-13). This could indicate the presence of very short G-overhangs (i.e. very little substrate available to extend the primer). However, subsequent data obtained

with the T-OLA and in-gel methods (see below) indicate that a more likely explanation is that the 3' to 5' exonuclease activity of T4 DNA Pol removed G-overhangs. Although the TOPE method lacked the necessary specificity to provide useful information about *Arabidopsis* G-overhangs we were able to employ the 3' to 5' exonuclease activity of T4 DNA Pol to remove G-overhangs in the in-gel hybridization protocol (see below).

Telomere Oligonucleotide Ligation Assay (T-OLA)

The Telomere Oligonucleotide Ligation Assay (T-OLA) is another technique that has been used to measure the length of G-overhangs in human cells (258,261). T-OLA involves hybridization of radiolabeled oligonucleotides consisting of two or three telomere repeats, designed to anneal to single-strand G-overhang of non-denatured genomic DNA (261) (Figure 23). Oligonucleotides that perfectly anneal to single-strand G-rich DNA are ligated together. The specificity of this technique is achieved by performing annealing and ligation steps under stringent temperatures (261).

We were provided with a protocol for a modified version of T-OLA by the Riha lab. To test the applicability of this technique in *Arabidopsis*, we performed T-OLA with oligonucleotides that contained either two or three C-rich telomere repeats, a length used in the human cell studies. Unfortunately, we failed to observe ligation products Since *Arabidopsis* G-overhangs are predicted to be only 30 nucleotides long (217), shorter oligonucleotides were used that harbored only one telomere repeat directed to G-strand telomere repeats, dubbed monomer (5' CCCTAAA 3'). As a negative control, an oligonucleotide that was directed at any C-rich overhangs, anti-monomer (5' GGGTAAA 3'), was employed (Figure 23A). Because the G-overhang is G-rich products should only be observed with the monomer. To permit binding of these

smaller oligonucleotides, reactions had to be conducted under less stringent conditions. Figure 23 is a control demonstrating that both monomers and anti-monomers are efficiently ligated to denatured plasmids that contain either 31 or 57 telomere repeats (Figure 23B, lanes 1, 2 and 3, 4 respectively).

T-OLA was performed on *Arabidopsis* genomic DNA isolated from wild type and various mutants. Surprisingly, several independent T-OLA reactions utilizing genomic DNA obtained from wild type and *ku70* mutants, generated products using anti-monomer oligonucleotides (Figure 26A, lanes 4 and 6) indicating that *Arabidopsis* contained single-strand C-rich telomeric DNA. Curiously, anti-monomer products were even stronger than those obtained using the monomer (Figure 26A, compare lanes 4, 6 to 3, 5). These data suggest that both telomere strands must contain single-strand DNA available for binding by monomers and anti-monomers.

As an additional control, T-OLA was performed using single-strand G-rich or C-rich oligonucleotides containing 4 to 8 telomeric repeats. Figure 26B shows that monomers bind when the substrate is a single-strand G-rich telomere repeat (lanes 1, 4 and 5) and, conversely, only anti-monomers bind a single-strand C-rich telomere repeat (Figure 26B, lanes 2 and 3). Thus, monomers and anti-monomers bind the correct telomere substrates. Importantly, we found that products were also observed using monomers and anti-monomers when DNA was digested with a nuclease to remove any overhangs (data not shown). Therefore, ligation of both oligonucleotides is not dependent on the presence of single-strand DNA (see Figure 27 for alternative binding scenarios). The lack of specificity indicates that T-OLA is not a suitable method to study the status of G-overhangs in *Arabidopsis*.

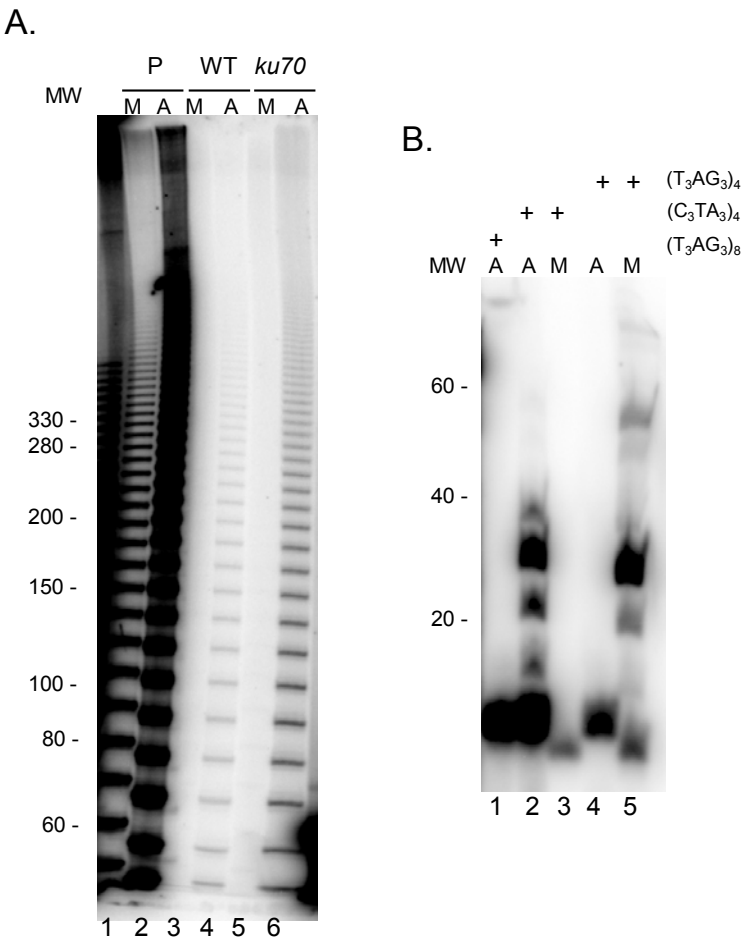

Figure 26. T-OLA performed on *Arabidopsis* DNA.

(A) Shown are results with a control plasmid containing 57 telomere repeats (lanes 1, 2), wild type genomic DNA (lanes 3, 4), G7 *ku70* DNA (lanes 5, 6). Monomer (M) or anti-monomer (A) reactions are indicated. (B) Control reacions to determine specificity of monomer and antimonomer oligonucleotides. T-OLA performed using the oligomer, $(T_3AG_3)_8$ (lane 1), $(C_3TA_3)_4$ (lanes 2, 3) or $(T_3AG_3)_4$ (lanes 4, 5). The oligomer was hybridized with either the monomer (M) or anti-monomer (A) indicated on the top of the gel. Molecular weight markers are shown on the left in base pairs.

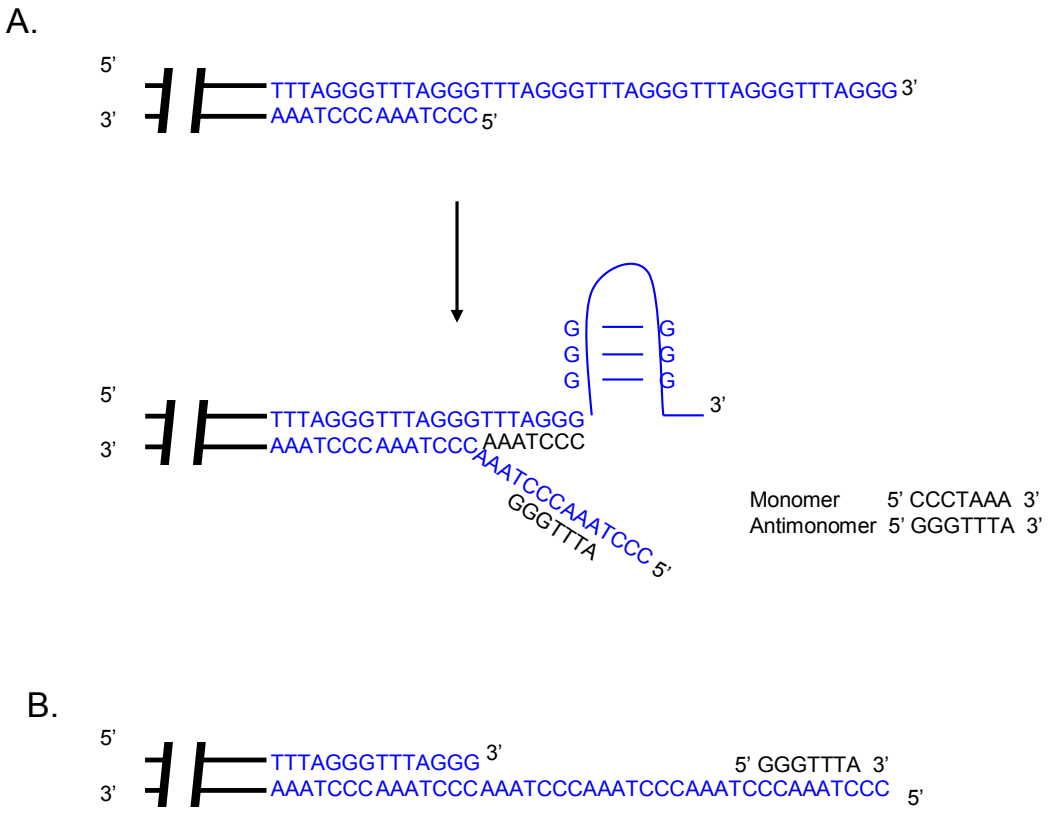

Figure 27. Possible explanations for the observed binding of the anti-monomer to telomeric genomic DNA. (A) G-overhang may form a G-quartet opening duplex DNA where monomer (5' AAATCCC 3') and anti-monomer (5' GGGTTTA 3') can gain access to double-strand telomeric DNA. (B) 5' C-strand overhangs.

Ligation-mediated primer extension (LMPE)

Ligation-mediated primer extension is another high resolution method to measure G-overhang length. Here, an anchor oligonucleotide is ligated onto the end of the G-overhang and is used as a site for primer extension (24). The principles of this assay are outlined in Figure 28. Briefly, a unique oligonucleotide is pre-annealed to a radiolabeled guide oligonucleotide. The guide oligonucleotide is complementary to the unique oligonucleotide in the 5' end, permitting annealing between the two oligonucleotides. The guide oligonucleotide also contains 5 nucleotides of C-strand telomere repeat in the 3' region, facilitating ligation by providing alignment to G-overhangs. Since G-overhangs are reported to terminate in a specific sequence, (24,109) several guide oligonucleotides are utilized to accommodate each permutation of the telomere repeat (Figure 28B). After ligation, guide oligonucleotides are primer extended from genomic DNA, denatured and separated in an acrylamide gel. Primer extension products are observed as a ladder corresponding to varying distances of primer extension, where the highest molecular weight band is the longest G-overhang. The advantage of this technique is that it can precisely measures the length of G-overhangs.

Since LMPE is dependent on several sequential steps, we tested its applicability by first determining if annealed anchor/guide oligonucleotide combinations can be efficiently ligated to G-overhangs in *Arabidopsis*. Radiolabeled unique oligonucleotides were separately annealed to each of the seven guide oligonucleotides (each representing a different permutation of the T_3AG_3 *Arabidopsis* telomere repeat) (Figure 28B). These oligonucleotides reactions were ligated to genomic DNA that had been previously digested to release intact telomere fragments. To test for specificity, we

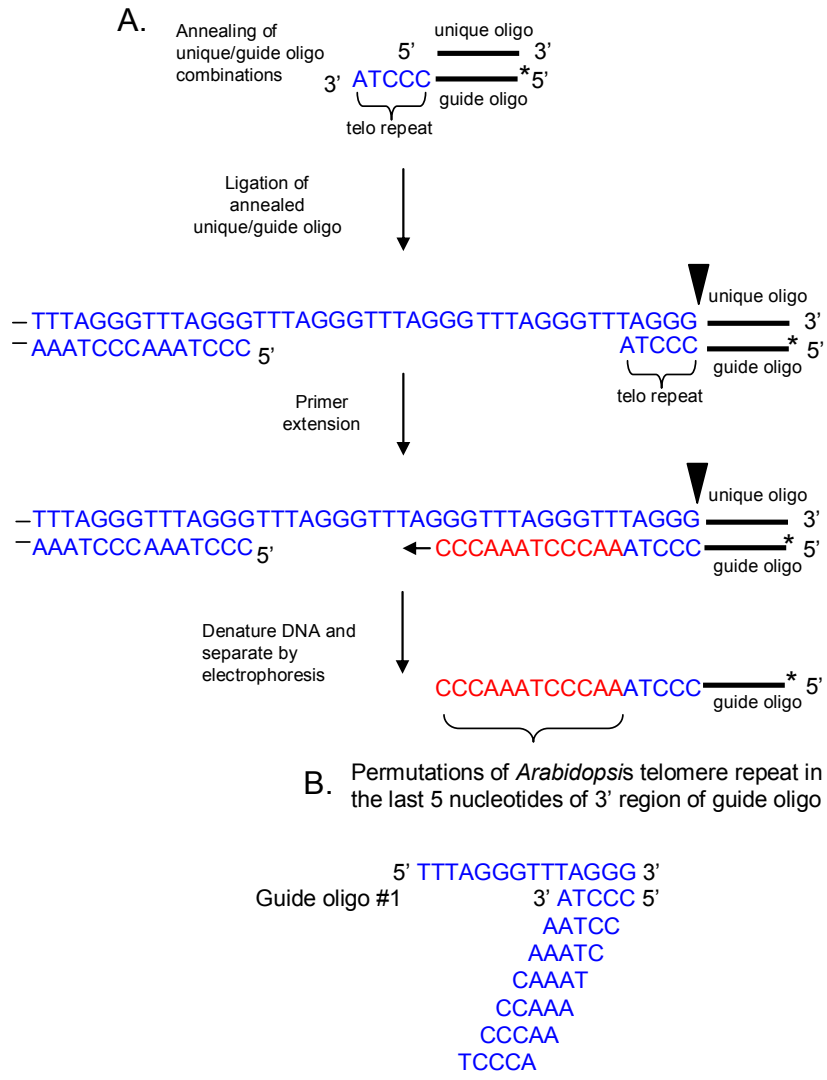

Figure 28. Overview of ligation-mediated primer extension (LMPE).

(A) Schematic of LMPE. A mixture of seven different guide oligonucleotides are radiolabeled and annealed to the guide oligonucleotide. Annealed unique/guide oligonucleotides are ligated to genomic DNA. Guide oligonucleotides are subjected to primer extension in the presence of Klenow fragment that lacks exonuclease activity. Primer extension products are denatured by boiling in SDS and products are separated in an acrylamide gel. Primer extension products are indicated in red. (B) The guide oligonucleotides harboring the seven different permutations of telomeric repeat.

used digested DNA obtained from G7 *ku70* mutants (telomeres above 10 kb in length) and G4 *tert* mutants (telomeres below 4 kb in length), where an obvious size difference should be observed. Figure 24B shows results of seven different ligation reactions for each a telomere permutation and for each genotype. Although hybridization signals were observed in all lanes, they are non-specific as no apparent size difference between *tert* and *ku70* samples was detected (Figure 24B, lanes 1-7 and 8-14 respectively). A similar result was obtained when undigested genomic DNA was employed (data not shown).

To ensure the method of DNA extraction was not the reason for the failure of this assay, we repeated this assay including the primer extension step, using highly-purified DNA (extracted with a GE genomic DNA extraction kit that allowed us to successfully reproduce detection of G-overhangs using in-gel hybridization (see below). The result of one of these experiments is shown in Figure 25. One major concern is that products were detected in reactions where DNA ligase was omitted (Figure 25, lane 1). Bands were also observed in samples where G-overhangs were removed (Figure 25, lanes 3 and 5). In addition, in contrast to previous data (117), the length of the G-overhang in *ku70* mutants was no different than wild type. It is noteworthy that the same DNA used in this assay was successfully used in an in-gel hybridization assay, where all controls worked. Thus, the LMPE method also fails to demonstrate specificity for G-overhangs in *Arabidopsis*.

In-gel hybridization

In-gel hybridization is similar to telomere restriction fragment (TRF) analysis which is used to determine bulk telomere lengths. In TRF analysis, genomic DNA is digested to

release intact telomere tracts and is separated in an agarose gel, denatured and transferred onto a membrane by Southern blotting. Telomere length is determined after hybridization with a radiolabeled oligonucleotide probe complementary to the telomere repeat. In-gel hybridization differs from TRF analysis in that DNA is not denatured or transferred to a membrane. Therefore, hybridization is performed "in-gel" and single-stranded DNA, in this case G-overhangs, should be the only accessible substrate for the C-strand telomere repeat oligonucleotide probe (Figure 29A). A limitation of this technique is it detects bulk single strand telomeres and can not precisely measure G-overhang lengths. As a consequence, subtle changes in length can not be observed.

Several modifications to the in-gel hybridization method enabled us to obtain consistent results from this technique. One major adjustment was to employ a new DNA extraction method. We used a commercially-available DNA extraction kit (GE genomic DNA extraction kit), recommended by the Price lab (111). In addition, to ensure DNA integrity, in-gel analysis was performed using restriction endonucleases that do not promote single-strand nicks and are active at 37°C (T. Cesare, personal communication). Lastly, we included single-strand binding protein during digestion reactions to protect single-strand G-overhangs from degradation (89).

When we performed the modified version of in-gel hybridization, the result was in agreement with previous data obtained in our lab (117). In particular, we were able to detect appropriate molecular weight differences and hybridization signals in G-overhangs between DNA from *ku70* and *tert ku70* mutants (117) (Figure 29B, compare lanes 2 and 4). As expected *ku70* and *tert ku70* mutants exhibited at least a five-fold increase in hybridization signal relative to wild type (Riha and Shippen 2003) (Figure 29B and Table 10). We found that the signal obtained from G-overhangs in *tert* mutants

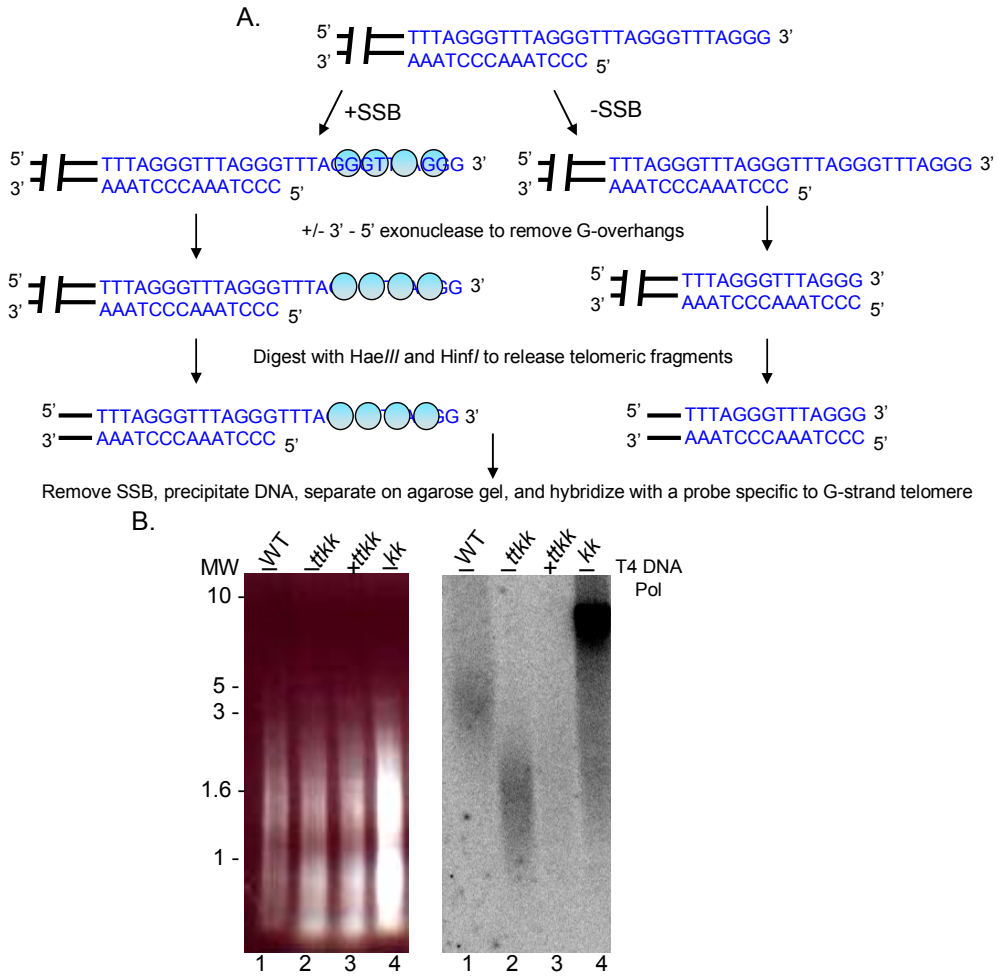

Figure 29. Overview of in-gel hybridization.

(A) Schematic of in-gel hybridization. Single-strand binding protein (blue circles) is added or omitted to genomic DNA. As a control, DNA is treated or untreated with the 3' – 5' exonuclease activity of T4 DNA Pol to remove 3' G-overhangs. DNA is digested with HaeIII and HinfI to release terminal fragments. Proteins are removed and DNA is isolated and separated on a native agarose gel. The agarose gel is dried and an oligonucleotide containing three G-rich telomere repeats is hybridized to single-strand genomic DNA. (B) Results of in-gel analysis for *Arabidopsis* G-overhangs. In-gel analysis performed on genomic DNA isolated from wild type (lane 1), *tert ku 70* (lanes 2 and 3) and *ku 70* mutants (lane 4). DNA treated with the 3' – 5' exonuclease activity of T4 DNA Pol exonuclease is indicated by a plus sign (+) at the top of each lane. Digested DNA is separated on a 0.9% agarose gel and G-overhangs are detected using a radiolabeled oligonucleotide, $(TA_3C_3)_3$. Ethidium stained gel is shown on left.

Table 10. Summary of in-gel analysis[a]

tert	*ku70*	*tert ku70*	*pot 1a*	*pot1a tert*	*pot 1b*	*pot 1a/b*	*POT 1c OE*	*cit1*	
1.9	4.2	0.9	3.3	1.8	0.8	0.8	0.3	3.2	
0.8	2.7	2.8	1.5	1.3	0.5	1.9	0.2	6.8	
0.5		8.0	2.0	0.9		2.0	0.2	3.3	
0.8		8.1	1.3			2.6	0.2	10.3	
0.9		4.8	0.9					4.7	
0.6		4.6	1.0					7.4	
0.5		3.2						5.8	
0.4		3.7							
		9.4							
		8.4							
		1.3							
		1.0							
0.8	3.4	4.7	1.7	1.4	0.7	1.8	0.2	5.9	AVG
0.5	1.1	3.1	0.9	0.4	0.2	0.8	0.1	2.5	SD

[a]Values are expressed as a ratio of hybridization signal intensity relative to wild type, where wild type is set to one. SD, standard deviation.

was only slightly reduced (0.8 fold +/- 0.5) compared to their wild type counterparts (Table 10). Most importantly, for the first time, we were able to consistently obtain a hybridization signal for G-overhangs including wild type plants. These controls provided the confidence to extend analysis of G-overhangs in different genetic backgrounds, and to investigate which telomere-related proteins make major contributions to the status of G-overhangs in *Arabidopsis*.

Loss of ATR does not alter G-overhang status in *Arabidopsis*

Several proteins in the DNA damage pathway are involved in telomere maintenance in *Arabidopsis*. These include KU70, ATM and ATR (117,159,196). ATR, a protein kinase that responds to single-strand DNA, is considered to be one of the master regulators of the DNA damage response (reviewed in (119)). ATR localizes to telomeres in yeast and mammals, and is implicated in telomere length regulation (30,149-151). While a single *atr* mutant does not exhibit a telomere phenotype in *Arabidopsis*, *atr tert* mutants demonstrate accelerated telomere shortening and end-to-end fusions involving telomere tracts (159). This accelerated telomere shortening phenotype is similar to that observed in *Arabidopsis tert ku70* mutants (117), suggesting ATR, like KU70, may be involved in protection of the C-strand telomere tract. To investigate this possibility, we performed in-gel analysis on DNA extracted from *atr* plants. Preliminary results shown in Figure 30 suggest the absence of ATR in plants does not significantly alter the status of G-overhangs: signal intensity is not changed relative to wild type (Figure 30A, lanes 1 and 5). Therefore, it appears that ATR does not act in the same manner as KU to protect the telomeric C-strand.

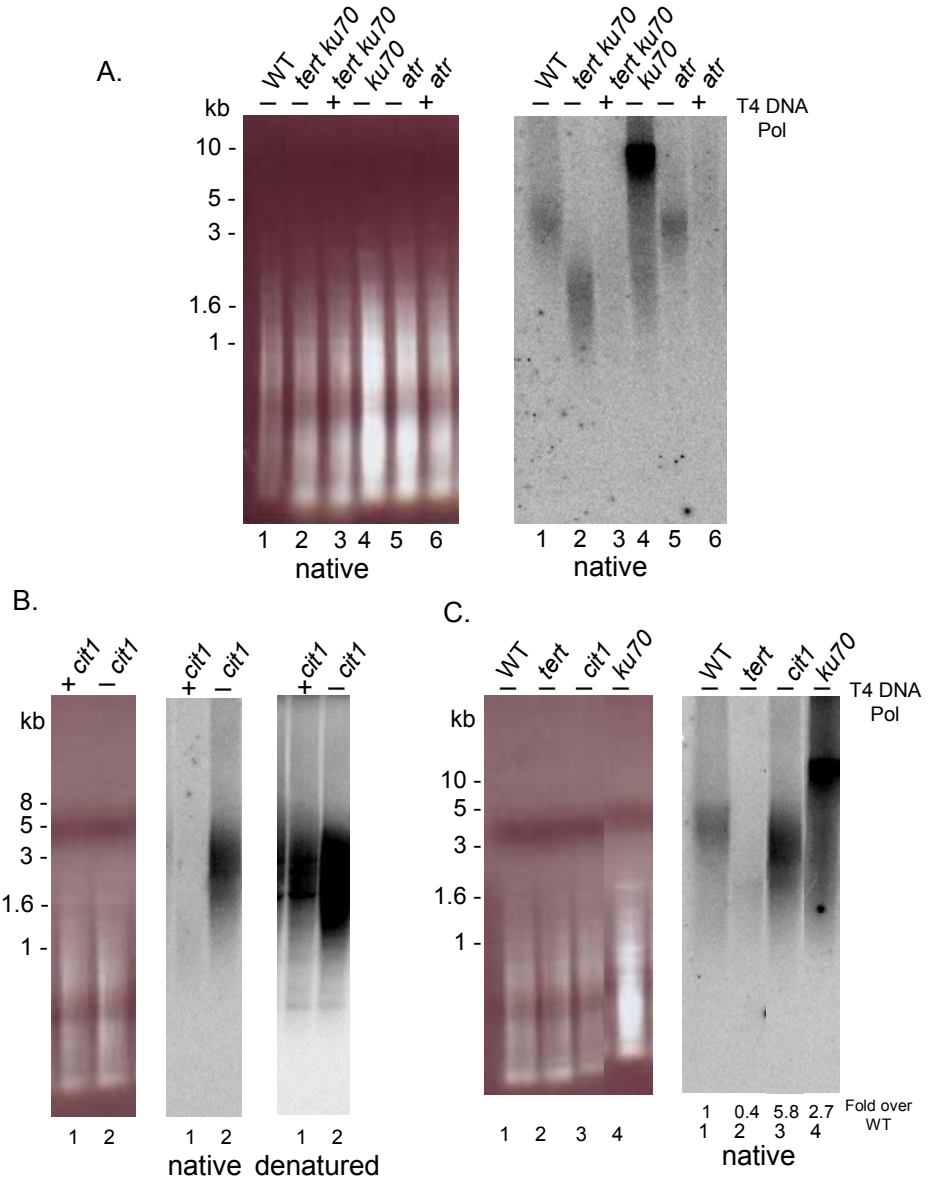

Figure 30. In-gel hybridization of *Arabidopsis* mutants.

Samples were treated (+) or mock-treated (-) with the 3' to 5' exonuclease activity of T4 DNA polymerase as indicated. (A) In-gel hybridization results for different *Arabidopsis* mutants. (B) In-gel hybridization with *cit1* mutants under native (left) and denaturing (right) conditions. (C) Native gel that is quantitated showing that *cit1* and *ku70* mutants have an increased G-overhang signal. Ethidium-stained gels are shown on the left.

POT proteins make distinct contributions to the G-overhang status

In-gel hybridization was also used to determine if *Arabidopsis* POT1 proteins function in maintenance of G-overhangs as observed in other organisms (see Table 9). We found that *pot1a* mutants possess slightly elongated G-overhangs, exhibiting a 1.7 fold (+/- 0.9) increase in overall size of G-overhangs relative to wild type (Table 10). This finding suggests that POT1a makes a small contribution to maintenance of G-overhangs. Interestingly, in-gel analysis of *pot1b* mutants indicates a modest *decrease* in length of G-overhangs, average of 0.7 fold (+/- 0.2) relative to wild-type. These observations indicate that POT1a and POT1b may play opposing roles in G-overhang maintenance where POT1a promotes degradation of the G-overhang and/or inhibits resection of the C-strand. However, in *pot1a pot1b* mutants G-overhang signals are increased over wild type ~ 1.8 fold (+/- 0.8), similar to that observed in single *pot1a* mutants, suggesting that POT1a plays a more dominant role in G-overhang maintenance than POT1b.

We also performed in-gel analysis on DNA obtained from plants containing a POT1c over-expression construct. Relative to wild type, plants harboring this construct exhibit a decreased G-overhang signal, 0.2 fold (+/- 0.1) less than wild-type (Table 10), implicating POT1c in the status of the G-overhang. This observation suggests that POT1c promotes G-overhang digestion and/or inhibits resection of the C-strand.

The *cit1* mutation results in dramatically increased G-overhang signals

G-overhangs were also analyzed from DNA obtained from *cit1* mutants (critical for the integrity of telomeres 1 (CIT1) (Y. Surovesteva and D.Shippen, unpublished data). *cit1* mutants exhibit severe telomere length deregulation and abundant end-to-end fusions, indicating that the gene is essential to multiple facets of telomere biology. In-gel

hybridization performed on DNA extracted from *cit1* plants showed dramatically increased G-overhang signals relative to wild type and *tert* mutants (Figure 30C, compare lane 3 with lanes 1 and 2; Table 10). Figure 30B shows controls for in-gel analysis performed on *cit1* mutants. Hybridization was increased up to 10 fold (avg. ~ 6 fold +/- 2.5) relative to wild-type plants (see Table 10). These data strongly indicate that *CIT1* is essential for G-overhang regulation.

Discussion

Here we discuss the development of reliable and sensitive methods to detect the status of G-overhangs in *Arabidopsis*. We were successful in modifying the current in-gel protocol to make it a useful tool for studying G-overhangs. The main adjustment was utilization of a commercially-available DNA kit. This extraction protocol differs from the commonly used CTAB method in that phenol/chloroform extraction is not employed and all incubations are performed at 37°C instead of 65°C. We speculate that the use of lower temperatures may prevent DNA degradation and breathing of DNA, which could have lowered specificity by allowing telomere oligonucleotides to inappropriately bind melted segments of double-strand telomere DNA. We also postulate that lack of specificity and reliability of the original in-gel protocol may be due to degradation of G-overhangs. To solve this problem, we included single-strand binding protein to protect G-overhangs and we used restriction enzymes that do not nick single-strand DNA ((89) and T. Cesare, personal communication). It is unclear which modification(s) led to success of this technique. Nevertheless, these changes resulted in a more reliable and sensitive method to detect bulk G-overhang signals.

Other ligation-based techniques were employed to evaluate G-overhangs with higher resolution with the goal of determining the length of the G-strand extension. However, these strategies failed to demonstrate any specificity when applied to *Arabidopsis* DNA. Our data indicate products from ligation-based primer extension protocols are non-specific. Non-specific ligation onto DNA ends, as a result of DNA shearing during DNA manipulation can not be ruled out. One essential difference between these protocols and that of in-gel hybridization is that the DNA is electrophoresed prior to hybridization in the later approach. It is tempting to speculate that the process of electrophoresis during in-gel hybridization may actually make G-overhangs more accessible to oligonucleotide hybridization, perhaps by disrupting secondary structures. The fact that the expected size differences in molecular weight were not observed for *tert* and *ku70* mutants indicates that oligonucleotides were not annealed and/or ligated onto telomeres. Therefore, if G-overhangs are inaccessible until DNA is electrophoresed, non-specific products would be favored.

Using the T-OLA method, we unexpectedly found binding of antimonomer oligonucleotides containing G-strand telomere repeats. This could be attributed to less stringent conditions under which hybridization and ligation steps were performed. Alternatively, *Arabidopsis* may actually harbor C-overhangs, as has been reported recently (262,263). C-overhangs reported in Cimino-Reale et al. were observed using T-OLA and were dependent on the presence of 3' single stranded G-rich telomeric DNA. However, the products we observed in the presence of anti-monomers were not sensitive to an exonuclease that removes single-stranded DNA suggesting our products did not reflect binding to a C-strand overhang. Nonetheless, an exploration of potential C-overhangs in *Arabidopsis* is warranted.

Although we were unable to precisely measure the length of individual G-overhangs, the in-gel hybridization method provided some new insight into the role of known telomere proteins in G-overhang maintenance. We speculated ATR could affect the status of G-overhangs as *atr tert* mutants exhibit accelerated telomere shortening similar to *tert ku70* mutants (117,159). However, in-gel hybridization did not result in an increased signal for *atr* mutants, demonstrating that an *atr* deficiency, unlike a *ku70* deficiency, does not grossly affect G-overhang signals. Since it is likely that KU protects the C-strand of the telomere, these data suggest that ATR does not play a similar role. However, it will be important to monitor the status of G-overhangs in *atr tert* mutants to determine whether the accelerated rate of telomere shortening in *atr tert* mutants reflects a *combined* role for ATR and TERT in protection of the chromosome terminus (159).

Our data suggest that *Arabidopsis* POT1a and POT1b may be involved in different aspects of G-overhang maintenance. G-strand hybridization signals are modestly increased in *pot1a* mutants, but are slightly decreased in *pot1b* mutants. These data suggest that POT1a either functions to promote G-overhang degradation and/or to inhibit of C-strand degradation, while POT1b appears to play an opposite role. Nevertheless, because the effect of POT1a and POT1b deficiency on G-overhangs is quite modest, further studies are necessary to explicitly implicate POT1a and POT1b in G-overhang maintenance. In contrast, overexpression studies suggest that POT1c may have a more significant role in regulating processing of C-strands. We find a five-fold decrease in G-overhang signals in these mutants.

It is important to note that these preliminary data suggest POT1a, POT1b and POT1c are not exclusive factors contributing to maintenance of G-overhangs as

complete deregulation is not observed in any of these mutants. A more precise method to detect G-overhangs is necessary to confirm these data and to carefully dissect the contribution of each protein to G-overhang status.

The most striking result we obtained with in-gel hybridization was with *cit1* mutants. These mutants harbor vastly increased G-overhang signals, greater even than *tert ku70* mutants (Figure 30; Table 10). Since *cit1* mutants have not been evaluated in a *tert* background, we can not rule out the possibility that depletion of Cit1 protein promotes G-overhang extension by telomerase. A more likely scenario is that CIT1 protects the C-strand. Loss of coordination of C-strand and G-strand synthesis as seen in Cdc13-deficient budding yeast (264), may also contribute to increased G-overhang signals in these mutants.

Our studies have provided the tools necessary to begin to define proteins that make major contributions to the status of the G-overhang in *Arabidopsis*, and have laid the groundwork to study fundamental aspects of the maintenance of the G-overhang in *Arabidopsis*. Further studies are necessary to understand the details of G-overhang dynamics in *Arabidopsis*.

CHAPTER V

CONCLUSIONS AND FUTURE DIRECTIONS

Telomeres act to protect chromosome ends from being inappropriately recognized as a DSB. When the protective telomere structure is perturbed either through loss of essential TBPs or telomere attrition, telomeres are revealed to DDR proteins. They are then recognized as a DSB (1,78) and are recruited into fusions, most often mediated by DDR proteins of the NHEJ pathway (reviewed in (3)). The genome instability that follows can lead to cellular senescence or full genetic rearrangements that result in tumorigenesis. Further studies of the molecular signatures that distinguish functional and dysfunctional telomeres are necessary to understand how telomeres provide genome stability.

Arabidopsis is a desirable model organism to study telomere dysfunction for several important reasons. One critical feature that distinguishes the *Arabidopsis* genome from other model systems is the presence of unique subtelomeric DNA sequences on a majority of chromosome ends. As discussed in this dissertation, I have employed novel PCR approaches that exploit these unique subtelomere sequences to precisely measure and assay for the participation of specific telomeres in end-to-end fusions. The detailed analysis of individual telomere dynamics gave us new insight into the relationship between telomere length and telomere function.

Arabidopsis is also highly tolerant to genome instability. Plants lacking telomerase can survive even though up to half of their chromosomes are engaged in anaphase bridges (187). This resiliency provides an abundance of material to study telomere dysfunction in the form of end-to-end fusions. Finally, knockouts in telomere-

related genes that are lethal in mammals are often viable in *Arabidopsis*, giving us the ability to uncover roles for these proteins in higher eukaryotes. Together, these features make *Arabidopsis* amenable to study fundamental aspects of telomere biology in a way that is not possible in other model systems.

Identification of two critical telomere lengths that mark distinct transitions to dysfunction

Cells possessing critically shortened telomeres elicit a DDR (1). Recognition of shortened telomeres occurs through accumulation of DDR proteins at chromosome ends, which subsequently leads to the formation of end-to-end fusions. Reports in mammalian systems indicate that the shortest telomeres are most often involved in fusions (185,186). However, these reports are limited in scope because relatively few telomere fusion junctions have been studied and in those that have, it was not possible to precisely determine the telomere length that triggers the fusion. Thus, little was known about how much telomeric DNA is needed for end protection before our studies.

Through exploitation of unique subtelomere regions present in *Arabidopsis*, we were able to develop two novel PCR-based techniques, PETRA and fusion PCR, to study telomere dysfunction in *Arabidopsis*. My analysis uncovered two discrete telomere lengths that appear to represent structural transitions a telomere undergoes as it reaches complete dysfunction (Chapter II and Figure 31).

The sequenced *Arabidopsis* genome indicated that sequences adjacent to telomere sequences were unique on 8/10 chromosome arms (13,214). Further

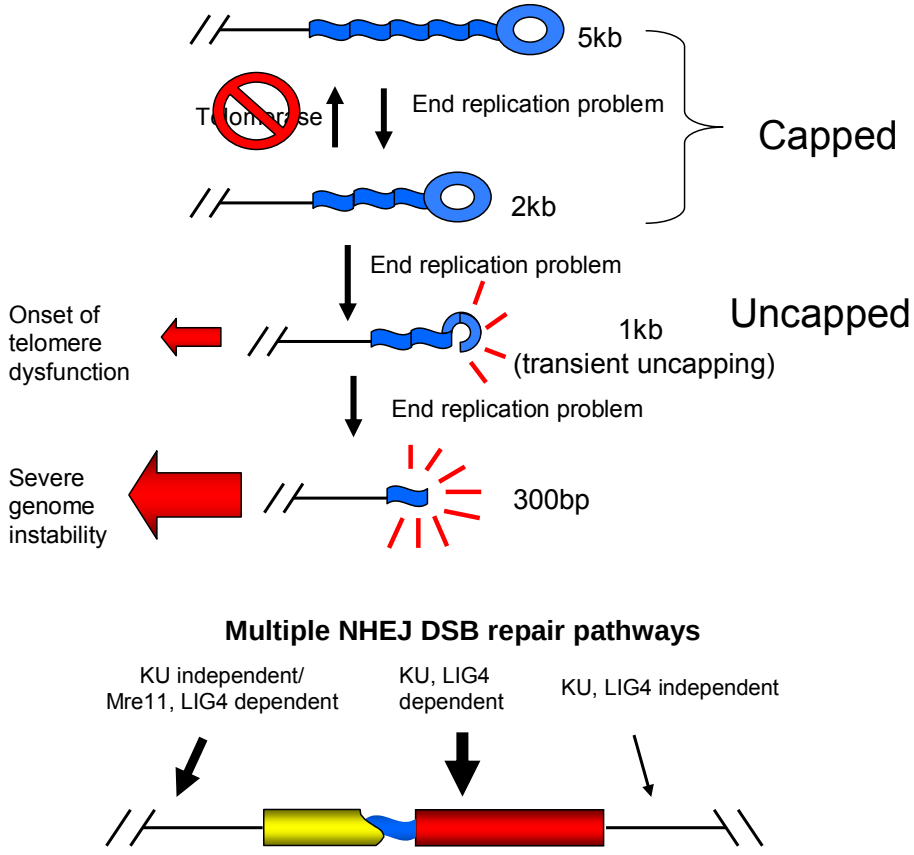

Figure 31. Summary of telomere dynamics in *Arabidopsis*.

Telomeres undergo two critical functional/structural transitions en-route to dysfunction. Telomeres that are between 2 - 5 kb in length are fully capped and refractory to eliciting a DDR, nuclease attack and end-joining. In the absence of telomerase, telomeres progressively shorten, reaching a transient uncapping length at 1 kb, where the onset of end-to-end chromosome fusions is observed. As telomeres continue to shorten, the incidence of fusions increases. Once telomeres reach a length of ~ 300 bp, they are rapidly recruited into fusions. Telomeres are joined by a hierarchy of end-joining mechanisms. KU is the predominant protein that joins dysfunctional telomeres. In the absence of KU, Mre11 is involved in end-joining and relies on microhomology. The robustness of end-joining is revealed by the fact that in the absence of KU and Mre11, telomeres continue to be end-joined. Thus, plants possess multiple pathways for end-joining.

sequencing of *Arabidopsis* subtelomeric regions allowed us to design primers that specifically target particular chromosome arms. By monitoring telomere length on many chromosome arms and simultaneously assessing the presence of fusions I was able to uncover a distinct telomere length at which telomeres begin to fuse. This first transition was observed when telomeres reached a length of ~ 1 kb. This length is likely to represent a structural transition as this same length was observed in a variety of mutants showing telomere fusions including: *tert*, *tert ku70*, *tert ku70 mre11*, *tert lig4* and *tert ku70 lig4.* In addition, even in mutants that exhibit a decrease in the frequency in end-joining (*tert ku70 lig4*), or those that result in accelerated telomere shortening (*tert ku70*), this same transition point was observed.

What is the significance of this length? We propose that at ~1 kb, *Arabidopsis* telomeres can no longer assume a proper capping structure, i.e. a t-loop. Instead an alternative structure is formed, that is not as secure, leading to transient uncapping. We conclude that telomeres are not completely unprotected because not all telomeres fuse when they reach this length. The alternative capping structure may not be conducive to full occupancy of TBPs. In line with this idea, studies in human cells show that TRF2 prefers to bind to ds/ss DNA junctions present in the t-loop structure (32,79). Since TBPs have been shown to block active sites of DDR proteins, this suggests that if TBPs are unable to bind the telomere, DDR proteins are unconstrained and are able to execute their activities on telomeres.

A study in the de Lange lab revealed that overexpression of TRF2 allowed cells to continue to divide even though telomeres were at a length that normally induced senescence (265). This study indicates that TRF2 is limiting at shortened telomeres. The authors speculate that the shortened telomeres may be forming an alternative

structure that TRF2 is unable to bind, requiring excess TRF2 to protect telomeres (265). When applied to *Arabidopsis*, this model would predict that at 1 kb, insufficient TBPs are able to bind the telomere, activating DDR proteins and, in turn, converting the telomere into a substrate for end-joining. Thus, although TBPs protect telomeres from end-joining reactions, their efficient localization is dependent on the telomere structure. We propose that telomeres at 1 kb assume an alternative telomere cap that is metastable (i.e. fluctuating between fully capped and uncapped) due to the inability of TBPs to efficiently associate with this structure.

I identified a second telomere length threshold that marks the onset of complete telomere dysfunction. A functional telomere must have an intact G-overhang. PETRA, an assay requiring the presence of a G-overhang, was used to measure and identify the shortest telomere in plants experiencing the terminal phenotype. Plants that exhibit the terminal phenotype harbor abundant anaphase bridges (up to half of anaphases contain bridges), are developmentally arrested in vegetative growth, and fail to produce seeds (are sterile) (187). Terminal plants from several different genotypes (*tert*, *tert ku70*, *tert ku70 mre11*, and *tert ku70 lig4*) were assessed for the shortest functional telomere. I found that the shortest functional telomere in *Arabidopsis* was consistently ~ 300 bp. We posit that at this length the telomere has completely lost the features that distinguish it from a DSB and it is rapidly recruited into an end-joining reaction. In accordance with this model, analysis of chromosome fusion junctions revealed the average length of the telomere tract retained in the fusion junction was 270 bp. Thus, once telomeres reach ~ 300 bp they are immediately processed by NHEJ machineries.

The fact that the shortest functional telomere in *Arabidopsis* is 300 bp is interesting when one considers that single-celled yeast telomeres are 300 bp. Yeast

telomeres are postulated to form a fold-back structure to cap their ends in lieu of a t-loop (36). Therefore, 300 bp may represent the minimum length necessary to form any type of protective structure. Once telomeres fall below this size they are recognized as a DSB (Figure 31).

Future directions

The localization of DDR proteins to telomeres appears to be a conserved feature of the telomere binding complex (reviewed in (3)). One specific DDR protein likely to reside at *Arabidopsis* is KU. This is based on its role in telomere length regulation (196), G-overhang maintenance (117) and protection against end-joining pathways. A capping role for KU70 in the context of shortened telomeres was revealed when it was discovered that *tert ku70* mutants exhibited ~ 4 fold increase in telomere-to-telomere fusions relative to *ku70* or *tert* mutants (Chapter II). These results agree with previous observations implicating KU70 in telomere biology (117,196,218). Telomere fusions are not present in *ku70* mutants which harbor elongated telomeres, suggesting the elongated telomeres suffice to keep chromosome ends protected. A role for KU in telomere capping is also observed in mice, where KU deficiency leads to telomere fusions (168,193).

Establishing which DDR proteins localize to *Arabidopsis* telomeres will help us understand the role that such factors play in telomere biology. ChIP and immunolocalization can help to identify which DDR proteins localize to telomeres and under what conditions. It is known that DDR proteins reside at wild type telomeres in other systems (reviewed in (3)), and activated DDR proteins (phosphorylated forms of ATM, Mre11 and Nbs1) only transiently localize to telomeres (30,149-151). However,

some proteins involved in signaling the presence of DSBs (e.g. γH2AX and 53BP1) only localize to telomeres in cases of telomere dysfunction (1,78). Therefore, understanding the context in which DDR proteins bind at telomeres may help us determine their functions at chromosome ends.

We would like to know if telomeres that reach the 1 kb threshold activate a DDR. Our model predicts that DDR pathways would not be activated at wild type telomeres, but would initiate at 1 kb telomeres and DDR activation would steadily increase as telomeres become shorter. This hypothesis could be tested through ChIP and immunolocalization using antibodies to the DDR signaling proteins that specifically localize to dysfunctional telomeres (e.g. γH2AX and 53BP1).

We would expect an even stronger association of activated and signaling DDR proteins at *Arabidopsis* telomeres that have reached 300 bp. It will be important to determine whether a prolonged association, as observed in uncapped and critically-shortened telomeres in other systems, is occurring as opposed to the transient association of DDR proteins at wild type telomeres seen in yeast and mammals (30,149-151). A correlation between the appearance of activated and signaling DDR proteins and telomere length could be attained by examining *Arabidopsis* telomere maintenance mutants through the use of PETRA. I predict that the concentration of TBPs would be reduced as telomeres decreased in length (i.e. forming an alternative structure) and that the reduction in TBPs would correlate with an increase in the concentration of activated and signaling DDR proteins at telomeres.

What is the mechanism that prevents DDR proteins from acting on wild type *Arabidopsis* telomeres? In all organisms studied at least one major TBP is responsible for bringing other factors, including DDR proteins, to the telomere and its absence can

result in telomere uncapping (reviewed in Riha et al. 2006). However, bona-fide TBPs remain to be discovered in *Arabidopsis*, although efforts are currently underway to find these proteins in the Shippen lab and elsewhere. When these proteins are identified it will be interesting to know whether they function in a similar manner to other TBPs such as TRF2, which plays dual roles at the telomere by acting in a capping capacity and by safeguarding telomeres against the action of telomere-localized DNA damage proteins (148). In addition, we would like to know whether overexpression of these TBPs would decrease the transient uncapping length, as been observed in human cells (265). If so, this would suggest that the primary cause of telomere dysfunction in *Arabidopsis* is a failure of TBPs to bind to alternative capping structure rather than the presence of very short telomere tracts.

Another outstanding question pertains to the mechanism that leads to an activated DDR at *Arabidopsis* telomeres. Cytological studies in mammalian systems have shown that the shortest telomeres are more apt to be involved in fusions (185,186). A study in *Arabidopsis* used fluorescently-labeled probes targeted to specific subtelomeres to detect which telomeres are involved in anaphase bridges (266). Therefore it may be possible to correlate the results of this type of cytological study with fusion PCR and PETRA to determine if the shortest telomeres are most often involved in fusions. A related question would be: does the presence of the shorter telomeres incite longer, “capped” telomeres into fusions? In other words, would fusions involving telomeres longer than 1 kb only be observed when a telomere less than 1 kb is present? Alternatively, are only those telomeres that have fallen below 1 kb involved in end-to-end fusions? Finally, are the only telomeres in the cell that show DDR localization the ones that are below 1 kb or does the presence of a critically shortened

telomere result in a genome-wide activated DDR? The relationship between these structural/functional transition points and DDR can now be addressed with the tools available in the Shippen lab.

Hierarchy of end-joining pathways used to join dysfunctional telomeres

Although terminal *Arabidopsis tert* mutants (G8 and G9) harbor abundant anaphase bridges (187), there was no direct evidence that these fusions involved telomere tracts. Moreover, there was no information on the mechanistic details for how dysfunctional telomere fuse. My work with fusion PCR revealed that prior to end-joining, telomeres are subjected to degradation. Interestingly, analysis of subtelomeric regions indicated that the degradation was constrained; we did not observe extensive degradation into the subtelomere tracts. In addition, I uncovered a hierarchy of end-joining pathways for dysfunctional telomeres in which KU predominates. In its absence, Mre11 mediates telomere fusions by a MMEJ mechanism (Chapter II, Figure 31). What is particularly striking about these observations is that they were the first to implicate Mre11 in NHEJ in higher eukaryotes, because Mre11 mutations are lethal in mammals (211).

Sequence analysis of the fusion junctions revealed while microhomology is present in all junctions, the average amount microhomology is highest in *tert ku70* mutants (avg. 4.6 bp) versus *tert* (avg. 3.6 bp) and *tert ku70 mre11* mutants (avg. 3.6 bp) (Chapters II and III). Strikingly, plasmid re-joining assays in yeast show that one feature of Mre11-dependent MMEJ is an average use of 5 bp perfect overlap is observed at fusion junctions (267). Thus, my data strongly implicate Mre11 in end-joining in the absence of KU70. While a role for Mre11 in end-joining reactions in *lig4* mutants has not been tested, the observation that an average of 2 bp microhomology is

present in fusion junctions of *tert ku70 lig4* mutants (Chapter III) suggests in the absence of LIG4, Mre11 does not mediate telomere end-joining. Together these data indicate that KU70, Mre11 and LIG4 may operate in a novel pathway distinct from KU-LIG4 independent end-joining.

We find that LIG4 is the predominant enzyme that covalently joins dysfunctional telomeres in *Arabidopsis*. This conclusion is based on decreased fusions, decreased G-overhang signals and a reduction in the amount of telomere repeat in fusions junctions when LIG4 is inactivated (Chapter III, Figure 32). Nonetheless, a back-up pathway for end-joining in the absence of LIG4 exists. DSB repair studies in human cells have shown that components of the base excision repair pathway, specifically PARP1 and LIG3, mediate end-joining in the absence of KU and LIG4 (136-138). While the *Arabidopsis* genome possesses PARP1, no clear homologue for LIG3 exists. However, it is possible that LIG1, an enzyme that joins single-strand breaks, can repair DSBs as LIG4 was found to be able to join one strand at a time (135,242). It remains to be determined which proteins are responsible for end-joining in KU/LIG4 deficient *Arabidopsis* plants.

Curiously, in mammalian cells, uncapped telomeres do not fuse in the absence of LIG4 (2,237). However, critically shortened telomeres are recruited into fusions with the same efficiency as when LIG4 is present (202). Thus, the cell must treat uncapped telomeres differently than telomeres that are critically shortened. One distinguishing feature may be the time during the cell cycle that telomeres become uncapped. Critically-shortened telomeres may experience additional shortening when the

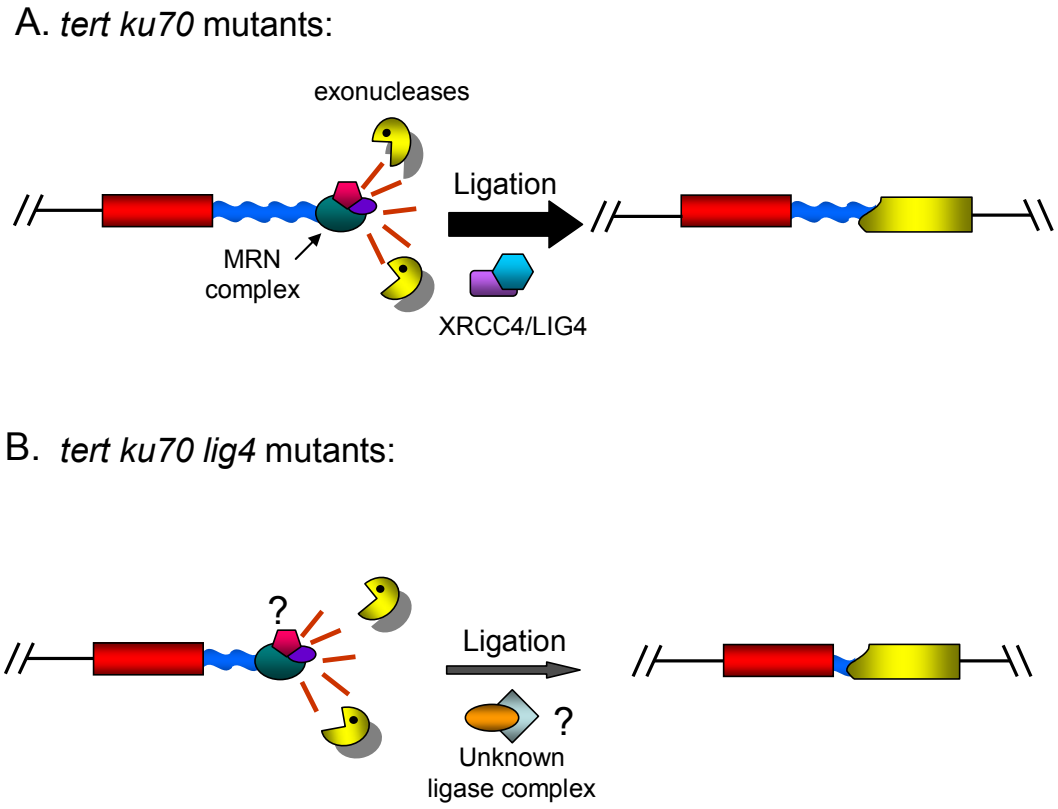

Figure 32. DNA ligase IV (LIG4) plays a key role in end-joining dysfunctional telomeres.

(A) Uncapped telomeres elicit a DNA damage response. LIG4 is recruited to dysfunctional telomeres which protects the ends from excessive degradation prior to fusion. (B) In the absence of LIG4, end-joining of dysfunctional telomeres is less efficient (indicated by narrower arrow), resulting in more degradation of the telomere prior to fusion. Because telomeres fuse even in the absence of LIG4, there must be a LIG4-independent pathway for end-joining, but the components of this pathway are unknown. Red and yellow rectangles denote subtelomeres; blue wavy lines, telomeres.

chromosome terminus is replicated. Thus, the time when a telomere reaches a critical length and loses the ability to form a protective structure is likely to occur at the end of S phase. In contrast, the failure to form a protective cap due to loss of essential TBPs may occur at any stage of the cell cycle. Therefore, it is possible that the choice of DNA repair used to join dysfunctional telomeres differs during the cell cycle. Support for this comes from yeast where the choice of joining DSBs by HR versus NHEJ is cell-cycle dependent (268). An alternative, but not mutually exclusive explanation involves the presence of TBPs. TRF1 remains bound to uncapped telomeres (77). Therefore, the presence of residual TBPs at longer telomere tracts may hinder LIG4-independent end-joining while shorter telomere tracts harbor less TBPs and this may not be as refractory to end-joining.

Finally, Yulia Surovtseva in the Shippen lab has shown that *Arabidopsis cit1* mutants experience rapid onset of telomere dysfunction, suggesting a role for this gene product in telomere capping (Y. Surovtseva et al. unpublished data). Strikingly, *cit1* mutants harbor increased G-overhangs signals (Chapter IV) even though abundant fusions are detected in these mutants (Y. Surovtseva et al. unpublished data). This finding contrasts with results in human cells, where the absence of G-overhangs is associated with telomere uncapping and subsequent telomere fusions (2). Thus, there may be a difference in treatment of uncapped telomeres in human cells versus *Arabidopsis*.

Future directions

One of the steps of DSB repair involves nucleolytic degradation to prepare ends for end-joining (reviewed in (131,206). Similarly, one fate of dysfunctional telomeres is that

they become more prone to nucleolytic attack (185,188). Analysis of subtelomere tracts in plants experiencing telomere dysfunction did not reveal extensive degradation into the subtelomere, even in cases where the frequency of end-joining is reduced (i.e. *tert ku70 lig4* mutants) (Chapter III). This finding is in contrast to what is observed in mice and yeasts where telomeric and subtelomeric tracts are lost prior to fusion (185,188,225). Thus, *Arabidopsis* subtelomeres are somehow protected from extensive nuclease digestion prior to fusion. How this occurs is unclear and may be due to a fundamental difference in the composition of TBPs at *Arabidopsis* telomeres.

To determine if uncapped telomeres and critically-shortened telomeres are differentially treated by the end-joining machinery, a comparison between the two types of telomere dysfunction is required. While a definitive telomere capping protein has not yet been described in plants, one promising candidate is CIT1. A comparison of the telomere fusion frequency of *cit1* versus *cit1 lig4* mutants might reveal if the dependency on LIG4 for telomere end-joining is restricted to uncapped telomeres. If LIG4 is required to join uncapped telomeres, what is the status of G-overhangs? Data from *tert ku70 lig4* mutants, where end-joining is less robust, show that G-overhangs are subjected to modest degradation (Chapter III). If LIG4 is absolutely required to join uncapped telomeres, would a complete loss of G-overhang signal be observed due to exonuclease digestion?

Development of a reliable G-overhang assay for *Arabidopsis*

G-overhangs are an essential feature of the telomere that is required for formation of the protective structure, the t-loop (31). The importance of sequestering the G-overhang is emphasized by the observation that exposure of G-overhangs leads to

telomere end-joining and senescence (2,105,106). G-overhangs have been reported to be asymmetric on different ends of the chromosome, suggesting telomeres replicated by leading versus lagging strand mechanisms are differentially regulated (24,246,248,249,260). Therefore, analysis of the status of the G-overhang is essential to more fully understand how telomeres provide genome stability and promote continued cell proliferation.

I employed several techniques to precisely measure G-overhangs in *Arabidopsis*, including telomere oligonucleotide primer extension (TOPE), telomere oligonucleotide ligation assay (T-OLA), and ligation-mediated primer extension (LMPE) (Chapter III). In all cases, these approaches resulted in non-specific products. One difference in these techniques relative to in-gel hybridization is that G-overhangs are assessed prior to electrophoresis. Perhaps the process of electrophoresis releases some secondary structure constraint, permitting greater access of the probe to the G-overhang.

Although I was unable to develop a strategy to precisely measure *Arabidopsis* G-overhangs, I did develop a sensitive and reliable assay to monitor bulk G-overhangs (Chapter IV). This addition to our toolkit will enable us to further dissect the roles of proteins that are known to contribute to telomere biology.

Using in-gel hybridization, I showed that *Arabidopsis* POT proteins make distinct contributions to G-overhang maintenance. Subtle changes in G-overhang signals for *pot1a* and *pot1b* mutants suggest that these two proteins play opposing roles at *Arabidopsis* G-overhangs. The increased G-strand signal in *pot1a* mutants suggests that POT1a promotes degradation of G-overhangs or inhibits resection of the C-strand. Since POT1a was recently found to promote telomerase activity in *Arabidopsis* (99), it

may assist in G-overhang preparation to allow binding of telomerase to the G-overhang. Conversely, analysis of *pot1b* mutants led to a decreased G-overhang signal. Although this result is subtle, so far this is the only phenotype observed in response to loss of the *POT1b* gene. Finally, overexpression of POT1c resulted in decreased G-overhangs, suggesting that POT1c promotes G-overhang digestion and/or inhibits C-strand resection. This finding suggests that POT1c may function in a similar capacity at G-overhangs as POT1a. Alternatively, because POT1a and POT1c share significant sequence similarity, overexpression of POT1c may simply titrate off POT1a from telomerase leading to a similar G-overhang phenotype. This possibility should be investigated further.

One of the most profound results obtained from G-overhang analysis was in studying *cit1* mutants. In-gel analysis performed on *cit1* mutants revealed a grossly increase in the G-overhang signal, up to 10 times that of wild type. Since telomeres are not elongated in these mutants, CIT1 may protect the C-strand from degradation, a role ascribed to Cdc13 in budding yeast (reviewed in (56)). Interestingly, in addition to an increased G-overhang signal, *cit1* mutants harbor abundant end-to-end fusions, implicating CIT1 in telomere capping (Y. Surovtseva et al. unpublished data). Currently, we can not rule out the possibility that the increased G-overhang signal in *cit1* mutants is dependent on telomerase. Examination of status of *cit1 tert* G-overhangs will be an important experiment to dissect the role of CIT1.

Future directions

In contrast to yeast and mammals, the factors that contribute to the G-overhang in *Arabidopsis* are largely unknown (reviewed in (255)). It is intriguing that G-overhangs are detected on only half of the *Arabidopsis* telomeres using a primer extension method, PENT (an assay that compares hybridization signals between telomeres containing G-overhangs versus those that do not) (217). What structure is present on remaining telomere ends? Since the limit of detection for PENT is 30 nucleotides (217), it is possible that the remaining ends contain overhangs less than 30 nucleotides. In support of this model, several studies report G-overhang length differences between lagging and leading strand telomeres (24,28,246,248,249). To address this issue in *Arabidopsis*, a higher resolution G-overhang assay is needed to determine exact telomere lengths. One major obstacle to overcome is the lack of specificity when higher resolution assays are employed in *Arabidopsis*. Therefore, further optimization is needed to apply these techniques to plant telomeres.

The exonucleases that contribute to G-overhang generation in *Arabidopsis* are unknown. For instance, which exonuclease degrades the C-strand in *ku70* mutants? Is it the same one responsible for increased G-overhang signals observed in *cit1* mutants? Mre11 and Exo1 are known to be involved in G-overhang maintenance (reviewed in (255)). However, the status of G-overhangs remains to be tested in *exo1* and *mre11* mutants in *Arabidopsis*. It is also unclear what factor(s) protect G-overhangs. Preliminary studies in Chapter IV indicate that POT1b makes a small contribution towards G-overhang protection, but additional exonucleases are clearly at play.

Experiments in yeast demonstrate that the length of G-overhangs increases in S-phase (26). Would this same trend be observed in higher eukaryotes? Here, our

synchronized *Arabidopsis* cell culture could be used to assay the status of G-overhangs during different stages of the cell cycle. Finally, do *Arabidopsis* telomeres terminate in a specific sequence as observed in *Tetrahymena* and human cells (24,109)? If so, do any of the *Arabidopsis* POT1 proteins contribute to this maintenance? Although much remains to be discovered regarding maintenance of G-overhangs in *Arabidopsis*, the optimization of the in-gel hybridization technique described in this dissertation has provided a great starting point.

Conclusions

Using a combination of genetic and molecular biology tools that exploit the unusual properties of *Arabidopsis* telomeres, I have participated in the development of novel techniques to examine the dynamics of telomeres and their involvement telomere fusions. These studies have provided new insights into the fate of dysfunctional telomeres and have laid the groundwork for understanding fundamental mechanisms of telomere maintenance and chromosome end protection.

REFERENCES

1. Meier, A., Fiegler, H., Munoz, P., Ellis, P., Rigler, D., Langford, C., Blasco, M.A., Carter, N. and Jackson, S.P. (2007) Spreading of mammalian DNA-damage response factors studied by ChIP-chip at damaged telomeres. *EMBO J*, **26**, 2707-2718.

2. Smogorzewska, A., Karlseder, J., Holtgreve-Grez, H., Jauch, A. and de Lange, T. (2002) DNA ligase IV-dependent NHEJ of deprotected mammalian telomeres in G1 and G2. *Curr. Biol*, **12**, 1635-1644.

3. Riha, K., Heacock, M.L. and Shippen, D.E. (2006) The role of the nonhomologous end-joining DNA double-strand break repair pathway in telomere biology. *Ann. Rev. Genet*, **40**, 237-277.

4. McClintock, B. (1938) The fusion of broken chromosome ends of sister half-chromatids following chromatid breakage at meiotic anaphases. *Missouri Agr. Exp. Sta. Res. Bull,* **290**, 1–48.

5. Muller, H.J. (1938) The remaking of chromosomes. *Collecting Net*, **8**, 182-198.

6. McClintock, B. (1941) The stability of broken ends of chromosomes in *Zea mays*. *Genetics*, **26**, 234-282.

7. Killan, A., Heller, K. and Kleinhofs, A. (1998) Development patterns of telomerase activity in barley and maize. *Plant Mol. Biol*, **37**, 621-628.

8. Olovnikov, A.M. (1971) [Principle of marginotomy in template synthesis of polynucleotides]. *Doklady Akademii nauk SSSR*, **201**, 1496-1499.

9. Watson, J.D. (1972) Origin of concatemeric T7 DNA. *Nature: New Biology*, **239**, 197-201.

10. Blackburn, E.H. and Gall, J.G. (1978) A tandemly repeated sequence at the termini of the extrachromosomal ribosomal RNA genes in *Tetrahymena*. *J. Mol. Biol*, **120**, 33-53.

11. Szostak, J.W. and Blackburn, E.H. (1982) Cloning yeast telomeres on linear plasmid vectors. *Cell*, **29**, 245-255.

12. Moyzis, R.K., Buckingham, J.M., Cram, L.S., Dani, M., Deaven, L.L., Jones, M.D., Meyne, J., Ratliff, R.L. and Wu, J.R. (1988) A highly conserved repetitive DNA sequence, (TTAGGG)n, present at the telomeres of human chromosomes. *Proc. Natl. Acad. Sci. USA*, **85**, 6622-6626

.

13. Richards, E.J. and Ausubel, F.M. (1988) Isolation of a higher eukaryotic telomere from *Arabidopsis thaliana*. *Cell*, **53**, 127-136.

14. LeBel, C. and Wellinger, R.J. (2005) Telomeres: what's new at your end? *J. Cell Sci*, **118**, 2785-2788.

15. Allshire, R.C., Dempster, M. and Hastie, N.D. (1989) Human telomeres contain at least three types of G-rich repeat distributed non-randomly. *Nucleic Acids Re.*, **17**, 4611-4627.

16. Kobryn, K. and Chaconas, G. (2001) The circle is broken: telomere resolution in linear replicons. *Curr. Opin. Microbiol,* **4**, 558-564.

17. Biessmann, H., Valgeirsdottir, K., Lofsky, A., Chin, C., Ginther, B., Levis, R.W. and Pardue, M.L. (1992) HeT-A, a transposable element specifically involved in "healing" broken chromosome ends in *Drosophila melanogaster*. *Mol. Cell Biol*, **12**, 3910-3918.

18. Reddel, R.R. (2003) Alternative lengthening of telomeres, telomerase, and cancer. *Cancer Lett*, **194**, 155-162.

19. Teng, S.C. and Zakian, V.A. (1999) Telomere-telomere recombination is an efficient bypass pathway for telomere maintenance in *Saccharomyces cerevisiae*. *Mol. Cell Biol*, **19**, 8083-8093.

20. Le, S., Moore, J.K., Haber, J.E. and Greider, C.W. (1999) RAD50 and RAD51 define two pathways that collaborate to maintain telomeres in the absence of telomerase. *Genetics*, **152**, 143-152
.

21. Lundblad, V. and Blackburn, E.H. (1993) An alternative pathway for yeast telomere maintenance rescues est1- senescence. *Cell*, **73**, 347-360.

22. Dionne, I. and Wellinger, R.J. (1996) Cell cycle-regulated generation of single-stranded G-rich DNA in the absence of telomerase. *Proc. Natl. Acad. USA,* **93**, 13902-13907.

23. Jacob, N.K., Kirk, K.E. and Price, C.M. (2003) Generation of telomeric G strand overhangs involves both G and C strand cleavage. *Mol. Cell*, **11**, 1021-1032.

24. Jacob, N.K., Skopp, R. and Price, C.M. (2001) G-overhang dynamics at *Tetrahymena* telomeres. *EMBO J*, **20**, 4299-4308
.

25. Wellinger, R.J., Wolf, A.J. and Zakian, V.A. (1992) Use of non-denaturing Southern hybridization and two dimensional agarose gels to detect putative intermediates in telomere replication in *Saccharomyces cerevisiae*. *Chromosoma*, **102**, S150-156.

26. Wellinger, R.J., Wolf, A.J. and Zakian, V.A. (1993) *Saccharomyces* telomeres acquire single-strand TG1-3 tails late in S phase. *Cell*, **72**, 51-60.

27. Wellinger, R.J., Ethier, K., Labrecque, P. and Zakian, V.A. (1996) Evidence for a new step in telomere maintenance. *Cell*, **85**, 423-433.

28. Chai, W., Sfeir, A.J., Hoshiyama, H., Shay, J.W. and Wright, W.E. (2006) The involvement of the Mre11/Rad50/Nbs1 complex in the generation of G-overhangs at human telomeres. *EMBO Rep*, **7**, 225-230.

29. Larrivee, M., LeBel, C. and Wellinger, R.J. (2004) The generation of proper constitutive G-tails on yeast telomeres is dependent on the MRX complex. *Genes Dev*, **18**, 1391-1396.

30. Verdun, R.E., Crabbe, L., Haggblom, C. and Karlseder, J. (2005) Functional human telomeres are recognized as DNA damage in G2 of the cell cycle. *Mol. Cell*, **20**, 551-561.

31. Griffith, J.D., Comeau, L., Rosenfield, S., Stansel, R.M., Bianchi, A., Moss, H. and de Lange, T. (1999) Mammalian telomeres end in a large duplex loop. *Cell*, **97**, 503-514.

32. Stansel, R.M., de Lange, T. and Griffith, J.D. (2001) T-loop assembly in vitro involves binding of TRF2 near the 3' telomeric overhang. *EMBO J*, **20**, 5532-5540.

33. Wang, R.C., Smogorzewska, A. and de Lange, T. (2004) Homologous recombination generates T-loop-sized deletions at human telomeres. *Cell*, **119**, 355-368.

34. Wei, C. and Price, M. (2003) Protecting the terminus: t-loops and telomere end-binding proteins. *Cell Mol. Life Sci*, **60**, 2283-2294.

35. Tomaska, L., Willcox, S., Slezakova, J., Nosek, J. and Griffith, J.D. (2004) Taz1 binding to a fission yeast model telomere: formation of telomeric loops and higher order structures. *J. Biol. Chem*, **279**, 50764-50772.

36. Grunstein, M. (1997) Molecular model for telomeric heterochromatin in yeast. *Curr. Opin. Cell Biol*, **9**, 383-387.

37. Greider, C.W. and Blackburn, E.H. (1985) Identification of a specific telomere terminal transferase activity in *Tetrahymena* extracts. *Cell*, **43**, 405-413.

38. Autexier, C. and Lue, N.F. (2006) The structure and function of telomerase reverse transcriptase. *Ann. Rev. Biochem*, **75**, 493-517.

39. Feng, J., Funk, W.D., Wang, S.S., Weinrich, S.L., Avilion, A.A., Chiu, C.P., Adams, R.R., Chang, E., Allsopp, R.C., Yu, J. *et al.* (1995) The RNA component of human telomerase. *Science*, **269**, 1236-1241.

40. Legassie, J.D. and Jarstfer, M.B. (2006) The unmasking of telomerase. *Structure*, **14**, 1603-1609.

41. Armbruster, B.N., Banik, S.S., Guo, C., Smith, A.C. and Counter, C.M. (2001) N-terminal domains of the human telomerase catalytic subunit required for enzyme activity *in vivo*. *Mol. Cell. Biol*, **21**, 7775-7786.

42. Beattie, T.L., Zhou, W., Robinson, M.O. and Harrington, L. (2000) Polymerization defects within human telomerase are distinct from telomerase RNA and TEP1 binding. *Mol. Biol. Cell*, **11**, 3329-3340.

43. Friedman, K.L. and Cech, T.R. (1999) Essential functions of amino-terminal domains in the yeast telomerase catalytic subunit revealed by selection for viable mutants. *Genes Dev*, **13**, 2863-2874.

44. Lai, C.K., Mitchell, J.R. and Collins, K. (2001) RNA binding domain of telomerase reverse transcriptase. *Molecular and cellular biology*, **21**, 990-1000.

45. Lue, N.F. (2004) Adding to the ends: what makes telomerase processive and how important is it? *Bioessays*, **26**, 955-962.

46. Autexier, C. and Greider, C.W. (1995) Boundary elements of the *Tetrahymena* telomerase RNA template and alignment domains. *Genes Dev,* **9**, 2227-2239.

47. Tzfati, Y., Fulton, T.B., Roy, J. and Blackburn, E.H. (2000) Template boundary in a yeast telomerase specified by RNA structure. *Science*, **288**, 863-867.

48. Tomlinson, R.L., Ziegler, T.D., Supakorndej, T., Terns, R.M. and Terns, M.P. (2006) Cell cycle-regulated trafficking of human telomerase to telomeres. *Mol. Biol. Cell*, **17**, 955-965.

49. Seimiya, H., Sawada, H., Muramatsu, Y., Shimizu, M., Ohko, K., Yamane, K. and Tsuruo, T. (2000) Involvement of 14-3-3 proteins in nuclear localization of telomerase. *EMBO J*, **19**, 2652-2661.

50. Cohen, S.B., Graham, M.E., Lovrecz, G.O., Bache, N., Robinson, P.J. and Reddel, R.R. (2007) Protein composition of catalytically active human telomerase from immortal cells. *Science*, **315**, 1850-1853.

51. Counter, C.M., Hirte, H.W., Bacchetti, S. and Harley, C.B. (1994) Telomerase activity in human ovarian carcinoma. *Proc. Natl. Acad. Sci. USA,* **91**, 2900-2904.

52. Wright, W.E., Piatyszek, M.A., Rainey, W.E., Byrd, W. and Shay, J.W. (1996) Telomerase activity in human germline and embryonic tissues and cells. *Dev. Gen*, **18**, 173-179.

53. Fitzgerald, M.S., Riha, K., Gao, F., Ren, S., McKnight, T.D. and Shippen, D.E. (1999) Disruption of the telomerase catalytic subunit gene from *Arabidopsis* inactivates telomerase and leads to a slow loss of telomeric DNA. *Proc. Natl. Acad. Sci. USA*, **96**, 14813-14818.

54. Cong, Y.S., Wright, W.E. and Shay, J.W. (2002) Human telomerase and its regulation. *Microbiol. Mol. Biol. Rev*, **66**, 407-425.

55. Nakamura, T.M., Morin, G.B., Chapman, K.B., Weinrich, S.L., Andrews, W.H., Lingner, J., Harley, C.B. and Cech, T.R. (1997) Telomerase catalytic subunit homologs from fission yeast and human. *Science*, **277**, 955-959.

56. Smogorzewska, A. and de Lange, T. (2004) Regulation of telomerase by telomeric proteins. *Ann. Rev. Biochem*, **73**, 177-208.

57. Karamysheva, Z., Wang, L., Shrode, T., Bednenko, J., Hurley, L.A. and Shippen, D.E. (2003) Developmentally programmed gene elimination in *Euplotes crassus* facilitates a switch in the telomerase catalytic subunit. *Cell*, **113**, 565-576.

58. Wong, J.M., Kusdra, L. and Collins, K. (2002) Subnuclear shuttling of human telomerase induced by transformation and DNA damage. *Nature Cell Biol*, **4**, 731-736.

59. Kramer, K.M. and Haber, J.E. (1993) New telomeres in yeast are initiated with a highly selected subset of TG1-3 repeats. *Genes Dev*, **7**, 2345-2356.

60. Hug, N. and Lingner, J. (2006) Telomere length homeostasis. *Chromosoma*, **115**, 413-425.

61. Blackburn, E.H. (2001) Switching and signaling at the telomere. *Cell*, **106**, 661-673.

62. Bianchi, A. and Shore, D. (2007) Early replication of short telomeres in budding yeast. *Cell*, **128**, 1051-1062.

63. Hayflick, L. (1965) The Limited in Vitro Lifetime of Human Diploid Cell Strains. *Exp. Cell Res*, **37**, 614-636.

64. Cosme-Blanco, W., Shen, M.F., Lazar, A.J., Pathak, S., Lozano, G., Multani, A.S. and Chang, S. (2007) Telomere dysfunction suppresses spontaneous tumorigenesis in vivo by initiating p53-dependent cellular senescence. *EMBO Rep*, **8**, 497-503.

65. Feldser, D.M. and Greider, C.W. (2007) Short telomeres limit tumor progression in vivo by inducing senescence. *Cancer Cell*, **11**, 461-469.

66. Verdun, R.E. and Karlseder, J. (2007) Replication and protection of telomeres. *Nature*, **447**, 924-931.

67. Bhattacharyya, M.K. and Lustig, A.J. (2006) Telomere dynamics in genome stability. *Trends Biochem. Sci*, **31**, 114-122.

68. Li, B. and Lustig, A.J. (1996) A novel mechanism for telomere size control in *Saccharomyces cerevisiae*. *Genes Dev,* **10**, 1310-1326.

69. Watson, J.M. and Shippen, D.E. (2007) Telomere rapid deletion regulates telomere length in *Arabidopsis thaliana*. *Mol. Cell Biol*, **27**, 1706-1715.

70. Johnson, J.E. and Broccoli, D. (2007) Telomere maintenance in sarcomas. *Curr. Opin. Oncol*, **19**, 377-382.

71. Crabbe, L. and Karlseder, J. (2005) In the end, it's all structure. *Curr. Mol. Med,* **5**, 135-143.

72. Grossi, S., Puglisi, A., Dmitriev, P.V., Lopes, M. and Shore, D. (2004) Pol12, the B subunit of DNA polymerase alpha, functions in both telomere capping and length regulation. *Genes Dev*, **18**, 992-1006.

73. Marcand, S., Brevet, V. and Gilson, E. (1999) Progressive cis-inhibition of telomerase upon telomere elongation. *EMBO J,* **18**, 3509-3519.

74. Marcand, S., Gilson, E. and Shore, D. (1997) A protein-counting mechanism for telomere length regulation in yeast. *Science*, **275**, 986-990.

75. Ray, S., Karamysheva, Z., Wang, L., Shippen, D.E. and Price, C.M. (2002) Interactions between telomerase and primase physically link the telomere and chromosome replication machinery. *Mol. Cell. Biol*, **22**, 5859-5868.

76. de Lange, T. (2005) Shelterin: the protein complex that shapes and safeguards human telomeres. *Genes Dev,* **19**, 2100-2110.

77. van Steensel, B., Smogorzewska, A. and de Lange, T. (1998) TRF2 protects human telomeres from end-to-end fusions. *Cell*, **92**, 401-413.

78. Takai, H., Smogorzewska, A. and de Lange, T. (2003) DNA damage foci at dysfunctional telomeres. *Curr. Biol*, **13**, 1549-1556.

79. Fouche, N., Cesare, A.J., Willcox, S., Ozgur, S., Compton, S.A. and Griffith, J.D. (2006) The basic domain of TRF2 directs binding to DNA junctions irrespective of the presence of TTAGGG repeats. *J.Biol. Chem*, **281**, 37486-37495.

80. Bradshaw, P.S., Stavropoulos, D.J. and Meyn, M.S. (2005) Human telomeric protein TRF2 associates with genomic double-strand breaks as an early response to DNA damage. *Nat. Genet*, **37**, 193-197.

81. Williams, E.S., Stap, J., Essers, J., Ponnaiya, B., Luijsterburg, M.S., Krawczyk, P.M., Ullrich, R.L., Aten, J.A. and Bailey, S.M. (2007) DNA double-strand breaks are not sufficient to initiate recruitment of TRF2. *Nat. Genet,* **39**, 696-698.

82. Smogorzewska, A., van Steensel, B., Bianchi, A., Oelmann, S., Schaefer, M.R., Schnapp, G. and de Lange, T. (2000) Control of human telomere length by TRF1 and TRF2. *Mol. Cell. Biol*, **20**, 1659-1668.

83. Loayza, D. and De Lange, T. (2003) POT1 as a terminal transducer of TRF1 telomere length control. *Nature*, **423**, 1013-1018.

84. Kelleher, C., Kurth, I. and Lingner, J. (2005) Human protection of telomeres 1 (POT1) is a negative regulator of telomerase activity in vitro. *Mol. Cell. Biol*, **25**, 808-818.

85. Zellinger, B. and Riha, K. (2007) Composition of plant telomeres. *Biochimica et Biophysica Acta*, **1769**, 399-409.

86. Karamysheva, Z.N., Surovtseva, Y.V., Vespa, L., Shakirov, E.V. and Shippen, D.E. (2004) A C-terminal Myb extension domain defines a novel family of double-strand telomeric DNA-binding proteins in *Arabidopsis*. *J.Biol. Chem*, **279**, 47799-47807.

87. Hwang, M.G. and Cho, M.H. (2007) *Arabidopsis thaliana* telomeric DNA-binding protein 1 is required for telomere length homeostasis and its Myb-extension domain stabilizes plant telomeric DNA binding. *Nucleic Acids Res*, **35**, 1333-1342.

88. Yang, S.W., Kim, S.K. and Kim, W.T. (2004) Perturbation of NgTRF1 expression induces apoptosis-like cell death in tobacco BY-2 cells and implicates NgTRF1 in the control of telomere length and stability. *Plant Cell*, **16**, 3370-3385.

89. Cesare, A.J., Quinney, N., Willcox, S., Subramanian, D. and Griffith, J.D. (2003) Telomere looping in *P. sativum* (common garden pea). *Plant J*, **36**, 271-279.

90. Lustig, A.J. (2001) Cdc13 subcomplexes regulate multiple telomere functions. *Nat. Struct. Biol*, **8**, 297-299.

91. Chandra, A., Hughes, T.R., Nugent, C.I. and Lundblad, V. (2001) Cdc13 both positively and negatively regulates telomere replication. *Genes Dev*, **15**, 404-414.

92. Evans, S.K. and Lundblad, V. (1999) Est1 and Cdc13 as comediators of telomerase access. *Science*, **286**, 117-120.

93. Baumann, P. and Cech, T.R. (2001) Pot1, the putative telomere end-binding protein in fission yeast and humans. *Science*, **292**, 1171-1175.

94. Colgin, L.M., Baran, K., Baumann, P., Cech, T.R. and Reddel, R.R. (2003) Human POT1 facilitates telomere elongation by telomerase. *Curr. Biol*, **13**, 942-946.

95. Lei, M., Podell, E.R. and Cech, T.R. (2004) Structure of human POT1 bound to telomeric single-stranded DNA provides a model for chromosome end-protection. *Nat. Struct. Mol. Biol*, **11**, 1223-1229.

96. Lei, M., Zaug, A.J., Podell, E.R. and Cech, T.R. (2005) Switching human telomerase on and off with hPOT1 protein in vitro. *J. Biol. Chem*, **280**, 20449-20456.

97. Armbruster, B.N., Linardic, C.M., Veldman, T., Bansal, N.P., Downie, D.L. and Counter, C.M. (2004) Rescue of an hTERT mutant defective in telomere elongation by fusion with hPot1. *Mol. Cell. Biol*, **24**, 3552-3561.

98. Zaug, A.J., Podell, E.R. and Cech, T.R. (2005) Human POT1 disrupts telomeric G-quadruplexes allowing telomerase extension in vitro. *Proc. Natl. Acad. Sci. USA*, **102**, 10864-10869.

99. Surovtseva, Y.V., Shakirov, E.V., Vespa, L., Osbun, N., Song, X. and Shippen, D.E. (2007) *Arabidopsis* POT1 associates with the telomerase RNP and is required for telomere maintenance. *EMBO J*, **26**, 3653-3661.

100. Shakirov, E.V., Surovtseva, Y.V., Osbun, N. and Shippen, D.E. (2005) The *Arabidopsis* Pot1 and Pot2 proteins function in telomere length homeostasis and chromosome end protection. *Mol. Cell. Biol*, **25**, 7725-7733.

101. Kwon, C. and Chung, I.K. (2004) Interaction of an *Arabidopsis* RNA-binding protein with plant single-stranded telomeric DNA modulates telomerase activity. *J. Biol. Chem*, **279**, 12812-12818.

102. Garvik, B., Carson, M. and Hartwell, L. (1995) Single-stranded DNA arising at telomeres in *cdc13* mutants may constitute a specific signal for the RAD9 checkpoint. *Mol. Cell. Biol*, **15**, 6128-6138.

103. Grandin, N., Damon, C. and Charbonneau, M. (2001) Ten1 functions in telomere end protection and length regulation in association with Stn1 and Cdc13. *EMBO J*, **20**, 1173-1183.

104. Grandin, N., Reed, S.I. and Charbonneau, M. (1997) Stn1, a new *Saccharomyces cerevisiae* protein, is implicated in telomere size regulation in association with Cdc13. *Genes Dev*, **11**, 512-527.

105. Li, G.Z., Eller, M.S., Firoozabadi, R. and Gilchrest, B.A. (2003) Evidence that exposure of the telomere 3' overhang sequence induces senescence. *Proc. Natl. Acad. Sci. USA*, **100**, 527-531.

106. Zhu, X.D., Niedernhofer, L., Kuster, B., Mann, M., Hoeijmakers, J.H. and de Lange, T. (2003) ERCC1/XPF removes the 3' overhang from uncapped telomeres and represses formation of telomeric DNA-containing double minute chromosomes. *Mol. Cell*, **12**, 1489-1498.

107. Yang, Q., Zheng, Y.L. and Harris, C.C. (2005) POT1 and TRF2 cooperate to maintain telomeric integrity. *Mol. Cell. Biol*, **25**, 1070-1080.

108. Klobutcher, L.A., Swanton, M.T., Donini, P. and Prescott, D.M. (1981) All gene-sized DNA molecules in four species of hypotrichs have the same terminal sequence and an unusual 3' terminus. *Proc. Natl. Acad. Sci. USA*, **78**, 3015-3019.

109. Sfeir, A.J., Chai, W., Shay, J.W. and Wright, W.E. (2005) Telomere-end processing the terminal nucleotides of human chromosomes. *Mol. Cell*, **18**, 131-138.

110. Hockemeyer, D., Sfeir, A.J., Shay, J.W., Wright, W.E. and de Lange, T. (2005) POT1 protects telomeres from a transient DNA damage response and determines how human chromosomes end. *EMBO J*, **24**, 2667-2678.

111. Churikov, D., Wei, C. and Price, C.M. (2006) Vertebrate POT1 restricts G-overhang length and prevents activation of a telomeric DNA damage checkpoint but is dispensable for overhang protection. *Mol. Cell. Biol*, **26**, 6971-6982.

112. Xin, H., Liu, D., Wan, M., Safari, A., Kim, H., Sun, W., O'Connor, M.S. and Songyang, Z. (2007) TPP1 is a homologue of ciliate TEBP-beta and interacts with POT1 to recruit telomerase. *Nature*, **445**, 559-562.

113. He, H., Multani, A.S., Cosme-Blanco, W., Tahara, H., Ma, J., Pathak, S., Deng, Y. and Chang, S. (2006) POT1b protects telomeres from end-to-end chromosomal fusions and aberrant homologous recombination. *EMBO J,* **25**, 5180-5190.

114. Hockemeyer, D., Daniels, J.P., Takai, H. and de Lange, T. (2006) Recent expansion of the telomeric complex in rodents: Two distinct POT1 proteins protect mouse telomeres. *Cell*, **126**, 63-77.

115. Cooper, J.P., Nimmo, E.R., Allshire, R.C. and Cech, T.R. (1997) Regulation of telomere length and function by a Myb-domain protein in fission yeast. *Nature*, **385**, 744-747.

116. Gravel, S., Larrivee, M., Labrecque, P. and Wellinger, R.J. (1998) Yeast Ku as a regulator of chromosomal DNA end structure. *Science*, **280**, 741-744.

117. Riha, K. and Shippen, D.E. (2003) Ku is required for telomeric C-rich strand maintenance but not for end-to-end chromosome fusions in *Arabidopsis*. *Proc. Natl. Acad. Sci. USA,* **100**, 611-615.

118. Wei, C., Skopp, R., Takata, M., Takeda, S. and Price, C.M. (2002) Effects of double-strand break repair proteins on vertebrate telomere structure. *Nucleic Acids Res,* **30**, 2862-2870.

119. O'Driscoll, M. and Jeggo, P.A. (2006) The role of double-strand break repair - insights from human genetics. *Nat. Rev. Genet*, **7**, 45-54.

120. Sancar, A., Lindsey-Boltz, L.A., Unsal-Kacmaz, K. and Linn, S. (2004) Molecular mechanisms of mammalian DNA repair and the DNA damage checkpoints. *Ann. Rev. Biochem*, **73**, 39-85.

121. Lavin, M.F. (2004) The Mre11 complex and ATM: a two-way functional interaction in recognising and signaling DNA double strand breaks. *DNA Repair*, **3**, 1515-1520.

122. Berkovich, E., Monnat, R.J., Jr. and Kastan, M.B. (2007) Roles of ATM and NBS1 in chromatin structure modulation and DNA double-strand break repair. *Nat. Cell Biol*, **9**, 683-690.

123. Block, W.D., Yu, Y., Merkle, D., Gifford, J.L., Ding, Q., Meek, K. and Lees-Miller, S.P. (2004) Autophosphorylation-dependent remodeling of the DNA-dependent protein kinase catalytic subunit regulates ligation of DNA ends. *Nucleic Acids Res*, **32**, 4351-4357.

124. Meek, K., Gupta, S., Ramsden, D.A. and Lees-Miller, S.P. (2004) The DNA-dependent protein kinase: the director at the end. *Immun. Rev*, **200**, 132-141.

125. Grawunder, U., Wilm, M., Wu, X., Kulesza, P., Wilson, T.E., Mann, M. and Lieber, M.R. (1997) Activity of DNA ligase IV stimulated by complex formation with XRCC4 protein in mammalian cells. *Nature*, **388**, 492-495.

126. Mimori, T., Akizuki, M., Yamagata, H., Inada, S., Yoshida, S. and Homma, M. (1981) Characterization of a high molecular weight acidic nuclear protein recognized by autoantibodies in sera from patients with polymyositis-scleroderma overlap. *J. Clin. Invest*, **68**, 611-620.

127. Critchlow, S.E. and Jackson, S.P. (1998) DNA end-joining: from yeast to man. *Trends Biochem. Sci*, **23**, 394-398.

128. Arosio, D., Cui, S., Ortega, C., Chovanec, M., Di Marco, S., Baldini, G., Falaschi, A. and Vindigni, A. (2002) Studies on the mode of Ku interaction with DNA. *J. Biol. Chem*, **277**, 9741-9748.

129. Dynan, W.S. and Yoo, S. (1998) Interaction of Ku protein and DNA-dependent protein kinase catalytic subunit with nucleic acids. *Nucleic Acids Res,* **26**, 1551-1559.

130. Walker, J.R., Corpina, R.A. and Goldberg, J. (2001) Structure of the Ku heterodimer bound to DNA and its implications for double-strand break repair. *Nature*, **412**, 607-614.

131. Wyman, C. and Kanaar, R. (2006) DNA double-strand break repair: all's well that ends well. *Ann. Rev. Genet*, **40**, 363-383.

132. Uematsu, N., Weterings, E., Yano, K., Morotomi-Yano, K., Jakob, B., Taucher-Scholz, G., Mari, P.O., van Gent, D.C., Chen, B.P. and Chen, D.J. (2007) Autophosphorylation of DNA-PKCS regulates its dynamics at DNA double-strand breaks. *J. Cell Biol*, **177**, 219-229.

133. Lee, S.E., Mitchell, R.A., Cheng, A. and Hendrickson, E.A. (1997) Evidence for DNA-PK-dependent and -independent DNA double-strand break repair pathways in mammalian cells as a function of the cell cycle. *Mol. Cell. Biol,* **17**, 1425-1433.

134. Wei, Y.F., Robins, P., Carter, K., Caldecott, K., Pappin, D.J., Yu, G.L., Wang, R.P., Shell, B.K., Nash, R.A., Schar, P. *et al.* (1995) Molecular cloning and expression of human cDNAs encoding a novel DNA ligase IV and DNA ligase III, an enzyme active in DNA repair and recombination. *Mol. Cell. Biol*, **15**, 3206-3216.

135. Ma, Y., Lu, H., Tippin, B., Goodman, M.F., Shimazaki, N., Koiwai, O., Hsieh, C.L., Schwarz, K. and Lieber, M.R. (2004) A biochemically defined system for mammalian nonhomologous DNA end joining. *Mol. Cell*, **16**, 701-713.

136. Audebert, M., Salles, B. and Calsou, P. (2004) Involvement of poly(ADP-ribose) polymerase-1 and XRCC1/DNA ligase III in an alternative route for DNA double-strand breaks rejoining. *J. Biol. Chem*, **279**, 55117-55126.

137. Wang, H., Rosidi, B., Perrault, R., Wang, M., Zhang, L., Windhofer, F. and Iliakis, G. (2005) DNA ligase III as a candidate component of backup pathways of nonhomologous end joining. *Cancer Res*, **65**, 4020-4030.

138. Wang, M., Wu, W., Wu, W., Rosidi, B., Zhang, L., Wang, H. and Iliakis, G. (2006) PARP-1 and Ku compete for repair of DNA double strand breaks by distinct NHEJ pathways. *Nucleic Acids Res*, **34**, 6170-6182.

139. Feldmann, E., Schmiemann, V., Goedecke, W., Reichenberger, S. and Pfeiffer, P. (2000) DNA double-strand break repair in cell-free extracts from Ku80-deficient cells: implications for Ku serving as an alignment factor in non-homologous DNA end joining. *Nucleic Acids Res*, **28**, 2585-2596.

140. Kabotyanski, E.B., Gomelsky, L., Han, J.O., Stamato, T.D. and Roth, D.B. (1998) Double-strand break repair in Ku86- and XRCC4-deficient cells. *Nucleic Acids Res*, **26**, 5333-5342.

141. Kemp, L.M., Sedgwick, S.G. and Jeggo, P.A. (1984) X-ray sensitive mutants of Chinese hamster ovary cells defective in double-strand break rejoining. *Mutation Res*, **132**, 189-196.

142. Smith, J., Riballo, E., Kysela, B., Baldeyron, C., Manolis, K., Masson, C., Lieber, M.R., Papadopoulo, D. and Jeggo, P. (2003) Impact of DNA ligase IV on the fidelity of end joining in human cells. *Nucleic Acids Res*, **31**, 2157-2167.

143. Tzung, T.Y. and Runger, T.M. (1998) Reduced joining of DNA double strand breaks with an abnormal mutation spectrum in rodent mutants of DNA-PKcs and Ku80. *Intl. J. Rad. Biol*, **73**, 469-474.

144. Daley, J.M., Palmbos, P.L., Wu, D. and Wilson, T.E. (2005) Nonhomologous end joining in yeast. *Ann. Rev. Genet*, **39**, 431-451.

145. van den Bosch, M., Bree, R.T. and Lowndes, N.F. (2003) The MRN complex: coordinating and mediating the response to broken chromosomes. *EMBO Rep*, **4**, 844-849.

146. Paull, T.T. and Gellert, M. (2000) A mechanistic basis for Mre11-directed DNA joining at microhomologies. *Proc. Natl. Acad. Sci. USA*, **97**, 6409-6414.

147. Ma, J.L., Kim, E.M., Haber, J.E. and Lee, S.E. (2003) Yeast Mre11 and Rad1 proteins define a Ku-independent mechanism to repair double-strand breaks lacking overlapping end sequences. *Mol. Cell Biol*, **23**, 8820-8828.

148. Karlseder, J., Hoke, K., Mirzoeva, O.K., Bakkenist, C., Kastan, M.B., Petrini, J.H. and de Lange, T. (2004) The telomeric protein TRF2 binds the ATM kinase and can inhibit the ATM-dependent DNA damage response. *PLoS Biol*, **2**, E240.

149. Takata, H., Kanoh, Y., Gunge, N., Shirahige, K. and Matsuura, A. (2004) Reciprocal association of the budding yeast ATM-related proteins Tel1 and Mec1 with telomeres *in vivo*. *Mol. Cell,* **14**, 515-522.

150. Takata, H., Tanaka, Y. and Matsuura, A. (2005) Late S phase-specific recruitment of Mre11 complex triggers hierarchical assembly of telomere replication proteins in *Saccharomyces cerevisiae*. *Mol. Cell,* **17**, 573-583.

151. Verdun, R.E. and Karlseder, J. (2006) The DNA damage machinery and homologous recombination pathway act consecutively to protect human telomeres. *Cell*, **127**, 709-720.

152. Lombard, D.B. and Guarente, L. (2000) Nijmegen breakage syndrome disease protein and MRE11 at PML nuclear bodies and meiotic telomeres. *Cancer Res*, **60**, 2331-2334.

153. Nakamura, T.M., Moser, B.A. and Russell, P. (2002) Telomere binding of checkpoint sensor and DNA repair proteins contributes to maintenance of functional fission yeast telomeres. *Genetics*, **161**, 1437-1452.

154. Zhu, X.D., Kuster, B., Mann, M., Petrini, J.H. and de Lange, T. (2000) Cell-cycle-regulated association of RAD50/MRE11/NBS1 with TRF2 and human telomeres. *Nat. Genet.*, **25**, 347-352.

155. Song, K., Jung, D., Jung, Y., Lee, S.G. and Lee, I. (2000) Interaction of human Ku70 with TRF2. *FEBS Lett.*, **481**, 81-85.

156. Greenwell, P.W., Kronmal, S.L., Porter, S.E., Gassenhuber, J., Obermaier, B. and Petes, T.D. (1995) TEL1, a gene involved in controlling telomere length in *S. cerevisiae*, is homologous to the human ataxia telangiectasia gene. *Cell*, **82**, 823-829.

157. Pandita, T.K. (2002) ATM function and telomere stability. *Oncogene*, **21**, 611-618.

158. Goudsouzian, L.K., Tuzon, C.T. and Zakian, V.A. (2006) *S. cerevisiae* Tel1p and Mre11p are required for normal levels of Est1p and Est2p telomere association. *Mol. Cell*, **24**, 603-610.

159. Vespa, L., Couvillion, M., Spangler, E. and Shippen, D.E. (2005) ATM and ATR make distinct contributions to chromosome end protection and the maintenance of telomeric DNA in *Arabidopsis*. *Genes Dev*, **19**, 2111-2115.

160. Bertuch, A.A. and Lundblad, V. (2003) Which end: dissecting Ku's function at telomeres and double-strand breaks. *Genes Dev*, **17**, 2347-2350.

161. Laroche, T., Martin, S.G., Gotta, M., Gorham, H.C., Pryde, F.E., Louis, E.J. and Gasser, S.M. (1998) Mutation of yeast Ku genes disrupts the subnuclear organization of telomeres. *Curr. Biol*, **8**, 653-656.

162. Aparicio, O.M., Billington, B.L. and Gottschling, D.E. (1991) Modifiers of position effect are shared between telomeric and silent mating-type loci in *S. cerevisiae*. *Cell*, **66**, 1279-1287.

163. Bertuch, A.A. and Lundblad, V. (2003) The Ku heterodimer performs separable activities at double-strand breaks and chromosome termini. *Mol. Cell. Biol*, **23**, 8202-8215.

164. Chai, W., Ford, L.P., Lenertz, L., Wright, W.E. and Shay, J.W. (2002) Human Ku70/80 associates physically with telomerase through interaction with hTERT. *J. Biol. Chem*, **277**, 47242-47247.

165. Stellwagen, A.E., Haimberger, Z.W., Veatch, J.R. and Gottschling, D.E. (2003) Ku interacts with telomerase RNA to promote telomere addition at native and broken chromosome ends. *Genes Dev*, **17**, 2384-2395.

166. Ting, N.S., Yu, Y., Pohorelic, B., Lees-Miller, S.P. and Beattie, T.L. (2005) Human Ku70/80 interacts directly with hTR, the RNA component of human telomerase. *Nucleic Acids Res*, **33**, 2090-2098.

167. Ribes-Zamora, A., Mihalek, I., Lichtarge, O. and Bertuch, A.A. (2007) Distinct faces of the Ku heterodimer mediate DNA repair and telomeric functions. *Nat. Struct. Mol. Biol,* **14**, 301-307.

168. Samper, E., Goytisolo, F.A., Slijepcevic, P., van Buul, P.P. and Blasco, M.A. (2000) Mammalian Ku86 protein prevents telomeric fusions independently of the length of TTAGGG repeats and the G-strand overhang. *EMBO Rep*, **1**, 244-252.

169. Espejel, S., Franco, S., Sgura, A., Gae, D., Bailey, S.M., Taccioli, G.E. and Blasco, M.A. (2002) Functional interaction between DNA-PKcs and telomerase in telomere length maintenance. *EMBO J*, **21**, 6275-6287.

170. Boulton, S.J. and Jackson, S.P. (1998) Components of the Ku-dependent non-homologous end-joining pathway are involved in telomeric length maintenance and telomeric silencing. *EMBO J*, **17**, 1819-1828.

171. Kironmai, K.M. and Muniyappa, K. (1997) Alteration of telomeric sequences and senescence caused by mutations in RAD50 of *Saccharomyces cerevisiae*. *Genes Cells*, **2**, 443-455.

172. Manolis, K.G., Nimmo, E.R., Hartsuiker, E., Carr, A.M., Jeggo, P.A. and Allshire, R.C. (2001) Novel functional requirements for non-homologous DNA end joining in *Schizosaccharomyces pombe*. *EMBO J*, **20**, 210-221.

173. Moreau, S., Ferguson, J.R. and Symington, L.S. (1999) The nuclease activity of Mre11 is required for meiosis but not for mating type switching, end joining, or telomere maintenance. *Mol. Cell. Biol*, **19**, 556-566.

174. Wilson, S., Warr, N., Taylor, D.L. and Watts, F.Z. (1999) The role of *Schizosaccharomyces pombe* Rad32, the Mre11 homologue, and other DNA damage response proteins in non-homologous end joining and telomere length maintenance. *Nucleic Acids Res*, **27**, 2655-2661.

175. Ueno, M., Nakazaki, T., Akamatsu, Y., Watanabe, K., Tomita, K., Lindsay, H.D., Shinagawa, H. and Iwasaki, H. (2003) Molecular characterization of the *Schizosaccharomyces pombe* nbs1+ gene involved in DNA repair and telomere maintenance. *Mol. Cell. Biol*, **23**, 6553-6563.

176. Lee, S.E., Moore, J.K., Holmes, A., Umezu, K., Kolodner, R.D. and Haber, J.E. (1998) *Saccharomyces* Ku70, Mre11/Rad50 and RPA proteins regulate adaptation to G2/M arrest after DNA damage. *Cell*, **94**, 399-409.

177. Tsubouchi, H. and Ogawa, H. (1998) A novel mre11 mutation impairs processing of double-strand breaks of DNA during both mitosis and meiosis. *Mol. Cell. Biol*, **18**, 260-268.

178. Tomita, K., Matsuura, A., Caspari, T., Carr, A.M., Akamatsu, Y., Iwasaki, H., Mizuno, K., Ohta, K., Uritani, M., Ushimaru, T. *et al.* (2003) Competition between the Rad50 complex and the Ku heterodimer reveals a role for Exo1 in processing double-strand breaks but not telomeres. *Mol. Cell Biol*, **23**, 5186-5197.

179. Ferreira, M.G. and Cooper, J.P. (2001) The fission yeast Taz1 protein protects chromosomes from Ku-dependent end-to-end fusions. *Mol. Cell,* **7**, 55-63.

180. Heacock, M., Spangler, E., Riha, K., Puizina, J. and Shippen, D.E. (2004) Molecular analysis of telomere fusions in *Arabidopsis*: multiple pathways for chromosome end-joining. *EMBO J*, **23**, 2304-2313.

181. Puizina, J., Siroky, J., Mokros, P., Schweizer, D. and Riha, K. (2004) Mre11 deficiency in *Arabidopsis* is associated with chromosomal instability in somatic cells and Spo11-dependent genome fragmentation during meiosis. *Plant Cell*, **16**, 1968-1978.

182. Bundock, P. and Hooykaas, P. (2002) Severe developmental defects, hypersensitivity to DNA-damaging agents, and lengthened telomeres in *Arabidopsis* MRE11 mutants. *Plant Cell*, **14**, 2451-2462.

183. Ranganathan, V., Heine, W.F., Ciccone, D.N., Rudolph, K.L., Wu, X., Chang, S., Hai, H., Ahearn, I.M., Livingston, D.M., Resnick, I. *et al.* (2001) Rescue of a telomere length defect of Nijmegen breakage syndrome cells requires NBS and telomerase catalytic subunit. *Curr. Biol*, **11**, 962-966.

184. Ferreira, M.G., Miller, K.M. and Cooper, J.P. (2004) Indecent exposure: when telomeres become uncapped. *Mol. Cell*, **13**, 7-18.

185. Hemann, M.T., Strong, M.A., Hao, L.Y. and Greider, C.W. (2001) The shortest telomere, not average telomere length, is critical for cell viability and chromosome stability. *Cell*, **107**, 67-77.

186. Zou, Y., Sfeir, A., Gryaznov, S.M., Shay, J.W. and Wright, W.E. (2004) Does a sentinel or a subset of short telomeres determine replicative senescence? *Mol. Biol. Cell*, **15**, 3709-3718.

187. Riha, K., McKnight, T.D., Griffing, L.R. and Shippen, D.E. (2001) Living with genome instability: plant responses to telomere dysfunction. *Science*, **291**, 1797-1800.

188. Chan, S.W. and Blackburn, E.H. (2003) Telomerase and ATM/Tel1p protect telomeres from nonhomologous end joining. *Mol. Cell*, **11**, 1379-1387.

189. Chan, S.W., Chang, J., Prescott, J. and Blackburn, E.H. (2001) Altering telomere structure allows telomerase to act in yeast lacking ATM kinases. *Curr. Biol*, **11**, 1240-1250.

190. Ritchie, K.B., Mallory, J.C. and Petes, T.D. (1999) Interactions of TLC1 (which encodes the RNA subunit of telomerase), TEL1, and MEC1 in regulating telomere length in the yeast *Saccharomyces cerevisiae*. *Mol. Cell. Biol*, **19**, 6065-6075.

191. Wong, K.K., Maser, R.S., Bachoo, R.M., Menon, J., Carrasco, D.R., Gu, Y., Alt, F.W. and DePinho, R.A. (2003) Telomere dysfunction and Atm deficiency compromises organ homeostasis and accelerates ageing. *Nature*, **421**, 643-648.

192. Qi, L., Strong, M.A., Karim, B.O., Armanios, M., Huso, D.L. and Greider, C.W. (2003) Short telomeres and ataxia-telangiectasia mutated deficiency cooperatively increase telomere dysfunction and suppress tumorigenesis. *Cancer Res,* **63**, 8188-8196.

193. d'Adda di Fagagna, F., Hande, M.P., Tong, W.M., Roth, D., Lansdorp, P.M., Wang, Z.Q. and Jackson, S.P. (2001) Effects of DNA nonhomologous end-joining factors on telomere length and chromosomal stability in mammalian cells. *Curr. Biol*, **11**, 1192-1196.

194. Espejel, S., Franco, S., Rodriguez-Perales, S., Bouffler, S.D., Cigudosa, J.C. and Blasco, M.A. (2002) Mammalian Ku86 mediates chromosomal fusions and apoptosis caused by critically short telomeres. *EMBO J,* **21**, 2207-2219.

195. Baumann, P. and Cech, T.R. (2000) Protection of telomeres by the Ku protein in fission yeast. *Mol. Biol. Cell,* **11**, 3265-3275.

196. Riha, K., Watson, J.M., Parkey, J. and Shippen, D.E. (2002) Telomere length deregulation and enhanced sensitivity to genotoxic stress in *Arabidopsis* mutants deficient in Ku70. *EMBO J*, **21**, 2819-2826.

197. Bailey, S.M., Meyne, J., Chen, D.J., Kurimasa, A., Li, G.C., Lehnert, B.E. and Goodwin, E.H. (1999) DNA double-strand break repair proteins are required to cap the ends of mammalian chromosomes. *Proc. Natl. Acad. Sci. USA*, **96**, 14899-14904.

198. Espejel, S., Klatt, P., Menissier-de Murcia, J., Martin-Caballero, J., Flores, J.M., Taccioli, G., de Murcia, G. and Blasco, M.A. (2004) Impact of telomerase ablation on organismal viability, aging, and tumorigenesis in mice lacking the DNA repair proteins PARP-1, Ku86, or DNA-PKcs. *J. Cell Biol*, **167**, 627-638.

199. Gilley, D., Tanaka, H., Hande, M.P., Kurimasa, A., Li, G.C., Oshimura, M. and Chen, D.J. (2001) DNA-PKcs is critical for telomere capping. *Proc. Natl. Acad. Sci. USA*, **98**, 15084-15088.

200. Bailey, S.M., Brenneman, M.A., Halbrook, J., Nickoloff, J.A., Ullrich, R.L. and Goodwin, E.H. (2004) The kinase activity of DNA-PK is required to protect mammalian telomeres. *DNA Repair*, **3**, 225-233.

201. Bailey, S.M., Cornforth, M.N., Kurimasa, A., Chen, D.J. and Goodwin, E.H. (2001) Strand-specific postreplicative processing of mammalian telomeres. *Science*, **293**, 2462-2465.

202. Maser, R.S., Wong, K.K., Sahin, E., Xia, H., Naylor, M., Hedberg, H.M., Artandi, S.E. and DePinho, R.A. (2007) DNA-dependent protein kinase catalytic subunit is not required for dysfunctional telomere fusion and checkpoint response in the telomerase-deficient mouse. *Mol. Cell. Biol*, **27**, 2253-2265.

203. McKnight, T.D. and Shippen, D.E. (2004) Plant telomere biology. *Plant Cell*, **16**, 794-803.

204. Bleuyard, J.Y., Gallego, M.E. and White, C.I. (2006) Recent advances in understanding of the DNA double-strand break repair machinery of plants. *DNA Repair*, **5**, 1-12.

205. Puchta, H., Dujon, B. and Hohn, B. (1993) Homologous recombination in plant cells is enhanced by in vivo induction of double strand breaks into DNA by a site-specific endonuclease. *Nucleic Acids Res*, **21**, 5034-5040.

206. Puchta, H. (2005) The repair of double-strand breaks in plants: mechanisms and consequences for genome evolution. *J. Exper. Bot*, **56**, 1-14.

207. Bundock, P., van Attikum, H. and Hooykaas, P. (2002) Increased telomere length and hypersensitivity to DNA damaging agents in an *Arabidopsis* KU70 mutant. *Nucleic Acids Res*, **30**, 3395-3400.

208. Gallego, M.E., Jalut, N. and White, C.I. (2003) Telomerase dependence of telomere lengthening in Ku80 mutant *Arabidopsis*. *Plant Cell*, **15**, 782-789.

209. Mieczkowski, P.A., Mieczkowska, J.O., Dominska, M. and Petes, T.D. (2003) Genetic regulation of telomere-telomere fusions in the yeast *Saccharomyces cerevisae*. *Proc. Natl. Acad. Sci. USA,* **100**, 10854-10859.

210. D'Amours, D. and Jackson, S.P. (2002) The Mre11 complex: at the crossroads of dna repair and checkpoint signalling. *Nature Rev*, **3**, 317-327.

211. Yamaguchi-Iwai, Y., Sonoda, E., Sasaki, M.S., Morrison, C., Haraguchi, T., Hiraoka, Y., Yamashita, Y.M., Yagi, T., Takata, M., Price, C. *et al.* (1999) Mre11 is essential for the maintenance of chromosomal DNA in vertebrate cells. *EMBO J* **18**, 6619-6629.

212. Kirik, A., Salomon, S. and Puchta, H. (2000) Species-specific double-strand break repair and genome evolution in plants. *EMBO J*, **19**, 5562-5566.

213. Alonso, J.M., Stepanova, A.N., Leisse, T.J., Kim, C.J., Chen, H., Shinn, P., Stevenson, D.K., Zimmerman, J., Barajas, P., Cheuk, R. *et al.* (2003) Genome-wide insertional mutagenesis of *Arabidopsis thaliana*. *Science*, **301**, 653-657.

214. *Arabidopsis* Genome Initiative. (2000) Analysis of the genome sequence of the flowering plant *Arabidopsis thaliana*. *Nature*, **408**, 796-815.

215. Kotani, H., Hosouchi, T. and Tsuruoka, H. (1999) Structural analysis and complete physical map of *Arabidopsis thaliana* chromosome 5 including centromeric and telomeric regions. *DNA Res*, **6**, 381-386.

216. Richards, E.J., Chao, S., Vongs, A. and Yang, J. (1992) Characterization of *Arabidopsis thaliana* telomeres isolated in yeast. *Nucleic Acids Res.*, **20**, 4039-4046.

217. Riha, K., McKnight, T.D., Fajkus, J., Vyskot, B. and Shippen, D.E. (2000) Analysis of the G-overhang structures on plant telomeres: evidence for two distinct telomere architectures. *Plant J*, **23**, 633-641.

218. Riha, K. and Shippen, D.E. (2003) Telomere structure, function and maintenance in *Arabidopsis*. *Chromosome Res*, **11**, 263-275.

219. McEachern, M.J., Iyer, S., Fulton, T.B. and Blackburn, E.H. (2000) Telomere fusions caused by mutating the terminal region of telomeric DNA. *Proc. Natl. Acad. Sci. USA*, **97**, 11409-11414.

220. Baird, D.M., Rowson, J., Wynford-Thomas, D. and Kipling, D. (2003) Extensive allelic variation and ultrashort telomeres in senescent human cells. *Nature Gen*, **33**, 203-207.

221. Hemann, M.T., Rudolph, K.L., Strong, M.A., DePinho, R.A., Chin, L. and Greider, C.W. (2001) Telomere dysfunction triggers developmentally regulated germ cell apoptosis. *Mol. Biol. Cell,* **12**, 2023-2030.

222. Forstemann, K., Hoss, M. and Lingner, J. (2000) Telomerase-dependent repeat divergence at the 3' ends of yeast telomeres. *Nucleic Acids Res*, **28**, 2690-2694.

223. Nugent, C.I., Hughes, T.R., Lue, N.F. and Lundblad, V. (1996) Cdc13p: a single-strand telomeric DNA-binding protein with a dual role in yeast telomere maintenance. *Science*, **274**, 249-252.

224. Lieber, M.R., Ma, Y., Pannicke, U. and Schwarz, K. (2003) Mechanism and regulation of human non-homologous DNA end-joining. *Nature Rev*, **4**, 712-720.

225. Hackett, J.A. and Greider, C.W. (2003) End resection initiates genomic instability in the absence of telomerase. *Mol. Cell. Biol*, **23**, 8450-8461.

226. Maringele, L. and Lydall, D. (2002) EXO1-dependent single-stranded DNA at telomeres activates subsets of DNA damage and spindle checkpoint pathways in budding yeast yku70Delta mutants. *Genes Dev*, **16**, 1919-1933.

227. Siroky, J., Zluvova, J., Riha, K., Shippen, D.E. and Vyskot, B. (2003) Rearrangements of ribosomal DNA clusters in late generation telomerase-deficient *Arabidopsis*. *Chromosoma*, **112**, 116-123.

228. Friesner, J. and Britt, A.B. (2003) Ku80- and DNA ligase IV-deficient plants are sensitive to ionizing radiation and defective in T-DNA integration. *Plant J*, **34**, 427-440.

229. Gallego, M.E., Bleuyard, J.Y., Daoudal-Cotterell, S., Jallut, N. and White, C.I. (2003) Ku80 plays a role in non-homologous recombination but is not required for T-DNA integration in *Arabidopsis*. *Plant J*, **35**, 557-565.

230. van Attikum, H., Bundock, P., Overmeer, R.M., Lee, L.Y., Gelvin, S.B. and Hooykaas, P.J. (2003) The *Arabidopsis* AtLIG4 gene is required for the repair of DNA damage, but not for the integration of Agrobacterium T-DNA. *Nucleic Acids Res*, **31**, 4247-4255.

231. Hefferin, M.L. and Tomkinson, A.E. (2005) Mechanism of DNA double-strand break repair by non-homologous end joining. *DNA Repair*, **4**, 639-648.

232. Boulton, S.J. and Jackson, S.P. (1996) *Saccharomyces cerevisiae* Ku70 potentiates illegitimate DNA double-strand break repair and serves as a barrier to error-prone DNA repair pathways. *EMBO J*, **15**, 5093-5103.

233. Teo, S.H. and Jackson, S.P. (1997) Identification of *Saccharomyces cerevisiae* DNA ligase IV: involvement in DNA double-strand break repair. *EMBO J*, **16**, 4788-4795.

234. Hsu, H.L., Gilley, D., Galande, S.A., Hande, M.P., Allen, B., Kim, S.H., Li, G.C., Campisi, J., Kohwi-Shigematsu, T. and Chen, D.J. (2000) Ku acts in a unique way at the mammalian telomere to prevent end joining. *Genes Dev*, **14**, 2807-2812.

235. Jaco, I., Munoz, P. and Blasco, M.A. (2004) Role of human Ku86 in telomere length maintenance and telomere capping. *Cancer Res*, **64**, 7271-7278.

236. Myung, K., Ghosh, G., Fattah, F.J., Li, G., Kim, H., Dutia, A., Pak, E., Smith, S. and Hendrickson, E.A. (2004) Regulation of telomere length and suppression of genomic instability in human somatic cells by Ku86. *Mol. Cell. Biol*, **24**, 5050-5059.

237. Celli, G.B. and de Lange, T. (2005) DNA processing is not required for ATM-mediated telomere damage response after TRF2 deletion. *Nature Cell Biol*, **7**, 712-718.

238. Shakirov, E.V. and Shippen, D.E. (2004) Length regulation and dynamics of individual telomere tracts in wild-type *Arabidopsis*. *Plant Cell*, **16**, 1959-1967.

239. Mathur J., K., C. (1998) Callus culture and regeneration. *Meth. Mol. Biol,* **82**, 31-34.

240. Gleave, A.P. (1992) A versatile binary vector system with a T-DNA organisational structure conducive to efficient integration of cloned DNA into the plant genome. *Plant Mol. Biol*, **20**, 1203-1207.

241. Mengiste, T., Revenkova, E., Bechtold, N. and Paszkowski, J. (1999) An SMC-like protein is required for efficient homologous recombination in *Arabidopsis*. *EMBO J*, **18**, 4505-4512.

242. Jeggo, P.A. (1998) Identification of genes involved in repair of DNA double-strand breaks in mammalian cells. *Radiation Res*, **150**, S80-91.

243. Goetz, J.D., Motycka, T.A., Han, M., Jasin, M. and Tomkinson, A.E. (2005) Reduced repair of DNA double-strand breaks by homologous recombination in a DNA ligase I-deficient human cell line. *DNA Repair*, **4**, 649-654.

244. Bonatto, D., Revers, L.F., Brendel, M. and Henriques, J.A. (2005) The eukaryotic Pso2/Snm1/Artemis proteins and their function as genomic and cellular caretakers. *Brazilian Journal of Medical and Biological Research = Revista brasileira de pesquisas medicas e biologicas / Sociedade Brasileira de Biofisica ... [et al*, **38**, 321-334.

245. de Bruin, D., Kantrow, S.M., Liberatore, R.A. and Zakian, V.A. (2000) Telomere folding is required for the stable maintenance of telomere position effects in yeast. *Mol. Cell. Biol*, **20**, 7991-8000.

246. de Bruin, D., Zaman, Z., Liberatore, R.A. and Ptashne, M. (2001) Telomere looping permits gene activation by a downstream UAS in yeast. *Nature*, **409**, 109-113.

247. Makarov, V.L., Hirose, Y. and Langmore, J.P. (1997) Long G tails at both ends of human chromosomes suggest a C strand degradation mechanism for telomere shortening. *Cell*, **88**, 657-666.

248. Parenteau, J. and Wellinger, R.J. (2002) Differential processing of leading- and lagging-strand ends at *Saccharomyces cerevisiae* telomeres revealed by the absence of Rad27p nuclease. *Genetics*, **162**, 1583-1594.

249. Wright, W.E., Tesmer, V.M., Huffman, K.E., Levene, S.D. and Shay, J.W. (1997) Normal human chromosomes have long G-rich telomeric overhangs at one end. *Genes Dev*, **11**, 2801-2809.

250. Munoz-Jordan, J.L., Cross, G.A., de Lange, T. and Griffith, J.D. (2001) t-loops at trypanosome telomeres. *EMBO J,* **20**, 579-588.

251. Lingner, J. and Cech, T.R. (1996) Purification of telomerase from *Euplotes aediculatus*: requirement of a primer 3' overhang. *Proc. Natl. Acad. Sci. USA,* **93**, 10712-10717.

252. Hemann, M.T. and Greider, C.W. (1999) G-strand overhangs on telomeres in telomerase-deficient mouse cells. *Nucleic Acids Res*, **27**, 3964-3969.

253. Haber, J.E. (1998) The many interfaces of Mre11. *Cell*, **95**, 583-586.

254. Diede, S.J. and Gottschling, D.E. (2001) Exonuclease activity is required for sequence addition and Cdc13p loading at a de novo telomere. *Curr. Biol*, **11**, 1336-1340.

255. Frank, C.J., Hyde, M. and Greider, C.W. (2006) Regulation of telomere elongation by the cyclin-dependent kinase CDK1. *Mol. Cell*, **24**, 423-432.

256. Bertuch, A.A. and Lundblad, V. (2006) The maintenance and masking of chromosome termini. *Curr. Opin. Cell Biol*, **18**, 247-253.

257. Zubko, M.K., Guillard, S. and Lydall, D. (2004) Exo1 and Rad24 differentially regulate generation of ssDNA at telomeres of *Saccharomyces cerevisiae* cdc13-1 mutants. *Genetics*, **168**, 103-115.

258. Bertuch, A.A. and Lundblad, V. (2004) EXO1 contributes to telomere maintenance in both telomerase-proficient and telomerase-deficient *Saccharomyces cerevisiae*. *Genetics*, **166**, 1651-1659.

259. Stewart, S.A., Ben-Porath, I., Carey, V.J., O'Connor, B.F., Hahn, W.C. and Weinberg, R.A. (2003) Erosion of the telomeric single-strand overhang at replicative senescence. *Nat. Genet*, **33**, 492-496.

260. Chai, W., Shay, J.W. and Wright, W.E. (2005) Human telomeres maintain their overhang length at senescence. *Mol. Cell. Biol*, **25**, 2158-2168.

261. Chai, W., Du, Q., Shay, J.W. and Wright, W.E. (2006) Human telomeres have different overhang sizes at leading versus lagging strands. *Mol. Cell*, **21**, 427-435.

262. Cimino-Reale, G., Pascale, E., Battiloro, E., Starace, G., Verna, R. and D'Ambrosio, E. (2001) The length of telomeric G-rich strand 3'-overhang measured by oligonucleotide ligation assay. *Nucleic Acids Res*, **29**, E35.

263. Cimino-Reale, G., Pascale, E., Alvino, E., Starace, G. and D'Ambrosio, E. (2003) Long telomeric C-rich 5'-tails in human replicating cells. *J. Biol. Chem*, **278**, 2136-2140.

264. Xhemalce, B., Riising, E.M., Baumann, P., Dejean, A., Arcangioli, B. and Seeler, J.S. (2007) Role of SUMO in the dynamics of telomere maintenance in fission yeast. *Proc. Natl. Acad. Sci. USA*, **104**, 893-898.

265. Diede, S.J. and Gottschling, D.E. (1999) Telomerase-mediated telomere addition *in vivo* requires DNA primase and DNA polymerases alpha and delta. *Cell*, **99**, 723-733.

266. Karlseder, J., Smogorzewska, A. and de Lange, T. (2002) Senescence induced by altered telomere state, not telomere loss. *Science*, **295**, 2446-2449.

267. Mokros, P., Vrbsky, J. and Siroky, J. (2006) Identification of chromosomal fusion sites in *Arabidopsis* mutants using sequential bicolour BAC-FISH. *Genome / National Research Council Canada = Genome / Conseil national de recherches Canada*, **49**, 1036-1042.

268. Decottignies, A. (2007) Microhomology-mediated end joining in fission yeast is repressed by pku70 and relies on genes involved in homologous recombination. *Genetics*, **176**, 1403-1415.

269. Ferreira, M.G. and Cooper, J.P. (2004) Two modes of DNA double-strand break repair are reciprocally regulated through the fission yeast cell cycle. *Genes Dev*, **18**, 2249-2254.

270. Scharer, O.D. (2003) Chemistry and biology of DNA repair. *Angewandte Chemie (International ed)*, **42**, 2946-2974.

271. Bray, C.M. and West, C.E. (2005) DNA repair mechanisms in plants: crucial sensors and effectors for the maintenance of genome integrity. *New Phyto.,* **168**, 511-528.

272. Sandell, L.L. and Zakian, V.A. (1993) Loss of a yeast telomere: arrest, recovery, and chromosome loss. *Cell*, **75**, 729-739.

273. Lieber, M.R. and Karanjawala, Z.E. (2004) Ageing, repetitive genomes and DNA damage. *Nature Rev*, **5**, 69-75.

274. Murti, K.G. and Prescott, D.M. (1999) Telomeres of polytene chromosomes in a ciliated protozoan terminate in duplex DNA loops. *Proc. Natl. Acad. Sci. USA,* **96**, 14436-14439.

275. Blasco, M.A. (2005) Telomeres and human disease: ageing, cancer and beyond. *Nat. Rev. Genet*, **6**, 611-622.

276. Lansdorp, P.M. (2005) Major cutbacks at chromosome ends. *Trends Biochem. Sci*, **30**, 388-395.

277. Bucholc, M., Park, Y. and Lustig, A.J. (2001) Intrachromatid excision of telomeric DNA as a mechanism for telomere size control in *Saccharomyces cerevisiae*. *Mol. Cell. Biol*, **21**, 6559-6573.

278. Greider, C.W. and Blackburn, E.H. (1987) The telomere terminal transferase of Tetrahymena is a ribonucleoprotein enzyme with two kinds of primer specificity. *Cell*, **51**, 887-898.

279. Beattie, T.L., Zhou, W., Robinson, M.O. and Harrington, L. (1998) Reconstitution of human telomerase activity in vitro. *Curr. Biol*, **8**, 177-180.

280. Collins, K. and Gandhi, L. (1998) The reverse transcriptase component of the *Tetrahymena* telomerase ribonucleoprotein complex. *Proc. Natl. Acad. Sci., USA*, **95**, 8485-8490.

281. Weinrich, S.L., Pruzan, R., Ma, L., Ouellette, M., Tesmer, V.M., Holt, S.E., Bodnar, A.G., Lichtsteiner, S., Kim, N.W., Trager, J.B. *et al.* (1997) Reconstitution of human telomerase with the template RNA component hTR and the catalytic protein subunit hTRT. *Nature Genet*, **17**, 498-502.

282. Vega, L.R., Mateyak, M.K. and Zakian, V.A. (2003) Getting to the end: telomerase access in yeast and humans. *Nature Rev*, **4**, 948-959.

283. Holt, S.E., Aisner, D.L., Baur, J., Tesmer, V.M., Dy, M., Ouellette, M., Trager, J.B., Morin, G.B., Toft, D.O., Shay, J.W. *et al.* (1999) Functional requirement of p23 and Hsp90 in telomerase complexes. *Genes Dev*, **13**, 817-826.

284. Mitchell, J.R., Wood, E. and Collins, K. (1999) A telomerase component is defective in the human disease dyskeratosis congenita. *Nature*, **402**, 551-555.

285. de Lange, T. (2004) T-loops and the origin of telomeres. *Nature Rev,* **5**, 323-329.

286. Stewart, S.A. and Weinberg, R.A. (2000) Telomerase and human tumorigenesis. *Sem. Cancer Biol*, **10**, 399-406.

287. Pardue, M.L., Rashkova, S., Casacuberta, E., DeBaryshe, P.G., George, J.A. and Traverse, K.L. (2005) Two retrotransposons maintain telomeres in *Drosophila*. *Chromosome Res*, **13**, 443-453.

288. Cenci, G., Siriaco, G., Raffa, G.D., Kellum, R. and Gatti, M. (2003) The *Drosophila* HOAP protein is required for telomere capping. *Nature Cell Biol*, **5**, 82-84.

289. Theobald, D.L. and Wuttke, D.S. (2004) Prediction of multiple tandem OB-fold domains in telomere end-binding proteins Pot1 and Cdc13. *Structure*, **12**, 1877-1879.

290. Grandin, N., Damon, C. and Charbonneau, M. (2000) Cdc13 cooperates with the yeast Ku proteins and Stn1 to regulate telomerase recruitment. *Mol. Cell. Biol*, **20**, 8397-8408.

291. Liu, D., Safari, A., O'Connor, M.S., Chan, D.W., Laegeler, A., Qin, J. and Songyang, Z. (2004) PTOP interacts with POT1 and regulates its localization to telomeres. *Nature Cell Biol*, **6**, 673-680.

292. Veldman, T., Etheridge, K.T. and Counter, C.M. (2004) Loss of hPot1 function leads to telomere instability and a cut-like phenotype. *Curr. Biol*, **14**, 2264-2270.

293. Ye, J.Z., Hockemeyer, D., Krutchinsky, A.N., Loayza, D., Hooper, S.M., Chait, B.T. and de Lange, T. (2004) POT1-interacting protein PIP1: a telomere length regulator that recruits POT1 to the TIN2/TRF1 complex. *Genes Dev*, **18**, 1649-1654.

294. Houghtaling, B.R., Cuttonaro, L., Chang, W. and Smith, S. (2004) A dynamic molecular link between the telomere length regulator TRF1 and the chromosome end protector TRF2. *Curr. Biol*, **14**, 1621-1631.

295. Cohen, H.Y., Miller, C., Bitterman, K.J., Wall, N.R., Hekking, B., Kessler, B., Howitz, K.T., Gorospe, M., de Cabo, R. and Sinclair, D.A. (2004) Calorie restriction promotes mammalian cell survival by inducing the SIRT1 deacetylase. *Science*, **305**, 390-392.

296. Sawada, M., Sun, W., Hayes, P., Leskov, K., Boothman, D.A. and Matsuyama, S. (2003) Ku70 suppresses the apoptotic translocation of Bax to mitochondria. *Nature Cell Biol*, **5**, 320-329.

297. Koike, M. (2002) Dimerization, translocation and localization of Ku70 and Ku80 proteins. *J. Rad. Res*, **43**, 223-236.

298. Martinez, J.J., Seveau, S., Veiga, E., Matsuyama, S. and Cossart, P. (2005) Ku70, a component of DNA-dependent protein kinase, is a mammalian receptor for Rickettsia conorii. *Cell*, **123**, 1013-1023.

299. Pang, D., Yoo, S., Dynan, W.S., Jung, M. and Dritschilo, A. (1997) Ku proteins join DNA fragments as shown by atomic force microscopy. *Cancer Res*, **57**, 1412-1415.

300. d'Adda di Fagagna, F., Reaper, P.M., Clay-Farrace, L., Fiegler, H., Carr, P., Von Zglinicki, T., Saretzki, G., Carter, N.P. and Jackson, S.P. (2003) A DNA damage checkpoint response in telomere-initiated senescence. *Nature*, **426**, 194-198.

301. Weller, G.R., Kysela, B., Roy, R., Tonkin, L.M., Scanlan, E., Della, M., Devine, S.K., Day, J.P., Wilkinson, A., d'Adda di Fagagna, F. *et al.* (2002) Identification of a DNA nonhomologous end-joining complex in bacteria. *Science*, **297**, 1686-1689.

302. Chovanec, M., Kysela, G., Dudasova, Z., & Doherty, A.J. (2006) *DNA Non-Homologous End-Joining in Unicellular Organisms*. Nova Science Publishers Inc., New York.

303. Liang, F. and Jasin, M. (1996) Ku80-deficient cells exhibit excess degradation of extrachromosomal DNA. *J. Biol. Chem*, **271**, 14405-14411.

304. Ma, Y., Lu, H., Schwarz, K. and Lieber, M.R. (2005) Repair of double-strand DNA breaks by the human nonhomologous DNA end joining pathway: the iterative processing model. *Cell cycle (Georgetown, Tex)*, **4**, 1193-1200.

305. Cary, R.B., Peterson, S.R., Wang, J., Bear, D.G., Bradbury, E.M. and Chen, D.J. (1997) DNA looping by Ku and the DNA-dependent protein kinase. *Proc. Natl. Acad. Sci. USA,* **94**, 4267-4272.

306. Ramsden, D.A. and Gellert, M. (1998) Ku protein stimulates DNA end joining by mammalian DNA ligases: a direct role for Ku in repair of DNA double-strand breaks. *EMBO J*, **17**, 609-614.

307. DeFazio, L.G., Stansel, R.M., Griffith, J.D. and Chu, G. (2002) Synapsis of DNA ends by DNA-dependent protein kinase. *EMBO J*, **21**, 3192-3200.

308. Frank-Vaillant, M. and Marcand, S. (2002) Transient stability of DNA ends allows nonhomologous end joining to precede homologous recombination. *Mol. Cell*, **10**, 1189-1199.

309. Chen, L., Trujillo, K., Sung, P. and Tomkinson, A.E. (2000) Interactions of the DNA ligase IV-XRCC4 complex with DNA ends and the DNA-dependent protein kinase. *J. Biol. Chem*, **275**, 26196-26205.

310. Nick McElhinny, S.A., Snowden, C.M., McCarville, J. and Ramsden, D.A. (2000) Ku recruits the XRCC4-ligase IV complex to DNA ends. *Mol. Cell. Biol*, **20**, 2996-3003.

311. Kysela, B., Doherty, A.J., Chovanec, M., Stiff, T., Ameer-Beg, S.M., Vojnovic, B., Girard, P.M. and Jeggo, P.A. (2003) Ku stimulation of DNA ligase IV-dependent ligation requires inward movement along the DNA molecule. *J. Biol. Chem*, **278**, 22466-22474.

312. Goedecke, W., Eijpe, M., Offenberg, H.H., van Aalderen, M. and Heyting, C. (1999) Mre11 and Ku70 interact in somatic cells, but are differentially expressed in early meiosis. *Nat. Genet*, **23**, 194-198.

313. Li, B. and Comai, L. (2001) Requirements for the nucleolytic processing of DNA ends by the Werner syndrome protein-Ku70/80 complex. *J. Biol. Chem*, **276**, 9896-9902.

314. Li, B., Conway, N., Navarro, S., Comai, L. and Comai, L. (2005) A conserved and species-specific functional interaction between the Werner syndrome-like exonuclease atWEX and the Ku heterodimer in *Arabidopsis*. *Nucleic Acids Res*, **33**, 6861-6867.

315. Palmbos, P.L., Daley, J.M. and Wilson, T.E. (2005) Mutations of the Yku80 C terminus and Xrs2 FHA domain specifically block yeast nonhomologous end joining. *Mol. Cell. Biol*, **25**, 10782-10790.

316. Wilson, T.E., Grawunder, U. and Lieber, M.R. (1997) Yeast DNA ligase IV mediates non-homologous DNA end joining. *Nature*, **388**, 495-498.

317. Frank, K.M., Sekiguchi, J.M., Seidl, K.J., Swat, W., Rathbun, G.A., Cheng, H.L., Davidson, L., Kangaloo, L. and Alt, F.W. (1998) Late embryonic lethality and impaired V(D)J recombination in mice lacking DNA ligase IV. *Nature*, **396**, 173-177.

318. Herrmann, G., Lindahl, T. and Schar, P. (1998) *Saccharomyces cerevisiae* LIF1: a function involved in DNA double-strand break repair related to mammalian XRCC4. *EMBO J*, **17**, 4188-4198.

319. Sibanda, B.L., Critchlow, S.E., Begun, J., Pei, X.Y., Jackson, S.P., Blundell, T.L. and Pellegrini, L. (2001) Crystal structure of an Xrcc4-DNA ligase IV complex. *Nat. Struct. Biol*, **8**, 1015-1019.

320. Grawunder, U., Zimmer, D., Fugmann, S., Schwarz, K. and Lieber, M.R. (1998) DNA ligase IV is essential for V(D)J recombination and DNA double-strand break repair in human precursor lymphocytes. *Mol. Cell,* **2**, 477-484.

321. McVey, M., Radut, D. and Sekelsky, J.J. (2004) End-joining repair of double-strand breaks in *Drosophila melanogaster* is largely DNA ligase IV independent. *Genetics*, **168**, 2067-2076.

322. Frank-Vaillant, M. and Marcand, S. (2001) NHEJ regulation by mating type is exercised through a novel protein, Lif2p, essential to the ligase IV pathway. *Genes Dev*, **15**, 3005-3012.

323. Kegel, A., Sjostrand, J.O. and Astrom, S.U. (2001) Nej1p, a cell type-specific regulator of nonhomologous end joining in yeast. *Curr. Biol*, **11**, 1611-1617.

324. Valencia, M., Bentele, M., Vaze, M.B., Herrmann, G., Kraus, E., Lee, S.E., Schar, P. and Haber, J.E. (2001) NEJ1 controls non-homologous end joining in *Saccharomyces cerevisiae*. *Nature*, **414**, 666-669.

325. Ahnesorg, P., Smith, P. and Jackson, S.P. (2006) XLF interacts with the XRCC4-DNA ligase IV complex to promote DNA nonhomologous end-joining. *Cell*, **124**, 301-313.

326. Buck, D., Malivert, L., de Chasseval, R., Barraud, A., Fondaneche, M.C., Sanal, O., Plebani, A., Stephan, J.L., Hufnagel, M., le Deist, F. *et al.* (2006) Cernunnos, a novel nonhomologous end-joining factor, is mutated in human immunodeficiency with microcephaly. *Cell*, **124**, 287-299.

327. Bassing, C.H., Swat, W. and Alt, F.W. (2002) The mechanism and regulation of chromosomal V(D)J recombination. *Cell*, **109 Suppl**, S45-55.

328. Collis, S.J., DeWeese, T.L., Jeggo, P.A. and Parker, A.R. (2005) The life and death of DNA-PK. *Oncogene*, **24**, 949-961.

329. Falck, J., Coates, J. and Jackson, S.P. (2005) Conserved modes of recruitment of ATM, ATR and DNA-PKcs to sites of DNA damage. *Nature*, **434**, 605-611.

330. Hammarsten, O. and Chu, G. (1998) DNA-dependent protein kinase: DNA binding and activation in the absence of Ku. *Proc. Natl. Acad. Sci. USA*, **95**, 525-530.

331. Kysela, B., Chovanec, M. and Jeggo, P.A. (2005) Phosphorylation of linker histones by DNA-dependent protein kinase is required for DNA ligase IV-dependent ligation in the presence of histone H1. *Proc. Natl. Acad. Sci. USA*, **102**, 1877-1882.

332. Chan, D.W., Chen, B.P., Prithivirajsingh, S., Kurimasa, A., Story, M.D., Qin, J. and Chen, D.J. (2002) Autophosphorylation of the DNA-dependent protein kinase catalytic subunit is required for rejoining of DNA double-strand breaks. *Genes Dev*, **16**, 2333-2338.

333. Park, E.J., Chan, D.W., Park, J.H., Oettinger, M.A. and Kwon, J. (2003) DNA-PK is activated by nucleosomes and phosphorylates H2AX within the nucleosomes in an acetylation-dependent manner. *Nucleic Acids Res*, **31**, 6819-6827.

334. Moshous, D., Callebaut, I., de Chasseval, R., Corneo, B., Cavazzana-Calvo, M., Le Deist, F., Tezcan, I., Sanal, O., Bertrand, Y., Philippe, N. *et al.* (2001) Artemis, a novel DNA double-strand break repair/V(D)J recombination protein, is mutated in human severe combined immune deficiency. *Cell*, **105**, 177-186.

335. Rooney, S., Sekiguchi, J., Zhu, C., Cheng, H.L., Manis, J., Whitlow, S., DeVido, J., Foy, D., Chaudhuri, J., Lombard, D. *et al.* (2002) Leaky Scid phenotype associated with defective V(D)J coding end processing in Artemis-deficient mice. *Mol. Cell*, **10**, 1379-1390.

336. Ma, Y., Pannicke, U., Schwarz, K. and Lieber, M.R. (2002) Hairpin opening and overhang processing by an Artemis/DNA-dependent protein kinase complex in nonhomologous end joining and V(D)J recombination. *Cell*, **108**, 781-794.

337. Riballo, E., Kuhne, M., Rief, N., Doherty, A., Smith, G.C., Recio, M.J., Reis, C., Dahm, K., Fricke, A., Krempler, A. *et al.* (2004) A pathway of double-strand break rejoining dependent upon ATM, Artemis, and proteins locating to gamma-H2AX foci. *Mol. Cell,* **16**, 715-724.

338. Gao, Y., Chaudhuri, J., Zhu, C., Davidson, L., Weaver, D.T. and Alt, F.W. (1998) A targeted DNA-PKcs-null mutation reveals DNA-PK-independent functions for KU in V(D)J recombination. *Immunity*, **9**, 367-376.

339. Rooney, S., Alt, F.W., Lombard, D., Whitlow, S., Eckersdorff, M., Fleming, J., Fugmann, S., Ferguson, D.O., Schatz, D.G. and Sekiguchi, J. (2003) Defective DNA repair and increased genomic instability in Artemis-deficient murine cells. *J. Exp. Med*, **197**, 553-565.

340. Hudson, J.J., Hsu, D.W., Guo, K., Zhukovskaya, N., Liu, P.H., Williams, J.G., Pears, C.J. and Lakin, N.D. (2005) DNA-PKcs-dependent signaling of DNA damage in Dictyostelium discoideum. *Curr. Biol*, **15**, 1880-1885.

341. de Jager, M., van Noort, J., van Gent, D.C., Dekker, C., Kanaar, R. and Wyman, C. (2001) Human Rad50/Mre11 is a flexible complex that can tether DNA ends. *Mol. Cell*, **8**, 1129-1135.

342. Hopfner, K.P., Craig, L., Moncalian, G., Zinkel, R.A., Usui, T., Owen, B.A., Karcher, A., Henderson, B., Bodmer, J.L., McMurray, C.T. *et al.* (2002) The Rad50 zinc-hook is a structure joining Mre11 complexes in DNA recombination and repair. *Nature*, **418**, 562-566.

343. Lee, J.H. and Paull, T.T. (2005) ATM activation by DNA double-strand breaks through the Mre11-Rad50-Nbs1 complex. *Science*, **308**, 551-554.

344. Lisby, M., Barlow, J.H., Burgess, R.C. and Rothstein, R. (2004) Choreography of the DNA damage response: spatiotemporal relationships among checkpoint and repair proteins. *Cell*, **118**, 699-713.

345. Shroff, R., Arbel-Eden, A., Pilch, D., Ira, G., Bonner, W.M., Petrini, J.H., Haber, J.E. and Lichten, M. (2004) Distribution and dynamics of chromatin modification induced by a defined DNA double-strand break. *Curr. Biol*, **14**, 1703-1711.

346. Nairz, K. and Klein, F. (1997) mre11S--a yeast mutation that blocks double-strand-break processing and permits nonhomologous synapsis in meiosis. *Genes Dev*, **11**, 2272-2290.

347. Neale, M.J., Pan, J. and Keeney, S. (2005) Endonucleolytic processing of covalent protein-linked DNA double-strand breaks. *Nature*, **436**, 1053-1057.

348. Dudasova, Z., Dudas, A. and Chovanec, M. (2004) Non-homologous end-joining factors of *Saccharomyces cerevisiae*. *FEMS Microbiol. Rev*, **28**, 581-601.

349. Chen, L., Trujillo, K., Ramos, W., Sung, P. and Tomkinson, A.E. (2001) Promotion of Dnl4-catalyzed DNA end-joining by the Rad50/Mre11/Xrs2 and Hdf1/Hdf2 complexes. *Mol. Cell,* **8**, 1105-1115.

350. Moore, J.K. and Haber, J.E. (1996) Cell cycle and genetic requirements of two pathways of nonhomologous end-joining repair of double-strand breaks in *Saccharomyces cerevisiae*. *Mol. Cell. Biol,* **16**, 2164-2173.

351. Rassool, F.V. (2003) DNA double strand breaks (DSB) and non-homologous end joining (NHEJ) pathways in human leukemia. *Cancer Lett*, **193**, 1-9.

352. Di Virgilio, M. and Gautier, J. (2005) Repair of double-strand breaks by nonhomologous end joining in the absence of Mre11. *J. Cell Biol*, **171**, 765-771.

353. Wu, X., Wilson, T.E. and Lieber, M.R. (1999) A role for FEN-1 in nonhomologous DNA end joining: the order of strand annealing and nucleolytic processing events. *Proc. Natl. Acad. Sci. USA,* **96**, 1303-1308.

354. Li, B. and Comai, L. (2002) Displacement of DNA-PKcs from DNA ends by the Werner syndrome protein. *Nucleic Acids Res*, **30**, 3653-3661.

355. Daley, J.M., Laan, R.L., Suresh, A. and Wilson, T.E. (2005) DNA joint dependence of pol X family polymerase action in nonhomologous end joining. *J. Biol. Chem*, **280**, 29030-29037.

356. Tseng, H.M. and Tomkinson, A.E. (2002) A physical and functional interaction between yeast Pol4 and Dnl4-Lif1 links DNA synthesis and ligation in nonhomologous end joining. *J. Biol. Chem*, **277**, 45630-45637.

357. Tseng, H.M. and Tomkinson, A.E. (2004) Processing and joining of DNA ends coordinated by interactions among Dnl4/Lif1, Pol4, and FEN-1. *J. Biol. Chem*, **279**, 47580-47588.

358. Nick McElhinny, S.A., Havener, J.M., Garcia-Diaz, M., Juarez, R., Bebenek, K., Kee, B.L., Blanco, L., Kunkel, T.A. and Ramsden, D.A. (2005) A gradient of template dependence defines distinct biological roles for family X polymerases in nonhomologous end joining. *Mol. Cell*, **19**, 357-366.

359. Uchiyama, Y., Kimura, S., Yamamoto, T., Ishibashi, T. and Sakaguchi, K. (2004) Plant DNA polymerase lambda, a DNA repair enzyme that functions in plant meristematic and meiotic tissues. *Europ. J. Biochem. / FEBS*, **271**, 2799-2807.

360. Burgers, P.M., Koonin, E.V., Bruford, E., Blanco, L., Burtis, K.C., Christman, M.F., Copeland, W.C., Friedberg, E.C., Hanaoka, F., Hinkle, D.C. *et al.* (2001) Eukaryotic DNA polymerases: proposal for a revised nomenclature. *J. Biol. Chem*, **276**, 43487-43490.

361. McClintock, B. (1939) The behavior in successive nuclear divisions of a chromosome broken at meiosis. *Proc. Natl. Acad. Sci. USA,* **25**, 405-416.

362. Feldser, D.M., Hackett, J.A. and Greider, C.W. (2003) Telomere dysfunction and the initiation of genome instability. *Nat. Rev. Cancer*, **3**, 623-627.

363. Maser, R.S. and DePinho, R.A. (2002) Connecting chromosomes, crisis, and cancer. *Science*, **297**, 565-569.

364. Maser, R.S. and DePinho, R.A. (2004) Telomeres and the DNA damage response: why the fox is guarding the henhouse. *DNA Repair*, **3**, 979-988.

365. Pennaneach, V., Putnam, C.D. and Kolodner, R.D. (2006) Chromosome healing by de novo telomere addition in *Saccharomyces cerevisiae*. *Mol. Microbiol*, **59**, 1357-1368.

366. Karlseder, J., Broccoli, D., Dai, Y., Hardy, S. and de Lange, T. (1999) p53- and ATM-dependent apoptosis induced by telomeres lacking TRF2. *Science*, **283**, 1321-1325.

367. Miller, K.M., Ferreira, M.G. and Cooper, J.P. (2005) Taz1, Rap1 and Rif1 act both interdependently and independently to maintain telomeres. *EMBO J,* **24**, 3128-3135.

368. Pardo, B. and Marcand, S. (2005) Rap1 prevents telomere fusions by nonhomologous end joining. *EMBO J*, **24**, 3117-3127.

369. Pardo, B., Ma, E. and Marcand, S. (2006) Mismatch tolerance by DNA polymerase Pol4 in the course of nonhomologous end joining in *Saccharomyces cerevisiae*. *Genetics*, **172**, 2689-2694.

370. Nakamura, T.M., Cooper, J.P. and Cech, T.R. (1998) Two modes of survival of fission yeast without telomerase. *Science*, **282**, 493-496.

371. Liti, G. and Louis, E.J. (2003) NEJ1 prevents NHEJ-dependent telomere fusions in yeast without telomerase. *Mol. Cell*, **11**, 1373-1378.

372. Cheung, I., Schertzer, M., Rose, A. and Lansdorp, P.M. (2006) High incidence of rapid telomere loss in telomerase-deficient *Caenorhabditis elegans*. *Nucleic Acids Res*, **34**, 96-103.

373. Hackett, J.A., Feldser, D.M. and Greider, C.W. (2001) Telomere dysfunction increases mutation rate and genomic instability. *Cell*, **106**, 275-286.

374. White, J.H., Green, S.R., Barker, D.G., Dumas, L.B. and Johnston, L.H. (1987) The CDC8 transcript is cell cycle regulated in yeast and is expressed coordinately with CDC9 and CDC21 at a point preceding histone transcription. *Exper. Cell Res*, **171**, 223-231.

375. Mattern, K.A., Swiggers, S.J., Nigg, A.L., Lowenberg, B., Houtsmuller, A.B. and Zijlmans, J.M. (2004) Dynamics of protein binding to telomeres in living cells: implications for telomere structure and function. *Mol. Cell. Biol*, **24**, 5587-5594.

376. Gisselsson, D. (2005) Mitotic instability in cancer: is there method in the madness? *Cell cycle (Georgetown, Tex)*, **4**, 1007-1010.

377. Lengauer, C. (2001) How do tumors make ends meet? *Proc. Natl. Acad. Sci. USA*, **98**, 12331-12333.

378. Shimizu, N., Shingaki, K., Kaneko-Sasaguri, Y., Hashizume, T. and Kanda, T. (2005) When, where and how the bridge breaks: anaphase bridge breakage plays a crucial role in gene amplification and HSR generation. *Exper. Cell Res*, **302**, 233-243.

379. Tsujimoto, H., Yamada, T. and Sasakuma, T. (1997) Molecular structure of a wheat chromosome end healed after gametocidal gene-induced breakage. *Proc. Natl. Acad. Sci. USA*, **94**, 3140-3144.

380. Han, F., Lamb, J.C. and Birchler, J.A. (2006) High frequency of centromere inactivation resulting in stable dicentric chromosomes of maize. *Proc. Natl. Acad. Sci. USA*, **103**, 3238-3243.

381. Melek, M. and Shippen, D.E. (1996) Chromosome healing: spontaneous and programmed de novo telomere formation by telomerase. *Bioessays*, **18**, 301-308.

382. Myung, K., Chen, C. and Kolodner, R.D. (2001) Multiple pathways cooperate in the suppression of genome instability in *Saccharomyces cerevisiae*. *Nature*, **411**, 1073-1076.

383. Myung, K., Datta, A. and Kolodner, R.D. (2001) Suppression of spontaneous chromosomal rearrangements by S phase checkpoint functions in *Saccharomyces cerevisiae*. *Cell*, **104**, 397-408.

384. Schulz, V.P. and Zakian, V.A. (1994) The *Saccharomyces* PIF1 DNA helicase inhibits telomere elongation and de novo telomere formation. *Cell*, **76**, 145-155.

385. Bender, C.F., Sikes, M.L., Sullivan, R., Huye, L.E., Le Beau, M.M., Roth, D.B., Mirzoeva, O.K., Oltz, E.M. and Petrini, J.H. (2002) Cancer predisposition and hematopoietic failure in Rad50(S/S) mice. *Genes Dev*, **16**, 2237-2251.

386. Zhang, Y., Lim, C.U., Williams, E.S., Zhou, J., Zhang, Q., Fox, M.H., Bailey, S.M. and Liber, H.L. (2005) NBS1 knockdown by small interfering RNA increases ionizing radiation mutagenesis and telomere association in human cells. *Cancer Res,* **65**, 5544-5553.

387. Hartsuiker, E., Vaessen, E., Carr, A.M. and Kohli, J. (2001) Fission yeast Rad50 stimulates sister chromatid recombination and links cohesion with repair. *EMBO J,* **20**, 6660-6671.

388. Gallego, M.E. and White, C.I. (2001) RAD50 function is essential for telomere maintenance in *Arabidopsis. Proc. Natl. Acad. Sci. USA*, **98**, 1711-1716.

389. Muntoni, A. and Reddel, R.R. (2005) The first molecular details of ALT in human tumor cells. *Hum. Mol. Genet.*, **14 Spec No. 2**, R191-196.

390. Wu, G., Lee, W.H. and Chen, P.L. (2000) NBS1 and TRF1 colocalize at promyelocytic leukemia bodies during late S/G2 phases in immortalized telomerase-negative cells. Implication of NBS1 in alternative lengthening of telomeres. *J. Biol. Chem*, **275**, 30618-30622.

391. Jiang, W.Q., Zhong, Z.H., Henson, J.D., Neumann, A.A., Chang, A.C. and Reddel, R.R. (2005) Suppression of alternative lengthening of telomeres by Sp100-mediated sequestration of the MRE11/RAD50/NBS1 complex. *Mol. Cell. Biol*, **25**, 2708-2721.

392. Lewis, L.K. and Resnick, M.A. (2000) Tying up loose ends: nonhomologous end-joining in *Saccharomyces cerevisiae*. *Mutation Res*, **451**, 71-89.

393. Tsukamoto, Y., Taggart, A.K. and Zakian, V.A. (2001) The role of the Mre11-Rad50-Xrs2 complex in telomerase- mediated lengthening of *Saccharomyces cerevisiae* telomeres. *Curr. Biol*, **11**, 1328-1335.

394. Krogh, B.O., Llorente, B., Lam, A. and Symington, L.S. (2005) Mutations in Mre11 phosphoesterase motif I that impair *Saccharomyces cerevisiae* Mre11-Rad50-Xrs2 complex stability in addition to nuclease activity. *Genetics*, **171**, 1561-1570.

395. Jazayeri, A., Falck, J., Lukas, C., Bartek, J., Smith, G.C., Lukas, J. and Jackson, S.P. (2006) ATM- and cell cycle-dependent regulation of ATR in response to DNA double-strand breaks. *Nat. Cell Biol*, **8**, 37-45.

396. Gottschling, D.E., Aparicio, O.M., Billington, B.L. and Zakian, V.A. (1990) Position effect at *S. cerevisiae* telomeres: reversible repression of Pol II transcription. *Cell*, **63**, 751-762.

397. Baur, J.A., Zou, Y., Shay, J.W. and Wright, W.E. (2001) Telomere position effect in human cells. *Science*, **292**, 2075-2077.

398. Nugent, C.I., Bosco, G., Ross, L.O., Evans, S.K., Salinger, A.P., Moore, J.K., Haber, J.E. and Lundblad, V. (1998) Telomere maintenance is dependent on activities required for end repair of double-strand breaks. *Curr. Biol*, **8**, 657-660.

399. Porter, S.E., Greenwell, P.W., Ritchie, K.B. and Petes, T.D. (1996) The DNA-binding protein Hdf1p (a putative Ku homologue) is required for maintaining normal telomere length in *Saccharomyces cerevisiae*. *Nucleic Acids Res*, **24**, 582-585.

400. Chahwan, C., Nakamura, T.M., Sivakumar, S., Russell, P. and Rhind, N. (2003) The fission yeast Rad32 (Mre11)-Rad50-Nbs1 complex is required for the S-phase DNA damage checkpoint. *Mol. Cell. Biol*, **23**, 6564-6573.

401. Conway, C., McCulloch, R., Ginger, M.L., Robinson, N.P., Browitt, A. and Barry, J.D. (2002) Ku is important for telomere maintenance, but not for differential expression of telomeric VSG genes, in African trypanosomes. *J. Biol. Chem*, **277**, 21269-21277.

402. Dreesen, O., Li, B. and Cross, G.A. (2005) Telomere structure and shortening in telomerase-deficient *Trypanosoma brucei*. *Nucleic Acids Res,* **33**, 4536-4543.

403. Janzen, C.J., Lander, F., Dreesen, O. and Cross, G.A. (2004) Telomere length regulation and transcriptional silencing in KU80-deficient *Trypanosoma brucei*. *Nucleic Acids Res*, **32**, 6575-6584.

404. Uegaki, K., Adachi, N., So, S., Iiizumi, S. and Koyama, H. (2006) Heterozygous inactivation of human Ku70/Ku86 heterodimer does not affect cell growth, double-strand break repair, or genome integrity. *DNA Repair*, **5**, 303-311.

405. Hande, P., Slijepcevic, P., Silver, A., Bouffler, S., van Buul, P., Bryant, P. and Lansdorp, P. (1999) Elongated telomeres in scid mice. *Genomics*, **56**, 221-223.

406. Espejel, S., Martin, M., Klatt, P., Martin-Caballero, J., Flores, J.M. and Blasco, M.A. (2004) Shorter telomeres, accelerated ageing and increased lymphoma in DNA-PKcs-deficient mice. *EMBO Rep,* **5**, 503-509.

407. Singer, M.S., Kahana, A., Wolf, A.J., Meisinger, L.L., Peterson, S.E., Goggin, C., Mahowald, M. and Gottschling, D.E. (1998) Identification of high-copy disruptors of telomeric silencing in *Saccharomyces cerevisiae*. *Genetics*, **150**, 613-632.

408. Fisher, T.S., Taggart, A.K. and Zakian, V.A. (2004) Cell cycle-dependent regulation of yeast telomerase by Ku. *Nat. Struct. Mol. Biol*, **11**, 1198-1205.

409. Fisher, T.S. and Zakian, V.A. (2005) Ku: a multifunctional protein involved in telomere maintenance. *DNA Repair*, **4**, 1215-1226.

410. Wu, X. and Lieber, M.R. (1997) Interaction between DNA-dependent protein kinase and a novel protein, KIP. *Mutation Res*, **385**, 13-20.

411. Lee, G.E., Yu, E.Y., Cho, C.H., Lee, J., Muller, M.T. and Chung, I.K. (2004) DNA-protein kinase catalytic subunit-interacting protein KIP binds telomerase by interacting with human telomerase reverse transcriptase. *J. Biol. Chem*, **279**, 34750-34755.

412. Difilippantonio, M.J., Zhu, J., Chen, H.T., Meffre, E., Nussenzweig, M.C., Max, E.E., Ried, T. and Nussenzweig, A. (2000) DNA repair protein Ku80 suppresses chromosomal aberrations and malignant transformation. *Nature*, **404**, 510-514.

413. Vogel, H., Lim, D.S., Karsenty, G., Finegold, M. and Hasty, P. (1999) Deletion of Ku86 causes early onset of senescence in mice. *Proc. Natl. Acad. Sci. USA*, **96**, 10770-10775.

414. Goytisolo, F.A., Samper, E., Edmonson, S., Taccioli, G.E. and Blasco, M.A. (2001) The absence of the DNA-dependent protein kinase catalytic subunit in mice results in anaphase bridges and in increased telomeric fusions with normal telomere length and G-strand overhang. *Mol. Cell Biol*, **21**, 3642-3651.

415. Bailey, S.M., Cornforth, M.N., Ullrich, R.L. and Goodwin, E.H. (2004) Dysfunctional mammalian telomeres join with DNA double-strand breaks. *DNA Repair*, **3**, 349-357.

416. Barnes, G. and Rio, D. (1997) DNA double-strand-break sensitivity, DNA replication, and cell cycle arrest phenotypes of Ku-deficient *Saccharomyces cerevisiae*. *Proc. Natl. Acad. Sci. USA,* **94**, 867-872.

417. Feldmann, H. and Winnacker, E.L. (1993) A putative homologue of the human autoantigen Ku from *Saccharomyces cerevisiae*. *J. Biol. Chem*, **268**, 12895-12900.

418. Gravel, S. and Wellinger, R.J. (2002) Maintenance of double-stranded telomeric repeats as the critical determinant for cell viability in yeast cells lacking Ku. *Mol. Cell. Biol*, **22**, 2182-2193.

419. Teo, S.H. and Jackson, S.P. (2001) Telomerase subunit overexpression suppresses telomere-specific checkpoint activation in the yeast yku80 mutant. *EMBO Rep*, **2**, 197-202.

420. Polotnianka, R.M., Li, J. and Lustig, A.J. (1998) The yeast Ku heterodimer is essential for protection of the telomere against nucleolytic and recombinational activities. *Curr. Biol*, **8**, 831-834.

421. DuBois, M.L., Haimberger, Z.W., McIntosh, M.W. and Gottschling, D.E. (2002) A quantitative assay for telomere protection in *Saccharomyces cerevisiae*. *Genetics*, **161**, 995-1013.

422. Miyoshi, T., Sadaie, M., Kanoh, J. and Ishikawa, F. (2003) Telomeric DNA ends are essential for the localization of Ku at telomeres in fission yeast. *J. Biol Chem*, **278**, 1924-1931.

423. Hsu, H.L., Gilley, D., Blackburn, E.H. and Chen, D.J. (1999) Ku is associated with the telomere in mammals. *Proc. Natl. Acad. Sci. USA*, **96**, 12454-12458.

424. Martin, S.G., Laroche, T., Suka, N., Grunstein, M. and Gasser, S.M. (1999) Relocalization of telomeric Ku and SIR proteins in response to DNA strand breaks in yeast. *Cell*, **97**, 621-633.

425. Melnikova, L., Biessmann, H. and Georgiev, P. (2005) The Ku protein complex is involved in length regulation of *Drosophila* telomeres. *Genetics*, **170**, 221-235.

426. Cenci, G., Ciapponi, L. and Gatti, M. (2005) The mechanism of telomere protection: a comparison between *Drosophila* and humans. *Chromosoma*, **114**, 135-145.

427. Ciapponi, L., Cenci, G., Ducau, J., Flores, C., Johnson-Schlitz, D., Gorski, M.M., Engels, W.R. and Gatti, M. (2004) The *Drosophila* Mre11/Rad50 complex is required to prevent both telomeric fusion and chromosome breakage. *Curr. Biol*, **14**, 1360-1366.

428. Bi, X., Wei, S.C. and Rong, Y.S. (2004) Telomere protection without a telomerase; the role of ATM and Mre11 in *Drosophila* telomere maintenance. *Curr. Biol*, **14**, 1348-1353.

429. Driller, L., Wellinger, R.J., Larrivee, M., Kremmer, E., Jaklin, S. and Feldmann, H.M. (2000) A short C-terminal domain of Yku70p is essential for telomere maintenance. *J. Biol. Chem,* **275**, 24921-24927.

430. Wright, W.E. and Shay, J.W. (2005) Telomere-binding factors and general DNA repair. *Nature Gen*, **37**, 116-118.

APPENDIX A

THE ROLE OF THE NON-HOMOLOGOUS END-JOINING DNA DOUBLE-STRAND BREAK REPAIR PATHWAY IN TELOMERE BIOLOGY*

Summary

Double-strand breaks are a cataclysmic threat to genome integrity. In higher eukaryotes the predominant recourse is the non-homologous end-joining (NHEJ) double-strand break repair pathway. NHEJ is a versatile mechanism employing the Ku heterodimer, Ligase IV/XRCC4 and a host of other proteins that juxtapositions two free DNA ends for ligation. A critical function of telomeres is their ability to distinguish the ends of linear chromosomes from double-strand breaks, and avoid NHEJ. Telomeres accomplish feat this by forming a unique higher order nucleoprotein structure. Paradoxically, key components of NHEJ associate with normal telomeres and are required for proper length regulation and end protection. Here we review the biochemical mechanism of NHEJ in double-strand break repair, and in the response to dysfunctional telomeres. We discuss the ways in which NHEJ proteins contribute to

_____

*Reprinted, with permission, from the Annual Review of Genetics, Volume 40 © 2006 by Annual Reviews.

telomere biology, and highlight how the NHEJ machinery and the telomere complex are evolving to maintain genome stability

Introduction

Environmental factors and genotoxic products of endogenous metabolic processes pose a constant threat to genome integrity by generating hundreds of thousands DNA modifications in each cell everyday (269,270). Among these, DSBs are the most deleterious; a single lesion of this type leads to cell cycle arrest (271). DSBs are repaired by homologous recombination (HR) or by NHEJ. HR is the predominant DSB repair mechanism in prokaryotes and in eukaryotes it plays a principal role during the S and G2 phases of the cell cycle. By contrast, NHEJ is highly preferred over HR in G1, especially in multicellular organisms with complex genomes, where ectopic recombination can lead to chromosomal rearrangements (272).

The linear genomes of eukaryotes present an interesting conundrum to the DNA repair machinery, as chromosome ends must be excluded from DSB repair (Figure 33). Telomeres are distinguished from DSBs by their specialized architecture consisting of tandem arrays of simple repeats bound by sequence-specific telomeric DNA binding proteins. These core components assemble with a plethora of additional proteins into a higher order non-nucleosomal structure that is refractory to NHEJ. If this protective cap is perturbed by deletion of essential telomere proteins, or by inactivation of the telomerase reverse transcriptase, which maintains telomeric DNA repeats, telomeres become susceptible to NHEJ. Remarkably, recent studies reveal that NHEJ components not only associate with the chromosome terminus in wild type cells, but

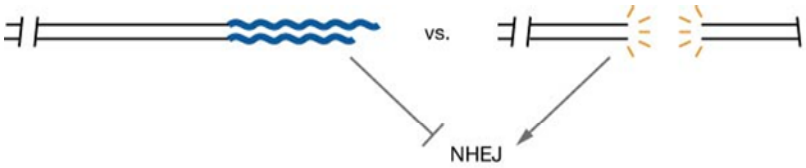

Figure 33. A functional telomere is distinguished from a double-strand break.

Although telomeres resemble a DSB, their specialized architecture prevents them from being detected as DNA damage and subjected to NHEJ (see text for details). Blue wavy lines indicate telomeres; black lines indicate non-telomeric sequence; small dashes radiating outward denote signaling to the DSB repair pathway.

also play crucial roles in telomere biology. Here we consider chromosome termini in the context of intact telomeres and as double-strand breaks, examining the molecular features of the NHEJ machinery and its response to DNA ends presented in these two settings.

Telomere structure and maintenance

In most eukaryotes telomeric DNA consists of extended tracts of simple G-rich repeat arrays. The G-rich strand forms a short 3' single-strand protrusion called the G-overhang. Recent data in ciliates and mammals indicate that the final nucleotide on the C-rich and G-rich strands of the telomere is precisely defined (24) (23) (109), allowing the physical end of the chromosome to be specifically recognized by proteins that form a protective cap. The G-overhang mediates the formation of a complex secondary structure called a t-loop (Figure 34), which sequesters the chromosome terminus in a sheltered position (31) (273) (89). During S phase, the t-loop is thought to unfold, allowing telomerase access to the G-overhang for telomere length maintenance (14).

The length of the duplex telomeric DNA tract varies widely, but in all cases a species-specific set point is attained. For example, in *Saccharomyces cerevisiae*, telomeres range in size from approximately 200-300 bp, and in *Arabidopsis thaliana* from 2-5 kb in length (13). Mouse telomeres are considerably longer, ranging from 25 to 40 (274). Telomere length homeostasis is achieved by a balance of forces that expand and contract the telomeric DNA tract. The inability of the conventional DNA polymerase machinery to fully duplicate the extreme 3' end of the chromosome by

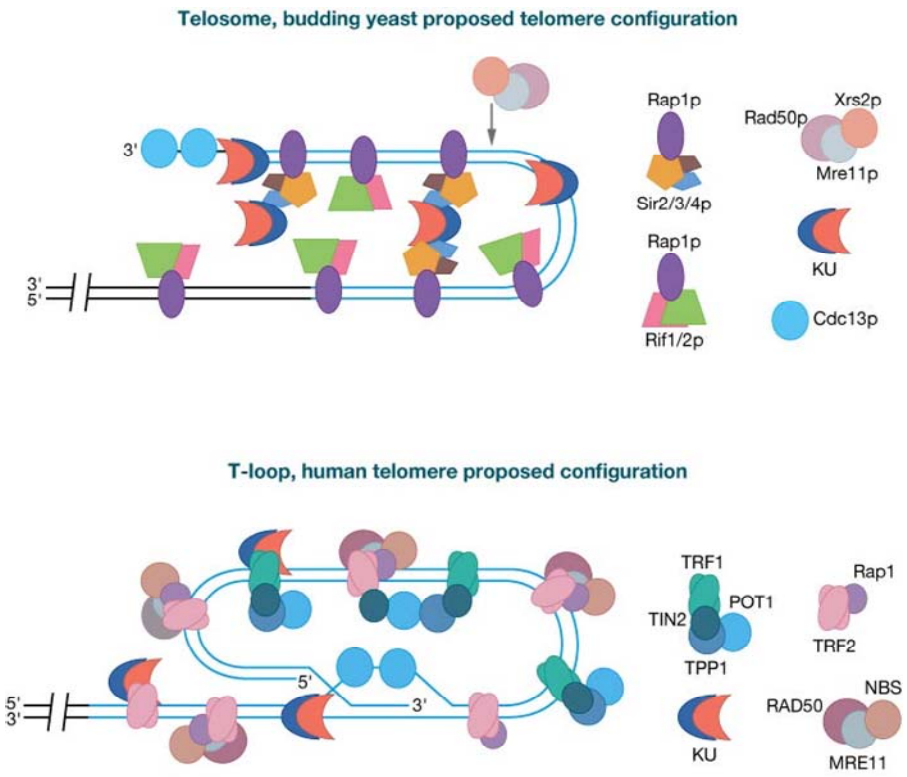

Figure 34. A model for telomere architecture in budding yeast and humans.

Top. Budding yeast telomeric DNA is proposed to fold back onto the subtelomere region. This fold is mediated by association of the dsTBP Rap1p with Sir2p, Sir3p, and Sir4p or Rif1p, and Rif2p. Cdc13p binds the single-strand G-overhang. Both the Ku heterodimer and the Mre11 complex localize to telomeres, although their precise mode of interaction is unclear. Here we show Ku positioned within the fold via interaction with Sir4p. Bottom. Human telomeres are proposed to assume a t-loop conformation in which the 3' G-overhang folds back to invade the telomeric duplex region. The dsTBPs, TRF1 and TRF2 directly contact telomeric DNA and together with four additional subunits, including the ssTBP POT1, comprise the shelterin complex. Interaction partners for TRF1 include TIN2, TPP1 and POT1, and for TRF2, Rap1. The MRE11 complex associates with telomeres via TRF2, whereas Ku can bind both TRF1 and TRF2. Although a many other proteins associate with human telomeres, only the components of shelterin and relevant NHEJ proteins are shown for simplicity.

lagging strand replication results in telomere shortening. Mammalian telomeres are likely to be subject to further nuclease processing (275), accelerating the rate of shortening in telomerase-deficient cells. In some circumstances, telomeres can undergo telomere rapid telomere deletion (TRD), a homologous recombination mechanism that truncates the telomeric DNA tract (276). To balance the loss of DNA, telomerase replenishes telomere tracts by adding G-rich telomere repeats through de novo synthesis.

Telomerase is a ribonucleoprotein reverse transcriptase that uses a sequence embedded within its internal RNA subunit (Tlc1 in yeast, TER in mammals) as a template for the reverse transcriptase subunit, TERT (telomerase reverse transcriptase) (37) (277). While TERT and the telomerase RNA are sufficient to reconstitute enzyme activity *in vitro* (278,279) (280), a host of other proteins associate with the core RNP *in vivo*. Among these in budding yeast is Est1p, a non-catalytic protein involved in the recruitment and/or activation of the telomerase RNP at telomeres *in vivo* (281). The mammalian telomerase complex includes molecular chaperones (282) and the snoRNA binding protein dyskerin (283), both of which appear to facilitate proper RNP assembly. The action of telomerase can be regulated by modulating enzyme activity levels (38) or by controlling its access to the chromosome terminus in cis by telomere binding proteins (see below).

Although telomerase is by far the most prevalent mechanism for telomere maintenance, alternative means to circumvent the end replication problem include recombination-based mechanisms such as alternative lengthening of telomeres (ALT) and retrotransposition (284). While most telomerase-deficient yeast cells die, survivors can be obtained that maintain chromosome end integrity through amplification of

subtelomeric or telomeric DNA repeats (21). In mammals, ALT is utilized by the 10-15% of human cancers that fail to reactivate telomerase (285). *Drosophila melanogaster* provides a more extreme example of telomerase-independent telomere maintenance. Fly telomeres lack canonical G-rich telomeric repeats, and instead are composed of tandem arrays of two retroelements called HetA and TART (286). The end replication problem is solved by intermittent retrotransposition events at the chromosome terminus. *Drosophila* telomeres are bound by two major double-strand DNA binding proteins, HP1 and HAOP (HP1 ORC2 associated protein). Disruption of either of these genes leads to massive end-to-end chromosome fusion (287).

A constellation of non-nucleosomal proteins associate with telomeric DNA to control telomerase access, and to prevent inappropriate nucleolytic or recombinogenic processing of the terminus (Figure 34). A core of single-strand and double-strand telomere DNA proteins (ssTBP and dsTBP) bind directly to the telomeric DNA tract, and coordinate the assembly of a higher order nucleoprotein complex that harbors additional proteins, including components of the NHEJ machinery (283).

The dsTBPs are distinguished by the presence of a Myb-like DNA binding domain. In budding and fission yeast, these are Rap1 (Figure 34 top) and Taz1, respectively, while in mammals, two dsTBPs, TRF1 and TRF2 (Figure 34 bottom), have evolved to perform distinct roles in telomere length regulation and end protection. TRF1 is a negative regulator of telomere length (82) (83), while TRF2 facilitates t-loop formation *in vitro* (32) and is necessary to prevent end-to-end chromosome fusion (77) and degradation of the G-overhang by the ERCC1/XPF nucleotide excision repair endonucleases (106).

At the physical terminus of the chromosome are proteins that bind the single-stranded G-overhang via an oligonucleotide-oligosaccharide fold (OB-fold) (288). The best studied of these is Cdc13p from budding yeast (56). Cdc13p is a multifunctional protein that, depending upon its binding partner, can promote or limit telomerase action at telomeres. Cdc13p simultaneously protects the terminus against excessive C-strand degradation and facilitates replication of the C-rich strand of the telomere by the lagging strand replication machinery (281) (289) (91).

The presumed ortholog of Cdc13p in *Schizosaccharomyces pombe* and in higher eukaryotes is Protection of telomeres 1 (Pot1) (93). Like Cdc13p, Pot1 is implicated in telomere length regulation, in some studies as a positive regulator (94) (97) (290), but in others as a negative regulator (83,107,110,291,292. Pot1 also appears to play a significant role in G-overhang maintenance and in protection against chromosome end-joining {Baumann, 2001 #453). Intriguingly, *Arabidopsis* harbors three Pot1-like genes, which share limited sequence similarity to each other and appear to encode distinct functions in a manner similar to mammalian TRF1 and TRF2 (100) (E. Shakirov, Y. Surovsteva and D. Shippen, unpublished data).

Although Pot1 proteins can bind single-strand telomeric DNA *in vitro*, they appear to localize at telomeres primarily through interactions with the TPP1 protein (83). Human Pot1 is part of a six-subunit “core” complex that includes TRF1, TRF2, hRap1, Tin2 and TPP1 (290,292,293) and has been dubbed shelterin (76) to reflect its essential role in chromosome end protection. While there is no evidence for a t-loop in budding yeast, telomeres appear to fold back on themselves forming a higher order chromatin structure (244,245) (Figure 34 top).

Recent studies in both yeast and mammals reveal that the central DNA damage response proteins, ATM and ATR physically associate with telomeres (30,149) in wild type cells, but fail to activate a full-blown DNA damage response (30). Even more surprising, key components of NHEJ, including the Ku heterodimer and the Mre11 complex not only bind telomeres (Figure 34), but also are absolutely required for telomere length homeostasis and chromosome end protection. Below we review the salient features of the NHEJ repair pathway, and discuss the biochemical properties of these components that enable them to act on chromosome termini.

Non-homologous end-joining repair

NHEJ repair directly rejoins broken ends of double-strand DNA molecules. The repair reaction requires alignment of two DNA ends in a manner robust enough to support subsequent DNA ligation. Repair of cohesive DNA ends can be achieved, in principle, using only one of the NHEJ components, ligase IV (125). However, the majority of spontaneous DNA breaks that occur in cells as a consequence of ionizing radiation, DNA replication, or oxidative metabolism, produce incompatible DNA ends that must be processed before ligation. Several NHEJ repair complexes are involved in the end-joining reaction and their utilization depends on the nature of the DNA lesion. The requirement for certain NHEJ factors varies among organisms, arguing that the composition of NHEJ machinery reflects a substantial degree of evolutionary flexibility. Ku and ligase IV/XRCC4 are required for NHEJ in both yeast and mammals. In contrast, the Mre11 complex plays a substantial role in NHEJ in yeast, but not in mammals. Likewise, mammalian NHEJ has a requirement for DNA-PKcs, but this protein is absent in non-vertebrates. In the following section we discuss individual

protein components of the NHEJ repair pathway and their roles in the end-joining reaction.

The Ku complex

The Ku complex is a heterodimer formed by Ku70 and Ku80 subunits which was originally identified as an autoantigen in the sera of patients suffering from polymyositis-scleroderma overlap syndrome (126). Ku has adopted multiple cellular functions. Its nuclear roles involve DNA replication, telomere maintenance and regulation of transcription, while in the cytoplasm, Ku inhibits apoptosis by sequestering Bax protein outside of mitochondria (294,295). Ku has also been localized in the plasma membrane, where it participates in cell adhesion (296,297).

The Ku complex is best known for its function in the NHEJ DNA repair. Ku has strong affinity for the ends of double-stranded DNA that is independent of DNA sequence as well as the exact structure of DNA ends. Ku can bind to blunt ends, to the ends with 5' and 3' single stranded protrusions or to hairpins (128,129). Ku also binds to heterologous DNA ends produced by ionizing radiation (298). The crystal structure of the human Ku70/80 heterodimer provides an elegant explanation for its affinity to DNA ends (130). Ku70 and Ku80 proteins share a similar three-domain topology, consisting of a □□-domain at the N-terminus, a central □-barrel domain and a helical C-terminal arm. The central domains of Ku70 and Ku80 form a double ring that encircles the DNA molecule. However, Ku makes no contacts with the DNA bases and few contacts with the sugar-phosphate backbone, explaining its sequence-independent mode of DNA interaction. Electrophoretic mobility shift assay, electron microscopy and footprinting experiments reveal that multiple Ku molecules can bind a single linear DNA molecule *in*

vitro (129), but Ku does not efficiently interact with closed circular plasmids. This observation supports a model in which the initial binding of Ku to DNA occurs through a DNA end followed by translocation inwards. The ability of Ku to move inward from the DNA terminus might be important for efficient NHEJ reaction, as it frees the DNA end for subsequent enzymatic processing.

The N-terminal α/ß domains and helical C-termini of Ku70 and Ku80 lie at the periphery of the complex and do not significantly contribute to DNA interactions or heterodimer formation. Rather, these domains provide an interface for binding other DNA repair proteins. Notably, Ku-like proteins capable of binding DNA ends have been found in bacteria and bacteriophages (299,300). They share sequence similarity with the central domain of their eukaryotic counterparts, but lack the conserved domains at the N and C terminus. Thus, eukaryotic Ku70 and Ku80 proteins appear to have evolved from an ancestral prokaryotic *ku* gene; the DNA end binding activity is the most conserved biochemical property of the Ku complex (301).

The efficiency and accuracy of NHEJ decreases dramatically in cells deficient in Ku as demonstrated by assays utilizing repair of site-specific breaks produced either by transforming cells with a linearized plasmid (plasmid religation assay) or by induction of site specific endonucleases such as HO or I-*Sce*I (chromosomal DSB assay) (232,302). Ku is one of the most abundant nuclear proteins, and thus it is likely to be the first protein to bind a DSB (224,303). Ku participates in several steps of NHEJ and is implicated in alignment and synapsis of DNA ends, ligation, suppression of exonuclease resection and recruitment of additional factors that are important for processing of DNA breaks. It is still a matter of debate whether the association of Ku with broken DNA plays a structural role in NHEJ by directly stabilizing DNA ends and facilitating their

synapsis, or whether it simply serves as a platform for loading other repair proteins. The role of the Ku in DNA end synapsis was inferred from visualization of the human Ku:DNA complexes by atomic force microscopy (298,304) and supported by the observation that Ku is capable of bridging two DNA fragments in an *in vitro* pull-down assay (305). However, an independent study suggested that DNA-PKcs, rather than Ku, mediates synapsis (306). Thus, the extent to which Ku facilitates the association of DNA ends *in vivo* is still unclear.

Another aspect of NHEJ where Ku contributes is protection of DSBs from excessive nucleolytic processing. Sequence analysis of the fusion junctions derived from the cells lacking Ku (232,302) or produced in cell-free system using protein extracts depleted of Ku (139) revealed deletions encompassing up to hundreds of nucleotides around the break site. The propensity of the NHEJ reaction towards deletions in the absence of Ku strongly indicates that the Ku heterodimer stabilizes DNA ends and protects them from excessive nucleolytic degradation before ligation ensues. Nevertheless, there are only a few studies directly addressing the interplay between Ku and nucleolytic activities at intrachromosmal DSBs. A two-fold increase in the rate of 5' to 3' end resection has been reported in budding yeast deficient for Ku when a DSB was induced in proliferating cells (176). The increased resection rate was suppressed by concomitant mutation in the *MRE11* gene. On the other hand, the stability of the 5' end was indistinguishable in wild type and *ku* deficient strains when a break was induced in cells arrested in G1 (307). These differences may be attributed to a variable availability of the nuclease activity during the cell cycle.

Besides its function in stabilizing DNA ends, Ku has also been shown to directly facilitate break ligation. The stimulatory effect may reflect the capability of the Ku

complex to juxtapose two DNA ends (305). In addition, it has been reported that the ligase IV/XRCC4 complex is recruited to DNA ends via interaction with Ku (308,309). Interestingly, Ku stimulates ligation under conditions where one or two molecules bind per DNA end; Ku is inhibitory at higher concentrations that would promote binding of multiple Ku heterodimers (305,310). Further biochemical experiments demonstrated that recruitment of ligase IV/XRCC4 to the break results in inward translocation of Ku, freeing DNA end for subsequent ligation (310). The ability of the ligase IV-XRCC4 to cause the translocation appears to be restricted by the presence of only a few internally bound Ku molecules.

One of the key functions of Ku in NHEJ is to recruit and coordinate end-processing activities to make DNA ends amenable to ligation (see below). Reconstitution of the NHEJ reaction *in vitro* demonstrated that Ku stimulates association of human polymerases μ and λ with DNA fragments (135). Polymerases μ and λ belong to the Pol X family, and are implicated in filling in gaps arising during alignment of DNA ends. Ku is also important for recruitment of Artemis, a structure-specific nuclease essential for processing coding joints during V(D)J recombination. Finally, Ku has been shown to directly interact with Werner syndrome helicase and the Mre11 complex, both of which are implicated in nucleolytic processing of DNA ends (311-314).

The Ligase IV/XRCC4 complex

Three DNA ligases (ligase I, III and IV) are present in mammalian cells. Genetic studies in budding yeast (233,315) and mouse (316) revealed that the NHEJ ligase activity is provided by ligase IV. Ligase IV forms a complex with the XRCC4 protein (*S. cerevisiae*

orthologs are called Lig4 and Lif1 respectively), which is also required for ligase activity (125,317). Crystallographic indicated that the stoichiometry of the human ligase IV/XRCC4 complex is 1:2 (318). Biochemical analysis of *in vitro* reconstituted NHEJ reaction revealed that the ligase IV/XRCC4 complex possess a unique single-strand ligation activity that permits joining of one DNA strand across a gap in the opposite strand (135). Ligase IV is the major NHEJ ligase, nevertheless yeast *lig4* mutants are still capable of plasmid relegation, though with significantly reduced efficiency and accuracy (233). Ligase IV independent end-joining appears also to occur in higher eukaryotes; knock-out of ligase IV in a human cell line does not completely abolish V(D)J recombination (319). Furthermore, ligase IV deficiency does not prevent non-homologous chromosomal integration of a *P* element and T-DNA in *Drosophila* and *Arabidopsis*, respectively (230,320). It remains to be determined which ligase is responsible for the residual end-joining activity.

Two additional NHEJ factors associated with ligase IV/XRCC4 have been identified. *S. cerevisiae* Nej1 is a haploid-specific protein whose expression is repressed by Mata1/α2 repressor (321-323). Nej1 interacts with Lif1 and *nej1*□ mutants are deficient in plasmid religation and chromosomal DSB repair assays. Two independent studies have recently reported discovery of a novel human protein, Cernunnos/XLF, which interacts with the ligase IV/XRCC4 complex (324,325). Intriguingly, Cernunnos/XLF is predicted to share a structural similarity with the XRCC4. Patients carrying a mutation in the Cernunnos/XLF gene or cell lines in which the protein was depleted by RNAi display impaired NHEJ. A more detailed understanding of the molecular function of NHEJ-associated proteins awaits further genetic and biochemical analyses.

DNA-PKcs/Artemis

In addition to the Ku heterodimer and XRCC4/Ligase IV, the mammalian NHEJ core components consist of the DNA-dependent protein kinase catalytic subunit (DNA-PKcs) and Artemis. DNA-PKcs is a member of phosphoinositide-3-kinase-related family, which also includes ataxia telangectasia mutated (ATM) and ataxia telangectasia-related (ATR) DNA damage signaling proteins. The essential role of DNA-PKcs in DSB repair was demonstrated by studies of severe combined immunodeficient (SCID) mice with defective DNA-PKcs gene. SCID mice display aberrant V(D)J recombination while DNA-PKcs deficient cells exhibit a radiosensitive phenotype (224,326,327). DNA-PKcs physically associates with the Ku heterodimer forming a catalytically active DNA-PK holoenzyme. Ku recruits DNA-PKcs to a DSB via the C-terminal domain of the Ku80 protein (328), leading to a rapid activation of DNA-PK in response to DNA damage. Activation of the kinase activity appears to require a direct interaction of DNA-PKcs with free DNA. Although DNA-PKcs can also bind to DNA termini and activate its kinase activity in the absence of Ku, this occurs at much lower efficiency (329).

The requirement for DNA-PKcs in NHEJ is well established, but little is known about its function in DSB rejoining or its *in vivo* phosphorylation targets. *In vitro* studies indicate a stimulatory role of DNA-PKcs in DNA synapsis (306) and ligation (123,330). Ligation stimulation may be implemented via autophosphorylation of DNA-PKcs, resulting in remodeling of the DNA-end-bound DNA-PK complex (123,331). In addition, DNA-PK phosphorylates histones H2AX and H1 (330,332) and histone H1 phosphorylation by DNA-PK has been shown to de-repress ligation of *in vitro* reconstituted nucleosomes by ligase IV (330). These observations indicate that DNA-

PK may facilitate the NHEJ reaction by modifying the local chromatin environment to provide access of other DNA repair complexes to DSBs.

New insight into the role of DNA-PKcs in NHEJ has emerged with the identification of Artemis, a structure-specific nuclease important for processing DNA ends during V(D)J recombination (333,334). Artemis is recruited to DNA ends by DNA-PK, which activates its endonuclease-hairpin opening activity and permits ligation of the coding ends (335). Increased sensitivity of Artemis-deficient cells to ionizing radiation and failure to rejoin ~ 10% of radiation induced DSBs suggests a NHEJ function outside of V(D)J recombination (336). However, the radiosensitive phenotype of both DNA-PKcs and Artemis-defective cells is significantly lower than in cells depleted of Ku or XRCC4 (334,337,338). The different genetic requirements for repair radiation induced DSBs or breaks occurring during V(D)J and class switch recombination indicate that, in contrast to Ku70/80 heterodimer and ligase IV/XRCC4, DNA-PKcs/Artemis are important for only a subset of NHEJ reactions. The less stringent requirement for DNA-PKcs/Artemis in NHEJ is in accordance with the fact that orthologs have been found only in vertebrates and slime moulds (339), but not in invertebrates, plants or fungi.

The Mre11 complex

The Mre11 complex consists of the evolutionary conserved Mre11 and Rad50 subunits and the less conserved Nbs1/Xrs2 protein (MRN/X; reviewed in (210)). Like Artemis, Mre11 is a structure-specific nuclease. Mre11 exhibits 3'-5' dsDNA exonuclease and ssDNA and dsDNA endonuclease activities. The Rad50 protein is a member of SMC (structural maintenance of chromosome) protein family, which also includes cohesin and condensin subunits. Rad50 forms a structural scaffold, containing C- and N-

terminal ATPase domains that are connected by a long coiled-coil region separated in the middle by a flexible hinge. Scanning force microscopy revealed that Rad50 protein folds back in the hinge region to bring together terminal ATPase domains. The whole structure is stabilized by anti-parallel association of the coiled-coil regions (340). Dimerization of two Rad50 proteins is mediated by a zinc-finger-like hook in the hinge domain (341). One Nbs1/Xrs2 and two Mre11 molecules interact with the Rad50 dimer, forming a complex capable of binding and tethering DNA ends.

The Mre11 complex plays a central role in DSB repair. It is involved in DNA damage detection and signaling, as well as in homologous recombination and NHEJ. The Mre11 complex is among the first enzymatic complexes arriving at a DSB suggesting that it acts as a DSB sensor to initiate DNA damage signaling and repair through a pathway that includes activation of the ATM kinase (342-344). The Mre11 complex is also essential for early steps of meiotic recombination, where it mediates nucleolytic processing of 5' DNA ends at meiotic breaks (345,346).

The NHEJ function of the Mre11 complex is only definitely established in budding yeast. Deletion of any component of the complex results in a 10 to 100 fold decrease in the efficiency of DNA end joining assays (347) (301). Biochemical analysis showed that the yeast Mre11 complex has a DNA end bridging activity and facilitates joining of linear DNA molecules by Dnl4/Lif1 (348). Epistasis analysis suggests that Ku, Mre11 and Lig4/Lif1 complexes participate in the same NHEJ pathway (232,314,349). This hypothesis is further supported by the observation that Ku augments the stimulatory role of the Mre11 in the Lig4-dependant ligation of DNA ends *in vitro* (348). Thus, genetic and biochemical experiments indicate that Mre11 complex acts in concert with Ku to promote efficient alignment of DNA ends and recruitment of ligase IV.

The Mre11 complex can also function independently from Ku in the end-joining mechanism that processes noncomplementary DNA ends (147). Characteristic features of this pathway include fusion products with deletions spanning up to 300 nucleotides and sequence microhomology at the fusion points. Accordingly, this mechanism has been dubbed microhomology-mediated end joining (MMEJ). The efficiency of the MMEJ pathway significantly decreases in the cells lacking Mre11 complex or Rad1/Rad10 3´ flap nuclease, but does not require Ku heterodimer. Interestingly, MMEJ is not entirely dependant on Lig4, indicating that its function can be substituted by another ligase, most likely Cdc9 (the yeast ligase I ortholog required for ligation of Okazaki fragments). The model of MMEJ predicts that nucleolytic processing of 5' ends of DSBs by Mre11 uncover microhomology that can be utilized for annealing and alignment of broken termini. The resulting 3´ flaps are removed by Rad1/Rad10 endonuclease generating 3´ ends suitable for gap-filling reaction and ligation (147).

The role of the Mre11 complex in NHEJ in other organisms is currently unclear. Repair of DSBs in higher eukaryotes frequently occurs by a MMEJ-like mechanism that generates microhomology at fusion junctions (350). The human Mre11 complex has been shown to possess exonuclease activity, which is stimulated by non-cohesive DNA ends, but is inhibited when a 3´ end anneals to a homologous region of another DNA molecule. This enzymatic property of the Mre11 complex is consistent with its role in MMEJ (146). However, there is no strong *in vivo* evidence demonstrating a significant contribution of the Mre11 complex to DNA end-joining repair outside of budding yeast (172,211,351).

Additional DNA end processing factors

DSBs that occur in nuclei as a result of cellular metabolism or external genotoxic stress are most likely not amenable for a direct ligation. Such ends may be formed by incompatible 3´ or 5 ´end protrusions or contain unusual chemical structures that must be removed to restore 3´-OH or 5´-phosphate groups. Rejoining of such substrates usually requires nuclease and polymerase activities that trim incompatible sequences and fill-in gaps. So far the only nuclease identified to be required specifically for NHEJ is Artemis. Two nuclease complexes that cleave branched DNA structures have been shown to contribute to efficient DNA end-joining in budding yeast. As discussed above, the Rad1/Rad10 nuclease participates in MMEJ by removing 3´ flaps (147), whereas removal of the 5´ flap intermediates arising during NHEJ is dependent, at least in part, on Rad27 (yeast homologue of FEN1) (352). Both Rad1/Rad10 and Rad27 play more general role in DNA repair; Rad27 is required for processing replication intermediates, while Rad1/Rad10 is involved in base excision repair and homologous recombination. Another enzyme implicated in nuclease processing during NHEJ is human Werner syndrome helicase (WRN). *In vitro* studies showed that WRN is recruited to DNA ends via physical interaction with Ku. This interaction stimulates 3´- 5´ exonuclease activity of WRN (312,353). It remains to be established whether WRN plays a physiological function in NHEJ *in vivo*.

DNA polymerization and gap-filling activities during NHEJ are mediated mainly by members of the Pol X family of non-replicative DNA polymerases. Genetic data implicate polymerase 4 (Pol4), the only member of the Pol X family in budding yeast, in the repair of subclass of DSBs that require gap filling and flap removing activities (174,354). Biochemical analysis revealed that the DNA synthesis activity of Pol4 is

stimulated by association with Lig4/Lif1, and that the both protein complexes interact with Rad27. Together, these proteins have been shown to coordinate processing and ligation of DNA ends with non-complementary 5´ends (355,356). Four Pol X polymerases have been found in mammalian cells and three of them, Pol λ, Pol μ and terminal deoxynucleotidyl transferase (TdT) are involved in NHEJ (135). The polymerases display distinct catalytic properties, which may allow efficient NHEJ at a wide spectrum of substrates. While TdT adds random nucleotides to DNA termini, both Pol λ and Pol μ can perform template-dependant gap filling synthesis on mismatched ends. Similar to TdT and in contrast to Pol λ, Pol μ does not require alignment of the primer with the template DNA strand (357). Interestingly, plants and yeast posses a single Pol X polymerase (most related to Pol λ) (358), while *C. elegans* and *D. melanogaster* completely lack this class of polymerases (359). Hence, expansion of the Pol X family in mammals may reflect their unique function in rearrangement of genes encoding immunoglobulins and T-cell receptors.

Model for non-homologous end joining

The NHEJ machinery must be remarkably flexible to process and efficiently ligate such a wide range of DNA damage induced structures, while at the same time preventing excessive loss of DNA sequence surrounding the breakage site. This coordination is facilitated by the existence of a NHEJ “toolkit” comprised of several distinct enzymatic activities that mediate DSB recognition and binding, end-synapsis, nucleolytic processing, DNA synthesis and ligation (Figure 35) (for recent reviews see (144,224,303,347). Binding of the Ku heterodimer to a DSB is the first step in blocking unregulated degradation of DNA, while simultaneously allowing for efficient assembly of

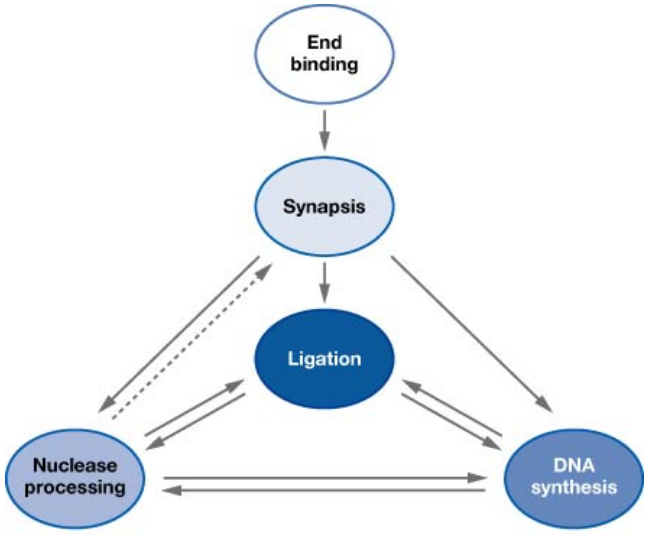

Figure 35. Iterative processing model for NHEJ.

The NHEJ reaction consists of several distinct enzymatic steps, different combinations of which result in ligation of DNA ends. A flexible series of DNA processing events (indicated by arrows) can occur depending upon the structure of the DNA lesion, and the availability of DNA repair enzymes. The order of events is not completely random, however, as DNA end binding by Ku typically initiates NHEJ, while ligation concludes the reaction. The timing of each reaction during NHEJ is illustrated by the intensity of the circle shading, with later steps indicated in darker colors. The dashed arrow suggests a situation where nucleolytic resection precedes synapsis to expose microhomology for end alignment.

other enzymatic components. The exact sequence of downstream reactions is not strictly defined. The recent discovery that ligase IV is able to join one strand leaving a free end on the other strand provides the impetus for an iterative processing model of NHEJ (135,303). This model predicts that nuclease, polymerase and ligase activities are recruited to DNA ends by Ku in a random order, which allows ligation of one strand to precede end-processing of the complementary DNA strand (Figure 35). This model contrasts with the classical view of NHEJ, which holds that ligation of both strands is the final step of NHEJ. The suggestion that that individual enzymatic activities can act independently on each strand in a random order provides an explanation for the efficient and timely repair of any two DNA ends regardless of their complexity.

Another factor that contributes to the versatility of the NHEJ reaction is an optional recruitment of other DNA repair proteins. So far no genetic conditions have been reported that completely suppress DNA end-joining. Even in the absence of ligase IV, which together with Ku defines the NHEJ machine, end-joining occurs demonstrating that another ligase can partially substitute for ligase IV {Ma, 2003 #54; McVey, 2004 #690; Teo, 1997 #73; van Attikum, 2003 #76}. The flexibility of the composition of NHEJ machinery is further illustrated by DNA lesion-specific or species-specific requirements for NHEJ proteins. For example, efficient alignment of broken DNA ends requires the Mre11 complex in yeast (348), whereas DNA-PKcs can apparently substitute for Mre11 function in mammals (306). Interestingly, none of these complexes are important for NHEJ in fission yeast. Because current models of NHEJ are based primarily on studies of NHEJ in budding yeast and V(D)J recombination in mammals, it is very likely that more examples of evolutionary substitutions, especially in DNA processing steps, will be uncovered in

other organisms. In summary, we can conclude that a crucial characteristic of NHEJ mechanism is a modular employment of individual enzymatic activities, the utilization of which depends on structural features of the broken ends and on the availability of individual NHEJ proteins in the cell.

The role of NHEJ in genome instability triggered by telomere dysfunction

One hallmark of telomere dysfunction is the formation of dicentric chromosomes as a consequence of chromosome end-joining. If the two kinetochores of a dicentric chromosome attach to opposite spindle poles, centromeres are pulled apart and chromosome will break during anaphase. The new break sites are then repaired by fusion with other DSBs forming a new dicentric chromosome. This process, called the breakage-fusion-bridge (BFB) cycle, can continue over multiple cell divisions, resulting in the generation of complex chromosomal rearrangements. Studies performed by Barbara McClintock have shown that the BFB cycle can be disrupted by “healing” broken chromosome ends by de novo telomere addition (6,306,360). Recently, it has been suggested that telomere attrition and the perpetuating BFB cycle is one of the key mechanisms initiating genome instability during early tumorigenesis (361,362). Although scarce information is available regarding the molecular aspects of the BFB cycle, the NHEJ DNA repair pathway appears to play a central role in both the formation of dicentric chromosomes and in the chromosome healing reaction (for recent reviews see (184,363,364).

Mechanisms of chromosome end-to-end fusion

While dicentric chromosomes can theoretically arise by recombination between ectopic regions of homology located at different chromosomes, the vast majority of chromosome fusions observed in cells with dysfunctional telomeres occur through a DNA end-joining reaction. Telomere dysfunction can either be induced by depletion of a crucial protein component of the telomere cap, or by telomerase inactivation and the slow attrition of telomeric DNA that arises from the end-replication problem.

The best established systems for studying telomere dysfunction in human cells utilize reduction of TRF2, accomplished by RNAi or through the expression of a dominant negative allele, to remove endogenous TRF2 from telomeres. TRF2-depleted telomeres induce a DNA damage response that is characterized by the formation of telomere-damage induced foci, consisting of □-H2AX, Mre11, ATM and other DNA repair factors, and the activation of the ATM/p53-dependent checkpoint pathway (78,365). Furthermore, cell lines transformed with the dominant negative TRF2$^{\Delta B \Delta M}$ construct exhibit a high frequency chromosome end-to-end associations (2,77). These findings argue that defective telomeres are recognized as DNA damage and subjected to repair by NHEJ. Importantly, chromosome fusions arising from TRF2 dysfunction are significantly reduced in mouse cells deficient for ligase IV, demonstrating direct involvement of NHEJ in telomere fusion (2,237). As discussed above, efficient NHEJ reaction requires alignment of both DNA ends in a ligatable conformation. The fact that telomeres carry 3´ overhangs precludes efficient juxtaposition of the 3´ ends, and hence poses an obstacle for efficient ligation. Further, the presence of a long telomeric DNA tract at the fusion sites in TRF2 deficient cells also argues against excessive exonucleolytic degradation, which might uncover regions of microhomology. Instead,

telomere ligation is facilitated by removal of 3´overhangs by the ERCC1/XPF 3´ flap endonuclease, a mammalian homologue of the *S. cerevisiae* Rad1/Rad10 (106).

Under certain growth conditions, fission yeast lacking Taz1, an ortholog of mammalian TRF1 and TRF2 arrest in G1 with massive telomere fusion and loss of viability. Chromosome fusion requires Ku and ligase IV, and like the fusion junctions in TRF2 mutants, a majority of the telomeric sequence is retained (179). Additional studies indicate that telomeres depleted of Taz1 are prone to DNA repair by HR or NHEJ, and the utilization of the DSB pathways depends on the stage of the cell cycle. While homologous recombination is the predominant mechanism for DSB repair during G2, NHEJ prevails in G1 resulting in the formation of lethal interchromosomal fusions in *taz*$^{-}$ strains (179,268). Ku- /ligase IV- dependent chromosome end-to-end fusions specifically occurring during G1 have recently been observed in the cells lacking Taz1 interacting protein Rap1 (366).

Inactivation of the Rap1 also results in telomere fusions in budding yeast (367). Because deletion of the Rap1 is lethal in *S. cerevisiae*, a conditional allele was utilized resulting in the inactivation of Rap1 after the cell culture exits stationary phase of growth. PCR amplification of the fusion products suggested that telomeres of nearly wild type length fuse with each other. Genetic analysis showed that all known core components of the yeast NHEJ pathway, Ku70, Ku80, Lig4, Lif1, Nej1, Mre11, Rad50 and Xrs2 are required for fusion formation (367). Moreover, chromosome end-joining decreased by two to three orders of magnitude in *pol4* mutants, suggesting that gap filling is important for the NHEJ reaction between telomeres (368).

Another instance of chromosome end-joining that occurs in budding yeast is found in cells doubly deficient for telomerase and Tel1 (the ATM ortholog). Using a

PCR-based assay, Chan and Blackburn (188) showed that *tel1 tlc1* cells accumulate telomere-DSB fusions immediately after induction of HO. The fusions are dependant on ligase IV and preferentially occur during G1. Interestingly, an average of only 33 bp of telomeric sequence was retained at the fusion junction, while the shortest telomeres in these cells were above 190 bp (188). Thus, in contrast to telomere uncapping by inactivation of Rap1 (367), extensive telomere shortening precedes ligation in *tel1 tlc1* strains. Similar observations have been made in *S. cerevisiae* lacking Tel1 and Mec1 (the ATR ortholog). Analysis of telomere-telomere fusions in *tel1 mec1* mutants showed extensive loss of telomeric DNA, and in some cases erosion into the subtelomeric region (209).

The studies discussed above strongly implicate NHEJ machinery in fusing chromosome termini when telomere deprotection is caused by depletion of dsTBPs or Tel1. However, a requirement for core NHEJ factors in processing chromosome ends that undergo progressive telomeric DNA loss as a consequence of telomerase inactivation is less stringent. Analysis of the NHEJ genes involved in fusing chromosome ends in telomerase-deficient mouse is complicated by the fact that ligase IV knock-outs are lethal, and strains lacking Ku or DNA-PKcs exhibit a high-level of chromosome fusions (168,193,234). Ku80 deficiency in mouse leads to an increased incidence of telomere-telomere fusions that retain long tracks of telomeric sequence at the fusion points, consistent with a role for Ku in chromosome end protection. Nevertheless, inactivation of Ku80 in mice propagated for three or four generations without functional telomerase suppresses formation of fusions that lack telomeric sequence, although it does not influence frequency of fusions that include long telomeres (194). Similar observations have been made in mice lacking telomerase and

DNA-PKcs (169), implying that Ku/DNA-PKcs is important for ligation of critically short telomeres arising as a consequence of telomerase deficiency. In contrast, neither Ku nor ligase IV appear to be essential for chromosome end-to-end fusions in fission yeast deficient for the catalytic subunit of telomerase (195). Telomerase-deficient *S. pombe* escape telomere-loss induced senescence by intramolecular ligation, resulting in circular chromosomes (369). Deletion of *ku70* or *lig4* genes does not abrogate this survival strategy (195). Paradoxically, formation of circular chromosomes in telomerase-deficient *S. cerevisiae* is promoted in the absence of Nej1, but still depends on functional ligase IV (370).

Mechanisms leading to end-to-end chromosome fusions were also studied in *Arabidopsis* mutants lacking telomerase reverse transcriptase (TERT). Sequence analysis of fusion junctions amplified from the late generation *tert* mutants reveal deletions reaching up to several hundreds bases pairs within the subtelomeric region. The size of the shortest telomeres with intact G-overhangs detected in the same plants is approximately 300 bp, indicating that rapid degradation precedes ligation once telomeres shorten below a critical length (180). This finding is similar to the situation in budding yeast and *Caenorhabditis elegans* where terminal deletions involving up to several kb of subtelomeric sequence occur prior to chromosome fusions in telomerase deficient strains (371,372). Inactivation of *ku70* in *Arabidopsis tert* mutants does not prevent chromosome fusions in plants with critically short telomeres (117). While more than 50% of the fusion junctions harbor untemplated insertions of a filler DNA in Ku70 proficient plants, the frequency of insertions is dramatically reduced in *ku70 tert* mutants and majority of the fusion junctions feature microhomology (180). The use of sequence microhomology is partially dependent on Mre11. These data indicate that plant cells can

fuse dysfunctional telomeres using both Ku-dependant and Ku-independent end-joining pathways.

While the experiments with yeast, plant and mammalian cells highlight the critical contributions of ligase IV and Ku in mediating end-to-end chromosome fusions, they also uncover significant differences in the requirements for these NHEJ factors. These differences might partially reflect species-specific redundancy and robustness in the NHEJ mechanism. However, the observations that Ku and ligase IV are essential for fusing telomeres in *taz*$^{-}$, but not in *trt*$^{-}$ *S. pombe* strains (179,195), and that the Ku86 deficiency in mouse promotes one type of chromosome fusions, but suppresses another type (194) strongly argue that the mode of telomere uncapping also influences chromosome end processing.

The data further indicate that deletion of dsTBPs, such as TRF2, Taz1 and Rap1 result in immediate end-joining (Figure 36), while chromosome end de-protection from progressive attrition of telomeric DNA in the absence of telomerase or Tel1 is followed by rapid degradation of chromosome termini (Figure 37). Ligation of chromosome ends in the latter case appears to be less dependent on the core components of NHEJ (Ku, ligase IV or Nej1) (117,195,209,370). While it is formally possible that the chromosomes depleted of dsTBPs are seen differently by DNA damage checkpoints than very short telomeres, this does not seem to be the case in mammals. Both TRF2 depleted telomeres and telomeres critically shortened due to telomerase inactivation induce telomere-damage foci consisting of a similar set of proteins (78,299). Accessibility of de-protected chromosome termini to DNA repair proteins might be another factor contributing to the different fates of dysfunctional telomeres. For example, telomeres

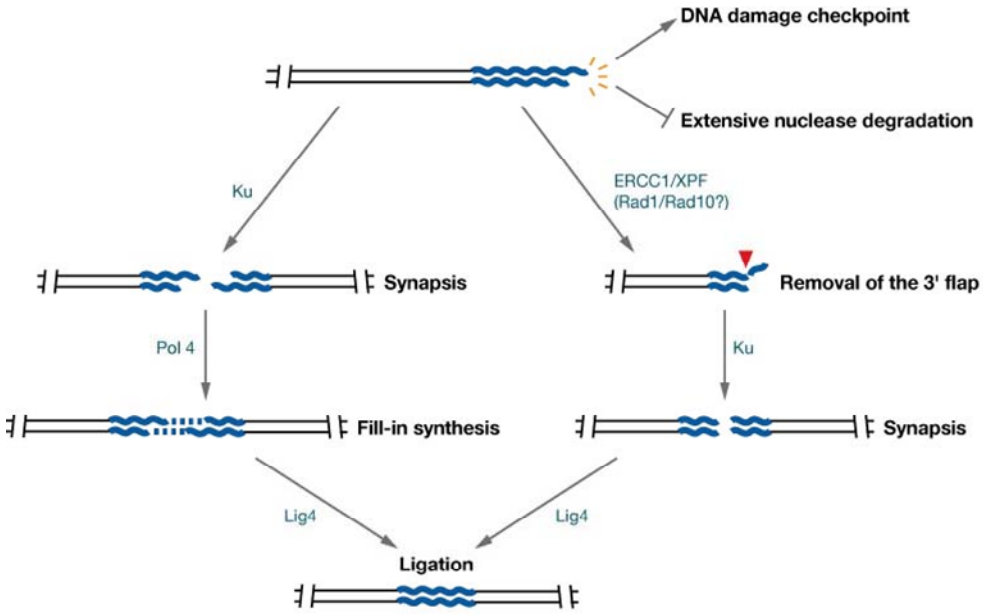

Figure 36. Model for telomere fusions in cells lacking capping dsTBPs.

End processing steps involved in fusing dysfunctional telomeres that arise from depletion of dsTBPs (see text for details). Left pathway shows the consequences of depleting Rap1 in budding yeast, while the right pathway illustrates events leading to fusion of TRF2-deficient telomeres in mammals.

lacking dsTBP may become permissible to NHEJ by Ku and ligase IV (Figure 37, right pathway), while the long tracks of telomeric DNA and the remaining telomere proteins may confer protection against exonuclease processing and/or Ku/ligase IV independent ligation. This model is supported by the observation that telomeres in *TRF2*$^{-/-}$ *Lig4*$^{-/-}$ *p53*$^{-/-}$ cells do not fuse, but rather persist in a free state without undergoing detectable DNA degradation (237) (Figure 36, right pathway). On the other hand, critically shortened telomeres that arise in yeast Δ*est1* strains are subjected to an extensive resection by exonuclease 1 (225) (Figure 37). Hence, the loss of functional telomeric DNA may result in a more severe mode of chromosome end de-protection, leaving termini vulnerable to a wider range of DNA repair factors.

The timing of when telomeres become uncapped may also influence their fate. In telomerase-deficient cells loss of telomeric sequence due to the end replication problem occurs in a relatively narrow window at the end of the S-phase, and telomere damage likely reflects a failure to reassemble a functional nucleoprotein complex after passage of the replication machinery. Because the majority of DSB repair proteins are up-regulated during S-phase, and many directly assist in repair and processing of replication intermediates, the local environment could provide more alternative pathways to act on dysfunctional telomeres. For example, the end-joining function of the ligase IV can be partially substituted by activity of the ligase I, which is induced in S-phase, but suppressed in other stages of the cell cycle (373). Similarly, abundant nuclease activities expressed during S-phase may expose regions of microhomology and facilitate DNA end synapsis through base pairing, alleviating a need for the Ku heterodimer (Figure 37, left pathway).

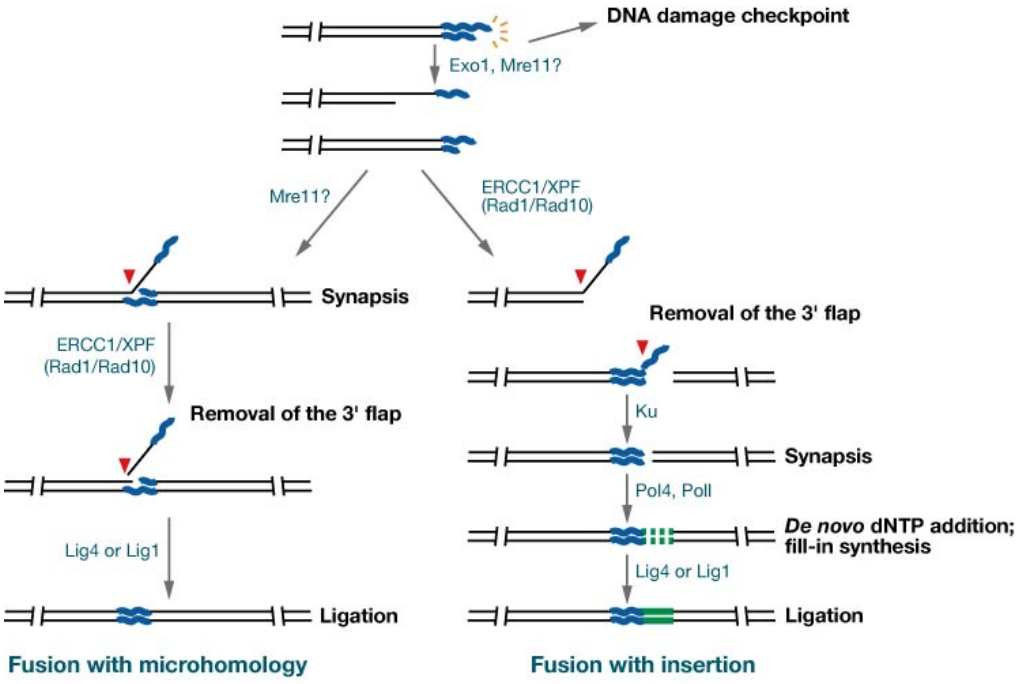

Figure 37. Model for end-joining of critically shortened telomeres.

End processing steps involved in fusing critically shortened telomeres that arise from telomerase inactivation (see text for details). Left pathway shows the Ku-independent MMEJ pathway. The right pathway illustrates a sequence of reactions leading to telomere-telomere ligation with non-templated insertions at the fusion point.

In contrast, the immediate consequences of Rap1, Taz1 or TRF2 depletion are likely to be manifested outside of S phase. For example, chromosome fusions in fission yeast lacking Taz1 form during G1 (179). It is also likely that chromosome fusions arising from TRF2 form predominantly outside of S phase. Inactivation of TRF2 has been achieved by transfection of asynchronous mammalian cells with vectors expressing either a dominant negative allele or an RNAi construct, or by infecting cells with a *cre*-retrovirus resulting in conditional deletion of the *TRF2* gene. Because the TRF2 protein exhibits a very dynamic interaction with telomeric DNA, with a residence time of up to 11 minutes (374), the pool of telomere-bound protein could be rapidly depleted in these experiments, causing telomeres become deprotected at any stage of the cell cycle, including G1. Consistent with this idea, the telomeric NHEJ reaction in TRF2-deficient cells has been detected before and after telomere replication (2). Therefore, end-joining reactions that occur in G1 may rely more on the conserved NHEJ pathway, which is the primary DSB repair mechanism at this stage of the cell cycle.

In summary, we can conclude that telomere-telomere ligation resembles joining of complex non-cohesive DSB breaks in many aspects. Single-stranded telomeric 3´ overhangs do not permit direct alignment of the ends in a ligatable conformation and hence the telomeric end-joining reaction must involve several DNA processing steps (Figure 36 model for telomeric end-joining). The studies discussed above suggest that processing of dysfunctional telomeres prior to ligation does not follow a uniform pattern, and instead depends on the mode of telomere de-protection and the cell cycle context in which the damage is incurred. These observations, together with the flexible requirements for individual DNA repair factors, support the iterative processing model of

the NHEJ (Figure 35 NHEJ model) and demonstrate the remarkable versatility of the DNA end-joining pathways (303).

BFB cycle propagation

End-to-end chromosome fusion will lead to the formation of a dicentric chromosome, which in turn triggers further genome instability via BFB cycles. Although the impact of the BFB cycle on genome structure is well documented cytologically (for reviews see (375,376), the molecular mechanisms that govern BFB cycles have not been extensively examined. It is assumed that breakage of the dicentric chromatid is caused by the mechanical tension produced by separating kinetochores during anaphase. If this is the case, then the anaphase bridge is expected to break anywhere between the two centromeres. Interestingly, analysis of the breakpoint frequency of dicentric chromosomes in budding yeast reveals that although breaks occur throughout whole chromosome arm, they tend to be more frequent in telomere proximal regions (225). Similarly, live imaging of dicentric chromosomes in human cell lines together with cytological characterization of chromosomal rearrangements arising from the BFB cycle indicated that anaphase bridges are most frequently severed in the middle (377). Thus, regions surrounding fusion points appear to be more fragile and prone to breakage. This conclusion is supported by the recovery of complex chromosome fusion junctions in wheat and *Arabidopsis,* which have structures consistent with breakage and secondary fusion occurring within several hundreds of nucleotides of the primary fusion site (180,378).

Because the two DSBs generated by breakage of the anaphase bridge segregate to opposite nuclei, they can not be repaired by direct rejoining. The DSBs

can either ligate with another break or with a dysfunctional telomere at the end of mitosis or during G1, or it can persist until the following S phase and cause fusion of newly replicated sister chromatids. Similar to the primary telomeric fusions, it is very likely that the secondary fusions are mediated by NHEJ.

De novo telomere addition

Since the BFB cycle produces extensive genome rearrangements including deletions, the presence of dicentric chromosomes is incompatible with long-term cell survival under physiological conditions. A study analyzing transmission of dicentric chromosomes in maize demonstrated that BFB cycle can be interrupted by inactivation of one centromere (379). Alternatively, broken chromatids can acquire a functional telomere by translocation of the terminal part of another chromosome. In yeast cells lacking telomerase, translocations mediated by break-induced replication appear to prevail (372). However, when telomerase is present, de novo telomere formation is the predominant form of chromosome healing. We will restrict our discussion to the chromosome healing pathway that involves Ku heterodimer. For a more comprehensive overview of de novo telomere addition we refer to specialized reviews (364,380).

Genetic assays developed in budding yeast to detect frequency of gross chromosomal rearrangements (GCR) such as terminal deletions indicate that telomerase dependent telomere addition to a DSB is the major cause of GCRs (380-382). Mutagenic repair of DSBs by telomerase is suppressed in yeast by Pif1 helicase (383); inactivation of Pif1 results in a 1,000 fold increase in spontaneous genome instability (381). Further genetic analyses revealed that inactivation of the Ku

heterodimer suppresses the mutagenic phenotype of *pif1* (381), suggesting that Ku facilitates telomere synthesis at DSBs. As discussed below, Ku directly interacts with telomerase RNA subunit TLC1 (Peterson 2001 11138000). This interaction appears to be important for de novo telomere addition (165) and hence it is likely that Ku promotes chromosome healing by directly recruiting telomerase to DSBs. Although a physical interaction between Ku and telomerase exists in mammals (164,166), it is currently unclear whether Ku contributes to de novo telomere formation at DSBs in higher eukaryotes.

The role of NHEJ in telomere biology

While no compelling data exist to support a role for Ligase IV or XRCC4 at wild type telomeres, the Mre11 and Ku complexes make essential contributions to multiple facets of telomere biology. Here we discuss the interactions and functions of these proteins at telomeres in different model organisms.

The Mre11 complex

All three components of the Mre11 complex (Mre11, Rad50 and Nbs1/Xrs1) bind telomeres (150,152-154). Although it is still unclear how this association occurs in yeast, in mammals Mre11 and Rad50 interact with the dsTBP TRF2 (154). Recent studies in both yeast and mammals reveal a striking cell-cycle regulated profile of Mre11p complex association with telomeres. In *S. cerevisiae*, all three Mre11 complex components associate with telomeres in late S phase. Mre11p is essential for the recruitment of Mec1p (ATR) to telomeres, which in turn leads to binding of Cdc13p and the telomerase-associated protein, Est1p (150). The temporal localization of Mre11 components at mammalian telomeres appears to be somewhat different than in yeast.

While Mre11 and Rad50 are present throughout the cell cycle, Nbs1 localizes to telomeres only during S phase (154). A more recent study has shown that Mre11 and then phosphorylated Nbs1 are recruited to telomeres in G2, followed by phosphorylated ATM (30).

Although the Mre11 complex is best known for its role in DSB repair, studies in mammals and in *Arabidopsis* indicate that it also helps distinguish the telomere from a double-strand break. It has been reported that the $Rad50^{S/S}$ mutation in a p53 null background results in a low frequency of chromosome end-joining events (384). Similarly, RNAi-mediated knockdown of NBS1 in human lymphoblastoid cells leads to an ~4-fold increase in the incidence of telomere fusions (385). Consistent with these findings, fusions that involve chromosome termini have also been observed in *Arabidopsis mre11* mutants (181).

Perturbations in the Mre11 complex result in telomere length deregulation in most organisms, where it has been studied. In *S. cerevisiae*, telomeres decline by approximately 65% in the absence of Mre11, Rad50 or Xrs2 (170,171,173). Fission yeast deficient in Mre11 or Rad50 exhibit a similar decrease in telomere length (153,172,174,386). Intriguingly, only slight telomere shortening is observed with Nbs1 mutants (175), suggesting that Nbs1 may act in a separate pathway. Analysis of the Mre11 complex at *Arabidopsis* telomeres has lead to somewhat conflicting results. Although one study reported that *mre11* mutants display telomere elongation (182), this phenotype was not observed in analysis of two other independent *mre11* alleles (J. Puizina and K. Riha, unpublished results). In addition, no difference in the telomere length was detected between *ku tert* and *ku tert mre11* mutants (180). Since telomere length varies slightly among *Arabidopsis* individuals, even those within the same

ecotype (238), this could account for the two different findings. *Arabidopsis rad50* mutants exhibit wild type telomere length (387). However, the dedifferentiated callus derived from this line initially exhibited slight telomere shortening, but after several weeks displayed a significant increase in telomere length.

Mre11 is strongly implicated in telomere length maintenance in mammalian cells. In fibroblasts derived from NBS syndrome patients telomeres decline by approximately 25% (183). Expression of telomerase (TERT) or Nbs1 in these cells failed to extend the shortened telomeres. However, when telomerase and Nbs1 were expressed simultaneously, telomere length was substantially increased and proliferation capacity was restored. Thus, the Mre11 complex appears to cooperate with telomerase in telomere maintenance.

The Mre11 complex is also implicated in telomerase-independent telomere maintenance in both yeast and mammals (388). NBS1 and TRF1 co-localize at promyelocytic leukemia (PML) bodies, intracellular structures characteristic of ALT cells (154) (389). A physical interaction between the C-terminus of Nbs1 and TRF1 is observed in PML bodies during late S and G2 phases (389). Moreover, knockdown of NBS1 inhibits the formation of PML bodies, and as a consequence, prevents activation of ALT (390).

In conjunction with its role in maintaining the overall length of the telomere tract, the Mre11 complex, and in particular Mre11 itself, is implicated in the formation and maintenance of the G-overhang. Although a G-overhang is found on both ends of telomeres, leading strand replication of the telomere results in the formation of a blunt end. Thus, nucleolytic processing of the telomeric C-rich strand is postulated to create the G-overhang on the other chromosome terminus (27). Several lines of evidence

indicate that Mre11 participates in this processing. First, Mre11 is required for the loading of the single-strand telomere binding protein Cdc13p in a de novo telomere formation assay in budding yeast (253). Second, Mre11 is associated with a variety of different nuclease activities and is involved in the formation of 3' single-strand overhangs at double-strand breaks (210,252). Third, Wellinger and colleagues found a significant reduction in the G-overhang signal in *S. cerevisiae mre11* mutants (29). Fourth, the elongated G-overhangs found in *taz1-* mutants from *S. pombe* (179), are dramatically reduced in cells doubly deficient for *taz1$^-$ rad50$^-$ or taz1$^-$ rad32$^-$* (*S. pombe* ortholog of Mre11) (178). Finally, RNA interference of human *MRE11* results in transient shortening of the G-overhang in telomerase positive cells (260).

It is important to note, however, that in none of these mutants were G-overhangs completely eliminated. Moreover, Wei et al (118) failed to detect any perturbations to the G-overhang in chicken cells lacking Mre11. Therefore, nucleolytic activities other than Mre11 must contribute to the formation of G-overhangs. From a biochemical perspective, this inference would appear obvious. As discussed above, the exonucleolytic activity associated with Mre11 proceeds in the 3' to 5' direction (391), a polarity opposite of what is required to generate a 3' overhang. In addition, site-directed mutagenesis experiments reveal that the nuclease activity of Mre11 is not required for telomere maintenance (173,174,392). Despite these caveats, Mre11 remains a target of investigation in G-overhang biology. More extensive site-directed mutagenesis of the Mre11 protein reveals that its structural integrity is needed for telomere maintenance (393). Thus, Mre11 may help to recruit another nuclease to process telomeric DNA. In this regard it is noteworthy that in *Tetrahymena*, biochemical analysis reveals the 3' end

of the G-rich strand is also subjected to nucleolytic processing (23). Hence, both the C-stand and the G-strand of the telomere engage nuclease activities.

Recent studies indicate that the Mre11 complex may help to promote structural transitions at telomeres during discrete phases of the cell cycle. As discussed previously, the Mre11 complex is recruited to yeast telomeres in late S-phase where it promotes ATR binding, the subsequent recruitment of the G-overhang binding protein Cdc13p and finally active telomerase (150) (Figure 38a). This finding implies that the telomere is transiently recognized as a double-strand break during S-phase, perhaps as a consequence of t-loop unfolding and presentation of the single-strand G-overhang to telomerase for elongation. In mammalian cells the Mre11 complex is recruited to telomeres later in the cell cycle, in G2 (30) (Figure 38b). Telomeres are susceptible to end-labeling reactions at this time in the cell cycle, and that inhibition of either Mre11 or ATM leads to telomere-end joining (30). Notably, the downstream DNA damage response proteins p53 or Chk2 are not phosphorylated in this interval, arguing that telomeres do not elicit a full-blown DNA damage response. This wave of transient DNA damage response may occur as the telomere reassembles into the t-loop configuration (30) (Figure 38b).

Taken together, the data argue that temporal perception of a chromosome termini as a DSB is important for assembly of a functional telomere capping structure and for telomerase action (30,149,150). In this regard, the role of the Mre11 complex in telomere maintenance parallels its function in perception and processing of a DSB. The Mre11 complex together with ATM promote activation of the ATR kinase in response to ionizing radiation in G2. The key step in the activation mechanism is Mre11-dependent

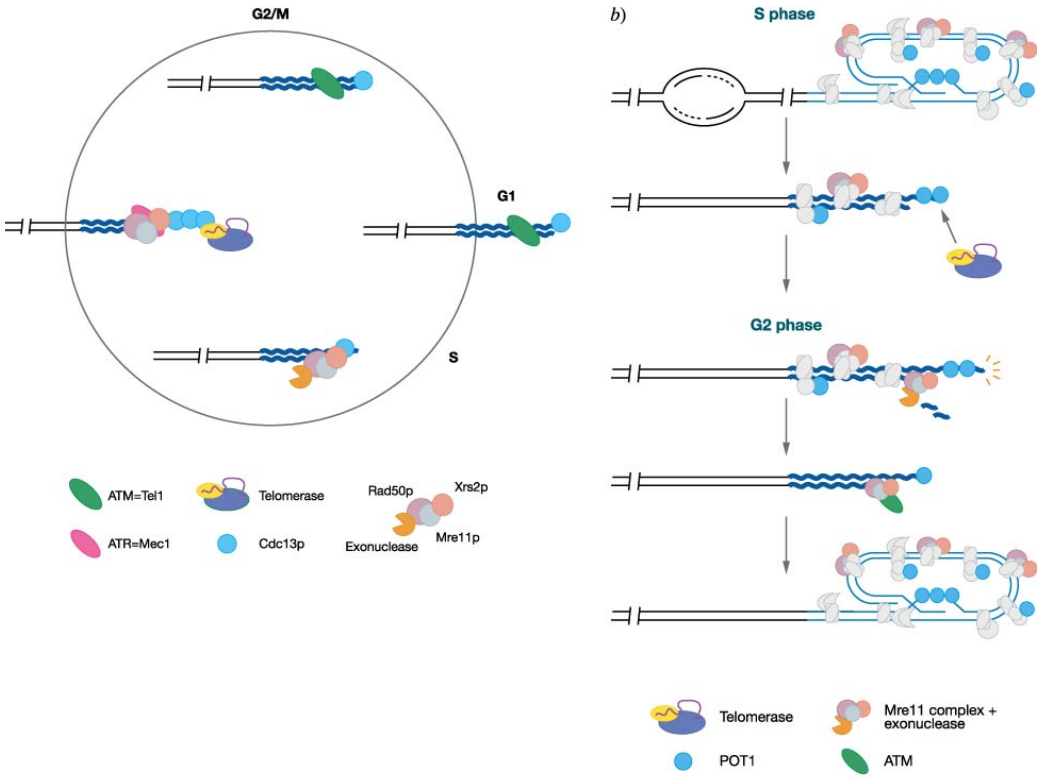

Figure 38. Model for telomere dynamics.

a. Model for telomere dynamics in budding yeast. Tel1 (ATM) and Mec1 (ATR) are reciprocally associated with the telomere in a cell cycle-dependent manner. In late S phase, the Mre11 complex is recruited to telomeres, where it is implicated in the formation of G-overhangs. However, as discussed in the text, it is likely that an additional nuclease assists in this process. Mec1 then binds the telomere facilitating the recruitment of Cdc13p and Est1p, a telomerase component. Following telomere replication, Mec1 is replaced by Tel1. b. Model for human telomere dynamics. During S phase the t-loop is likely to unfold to allow telomere replication by the conventional replication machinery (replication bubble) and by telomerase. At this stage, human telomeres may resemble DSBs, as indicated by the transient recruitment of ATM (not shown), and by analogy with yeast telomeres (see top). In G2, the telomere is bound by the Mre11 complex, which appears to promote processing the C-rich strand of the telomere through the association of another nuclease activity. There is partial release of Pot1 (depicted as removal from the G-overhang), followed by recruitment of ATM. The dynamic interplay of DNA damage response components with telomeres is proposed to help facilitate the formation of a protective cap for the transition through M and G1.

resection of DSBs leading to the formation of a RPA-coated ssDNA, which in turn may serve as a substrate for HR (394). This pathway is similar to the situation at yeast telomeres, where Mre11p is implicated in telomere resection (29), loading of Mec1p (yeast ATR homologue) during late S phase, and ultimately the recruitment of Cdc13p and telomerase (150). Thus, the telomeric function of Mre11 may reflect its role in DSB recognition and processing rather than its function in NHEJ.

The role of Ku in telomere length regulation

In all eukaryotes studied, the Ku heterodimer makes crucial contributions to telomere length homeostasis and chromosome end protection. In budding yeast, it also tethers telomeres at the nuclear periphery (161), and is required for telomere-proximal silencing (170,395). Telomere position effect (TPE) is mediated by Ku interactions with the silent information regulators proteins, Sir2-4 (162). In contrast, Ku does not play a role in TPE in fission yeast (172), and although TPE has recently been reported in mammalian cells (396), it remains to be determined whether Ku contributes to this mode of transcriptional regulation in higher eukaryotes. In vertebrates, DNA-PKcs is an essential component of this complex required for NHEJ and V(D)J recombination. Since this process is confined to vertebrates, the requirement for DNA-PKcs may be a reflection of its immunological role. Nevertheless, DNA-PKcs has also evolved to make key contributions to telomere function.

As with mutation of the Mre11 complex, telomere length is perturbed in Ku mutants. In *S. cerevisiae*, Ku-deficient telomeres decline to approximately 1/3 of their wild type length (116,170,397,398). A similar degree of telomere shortening occurs when Ku is deleted in *S. pombe* (172,174,399) or in trypanosomes (400-402). These

data argue that Ku is a positive regulator of telomere length in single-celled organisms. By contrast, Ku plays the opposite role in telomere length regulation in *Arabidopsis*. In the absence of Ku70 or Ku80, telomeres increase in size up to four-fold over wild type by the third generation (196,207,229). A new set point is then established and maintained ((229); (69)).

The contribution of Ku in mammalian telomere maintenance is less clear. d'Adda di Fagnana et al reported that telomeres shorten by ~40% in mouse embryonic fibroblasts (MEFs) derived from mice deficient in either subunit of Ku (193). MEFs from Ku heterozygous also exhibit telomere shortening, but to a level intermediate between wild type and homozygous mutants. On the other hand, Samper et al. observed slight telomere elongation in Ku deficient MEFs. Since Ku is essential for human cell viability, it has only recently been possible to address its function using RNAi or heterozygous mutant cell lines. Fluorescence in-situ hybridization (FISH) analysis of cells expressing an RNA-interference construct for Ku86 displayed dramatic telomere attrition, with 10% of the cells harboring signal-free ends (235). Similarly, telomeres declined by 50% in human cells heterozygous for Ku86 (236). In contrast, analysis of another human cell line heterozygous for Ku found a slight telomere elongation (403). One possible explanation for these conflicting results is that the level of telomerase activity differs in these cell lines. Telomere elongation in *Arabidopsis* Ku mutants is dependent on telomerase; its absence results in accelerated telomere shortening (117). Therefore, the extent to which telomere length is altered in MEFs may reflect the inherent level of telomerase activity and whether this is sufficient to counterbalance telomere loss in Ku deficient cells. As with Ku mutants, somewhat different conclusions have been reached concerning the contribution of DNA-PKcs to telomere length homeostasis. One study

found a slight increase in telomere length (404), another showed a slight decrease (405), and yet another reported wild type telomere length (199).

One important clue for how Ku can influence telomere length can be gleaned from its direct interaction with the telomerase RNP. Ku was identified as a suppressor of the telomere shortening/gene silencing defect displayed by mutants that over-express the telomerase RNA subunit, TLC1 (406). The deleterious effects of TLC1 over-expression presumably occur as a consequence of Ku titration from telomeres. Subsequent studies revealed that the Ku80 subunit recognizes a 48 nucleotide stem-loop structure in the telomerase RNA (165). Conversely, the N terminal alpha/beta domain of Ku80, which is proposed to function as a protein-protein interaction interface (163), is both necessary and sufficient for binding the telomerase RNA (165). Mutants where this interaction is disrupted display shortened telomeres. Ku binds TLC1 throughout the cell cycle, although the interaction is reduced during S (407). It is important to note that Ku is not absolutely essential for telomerase action at telomeres, otherwise a progressive loss of telomeric DNA should continue over multiple generations. It is hypothesized that Ku brings telomerase to telomeres in G1, while in S phase other components of telomerase position the enzyme at the extreme terminus (408).

Two separate studies have reported an interaction between Ku and telomerase in humans. One study found that Ku binds the 3' end of the human RNA in a region corresponding to the Ku binding site on the *S. cerevisiae* telomerase RNA (165,166). Another study found that Ku contacts TERT, and this interaction does not require the telomerase RNA or telomeric DNA (164). Whether the contacts made by Ku with TERT and the RNA are independent of each other or act in concert to stabilize the interaction

is currently unclear. However, one intriguing explanation for the differential behavior of Ku in regulating telomere length in single-celled organisms, where it is a positive regulator, and in *Arabidopsis*, where it is a negative regulator, is that Ku contacts the telomerase RNP in different manners in these two organisms.

Although a direct role for DNA-PKcs in telomere length homeostasis has not been established, DNA-PKcs interacts with a novel protein called KIP (kinase interacting protein), which displays structural similarity to calcineurin B (409). Intriguingly, KIP directly binds TERT (410). This interaction is independent of telomeric DNA and the telomerase RNA subunit. Over-expression of KIP leads to a two-fold increase in telomerase activity, and a 2kb increase in bulk telomere length, suggesting that KIP is involved in the positive regulation of telomerase.

The role of the Ku complex in chromosome end protection

Studies in mammalian cells reveal a role for Ku in chromosome end protection (168,193,197,234-236). Ku knock-out mice exhibit an early onset of senescence and a marked increase in chromosomal aberrations (411,412). Further cytogenetic analyses showed that Ku deficiency leads to chromosome-end-to-end fusions that in most cases retain telomeric DNA at the fusion junction (168,193,201,234). Similarly, most studies of Ku-deficient human cell lines find extensive chromosomal abnormalities, but report different degrees to which telomeric DNA is captured in the fusion junctions (235,236,385).

Like Ku, DNA-PKcs is strongly implicated in chromosome end protection in mammals. Numerous cytogenetic studies of cell lines deficient in DNA-PKcs and knockout mice reveal significant genome instability that apparently arises from end-to-

end chromosome fusion (199,200,385,405,413). In all cases wild type telomeric DNA length is retained at the fusion junction. Bailey et al (200) characterized DNA-PKcs MEFs using CO-FISH and determined that telomere fusion junctions were formed between telomeres replicated by leading synthesis. A similar conclusion was reached using human cell lines deficient in DNA-PKcs (385). Remarkably, this phenotype is dependent on the integrity of the catalytic subunit of DNA-PKcs as the pharmacological inhibition of the DNA-PKcs kinase domain results in a dose-dependent increase in telomere-to-telomere fusions (414). Since this type of fusion results after telomere replication, the data imply that the catalytic activity of DNA-PKcs is involved in the formation of a post-replicative chromosome cap at the telomere and, hence, supports the idea that telomeres are transiently recognized as double-strand breaks.

Remarkably, neither telomere fusions nor other genome instabilities were detected in Ku-deficient *Arabidopsis* (196,229). Similarly, no end-joining events were observed in Ku-deficient fission yeast. However, a low level of chromosome fusions could be discerned by a PCR–based method in budding yeast deficient in Ku80 (209).

Despite the failure to observe chromosome fusions in fission yeast and *Arabidopsis*, other evidence strongly implicates Ku in chromosome end protection in these organisms. Mutants doubly-deficient in Ku and telomerase experience a highly accelerated rate of telomere shortening. Although most *S. pombe* cells die as a result of inactivating Ku80 and Tert, the few remaining survivors circularize their chromosomes after having undergoing extensive erosion of terminal DNA sequences (195). Likewise, in *Arabidopsis ku70 tert* mutants telomeres shorten two to three times faster than in *tert* mutants (117,229). In striking contrast, when a Ku deficiency is introduced into telomerase-negative mice, no accelerated shortening is observed (194), although the

double mutants suffer a slight increase in mortality (405). However, a two-fold accelerated rate of telomere shortening occurs in telomerase-deficient mice that lack DNA-PKcs (198). Although no increase in the frequency of telomere fusions was observed, the double mutants age more rapidly and have a decreased lifespan. Since DNA-PKcs and Ku mutants display essentially the same loss of proliferative capacity and early onset of age-related pathologies in the absence of telomerase, these proteins appear to participate in the same DNA damage response pathway (198). However, since mutation of these two genes lead to dramatically different outcomes with respect to telomere maintenance, the data imply that DNA-PKcs and Ku make distinct contributions to telomere biology.

It likely that the accelerated rate of telomere shortening observed in Ku and DNA-PKcs mutants that lack telomerase reflects the combined failure of telomerase to maintain the telomeric G-strand and an increased susceptibility of the C-strand to nucleolytic processing. Although G-overhangs are not substantially extended in mice lacking DNA-PKcs (169), extensive resection of the telomeric C-strand was observed in *Arabidopsis ku70* mutants (117). This finding suggests that Ku protects the 5' chromosome terminus from extensive degradation.

In budding yeast, Ku mutants display a temperature-sensitive phenotype at 37°C (415,416). Cells arrest in G2 (416), eliciting a strong DNA damage checkpoint response that is dependent on RAD9, CHK1 and MEC1 (226,417). Strikingly, over-expression of telomerase components can suppress checkpoint activation (397,418), arguing that arrest can be attributed to some aspect of telomere dysfunction. Indeed, the G-overhangs in Ku mutants are significantly elongated, and in contrast to wild type,

persist through-out the cell cycle (116,419). Since the extended G-overhangs are created in the absence of telomerase (417), they are likely to arise from degradation of telomeric C-rich strand rather than enhanced engagement of telomerase. Notably, cell cycle arrest and extension of G-overhangs in Ku mutants are both dependent on the mismatch repair nuclease, Exo1 (226).

Although the status of the G-overhang in *S. pombe* Ku mutants has not been reported, G-overhangs are greatly elongated in cells deficient cells dsTBP Taz1 (179). Genetic evidence argues that Ku protects the C-strand from nucleolytic degradation. The extended G-overhangs in *taz1* mutants are lost when in a *taz1*$^{-}$ *rad32*$^{-}$ double mutant, but they reappear in *taz1*$^{-}$ *rad32*$^{-}$ *ku70*$^{-}$ triple mutants (178). These results are consistent with the idea that Mre11 promotes processing of the C-rich strand, while Ku protects it.

Further evidence that Ku is required for chromosome end integrity is the observation that homologous recombination at telomeres is dramatically increased in Ku-deficient yeast. Telomere rapid deletion is increased 50-fold in *S. cervisiae* Ku mutants (419,420). Similarly, *S. pombe* Ku70 and Ku80 mutants display a marked increased incidence of recombination at subtelomeric DNA (195,421).

Interaction of Ku with telomeres

The wide range of telomeric phenotypes associated with Ku deficiency in different organisms does not allow a unifying model for Ku's action at telomeres. This is not unexpected given Ku's very diverse functions in cellular metabolism. Alternatively, Ku may act in fundamentally similar way at telomeres, but how its function is limited may

reflect species-specific variations in the structure and maintenance of telomeric chromatin.

To gain more mechanistic insight in the telomeric role of Ku, it is essential to understand how Ku functionally interacts with telomeres. A physical association between the Ku complex with telomeres has been extensively reported (172,193,209,234,421-423). This contact persists in *S. cerevisiae* and human cell lines though-out the cell cycle (116,193,407). In mammals, it is noteworthy that Ku and DNA-PKcs interact with telomeres independently of each other (193,422), arguing that they can make unique contributions to telomere structure and/or function.

In principle, Ku can associate with telomeres via protein-protein interaction or by directly binding to the DNA as with DSBs (Figure 39). Several lines of evidence suggest that Ku associates with chromosome termini via dsTBPs (Figure 39a). In mammals, Ku interacts with telomeres through TRF1 and TRF2 (155,234) and in *S. cerevisiae*, through Rap1 association where it forms cytologically detectable foci (423). Moreover, in yeast cells exposed to DNA damage Ku rapidly re-localizes to DSBs, implying that bulk of the heterodimer is sequestered at chromosome termini through protein-protein interaction. Interestingly, in *S. pombe* Ku binds telomeres independently of Taz1 (421).

Although there is currently no proof for a physical interaction with telomeric DNA, binding of Ku may be facilitated through interactions with dsTBPs. This would be reminiscent of the recruitment of Pot1 to the single-stranded G-overhang (76). The direct binding of the Ku to the end of telomeric DNA (Figure 39b,c and d) would provide a mechanistic explanation for many of the functions attributed to the Ku complex,

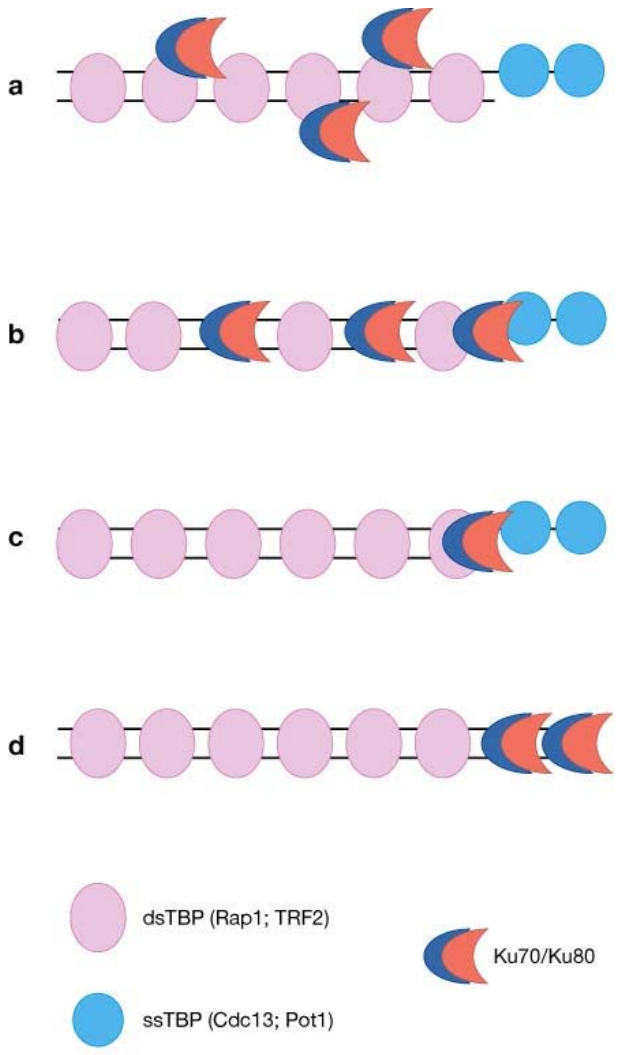

Figure 39. Possible modes of Ku association with telomeres.

Ku can associate with chromosome termini through protein-protein interaction (a) or via binding to the telomeric DNA (b, c, d). Since Ku can load onto DNA only through ends, binding of multiple Ku molecules along the entire length of the telomeric DNA tract (b) is unlikely, because other telomere-bound proteins would hinder Ku translocation from the terminus to more internal sites. Alternatively, Ku may bind at the transition between single stand and double strand DNA (c), where it could protect the 5' end of the telomere (C-rich strand) from extensive exonuclease resection; the 3' G-overhang is protected by ssTBPs. The telomere created by leading strand DNA replication will be "blunt ended" and hence unable to bind ssTBPs. Ku heterodimers could associate with such ends (d), protecting them extensive nuclease resection and NHEJ, until a proper G-overhang is formed. These modes of Ku-telomere interactions are not mutually exclusive, and their utilization may vary during the cell cycle and/or at different subsets of telomeres.

including its capacity to prevent extensive nucleolytic degradation of DSBs and at telomeres (116,117,178,226). By analogy to the situation at DSBs, we would predict that one or only a few Ku molecules could potentially load at the telomere through chromosome ends (Figure 39c and d). Suppression of 5´ end resection may also contribute to the anti-recombinogenic effect of Ku at yeast telomeres (419,420) (Figure 39b and c).

Positive regulation of telomerase by chromatin-bound Ku in yeast appears to be partially mediated by recruitment of the Est2/TLC1 holoenzyme to telomeric chromatin in G1 (407). Moreover, DNA-bound Ku may also directly contribute to the loading of telomerase to the 3' DNA end, which is evident from its role in de novo telomere synthesis at DSBs (165). Regulation of telomerase draws another parallel with the function of Ku at DSBs, where it controls activity of DNA repair polymerases. Thus, Ku may essentially perform very similar tasks at telomeres and DSBs; in both cases it stabilizes ends of DNA molecule and coordinates DNA processing activities. If the same molecular mechanism underlies the function of Ku at both DSBs and telomeres, why does Ku-binding facilitate ligation of internal breaks, but not chromosome end-joining? Biochemical analysis indicates that KU can both promote and suppress DNA end ligation, depending on the number of Ku molecules that bind the DNA (310). Thus, Ku has an intrinsic capability to act as *bona fide* telomere capping factor, protecting chromosome ends from nucleolytic, recombinogenic and even end-joining activities. The final outcome of Ku association with DNA termini is likely to be strongly influenced by the local chromatin environment. For example, dsTBPs may be important modulators of Ku, promoting its telomere protective function, while loss of the dsTBPs may unleash end joining reaction.

The role of NHEJ components at *Drosophila* telomeres

Remarkably, the essential role for the Ku complex in chromosome end biology is conserved even among organisms that do not have canonical telomere sequences or telomerase. Ku70 and Ku 80 heterozygous flies both display elongated telomeres, with a 100-fold increase in the rate of HeT-A and TART transposition (424). Thus, Ku is a negative regulator of retrotransposition at telomeres in much the same way that Ku negatively regulates telomerase-mediated telomere lengthening in *Arabidopsis* (196,207,229). Ku-deficient Drosophila do not show an increase in chromosome end fusion (425).

Although the Mre11 complex shows no specific localization to chromosome termini in Drosophila (426), flies that are deficient in either Mre11 or Rad50 exhibit massive telomere-to-telomere fusions, with more than 60-70% of the chromosome ends involved in fusions (426) (427). Intriguingly, Ciapponi et al also show that the loss of Mre11 or Rad50 results in a decreased occupancy of HP1 at telomeres. These results strongly suggest that Mre11 and Rad50 contribute to proper telomere formation by allowing the binding of HP1 and HOAP.

Conclusion and future directions

The necessity for NHEJ components at telomeres appears to be universal among eukaryotic organisms. Even Drosophila with its unconventional telomeres requires NHEJ machinery for proper maintenance of chromosome ends. Although the larger question of how NHEJ proteins are kept at bay remains unresolved, some insight may be gained from mutagenesis studies where mutations in Ku (428) (163,165,314) and

Mre11 (252) have begun to reveal functional regions in these proteins that separate NHEJ and telomere activities. Further biochemical dissection of NHEJ proteins will undoubtedly provide insight in this regard.

It will also be important to consider NHEJ proteins within the context of telomeric chromatin. Recent data reveal a dynamic interplay between telomere maintenance and the DNA damage pathway, notably the intriguing observation that telomeres elicit a transient, but incomplete, DNA damage response. Recent data indicate that TRF2 plays a central role in restraining this response. Over-expression of TRF2 inhibits the ability of ATM to phosphorylate its targets (80,148), which provides a compelling explanation for why downstream targets of ATM are not activated when normal telomeres are exposed in G2. Moreover, the ability of TRF2 to physically interact not only with ATM, but also with the Mre11 and Ku complexes provides an opportunity to dampen the DNA response at multiple levels.

Adding another layer of complexity in the telomere-DNA repair relationship is the recent discovery that TRF2 rapidly localizes to double-strand breaks, arriving before and independently of Ku (80). This observation raises the provocative possibility that TRF2 evolved from a general DNA damage protein, and as the need for chromosome end protection emerged so did the functions of TRF2 (429). It has been proposed that TRF2 may act to prevent inappropriate repair during telomere replication and re-establishment of the protective cap (429).

In principle, localization of a key component of the shelterin complex to an internal double-strand break could promote de novo telomere formation, but this does not occur. One possible explanation is that the recent finding that telomerase is sequestered to the nucleolus in response to DNA damage (58), which would preclude

its inappropriate action at double-strand breaks. Thus, although the relationships between telomere and DNA repair proteins are highly dynamic and functionally intertwined, the execution of their fundamental activities is restrained by their chromosome context.

VITA

Name:	Michelle L. Heacock
Address:	National Institutes of Enviromental Health P.O. Box 12233, Research Triangle Park North Carolina, USA, 27709
Education:	Ph.D. Biochemistry, Texas A&M University, 2007 B.S., Biochemistry, Delta State University, 2001